

# **Extracellular vesicle cargo: a source of biomarkers for severe malaria in paediatric patients**

**by Iris Simone Cheng**

Thesis submitted in fulfilment of the requirements for the degree of

**Doctor of Philosophy, PhD Thesis: Science (C02031)**

under the supervision of Associate Professor Valery Combes and Associate Professor Sheila Donnelly

University of Technology Sydney  
Faculty of Science

August 2024

## **Certificate of Original Authorship**

I, Iris Simone Cheng, declare that this thesis, is submitted in fulfilment of the requirements for the award of Doctor of Philosophy, in the Faculty of Science at the University of Technology Sydney.

This thesis is wholly my own work unless otherwise referenced or acknowledged. In addition, I certify that all information sources and literature used are indicated in the thesis. This document has not been submitted for qualifications at any other academic institution. This research is supported by the Australian Government Research Training Program.

**Signature:**      Production Note:  
                                 Signature removed prior to publication.

**Date:** 19/08/2024

# Table of Contents

Acknowledgements .....	xiii
Publications associated with this thesis .....	xv
Published abstracts related to this thesis .....	xv
Conferences and awards .....	xv
Abstract.....	xviii
<b>Chapter 1: Introduction and Background to the Area of Research .....</b>	<b>2</b>
<b>1.1 Aetiology.....</b>	<b>2</b>
<b>1.2 Epidemiology .....</b>	<b>2</b>
<b>1.3 Burden of Malaria .....</b>	<b>3</b>
<b>1.4 <i>Plasmodium</i> life cycle.....</b>	<b>3</b>
1.4.1 <i>Asexual liver stage - asymptomatic .....</i>	<i>3</i>
1.4.2 <i>Asexual erythrocytic cycle - symptomatic.....</i>	<i>4</i>
1.4.3 <i>Sexual stage .....</i>	<i>4</i>
<b>1.5 Clinical presentation and pathogenesis .....</b>	<b>5</b>
<b>1.6 Control, prevention, and diagnosis of malaria.....</b>	<b>7</b>
<b>1.7 Biomarkers of Malaria .....</b>	<b>9</b>
<b>1.8 Extracellular vesicles .....</b>	<b>10</b>
<b>1.9 Patient and collaborator acknowledgements.....</b>	<b>11</b>
<b>1.10 Thesis Aims .....</b>	<b>12</b>
<b>Chapter 2: Review of extracellular vesicles' role in pathogenesis and as biomarkers in cerebral malaria .....</b>	<b>14</b>
<b>2.1 Introduction to Malaria.....</b>	<b>16</b>
<b>2.2 Pathogenesis of CM: from host cells to extracellular vesicles .....</b>	<b>17</b>
<b>2.3 <i>In vitro</i> models of malaria - interactions between host cells and extracellular vesicles .....</b>	<b>20</b>
<b>2.4 <i>In vivo</i> models of malaria: what do extracellular vesicles bring to pathogenesis? ....</b>	<b>22</b>
<b>2.5 Extracellular vesicle cargo: effector, biomarker or both? .....</b>	<b>25</b>
<b>2.6 Conclusion .....</b>	<b>30</b>
<b>2.7 References .....</b>	<b>32</b>
<b>Chapter 3: Characterising extracellular vesicle microRNAs from Thai malaria patients.....</b>	<b>44</b>
<b>3.1 Background.....</b>	<b>46</b>
<b>3.2 Methods.....</b>	<b>47</b>
3.2.1 <i>Human samples collection and preparation.....</i>	<i>47</i>
3.2.2 <i>Extracellular vesicles isolation from human plasma .....</i>	<i>47</i>

3.2.3 Total RNA extraction .....	47
3.2.4 Total RNA concentration measurement and cleaning .....	47
3.2.5 Primers for miRNAs detection .....	47
3.2.6 Reverse transcriptase quantitative polymerase chain reaction (RT-qPCR) .....	47
3.2.7 Relative expression analysis .....	48
3.2.8 Target prediction and pathway involvement of dysregulated miRNAs .....	48
3.2.9 Evaluation of potential EVs-derived miRNA as biomarker .....	48
3.2.10 Statistical analysis .....	48
<b>3.3 Results</b> .....	<b>48</b>
3.3.1 Patient's characteristics .....	48
3.3.2 Relative expression of miRNAs in three biological groups .....	49
3.3.3 Target prediction and KEGG Pathway analysis of hsa-miR150-5p and hsa-miR-15b-5p .....	50
3.3.4 Evaluation of the diagnostic potential of extracellular vesicles-derived miRNAs ..	51
<b>3.4 Discussion</b> .....	<b>52</b>
<b>3.5 Conclusion</b> .....	<b>55</b>
<b>3.6 References</b> .....	<b>56</b>
<b>Chapter 4: Extracellular vesicle miRNAs in plasma as biomarkers for disease severity and neurocognitive impairment in children with severe malaria</b> .....	<b>61</b>
<b>4.1 Introduction</b> .....	<b>64</b>
<b>4.2 Materials and methods</b> .....	<b>68</b>
4.2.1 Study Participants .....	68
4.2.2 Informed consent and ethical approval .....	68
4.2.3 Experimental design .....	69
4.2.4 Neuropsychological/Cognitive tests .....	69
4.2.5 Blood collection and platelet-free plasma preparation and storage .....	71
4.2.6 Isolation of extracellular vesicles .....	71
4.2.7 Extracellular vesicle concentration and size .....	71
4.2.8 Total RNA extraction .....	72
4.2.9 miRNA library preparation .....	72
4.2.10 Quality Control before NGS .....	72
4.2.11 Denaturing, diluting, and sequencing the library .....	73
4.2.12 Mapping and expression analysis .....	73
4.2.13 Verification via RT-qPCR .....	74
4.2.14 RT-qPCR statistical analysis .....	75
<b>4.3 Results</b> .....	<b>75</b>



4.3.1 Nanoparticle tracking analysis profile of platelet-free plasma extracellular vesicle .....	75
4.3.2 Extracellular vesicle RNA population profile .....	76
4.3.3 Differential expression analysis between the clinical groups .....	77
4.3.4 Pathway analysis on miRNAs of interest .....	85
4.3.5 Selecting endogenous control for real-time quantitative PCR normalisation .....	89
4.3.6 MicroRNA verification via real-time quantitative PCR.....	89
4.3.7 Differing miRNA expression profiles between sequencing and PCR analysis .....	90
4.3.8 Receiver operator curves identified numerous miRNAs with prognostic potential	93
<b>4.4 Discussion</b> .....	<b>94</b>
<b>4.5 Conclusion</b> .....	<b>99</b>
<b>4.6 References</b> .....	<b>101</b>
<b>4.7 Supplementary data</b> .....	<b>110</b>
<b>Chapter 5: Proteomic analysis of paediatric plasma extracellular vesicles for the identification of prognostic biomarkers for severe malaria outcomes</b> .....	<b>118</b>
<b>5.1 Introduction</b> .....	<b>121</b>
<b>5.2 Materials and methods</b> .....	<b>124</b>
5.2.1 Study Participants .....	124
5.2.2 Ethical approval and informed consent .....	124
5.2.3 Study design .....	124
5.2.4 Platelet-free plasma preparation and storage .....	124
5.2.5 EV isolation, size measurement, and serum protein removal .....	126
5.2.6 Protein digestion and tandem mass spectrometry analyses .....	126
5.2.7 Mapping and bioinformatics.....	128
<b>5.3 Results</b> .....	<b>129</b>
5.3.1 EV size and concentration .....	129
5.3.2 Technical reproducibility .....	129
5.3.3 Proteomic analysis .....	132
5.3.4 Expression and pathway analysis for 5 sub-groups (community controls and malaria patients).....	135
5.3.5 Expression analysis for the clinically relevant malaria comparisons .....	139
5.3.6 Identification of biological processes and functional group networks .....	140
<b>5.4 Discussion</b> .....	<b>152</b>
<b>5.5 References</b> .....	<b>158</b>
<b>5.6 Supplementary data</b> .....	<b>166</b>

<b>Chapter 6: Comparative phenotype and numbers of extracellular vesicles in the plasma and the cerebrospinal fluid of children with severe malaria .....</b>	<b>174</b>
<b>6.1 Introduction.....</b>	<b>177</b>
<b>6.2 Materials and methods .....</b>	<b>180</b>
6.2.1 <i>Participants .....</i>	180
6.2.2 <i>Informed consent and ethical approval .....</i>	181
6.2.3 <i>Study Design.....</i>	181
6.2.4 <i>Cerebrospinal fluid and platelet-free plasma collection, preparation, and storage .....</i>	181
6.2.5 <i>Extracellular vesicle and cellular origin markers .....</i>	183
6.2.6 <i>Pre-analytical flow cytometer preparations .....</i>	183
6.2.7 <i>Staining and incubation .....</i>	184
6.2.8 <i>Sizing beads used for extracellular vesicle gating strategy .....</i>	184
6.2.9 <i>Acquisition strategy and gating protocol .....</i>	185
6.2.10 <i>Phenotype and statistical analysis.....</i>	185
<b>6.3 Results.....</b>	<b>186</b>
6.3.1 <i>Gating Strategy for EVs.....</i>	186
6.3.2 <i>Confirming events were extracellular vesicles .....</i>	187
6.3.3 <i>Phosphatidylserine profiles for CSF and PFP extracellular vesicles.....</i>	187
6.3.4 <i>Antibody+/PS-negative profiles of EVs in CSF and PFP during severe malaria .....</i>	192
6.3.5 <i>Antibody/PS double-positive profiles of EVs in CSF and PFP during severe malaria .....</i>	196
6.3.6 <i>Correlation between CSF and PFP EV profiles of severe malaria .....</i>	201
<b>6.4 Discussion .....</b>	<b>203</b>
<b>Acknowledgements.....</b>	<b>207</b>
<b>6.5 References .....</b>	<b>208</b>
<b>Chapter 7: Concluding remarks and future directions.....</b>	<b>216</b>
<b>Chapter 8: References (Chapter 1 and 7) .....</b>	<b>220</b>

## List of Tables

### Chapter 3

<b>Table 3.1</b> Primers used for quantitative PCR.....	48
<b>Table 3.2</b> Sample characteristic.....	48
<b>Table 3.3</b> Descriptive statistics of quantification cycle (C <sub>q</sub> ) values.....	50
<b>Table 3.4</b> Relative expression analysis of miRNAs.....	51

### Chapter 4

<b>Table 4.1</b> Characteristics of paediatric patient group baseline demographics and clinical findings.....	70
<b>Table 4.2</b> Genomic mapping of different small RNA species from Ugandan paediatric patient plasma EVs .....	80
<b>Table 4.3</b> Top 20 most abundant mature miRNA sequences identified in Ugandan paediatric plasma-derived EVs.....	82
<b>Table 4.4</b> MicroRNAs that regulate proteins from the malaria KEGG pathway .....	86
<b>Table 4.5</b> Comparison of next generation sequencing and RT-qPCR expression levels between severe malaria patient groups .....	91

### Chapter 5

<b>Table 5.1</b> Characteristics of paediatric patient group baseline demographics and clinical findings.....	125
<b>Table 5.2</b> Percentage similarity between patient technical replicates and number of proteins identified in each patient.....	131
<b>Table 5.3</b> Number of proteins and protein groups identified in each patient group via mass spectroscopy .....	133
<b>Table 5.4</b> Top 10 most highly dysregulated proteins for each severe malaria outcome comparison .....	141
<b>Table 5.5</b> Top 5 diseases and biological functions that were significantly altered by the differentially expressed proteins .....	145

### Chapter 6

<b>Table 6.1</b> Characteristics of paediatric patient group baseline demographics and clinical findings.....	182
---	-----

## List of Supplementary Tables

### Chapter 3

<b>Supplementary Table 3.1</b> Individual target prediction of up-regulated miRNAs and genes involved in malaria pathway .....	59
--	----

### Chapter 4

<b>Supplementary Table 4.1</b> Top 20 most abundant mature microRNA sequences identified in plasma-derived extracellular vesicles for each child .....	112
<b>Supplementary Table 4.2</b> Top 20 most abundant seed sequences identified in plasma-derived extracellular vesicles for each individual patient sample .....	113
<b>Supplementary Table 4.3</b> Top 20 most abundant novel seed sequences identified in plasma-derived extracellular vesicles for each patient sample .....	114
<b>Supplementary Table 4.4</b> Differentially expressed microRNAs for clinically relevant groups comparisons .....	115
<b>Supplementary Table 4.5</b> Top 20 GO term clusters with the corresponding miRNA of interest .....	116

### Chapter 5

<b>Supplementary Table 5.1</b> List of all differentially expressed proteins for the clinically relevant comparisons .....	168
--	-----

## List of Figures

### Chapter 1

<b>Figure 1.1</b> Plasmodium parasite life cycle .....	5
--	---

### Chapter 2

<b>Figure 2.1</b> Outline of the role that EVs play in the pathogenesis of cerebral malaria .....	24
---	----

### Chapter 3

<b>Figure 3.1</b> a Malaria infected patients with <i>P. vivax</i> or <i>P. falciparum</i> calculated as a percentage of parasitaemia .....	49
<b>Figure 3.2</b> Relative expression of hsa-miR-15b-5p, hsa-miR-16-5p, hsa-let-7a-5p and hsa-miR-150-5p were calculated using $2^{(-\Delta\Delta Cq)}$ method.....	50
<b>Figure 3.3</b> This dot plot demonstrates the miRNAs expression values in 3 biological groups (Uninfected, <i>P. vivax</i> -infected patients or <i>P. vivax</i> , and <i>P.falciparum</i> -infected patients or <i>P. falciparum</i> ).....	51
<b>Figure 3.4</b> Pathway enrichment analysis of up-regulated miRNAs were carried out by DIANA-mirPath v3.0 which searching against experimentally validated miRNAs targets on Tarbase v7.0.....	52
<b>Figure 3.5</b> Area Under the Receiver Operating Characteristic (ROC) curve (AUC) analysis...54	

### Chapter 4

<b>Figure 4.1</b> Study pipeline summarising the patient groups, EV and RNA purification from human paediatric samples and bioinformatics .....	67
<b>Figure 4.2</b> Quality control for library size and length, and extracellular vesicle size and concentration.....	76
<b>Figure 4.3</b> Characterisation of miRNA in malaria-infected Ugandan paediatric patient plasma EVs using next-generation sequencing.....	81
<b>Figure 4.4</b> Volcano plots of the mature miRNAs in the 5 comparisons of biological interest	83
<b>Figure 4.5</b> Heatmap representation of differentially expressed miRNAs in the 5 comparisons of biological interest .....	84
<b>Figure 4.6</b> Top 20 gene ontology terms for differentially expressed miRNA present in $\geq 50\%$ of patients .....	87
<b>Figure 4.7</b> Malaria KEGG pathway, hsa05144, 13 miRNAs of interest that regulate the 13 genes involved in malaria .....	88
<b>Figure 4.8</b> Validation of microRNA expression via RT-qPCR.....	92

### Chapter 5

<b>Figure 5.1</b> Study pipeline depicting the patient groups, sample collection and processing, protein purification from paediatric samples and bioinformatics .....	124
--	-----

<b>Figure 5.2</b> Measurement of size and concentration of extracellular vesicles using nanoparticle tracking analysis.....	130
<b>Figure 5.3</b> Venn diagram comparing the plasma EV proteins identified in each patient and malaria sub-group.....	133
<b>Figure 5.4</b> Comparison of proteins identified in the three main groups of children .....	134
<b>Figure 5.5</b> Comparison of <i>Plasmodium falciparum</i> proteins identified in all the patients ...	134
<b>Figure 5.6</b> Differentially expressed plasma extracellular vesicle proteins identified with PEAKS Xpro.....	137
<b>Figure 5.7</b> Summary of the major biological themes identified using Ingenuity Pathway Analysis. ....	138
<b>Figure 5.8</b> Volcano plots of three clinically relevant comparisons of severe malaria outcomes .....	139
<b>Figure 5.9</b> Most significant canonical pathway categories and networks for the comparison between children with severe malarial anaemia and cerebral malaria who fully recovered without complications. ....	144
<b>Figure 5.10</b> Most significant canonical pathway categories and networks for the comparison between children with cerebral malaria who died and children with cerebral malaria who fully recovered without complications.....	148
<b>Figure 5.11</b> Most significant canonical pathway categories and networks for the comparison between children with severe malarial anaemia who fully recovered without complications and children with severe malarial anaemia who survived but developed neurocognitive impairment .....	151

## Chapter 6

<b>Figure 6.1</b> Study pipeline, explaining the collection of paediatric samples and characterisation using flow cytometry .....	180
<b>Figure 6.2</b> Gating Strategy for particles between approximately 70-900 nm, acquisition on the CytoFLEX S flow cytometer.....	187
<b>Figure 6.3</b> Gating strategy for Annexin V and antibody labelled extracellular vesicles (EVs) .....	189
<b>Figure 6.4</b> Annexin V profiles for cerebrospinal fluid (CSF) and matching platelet-free plasma (PFP) extracellular vesicles (EVs).....	190
<b>Figure 6.5</b> Annexin V-positive events from the marker panels were used to compare the number of extracellular vesicles (EVs) between the severe malaria outcomes and the matching cerebrospinal fluid (CSF) and platelet-free plasma (PFP).....	191
<b>Figure 6.6</b> Comparison of antibody-positive/annexin V-negative EVs in cerebrospinal fluid (CSF) between the different severe malaria outcomes.....	193
<b>Figure 6.7</b> Comparison of antibody-positive/annexin -negative EVs in platelet-free plasma (PFP) between the different severe malaria outcomes.....	194
<b>Figure 6.8</b> Comparison of antibody-positive/annexin V-negative EVs between the cerebrospinal fluid (CSF) and platelet-free plasma (PFP) of children with severe malaria...	195
<b>Figure 6.9</b> Comparison of antibody-positive/annexin V-positive EVs in the cerebrospinal fluid (CSF) across the different severe malaria outcomes .....	198
<b>Figure 6.10</b> Comparison of antibody-positive/annexin V-positive EVs in the platelet free plasma (PFP) across the different severe malaria outcomes .....	199

**Figure 6.11.** Comparison of antibody-positive/annexin V-positive EVs between the cerebrospinal fluid (CSF) and platelet-free plasma (PFP) across the different severe malaria outcomes. ....200

**Figure 6.12** Spearman’s correlation matrix comparing the phenotypic profile of cerebrospinal fluid and platelet-free plasma extracellular vesicles from children with severe malaria .....202

## List of Supplementary Figures

### Chapter 4

<b>Supplementary Figure 4.1</b> CLC genomics workbench workflow .....	110
<b>Supplementary Figure 4.2</b> Top 50 gene ontology terms for differentially expressed miRNA present in $\geq 50\%$ of patients .....	111

### Chapter 5

<b>Supplementary Figure 5.1</b> Pearson correlation plots depicting the relationship between technical replicates of patient sample .....	166
<b>Supplementary Figure 5.2</b> Predicted up- and downstream regulators using Ingenuity Pathway Analysis .....	167
<b>Supplementary Figure 5.3</b> Canonical pathways for clinically relevant severe malaria comparisons .....	169
<b>Supplementary Figure 5.4</b> All diseases and biological functions significantly altered by the differentially expressed proteins between children with severe malarial anaemia (SMA) and cerebral malaria (CM) who fully recovered without complications .....	170
<b>Supplementary Figure 5.5</b> All diseases and biological functions significantly altered by the differentially expressed proteins between children with cerebral malaria who died (CM FO) and children with cerebral malaria who fully recovered without complications (CM FR)....	171
<b>Supplementary Figure 5.6</b> All diseases and biological functions significantly altered by the differentially expressed proteins between children with severe malarial anaemia who fully recovered without complications (SMA FR) and children with severe malarial anaemia who survived but developed neurocognitive impairment (SMA NCI).....	172



## Acknowledgements

This thesis reports on a genuinely thrilling time while completing my doctorate. The vast amount of techniques, skills, and experience I have gained while completing this thesis is truly priceless. Luckily, being blessed with the best supervisors I could ask for has allowed me to excel in fields I previously could not imagine and grow as a researcher and academic. All the researchers I have had the privilege to interact with have given me advice, information, and comfort, which has allowed me to complete this thesis. Thank you all.

I would first like to thank my amazing supervisors, A/Prof. Valery Combes and A/Prof. Sheila Donnelly, thank you for all the limitless help and guidance you have provided me throughout my honours and PhD. And a special thanks to A/Prof. Valery Combes, I greatly appreciate you for always being there and providing invaluable help with any questions I have, whether it be writing, lab work, or life.

Also, thank you to all those who spent time teaching me the essential lab skills needed to complete my candidature. Thank you to Nutpakal Ketprasit and Benjamin Sealy for teaching me how to culture malaria parasites, tissue culturing and various essential assays, Dr Nilesh Bokil for teaching me how to perform various assays for flow cytometry, and Dr Kay Anantanawat for going through RNA isolation, library preparation, all the QC assay and next-generation sequencing as well as bioinformatics. I would also like to thank Joyce To for all your help throughout the years; you know where everything is! Also, thank you to the lab managers and technical services assistance with learning how to use equipment and specific lab work, Drs Mercedes Ballesteros, Kun Xiao, Luke Beebe, Sarah Osvath, Fiona Ryan, Lalit Overlunde, and A/Prof. Matt Padula.

I am grateful to all the children and their guardians from Uganda and adults from Thailand who participated in the studies within my thesis, their invaluable contributions have allowed for new discoveries within the field of malaria. My deepest gratitude to Distinguished Prof. Chandy John, Prof. Robert Opoka, and Dr Paul Bangirana for providing guidance alongside the precious paediatric samples and data from Uganda. I greatly appreciate the assistance from A/Prof. Duangdao Palasuwan and Prof. Mallika Imwong for the valuable adult samples from Thailand.

Of course, I would also like to thank my peers who have gone through honours and PhD with me; I know that if there is anything we need help with, we will all step in and help. Love you guys, Inah Camaya, Mayra Loli, Glenna Travis, Giang Le, Louis de Couvreur, Bobby Fleck, Kiora Pillay and Neus Pelegri. Also, to Bobby's wonderful partner, Raissa Gill, thank you for your valuable help with RT-qPCR statistics; you saved me so much time. I also appreciate Drs Joel Steele and Penelope Dalla for proteomics data sorting tips and software.

Lastly, I am most grateful to my family for all their support throughout my candidature. Love you to my partner Zhi Xu, thank you for always picking me up from UTS after staying past the last train home and making sure I have snacks between long experiments.

Although I can call this my thesis, it is a bit of everyone's as there was no way I could have accomplished this without everyone's support. I am genuinely proud of the research reported here, and I am excited for anyone who reads it.

## Publications associated with this thesis

First co-author

**The characterization of extracellular vesicles-derived microRNAs in Thai malaria patients**

Cheng, I.S., Ketprasit, N., Deutsch, F. *et al.* Malaria Journal **19**, 285 (2020).

<https://malariajournal.biomedcentral.com/articles/10.1186/s12936-020-03360-z>

First co-author

**Extracellular vesicles, from pathogenesis to biomarkers: the case for cerebral malaria**

Cheng, I.S., Sealy, B.C., Tiberti, N., Combes, V. Vessel Plus **4**, 17 (2020).

<http://dx.doi.org/10.20517/2574-1209.2020.08>

## Published abstracts related to this thesis

**The role of extracellular vesicles in the modulation of endothelial junctions in an in vitro model of cerebral malaria**

Combes, V., Sealy, B. & Cheng, I. Journal of Extracellular Vesicles **7**, 188 (2018)

<https://www.proquest.com/docview/2116610283/abstract/CC83B2BF11514292PQ/1?accountid=17095>

**MicroRNA in human plasma extracellular vesicles during severe malaria – Potential biomarkers for disease severity?**

Cheng, I.S., Opoka, R.O., John, C.C., Combes, V. Life Sciences, Medicine and Biomedicine **6**, 1 (2022)

<https://doi.org/10.28916/lsm.6.1.2022.106>

## Conferences and awards

New Horizons 2017 poster award

Australia and New Zealand Society for Extracellular Vesicles 2018 and 2020 poster award

Women in Malaria 2021

International Congress for Tropical Medicine & Malaria 2022

## Abbreviations

ACAN	Aggrecan
AcN	Acetonitrile
AHSG	Alpha-2-HS-glycoprotein
ALAD	Aminolevulinic acid dehydratase
ALB	Albumin
APO	Apolipoprotein
APOH	Apolipoprotein H
AUC	Area under the curve
AV	Annexin V
AZGP1	Alpha-2-glycoprotein 1, zinc-binding
B2M	$\beta$ 2 microglobulin
BASP1	Brain acid soluble protein 1
C3	Complement C3
C8b	Complement component C8 beta chain
CA1	Carbonic anhydrase 1
CALM1	Calmodulin 1
CC	Community control
cDNA	Complementary DNA
CEACAM8	Carcinoembryonic antigen-related cell adhesion molecule 8
CETP	Cholesteryl ester transfer protein
CFHR	Complement factor H-related
CFL1	Cofilin 1
CFP	Cornified envelope protein
CLC-GWB	CLC genomics workbench
CLEC3B	C-type lectin domain family 3 member B
CM	Cerebral malaria
COL1A1	Collagen type I alpha one chain
CSF	Cerebrospinal fluid
DCD	Dermcidin
DEFA1	Defensin, alpha 1
DEPs	Differentially expressed proteins
EC	Endogenous control
EDTA	Ethylenediaminetetraacetic acid
EV	Extracellular vesicles
F10	Coagulation factor X
F13A1	Coagulation factor XIII A
FA	Formic acid
FCS	Flow cytometry standard
FO	Fatal outcome
FR	Fully recovered
FSC	Forward scattergram
GITC	Guanidinium isothiocyanate
GPX	Glutathione peroxidase
HP	Haptoglobin
HPX	Hemopexin

ICAM-1	Intercellular adhesion molecule 1
IG	Immunoglobulin
iRBCs	Infected red blood cell
ITIH2	Inter-alpha-trypsin 2
KNG1	Kininogen 1
KRT	Keratin
LCAT	Lecithin cholesterol acyltransferase
LDHA	Lactate dehydrogenase A
LDLR	Low-density lipoprotein receptor
LYZ	Lysozyme
NCI	Neurocognitive impairment
NGS	Next-generation sequencing
nt	Nucleotide
ORM1/2	Orosomucoid 1/2
PBS	Phosphate-buffered saline
PCS	Photon correlation spectroscopy
<i>Pf</i>	<i>Plasmodium falciparum</i>
PF4	Platelet factor 4
PfHRP2	<i>Plasmodium falciparum</i> histidine-rich protein 2
PFP	Platelet-free plasma
PGLYRP2	Peptidoglycan recognition protein 2
PPIA	Peptidylprolyl isomerase A
PROS1	Protein S 1
PS	Phosphatidylserine
PSMA1/4	Proteasome subunit alpha type-1/4
PTX3	Pentraxin 3
RBP4	Retinol-binding protein 4
ROC	Receiver operating characteristic
RT-qPCR	Real-time quantitative polymerase chain reaction
S100A/9	Calcium-binding protein 8/9
SAA2	Serum amyloid A2
SD	Standard deviation
SERPINA	Serum protease inhibitor, clade A [alpha-1 antiproteinase, antitrypsin]
SLC1A5	Solute carrier family 1 member 5
SM	Severe malaria
SMA	Severe malarial anaemia
SSC	Side scattergram
TCEP	Tris(2-carboxyethyl)phosphine
TFA	Trifluoroacetic acid
TFRC/CD71	Transferrin receptor
TNC	Tenascin C
TTR	Transthyretin
UMIs	Unique molecular indices
VCAN	Versican
VSSC	Violet side scattergram
VWF	von Willebrand factor
WHO	World health organisation

## Abstract

The burden caused by malaria infections in endemic countries has been persistent as morbidity and mortality case numbers remain high. Factors such as the COVID-19 pandemic also impeded the efforts to control the infections. Despite successes with the malaria control program, nearly half a million children under the age of 5 do not survive malaria complications. Malaria is caused by an infection with a *Plasmodium* species parasite, the most prevalent and deadly protozoan parasite being *Plasmodium falciparum*. In some patients, malaria can rapidly develop into severe malaria, which can then rapidly advance into vital organ dysfunction and failure. Major complications of severe malaria include cerebral malaria and severe malaria anaemia, and both can lead to a fatal outcome. However, even after successful treatment, patients can develop neurocognitive impairments (NCI) such as attention, behavioural and memory problems that can last for many years after the malaria episode. Upon admission to hospitals, many children have already progressed to severe malaria; therefore, there is a great need for predictive biomarkers of disease severity and progression, specifically for children who will develop NCI and children who will not survive severe malaria. Fortunately, increased interest has been in investigating markers of severe malaria outcomes in the last few years. Among elements that could be considered as new biomarkers, extracellular vesicles (EVs) or their microRNA and protein content are showing great promise. EVs are lipid-bound vesicles released into the extracellular space by all cell types. They are involved in disease pathogenesis and mirror their cell of origin through their content.

This PhD project focuses on identifying prognostic biomarkers of disease outcome in plasma and cerebrospinal fluid (CSF) extracellular vesicles (EVs) from children with cerebral malaria and severe malarial anaemia. Chapter 2 presents a detailed overview of EVs, the importance of biomarkers, and the reasoning behind why EVs are relevant to malaria. Chapter 3 investigates the presence of a set panel of microRNA in the EVs extracted from the plasma of adult Thai patients infected by two malaria parasite species, *Plasmodium falciparum* and *Plasmodium vivax*, using RT-qPCR. The results showed that the relative expression of hsa-let-7a-5p was higher in plasma EVs from patients infected with either malaria parasite species, and compared to healthy adults, plasma EVs from patients infected with *Plasmodium vivax*

had higher relative expressions of hsa-miR-150-5p and hsa-miR-15b-5p. Chapter 3 elucidated differences in EV microRNA cargo of patients with uncomplicated malaria, inspiring the investigation of EV cargo in patients with severe malaria. In Chapters 4, 5 and 6, the molecular signature, numbers, and cellular origins of EVs from a cohort of children from Uganda, healthy or suffering from several clinical presentations of severe malaria, namely severe malarial anaemia and cerebral malaria, were explored. Clinical outcomes, i.e., full recovery, development of neurological impairment or death, were available for all patients, allowing us to link these parameters to the disease severity. In Chapter 4, we expanded the study of microRNA by performing next-generation sequencing on the plasma EVs of patients from Uganda. By comparing the EV transcriptomes in the plasma of children with severe malaria, five microRNA were selected with high prognostic value, especially when distinguishing the outcomes of cerebral malaria (hsa-miR-1-3p, hsa-miR-19a, hsa-miR-30, hsa-miR-4516, and hsa-miR-590-3p). Proteomic analysis was conducted on children from the same Ugandan cohort in Chapter 5. Comparing the proteomic profiles allowed the identification of 94 differentially expressed proteins that could discriminate between children with cerebral malaria and severe malarial anaemia, as well as children who would develop neurocognitive impairment or succumb to complications. To understand the cellular origins of EV within CSF and plasma from children with severe malaria (cerebral malaria and/or severe malarial anaemia), the populations were phenotypically characterised and compared in Chapter 6. Overall, there were significantly more EVs in the plasma than in the CSF, and children with CM who developed NCI had a significantly strong negative correlation between CSF and plasma EV amounts.

This PhD thesis highlights the significance of EVs and their cargo regarding malaria pathogenesis and their role as prognostic biomarkers of severe malaria and its outcomes. For future development, the potential biomarkers identified in this PhD could be combined into a panel to identify children at risk of developing NCI or mortality, allowing earlier intervention. This could minimise the impact of malaria on the child's livelihood, education, and well-being.

# **Chapter One:**

## **Introduction and Aims**



# Chapter 1: Introduction and Background to the Area of Research

## **1.1 Aetiology**

Malaria is a mosquito-borne haematologic disease caused by six protozoan Plasmodium species, *P. falciparum*, *P. vivax*, *P. knowlesi*, *P. malariae*, *P. ovale curtisi* and *P. ovale wallikeri*. *P. falciparum* is most prevalent, accounting for 99.7% of malaria cases, especially in the World Health Organisation (WHO) defined African region (49 countries), and is commonly associated with severe fatal forms of malaria, termed severe malaria, such as cerebral malaria and severe malarial anaemia<sup>1,2</sup>. *P. vivax* is less deadly compared to *P. falciparum* but has also been shown to cause severe pathology. It was previously thought that *P. vivax* did not cause cerebral malaria; however, in 2005, clinical data indicated both sequestration-related and non-sequestration-related complications of severe malaria for this species<sup>3</sup>.

## **1.2 Epidemiology**

Despite progress in malaria prevention and treatment, this now preventable, treatable and curable disease remains a significant and persistent health burden worldwide, affecting millions of people, particularly in tropical and subtropical climates<sup>4</sup>. According to the WHO, in 2022 alone, there were approximately 249 million malaria cases, 18 million more than in 2015, with 94% occurring in the WHO-defined African Region<sup>5</sup>. A slight decrease in deaths was estimated, dropping from 619,000 deaths in 2021 to 608,000 deaths in 2022, although still affecting 77% of children under 5 years old<sup>5</sup>. Immunocompromised individuals, young children under the age of 5, and pregnant women are most at risk of developing severe complications<sup>2</sup>. This may result from an immature or suppressed immune response, lack of clinical immunity developed over years of exposure, or hormonal changes<sup>6-9</sup>.

### **1.3 Burden of Malaria**

Malaria's societal impact extends beyond the measures of morbidity and mortality as it also hinders cognitive development and reduces scholastic and work attendance and productivity<sup>10-13</sup>. The disruption caused by malaria in impoverished countries has lasting effects, affecting population growth, saving and investment, education, and migration decisions<sup>14</sup>. At the same time, low income and wealth, a lack of education, poor housing and occupations in farming may increase the risk of malaria infection<sup>15-20</sup>. Malaria infections then trigger income loss, a reduction in economic growth and development, and add unnecessary strain on fragile health systems, causing major socioeconomic disruption, consequently perpetuating the cycle of poverty<sup>7,15,21,22</sup>.

### **1.4 Plasmodium life cycle**

#### **1.4.1 Asexual liver stage - asymptomatic**

The *Plasmodium* parasites have complex life cycles requiring human and mosquito hosts (Figure 1.1)<sup>23</sup>. Malaria infection of the human host begins with the bite of a *Plasmodium* parasite-infected female *Anopheles* mosquito, which injects a minute amount of sporozoites from the salivary glands during a blood meal<sup>24</sup>. Within 30 to 60 minutes, the bloodstream carries the sporozoites to the liver for invasion and replication<sup>25</sup>. The sporozoites infect hepatocytes and undergo asexual liver-stage replication for 5-7 days (*P. falciparum*), 2-3 weeks (*P. vivax*, *knowlesi*, or *ovale*) and 18 days or longer (*P. malariae*), with an estimated 10,000 to 90,000 uninucleate exoerythrocytic merozoites forming in the mature parasite<sup>26-30</sup>. For some strains of *P. vivax* and *P. ovale* species, portions of the intrahepatic parasites become dormant, forming hypnozoites and reactivating weeks to months later, causing relapses<sup>31-33</sup>. Once hepatocytes rupture, motile merozoites are released into the bloodstream and invade erythrocytes, starting the asexual erythrocytic cycle of the *Plasmodium* parasite life cycle<sup>31,34</sup>.

#### 1.4.2 Asexual erythrocytic cycle - symptomatic

Characteristically the malaria parasites go through repeated cycles of red blood cell (RBC) invasion, replication, egress, and reinvasion, resulting in periodic fever spikes<sup>28</sup>. The febrile waves correspond to the erythrocytic cycle length, 48 hours (*P. falciparum, vivax, or ovale*) and 72 hours (*P. malariae*), where the parasite progresses through the ring, trophozoite and schizont stages<sup>35</sup>. Within the RBCs, merozoites develop into thin biconcave discs called the ring stage. As haemoglobin and nutrients are taken up from the RBC and plasma, respectively, the ring becomes a rounder trophozoite stage. The *Plasmodium* parasite is most active during the trophozoite stage as substantial growth in size and RBC modification of surface antigens for cytoadhesion occurs. The parasite feeds on more haemoglobin becoming complex as particles of dark haemozoin crystals appear. The parasite then develops into a schizont by undergoing nuclear division to create ~16 to 64 nuclei, each becoming a merozoite as the RBC ruptures, invading new RBCs<sup>23,35</sup>. The blood-stage development continues to multiply 6 to 20 fold every 48 to 72 hours and the symptomatic stage begins once the parasite densities reach ~50/μL of blood, which may vary depending on the patient's immune status and clinical history<sup>31,36</sup>.

#### 1.4.3 Sexual stage

A small portion of the blood-stage parasites will become sexual stage parasites, female, or male gametocytes, through a process called gametocytogenesis<sup>37</sup>. Similar to the asexual stage, gametocytes develop in RBCs, though they are not linked to disease pathology<sup>38</sup>. Once mature gametocytes are ingested by a female *Anopheles* mosquito during a blood meal, the parasites differentiate into gametes, after fertilisation they become zygotes and then oocysts that rupture, releasing haploid sporozoites that migrate to the salivary gland for transmission to humans<sup>24,39</sup>.

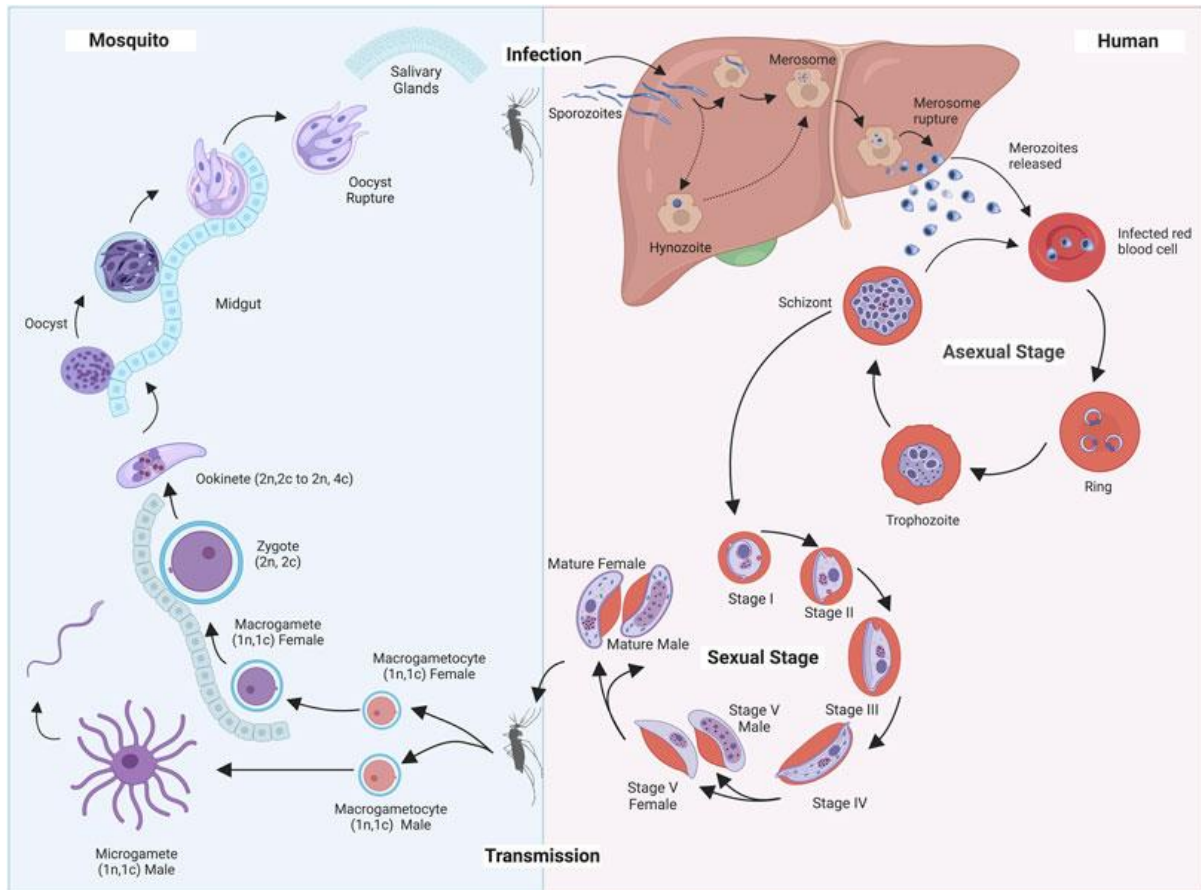


**Figure 1.1** Plasmodium parasite life cycle. Adapted from Chahine and Le Roch 2022<sup>23</sup>. Mosquito life cycle (left), human life cycle (right).

## **1.5 Clinical presentation and pathogenesis**

Many factors play a role in disease severity, such as prior exposure to malaria (clinical immunity), age, nutritional conditions, parasite and host genetics, geographical location, and socioeconomic environment<sup>40,41</sup>. Many people infected with malaria (asexual and gametocyte) are asymptomatic. Because these individuals are afebrile, they do not pursue treatment, but they can transmit malaria, impeding malaria elimination efforts<sup>38,42–45</sup>. Symptomatic malaria can be classified into two disease presentations, uncomplicated and severe. Most malaria patients develop uncomplicated infections, typically presenting with nonspecific signs and symptoms, including headaches, myalgia, diarrhoea, fever, and chills, which occur during the parasite rupture and reinvasion lifecycle<sup>46,47</sup>. Depending on the plasmodium species, fever typically cycles every 2-3 days<sup>47</sup>. Early detection and proper

treatment of malaria infections are critical, as the initial infection can quickly progress to life-threatening severe or complicated malaria that is single-organ, multi-organ, or systemically involved<sup>40,48,49</sup>. Approximately 4.5% of *P. falciparum*-infected patients with flu-like symptoms advance into severe malaria, where the disease progresses to loss of consciousness, seizures and severe anaemia, which could then worsen to neurological disturbances, coma, and death<sup>1,50,51</sup>.

Within hyperendemic regions, infants and children under 5 years of age are the individuals most affected by severe malaria. Most adults have developed clinical immunity, which makes the infection less symptomatic. However, within areas of low endemicity, severe malaria affects all ages<sup>52</sup>. Severe malaria mortality rates are well over 5%, representing a more than 50-fold increase in the risk of death<sup>49</sup>. Severe malaria is preventable with early administration of anti-malarial drugs; however, access and affordability prevent the widespread use of these in highly prevalent areas<sup>49,53</sup>. Therefore, malaria relapse rates are high, where symptoms re-occur for months after the initial infection<sup>53</sup>. In addition, there are many ways for the *Plasmodium* parasite to evade the immune system and drug treatments, such as surface antigen switching, hypnozoite dormancy, and ring-stage dormancy, which also impact the ability to control infection<sup>54,55</sup>. Recently evidence of extravascular reservoirs of blood-stage *Plasmodium* parasites in the bone marrow has been identified, showing a major reservoir for asexual parasites and a primary site of gametocyte development<sup>56–58</sup>. This shifts the fundamental understanding of malaria parasite biology and gives rise to a new field of research within malaria.

Fundamental features of *P. falciparum* that contribute to severe disease pathogenesis include exponential parasite growth, induction of host inflammatory responses, mature infected red blood cells (iRBCs) adhering to blood vessel walls obstructing the microvasculature and activating the endothelium<sup>59</sup>. Clinical symptoms of complicated malaria are mediated by secreted malarial toxins, which are known to stimulate macrophage secretion of pro-inflammatory cytokines such as tumour necrosis factor and interleukin-1<sup>60,61</sup>.

The initial malaria infection can quickly progress into severe malaria as parasites spread to the entire body via the bloodstream, of which high parasitaemia is reached due to exponential parasite growth, >10-fold every 48 hours<sup>48,62</sup>. Subsequently, malaria may affect the whole body causing complications such as cerebral malaria (CM), severe malarial anaemia (SMA),

metabolic complications such as hypoglycaemia and acidosis, acute respiratory distress syndrome, renal failure and pulmonary oedema<sup>63</sup>. These severe malaria complications can happen independently or in conjunction, rapidly progressing and becoming fatal within hours or days<sup>64</sup>. Subsequently, approximately 25% of patients successfully treated for malaria develop neurocognitive impairment (NCI) causing deficits such as declined cognitive ability, memory, behaviour, and fine motor skills<sup>65–68</sup>.

The effects of malaria can be long-term, as a child's poor cognitive outcome can start before birth, as during pregnancy malaria worsens maternal anaemia, which impedes nutrition to the foetus, limiting cognitive development later in life<sup>69</sup>. Early childhood severe malaria can also contribute to long-lasting neurocognitive impairment for as long as 9 years after disease onset<sup>13,70–74</sup>. Cognitive deficits are also observed up to 6 years after illness when prolonged and repeated malaria attacks in the absence of severe complications are experienced<sup>75–77</sup>.

This section is reviewed in more detail in Chapter 2, which focuses on pathogenesis, and the introductions of Chapters 4 and 5, which focus on CM, SMA, and neurocognitive impairment.

## **1.6 Control, prevention, and diagnosis of malaria**

Great success and progress have been made in controlling malaria over the last 20 years with significant reductions in overall cases (41%) and deaths (62%) between 2000 and 2015<sup>78</sup>. There was also a decline in the total percentage of malaria deaths among children under 5 years of age, from 87.3% to 76.8%; however, the rate of decline stalled in 2015 and malaria cases and deaths are on the rise<sup>2,5</sup>. As of today, a child under five dies of malaria nearly every minute. Malaria cases will expectedly continue to rise due to a plateau in funding, an increase in drug and insecticide resistance and climate change allowing malaria transmissions into new areas.

Between 2010 and 2021, approximately US\$39 billion was spent on malaria control, funding the distribution of 2.5 billion insecticide-treated bed nets, 3.5 billion rapid diagnostic tests, and 3.8 billion artemisinin combination treatments<sup>2</sup>. The COVID-19 pandemic, starting early 2020 contributed to the stall in progress and increasing malaria prevalence by disrupting essential malaria control and prevention services. The funding gap between investment

amounts and resources required for malaria control is also continuing to widen, increasing to UD\$3.8 billion in 2021<sup>2</sup>. There is a great need for investment in malaria for basic research and product development as well as to combat emerging threats like urban malaria and drug and insecticide resistance.

Malaria elimination progress is uneven as cases have become rare in Europe, Sri Lanka central Asia, and several Latin countries. Still, malaria elimination in high-transmission countries in Sub-Saharan Africa has proven to be more difficult<sup>46</sup>. In addition, most regions with civil disruption show a significant increase in malaria. Proper use of anti-malarial and insecticides can greatly protect against and decrease malaria cases, although resistance is an ongoing battle due to uninformed and improper usage. Therefore, new advanced insecticidal and anti-malarial treatments are being formulated, and research into transgenic mosquitoes is being conducted to disrupt transmission<sup>79</sup>.

Accurate diagnostic methods are necessary to differentiate malaria from other febrile diseases, monitor asymptomatic infections to reduce transmission, discriminate between *P. falciparum* and *P. vivax* to reduce G6PD-related haemolytic anaemia, and identification of cases in low malaria transmission areas<sup>5</sup>. The gold standard for malaria diagnosis has been microscopy, allowing for an inexpensive detailed examination of morphological differences and species identification. Microscopy can also allow the detection of other infections that may be mistaken for malaria. The downside is that this type of diagnosis is labour-intensive and requires skilled microscopists and electricity. Rapid diagnostic tests (RDTs) to detect parasite-specific blood antigens are a simpler way to detect malaria infection and can be completed in 5-20 minutes. In addition, RDTs require minimal training and can be used in the field. Polymerase Chain Reaction (PCR) approaches are also becoming more popular due to the sensitivity of the tool. With more accurate and simple techniques being developed, such as RT-PCR, there are growing choices for healthcare facilities with the correct equipment and expertise, although it can be relatively expensive.

Due to the complexity of the malaria life cycle, vaccines and treatment can sometimes be too stage-specific and allow the parasite to evade elimination. Malaria subunit vaccines establish immunity against proteins expressed at certain stages of the lifecycle. The sporozoite stage is targeted using a surface protein that helps navigate the parasite to the liver, reducing the incidence of infection. The most studied vaccine is the RTS,S/AS01, based on *P. falciparum*

circumsporozoite protein which has been shown to provide protection for 3-4 years in older children and was the first vaccine recommended by the WHO in 2021<sup>2,80</sup>. As of 2023, the WHO has recommended a second vaccine, R21/Matrix-M, to prevent malaria in children<sup>5</sup>. During 12 months after a 3-dose series, the R21/Matrix-M vaccine has shown to reduce symptomatic malaria cases by 75%, this efficacy can be maintained with a fourth dose a year after the third<sup>5,81</sup>. This new vaccine is promising as it has been safe in clinical trials, is expected to have a high impact in low and high transmission regions, and is cost-effective, ~US\$3 per dose<sup>5</sup>.

## **1.7 Biomarkers of Malaria**

The scarcity of reliable markers identifying patients at risk of death or NCI means treatment is delayed making it less effective. Identification of a prognostic biomarker that can predict the progression, regression or outcome of disease could greatly improve patient quality of life post-treatment. Most potential biomarkers identified for severe malaria are proteins, such as erythropoietin, *Plasmodium falciparum* histidine-rich protein 2 (PfHRP2), angiopoietin (ANG), inter-cellular adhesion molecule 1 (ICAM-1) and von Willebrand factor (VWF)<sup>82-90</sup>. Unfortunately, these proteins lacked specificity for malaria and results varied across studies.

Another source of biomarkers is microRNA (miRNA), a class of non-coding RNAs (17-25 nucleotides); with miRNAs gaining more interest over the years, more studies have focused on identifying severe malaria biomarkers. Most of the studies so far have focused on biomarkers for severe malaria, with only a couple investigating predictive biomarkers for severe malaria outcomes, such as neurocognitive impairment and mortality. One such study identified hsa-miR-3158-3p and hsa-miR-150-5p as potential plasma biomarker candidates for severe malaria in Indian teenagers and adults, ranging from 13 to 41 years old<sup>91</sup>. Both miRNAs were able to differentiate those with fatal CM from other CM and non-CM outcomes, as well as uncomplicated malaria and healthy controls<sup>91</sup>. This study also described a decrease of hsa-miR-3158-3p in plasma at day 30 compared to day 0 in CM patients<sup>91</sup>. Although adults can also develop severe malaria, the majority (77%) of deaths occur in children under 5 years old, yet very few studies have focused on prognostic biomarkers for the different outcomes of severe malaria.



Chapter 2 and the introductions of Chapters 4 and 5 review this section in more detail, focusing on potential protein and miRNA biomarkers of severe malaria.

## **1.8 Extracellular vesicles**

Extracellular vesicles (EVs) are bilayer lipid membranes that contain cytosolic proteins, lipids and nucleic acids, which contribute to intercellular communication and are involved in disease pathogenesis<sup>92</sup>. In the last three decades, EVs have been investigated in many different fields and described to have many functions. EVs are key pathophysiological players and have a variety of roles, such as drug/biomarker delivery vehicles, therapeutic resources, tools, and targets, immune system regulators, diagnostic liquid biopsies, vaccine platforms, and biomarkers<sup>92-102</sup>. There are three subtypes of EVs: exosomes, derived from multivesicular bodies (50 nm – 100 nm); microvesicles, shed by plasma membrane (100 nm – 1000 nm); and apoptotic bodies, during programmed cell death (apoptosis) (1000 nm – 5000 nm)<sup>103,104</sup>. This PhD project will focus on the characterisation of both exosomes and microvesicles, which will collectively be termed EVs.

A major discovery in the field of EV research was their function as mediators of cell-to-cell communication, showing that EVs delivered functional molecules to cells that altered their pathological and physiological functions<sup>105</sup>. In recent years, EV proteins and genetic cargo have been linked to roles in cellular signalling and intercellular communication<sup>92</sup>. EVs have also been described in terms of disease processes, pathogenic mechanisms, angiogenesis, programmed cell death, and inflammation<sup>106</sup>. EVs have also shown a strong relation with disease severity and progression, leading to EVs becoming drug targets. However, in neurodegenerative disease, EVs have been shown to transfer material from damaged tissue or transport neurotrophic/neuroprotective molecules to different regions of the body, continuing their effect<sup>107</sup>. Therefore, inhibiting EV production may worsen disease progression as it also plays a role in homeostasis<sup>107</sup>. EVs have become a new concept in the field of biomarkers, as they transfer molecules between cells and represent a promising source in many diseases, including malaria<sup>100,108-110</sup>.

Chapters 2, 4, and 5 review this section in more detail, discussing EVs' role in malaria pathogenesis, EVs as biomarkers, and EV cargo as biomarkers of severe malaria.

## **1.9 Patient and collaborator acknowledgements**

We greatly appreciate the adults who participated in the Thailand study and the children and their parents or guardians who participated in the Uganda studies (Chapters 3-6). The commitment to treatment and data collection by the teams at Buntharik Hospital, Mahidol University, Mulago Hospital, Makerere University, and the University of Minnesota are commendable. Great appreciation to A/Prof. Duangdao Palasuwan and Prof. Mallika Imwong for the adult samples from Thailand (Chapter 3) and Distinguished Prof. Chandy John, Prof. Robert Opoka, and Dr Paul Bangirana for the paediatric samples and clinical, biological, and neurological data required for Chapters 4, 5, and 6.

## **1.10 Thesis Aims**

The study of EVs in malaria is still in its infancy, with gaps in knowledge regarding their involvement in disease pathogenesis, prognosis, and outcome yet to be filled. Several studies, including those from our group, have previously identified links between EV production and malaria complications. However, this was only investigated in EVs originating from single cell types such as endothelial cells, red blood cells, and platelets. Thus, it is now essential to characterise the EV profiles from all vascular cells. This has proven challenging as we are working with paediatric samples; the limited volume makes the purification of EVs challenging; therefore, few studies characterise the population of circulating EVs. There is also a lack of practical prognostic markers for severe malaria that can be used to allow earlier treatment of patients with new adjunct therapies. This PhD project hypothesises that EVs derived from plasma and CSF from children with severe malaria can act as and contain biomarkers to predict disease outcomes. The overarching aims of the studies in this thesis are to use the molecular signature of EVs to identify predictive biomarkers for severe malaria outcomes and increase our understanding of malaria pathogenesis.

To achieve this, the following aims have been constructed:

- **Aim 1.** Characterise and compare the microRNA composition of plasma EVs from children with different clinical presentations and outcomes of severe malaria
- **Aim 2.** Characterise and compare the protein composition of plasma EVs from children with different clinical presentations and outcomes of severe malaria
- **Aim 3.** Characterise and compare the cellular origins of EVs in cerebrospinal fluid and plasma from children with cerebral malaria or combined cerebral malaria and severe malarial anaemia

**Chapter Two:**  
**Review of extracellular vesicles’  
role in pathogenesis and as  
biomarkers in cerebral malaria**

## Chapter 2: Review of extracellular vesicles' role in pathogenesis and as biomarkers in cerebral malaria

### Chapter overview

Extracellular vesicles (EVs) play key roles in malaria pathogenesis, especially in complicated malaria such as cerebral malaria. Increased amounts of EVs release by vascular cells have been described in patients with malaria. EVs have also been recognised as carriers of unique molecular markers for different outcomes of the infection. This chapter also discusses EVs capacity as biomarkers of disease severity and the current lack of effective biomarkers.

### Authors' contributions

Author	Concept	Writing-2.1, 2.6	Writing-2.2	Writing-2.3, 2.4	Writing-2.5	Figures	Writing-review & editing	Signature
Iris S. Cheng	X	X	X		X		X	Production Note: Signature removed prior to publication.
Benjamin C. Sealy	X		X	X		X	X	Production Note: Signature removed prior to publication.
Natalia Tiberti					X		X	Production Note: Signature removed prior to publication.
Valery Combes	X						X	Production Note: Signature removed prior to publication.

**Publication status:** Published

Cheng IS, Sealy BC, Tiberti N, Combes V. Extracellular vesicles, from pathogenesis to biomarkers: the case for cerebral malaria. *Vessel Plus* 2020;4:17.

**Link to publication:**

<http://dx.doi.org/10.20517/2574-1209.2020.08>

## Extracellular vesicles, from pathogenesis to biomarkers: the case for cerebral malaria

Iris S. Cheng<sup>1,#</sup>, Benjamin C. Sealy<sup>1,#</sup>, Natalia Tiberti<sup>2</sup>, Valery Combes<sup>1</sup>

<sup>1</sup>Faculty of Science, School of Life Sciences, University of Technology Sydney, Sydney 2007, Australia.

<sup>2</sup>Department of Infectious - Tropical Diseases and Microbiology, IRCCS Sacro - Cuore Don Calabria Hospital, Verona Area 37024, Italy.

#Co-equal first authors.

**Correspondence to:** Associate Prof. Valery Combes, Faculty of Science, School of Life Sciences, University of Technology Sydney, Australia. E-mail: [valery.combes@uts.edu.au](mailto:valery.combes@uts.edu.au)

**Received:** 5 Feb 2020 **First Decision:** 5 Mar 2020 **Revised:** 1 Apr 2020 **Accepted:** 7 Apr 2020

**Published:** 16 Jun 2020

**Science Editor:** Narasimham L. Parinandi **Copy Editor:** Jing-Wen Zhang **Production Editor:** Jing Yu

### Abstract

Malaria infections due to the Plasmodium parasite remains a major global health problem. Plasmodium falciparum is responsible for majority of the severe cases, resulting in more than 400,000 deaths per annum. Extracellular vesicles (EVs) released by vascular cells, including parasitised erythrocytes, have been detected with increased levels in patients with malaria. EVs are thought to be involved in the pathogenesis of severe malaria, particularly cerebral malaria, and represent a unique molecular signature for different forms of the infection. In this review, we will cover the known effects of EVs on the vasculature and discuss their potential use as a biomarker of disease severity.

**Keywords:** Cerebral malaria, extracellular vesicles, biomarker, pathogenesis, microvesicles, exosomes

## **2.1 Introduction to Malaria**

Malaria can be a life-threatening disease and remains a global health problem with an estimated incidence of 228 million cases and 405,000 deaths in 2018<sup>[1]</sup>. While its incidence has decreased significantly in the last 15 years, progress has stalled and case numbers are starting to increase again in some countries with drug resistance a major threat<sup>[1]</sup>. *Plasmodium falciparum* (*P. falciparum*) is one of six *Plasmodium* species, all of which can cause disease in humans, and is associated with the development of severe disease. Clinically, malaria can be either uncomplicated or severe. Uncomplicated malaria presents as a non-specific, flu-like syndrome and diagnosis is based only on clinical features, which is often unreliable. Approximately 1% of diagnosed cases will progress to severe malaria for reasons that are not fully understood<sup>[2]</sup> and amongst these, up to 30% will be at risk of developing life-threatening or debilitating complications<sup>[3]</sup>. Severe malaria is defined by precise diagnostic criteria related to specific signs and symptoms, with cerebral malaria (CM) and severe malarial anaemia (SMA) being two of the most serious life-threatening complications associated with *P. falciparum* infection. Both target children under the age of five and although not yet fully understood, the pathogenesis of CM and SMA is likely to be different. The clinical hallmark of CM is a diffuse, symmetrical encephalopathy with coma and a general absence of focal neurological signs. CM is characterised by the sequestration (binding) of infected red blood cells (iRBCs) in the vasculature of most organs, including the brain, coupled with an uncontrolled inflammatory response<sup>[4]</sup>. This sequestration of iRBCs during CM is associated with endothelial dysfunction leading to coma, respiratory distress syndrome and placental malaria when it occurs in the brain, lungs or during pregnancy, respectively. SMA is defined by a haemoglobin (Hb) concentration < 5g/dL and a packed cell volume (PCV) < 15% in children, and by Hb < 7g/dL and PCV < 20% in adults<sup>[5]</sup>. SMA is also associated with increased clearance of both iRBCs and non-infected red blood cells (nRBCs), as well as altered haematopoiesis<sup>[6-8]</sup>. In both CM and SMA cases however, iRBCs remain within the vasculature, adhere to and activate endothelial cells that are then likely to release pathogenic factors into the surrounding tissues such as the brain parenchyma. This review will focus mainly on CM and its association with extracellular vesicles.

## **2.2 Pathogenesis of CM: from host cells to extracellular vesicles**

As mentioned above, CM is characterised by sequestration of iRBCs within the cerebral vasculature although the neurological lesion extends beyond blood vessel alteration to damage to the brain parenchyma, with clear involvement of the blood-brain barrier (BBB). There is a fine and complex interplay between the cells on each side of the BBB, with vascular cells, (i.e., endothelial cells, platelets, T cell lymphocytes, macrophages and to lesser extent neutrophils), microglial cells, neurones, and astrocytes, all having either target or effector roles (and sometimes both) at some point in disease development<sup>[9]</sup>. In addition, extracellular vesicles (EVs) are potentially released by all these cells adding another level of complexity to this intercellular crosstalk. A combination of *ex vivo* studies using patient samples (biological fluids or *post-mortem* tissues), *in vitro* assays mimicking the intravascular lesion, and *in vivo* experiments using mostly murine models allows for a better understanding of the cellular interactions and pathogenesis of the disease.

How much of CM is attributable to the sequestration of iRBCs is still unknown. *Post-mortem* studies have shown various levels of iRBC accumulation within the microvasculature of the brain in patients with diagnosed CM, but this was similarly observed in patients who died of non-CM causes<sup>[10,11]</sup>. Of note, this observation is correlated with the severity of the disease in both children and adults<sup>[10,12]</sup>. *Post-mortem* histopathology in Malawian children with clinically defined CM (coma and *P. falciparum* parasitaemia) identified different disease patterns: (1) iRBCs sequestration only; (2) iRBCs sequestration with associated peri-vascular changes such as haemorrhages or micro-thrombi; and (3) little to no sequestration<sup>[11]</sup>. In the latter, the real cause of death was only identified after autopsy, adding to the complexity of CM and the difficulty in establishing a precise diagnosis. In this study<sup>[11]</sup>, only fundus examination allowed discrimination between malarial and non-malaria coma. In Vietnamese adults, iRBC sequestration was more frequent in patients with CM than in those without, and was correlated with coma and time of death<sup>[12]</sup>. Consequently, vascular congestion was proposed as a cause for coma since sequestration leads to decreased cerebral blood flow, impaired brain function and cerebral hypoxia.



Sequestration occurs via the binding of parasite-related ligands, expressed on the surface of iRBCs, to receptors on the surface of vascular endothelial cells. *P. falciparum* erythrocyte membrane protein 1 (PfEMP1) is one such molecule expressed on the surface of iRBCs that then binds to a series of endothelial receptors such as CD36, intercellular cell adhesion molecule-1 (ICAM-1), vascular cell adhesion molecule-1, P-selectin, E-selectin, endothelial protein C receptor or thrombospondin. The expression of these receptors is further modulated by pro-inflammatory cytokines such as tumour necrosis factor (TNF) or interferon-gamma (IFN- $\gamma$ ), thereby supporting inflammation as a critical player in the regulation of sequestration<sup>[13,14]</sup>.

Together with iRBCs and nRBCs, platelets also play an important role in CM<sup>[15]</sup>. Thrombocytopenia is a hallmark of CM but whether platelet counts can be predictive of lethality in CM is still controversial<sup>[16,17]</sup>. Platelets were found in high numbers in vascular lesions of the brain of Malawian children who succumbed to CM<sup>[18]</sup> and are thought to have contributed to the severity of the disease through clumping<sup>[19]</sup>, activation of endothelial cells<sup>[20]</sup> or increased sequestration via the transfer of CD36 to brain endothelial cells that are otherwise devoid of it<sup>[21]</sup>. On the other hand, platelets also are thought to have a protective role during CM by killing intra-erythrocytic parasites<sup>[22,23]</sup>. Therefore, platelets could have different roles at different stages of the disease, i.e., a protective role during the early phase of disease and a pathogenic role when severe<sup>[24]</sup>.

The BBB is at the centre of the neurovascular lesion occurring in CM although iRBCs do not actively cross this barrier as seen in other pathogens with brain tropism<sup>[25,9]</sup>. *Post-mortem* histopathological brain studies have demonstrated impairment of the BBB which suggests that the localised sequestration of iRBCs increases the pressure within microvessels to act on cellular tight junctions, thereby altering the permeability of the BBB which results in micro-haemorrhages when these junctions rupture. Neurological sequelae observed in children who have recovered from CM are also suggestive of neuronal damage<sup>[26]</sup>. Neuronal dysfunction is likely an indirect consequence of the sequestration of iRBCs, activation of the endothelium, alteration of junctional permeability and passage of cytokines, chemokines and other inflammatory mediators into the perivascular space<sup>[27,28]</sup>. However, in most cases, it is likely that these alterations are localised, as symptoms are quickly reversed once parasites have

been eliminated. More recently, Magnetic Resonance Imaging has been successfully used as a non-invasive way to predict fatal outcomes in paediatric CM, notably in Malawi<sup>[29,30]</sup>.

As mentioned earlier, crosstalk between vascular cells, including immune and brain parenchyma cells, via direct contact, soluble mediators and molecules leaking through the BBB, can all contribute to the neurological syndrome. In addition, subjecting all these cells to various stimuli can lead to the release of EVs that in turn, target other cells distant from their site of production. Long considered as inert cellular debris, EVs are now accepted as biological effectors in many infectious and inflammatory diseases including malaria<sup>[31,32]</sup>.

EVs represent an ensemble of membrane-bound structures grouped into three main categories: exosomes, microvesicles, and apoptotic bodies. This nomenclature can vary and the term EVs usually encompasses subpopulations of vesicles ranging in size from 30 nm to 4 µm, i.e., exosomes produced by membrane invagination of multivesicular bodies, microvesicles (MVs) released after budding of the plasma membrane, or apoptotic bodies that result from blebbing of the plasma membrane of apoptotic cells<sup>[33]</sup>. It is now clear that the role of EVs goes far beyond simple structural function to active mediators of important biological processes for parasitic infections such as immunomodulation, parasite virulence, target cell invasion and parasite-parasite communication<sup>[34,35]</sup>.

In malaria infection, two categories of EVs (i.e., exosomes and microvesicles) have been studied the most. While known in other illnesses for several decades, MVs in malaria patients were first described by our group in 2004 in Malawian children with CM<sup>[36]</sup>, where an elevation in the number of MVs of endothelial origin was described. MVs released by RBCs were later found to be increased in both *P. falciparum* and *P. vivax* malaria<sup>[37,38]</sup>. EVs have been shown to be involved throughout the entire life-cycle of malaria infection and at different stages, the parasite can affect various immune and vascular cell types in different ways, ultimately altering the endothelium and BBB function<sup>[32]</sup>.

A pan-vascular, cell-derived MV release was also observed in children with CM in Cameroon. Of these MVs, an increase in platelet MVs was most significantly correlated with disease severity<sup>[39]</sup>. Exosomes were first explored in 2011 in a murine model of malaria<sup>[40]</sup> and will be

discussed in a later section. While mostly descriptive, these clinical studies were essential for suggesting a role for these EVs as either markers of CM severity, or as players in the pathogenesis of CM infection, and paved the way for subsequent work on the composition and functional potential of EVs during malaria infection.

### **2.3 *In vitro* models of malaria - interactions between host cells and extracellular vesicles**

Most *in vitro* models of CM simulate the interactions between microvascular endothelial cells and circulating vascular cells (e.g., iRBCs, nRBCs, platelets, and leucocytes) in either static or shear stress environments<sup>[41,21]</sup>. The brain endothelial cells used can be of human, simian or murine origin (primary or immortalised), and co-cultured with one or more other cell types in two-dimensional systems<sup>[42-45]</sup>. The recent introduction of more complex three-dimensional models will help to examine and understand the pathogenesis of this disease better<sup>[46-48]</sup>.

Very much like their cells of origin, EVs interact with their target cells and modulate their responses. *In vitro*, platelet MVs behave in a similar fashion as platelets by increasing the adherence of iRBCs to human brain endothelial cells (HBECs) by providing iRBCs with surface receptors such as CD31 and CD36<sup>[49]</sup> such that platelet MVs act as a bridge between HBECs and iRBCs. The internalisation of platelet MVs by vascular endothelial cells is also associated with an alteration of their phenotype such that ultimately, their inflammatory effects and subsequent activation can be potentiated<sup>[50]</sup>.

RBCs release increased levels of EVs when infected with a *Plasmodium* parasite and late-stage infections are associated with even greater release of EVs<sup>[38]</sup>. This is mainly due to membrane changes occurring within iRBCs during parasite maturation. The composition of EVs derived from iRBCs is also dependent on the parasite's stage of development. Indeed, specific parasite proteins, considered as virulence factors, were present in EVs only at specific developmental stages and PfEMP1 was only detected in EVs from iRBCs with parasites at early stages.

Potentially, such developments would allow EVs to bind and prime endothelial cells for later adherence and sequestration of late-stage iRBCs<sup>[51]</sup>.

EVs from iRBCs have also been shown to contain a functional microRNA-argonaute 2 complex that can modulate gene expression and alter barrier function<sup>[52,53]</sup> when transferred to endothelial cells after vesicle uptake. Such EVs do not only affect endothelial cells but are also able to induce pro-inflammatory responses, particularly the activation of macrophages, monocytes as well as other immune cells through the upregulation of cytokines<sup>[54,55]</sup>. Interestingly, when these EVs were compared to their mother cells, they were able to activate inflammation and immune activation to a greater degree<sup>[54,55]</sup>. EVs from iRBCs also contain small RNAs and genomic DNA. After internalisation by monocytes, they can induce the innate immune cytosolic adaptor-dependent DNA sensing pathway (STING), leading to downstream alterations of DNA sensing pathways in target cells<sup>[56]</sup>. Activation of these pathways has been shown to correlate with parasite survival<sup>[57]</sup>. Thus, this could possibly be used as a decoy method for immune escape by the parasites<sup>[57]</sup>. Similarly, the release of PfEMP1-containing EVs as previously mentioned, has also been suggested as a decoy strategy as it is capable of inducing both the production of inflammatory cytokines (IL-12, CCL2, and CCL4) by monocytes after internalisation and transcriptomic changes<sup>[51]</sup>. Furthermore, as the majority of the body's natural immune response to *P. falciparum* targets PfEMP1, the secretion of PfEMP1-containing EVs could possibly work as a smokescreen by attracting neutralising antibodies that protect the parasite from the immune system<sup>[13,51]</sup>. EVs can also mediate immunosuppression in mice infected with malaria with EVs from *P. berghei*-iRBCs able to inhibit CD4+ T cell proliferation in response to antigen presentation. This process seems to be mediated by two potential virulence factors, histamine-releasing factor and elongation factor 1 $\alpha$  (EF-1 $\alpha$ ). Importantly, this work also showed that mice immunisation with EVs from *P. berghei*-iRBCs or recombinant *P. berghei*-EF-1 $\alpha$  resulted in resistance to infection, further suggesting the role of EVs in immune-modulation and potential for vaccine development<sup>[58]</sup>.

Exosome-like vesicles derived from iRBCs have been reported to facilitate communication between iRBCs and therefore, promoting gametocytogenesis between parasites *in vitro* via the transfer of a *P. falciparum* protein<sup>[59]</sup>. This communication is also used to improve parasite survival within the host as well as transmission to mosquitoes.

Although not specifically studied in an *in vitro* model of CM, endothelial MVs interacting with T lymphocytes have been found to assist cell proliferation by inducing cell activation and antigen presentation by immune cells<sup>[60]</sup>. In addition, when MVs from lipopolysaccharide-stimulated monocytes are internalised by HBECs, they release high levels of MVs (usually a sign of cell activation) and at the same time, display an increase in trans-endothelial resistance (i.e., tightening of endothelial junctions) which could have a protective effect on the BBB if occurring *in vivo*. This suggests that MVs from monocytes, as was shown for MVs from neutrophils, could trigger contrasting protective and pathogenic responses<sup>[61-63]</sup>.

*In vitro* models of malaria are limited in their ability to mirror the pathogenesis of CM and more complex systems are needed to understand the fine interplay between host cells and EVs during malaria infection.

## **2.4 *In vivo* models of malaria: what do extracellular vesicles bring to pathogenesis?**

Although there is still debate regarding the usefulness of murine models for studying the pathogenesis of CM, human studies are limited and often, *post-mortem* analyses are the only way to explore some parameters. However, the number of studies that find parallels between human and experimental CM (ECM) continues to grow. Most recently a study<sup>[64]</sup> observed that in *post-mortem* cases of paediatric CM, CD8+ T cells were found within both the vascular lumen as well as the juxtavascular space as was previously shown in murine CM studies<sup>[65,66]</sup>. Therefore, animal models can still provide relevant basic scientific knowledge and allow testing of important hypotheses related to the pathogenesis of the disease<sup>[67-71]</sup>. For instance, whole-animal imaging using transgenic fluorescent parasites has demonstrated that sequestration, and not only accumulation, of iRBCs, does occur in all organs similar to humans<sup>[72-74]</sup>. In addition, recent quantitative mapping of mice brains during ECM showed similar numbers compared to human CM despite the distinct aetiology<sup>[75]</sup>. However, as for any model, it is not perfect and should be used with caution and one should be aware of its limitations before drawing direct conclusions with human disease.

Two different *Plasmodium* species are commonly used in CM models, *P. yoelii*<sup>[40]</sup> and *P. berghei*<sup>[76]</sup>, notably *P. berghei* ANKA (PbA). During the acute phase of infection, mouse strains that are susceptible to CM (e.g., CBA/J, C57BL/6, DBA1) display increased levels of plasma MVs similar to that observed in humans<sup>[76-78]</sup>. We examined the ATP-binding cassette transporter A1, which modulates the distribution of phosphatidylserine to the outer leaflet of the cell plasma membrane at the time of MV production<sup>[76]</sup>. We found that mice lacking this ATP-binding cassette had resistance to the malaria-associated neurological syndrome in C57BL/6 mice<sup>[76]</sup>. These animals displayed basal levels of plasma MVs but numbers failed to increase following infection (as observed in wild type counterparts), had lower levels of plasma TNF, reduced expression of endothelial cell adhesion molecules and had increased survival of leukocytes and platelets. Another study examining the blocking of phosphatidylserine using low-molecular-weight thiol pantethine found a similar reduction in MV production, which correlated with reduction in inflammation and resistance to the disease<sup>[78]</sup>. When passively transferred into the circulation of mice, plasma MVs from infected animals localised to the inflamed vessels of infected animals, notably in the brain, which suggests that they could potentiate the neurovascular lesions by interacting with other vascular cells. In addition, healthy mice injected with TNF-generated endothelial MVs developed CM-like pathology with cerebral and pulmonary oedema and haemorrhage, the two main histopathological features of human and murine CM<sup>[77,79,80]</sup>.

Interaction with and internalisation of MVs derived from iRBCs by astrocytes and microglial cells leads to increased production of IFN- $\gamma$ -inducible protein 10 (IP-10), which coincided with increased levels of inflammatory cytokines within both plasma and brain tissue of PbA-infected mice<sup>[81]</sup>. Plasma MVs from PbA-infected mice were also able to activate immune cells, in particular macrophages, leading to the up-regulation of CD40 as well as TNF production<sup>[54]</sup>. Knock-out mice that lack pro-inflammatory cytokines (TNF-/-, IFN- $\gamma$ -/-, IL-12-/- and RAG-1-/-) displayed levels of plasma MVs similar to those of their wild-type counterparts<sup>[54]</sup>, suggesting that their production is not solely dependent on the presence of inflammation.

When exosomes, purified from the blood of *P. yoelii* (nonlethal strain, 17XNL)-infected mice, were injected into mice infected with *P. yoelii* (lethal strain, 17XL), these mice were protected against the lethal syndrome, showing that exosomes could also modulate the immune response<sup>[82,40]</sup>. We propose a model in Figure 2.1 that summaries the role EVs play in the pathogenesis of CM.

Figure 2.1 was designed by modifying free images provided by Smart Servier Medical Art (<https://smart.servier.com/>) and available under the creative commons license.

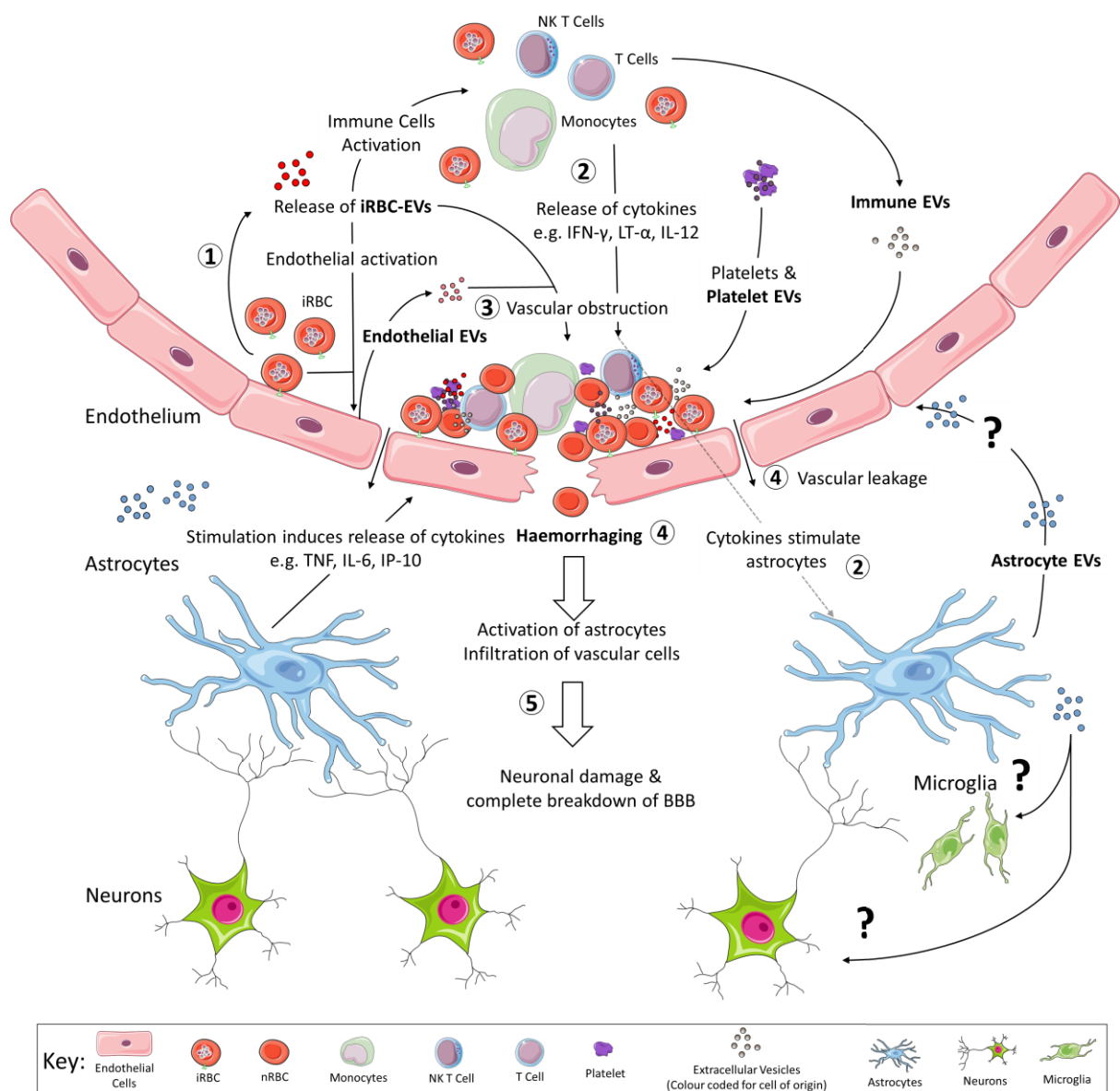


**Figure 2.1** Outline of the role that EVs play in the pathogenesis of cerebral malaria. (1) As iRBCs adhere to vascular ECs, they are also releasing EVs into the blood. These EVs from iRBCs stimulate all vascular cells including immune cells, ECs and

platelets to release EVs of their own<sup>[83]</sup> as reviewed by Babatunde et al.<sup>[84]</sup>. Both ECs and platelet EVs have been shown to assist with the formation of neurovascular lesions by providing mechanisms of binding for iRBCs and other vascular cells as reviewed by El-Assaad et al.<sup>[77]</sup>, 2014 and Faille et al.<sup>[49]</sup>. (2) EVs from iRBCs have been suggested to act not only as a decoy, by providing alternative targets expressing PfEMP-1 for immune cells to attack<sup>[51]</sup>, but also promote secretion of increased levels of pro-inflammatory cytokines, notably IFN- $\gamma$ , LT- $\alpha$  and IL-12 once internalised by immune cells<sup>[54,55]</sup>. These cytokines have also been shown to stimulate astrocytes, which then respond by secreting additional cytokines and chemokines of their own<sup>[13]</sup>. The effect of astrocyte EVs have not been studied in humans but these EVs could have effects on both endothelial cells and cells of the brain parenchyma. (3) The release of these pro-inflammatory cytokines and chemokines further activates the already stimulated ECs, leading to greater adherence of vascular cells and ultimately, formation of the neurovascular lesion. (4) Once the neurovascular lesion has formed, increased intravascular pressure on the endothelium leads to vascular leakage and ultimately results in haemorrhage. (5) The infiltration of vascular cells and cytokines or chemokines causes neuronal damage and subsequently, a localised breakdown of the blood brain barrier<sup>[32]</sup>. EVs: extracellular vesicles; ECs: endothelial cells; iRBCs: infected red blood cells; nRBC: non-infected red blood cell; BBB: blood-brain barrier; TNF: tumour necrosis factor; IFN- $\gamma$ : interferon-gamma; NK: natural killer; LT-a: lymphotoxin alpha; IL: Interleukin; IP-10: IFN- $\gamma$ -inducible protein 10

## **2.5 Extracellular vesicle cargo: effector, biomarker or both?**

Biomarkers have long been used as diagnostic and prognostic tools to determine the presence of disease as well as the regression, progression or outcome after treatment<sup>[85]</sup>. The field of malaria, especially severe malaria, currently lacks reliable markers for the prediction of morbidities such as neurocognitive impairment and/or mortality that can be widely applicable regardless of country or endemicity. Such biomarkers would allow for the prediction of severe complications and allow early implementation of adjunctive therapies. Current adjunctive therapies used to aid anti-malarial drugs have so far been ineffective<sup>[86]</sup>, possibly due to late implementation due to the lack of predictive biomarkers. Therefore, early identification of patients at risk of severe malaria complications (lethal or not) would allow for prompt treatment and potentially decrease the risk of long-term disabilities. Currently, only a handful of candidate markers have been identified for severe malaria, though they are not fully reliable. The proposed molecular markers include erythropoietin, angiopoietin 2, von Willebrand factor, *P. falciparum* histidine-rich protein 2 and ICAM-1 which, although indicative of severe disease when elevated, still has limited clinical utility. This is mainly due to the highly variable sensitivity and specificity for the detection of severe CM<sup>[41,87-90]</sup>. It is now clear that EVs and their cargo have potential as biomarkers. Their elevated numbers, notably endothelial-, platelet- and RBC-derived MVs, in the circulation of human patients with



CM has already been proven in multiple studies<sup>[39,84,91]</sup>. The role of EVs as a biomarker in severe malaria is still in its infancy and in-depth multi-centre studies are still needed to ascertain their predictive value to improve rapid detection in bodily fluids. In addition, although blood, urine, and saliva have all been used for diagnostics<sup>[92,93]</sup>, urine and saliva have not been investigated in malaria but we cannot exclude the possibility of them becoming a source of biomarkers to assess disease severity in the future. As mentioned above, all current markers have their limitations and one could hypothesise that the combination of these existing biomarkers with newly discovered EV-associated markers could significantly improve both the specificity and sensitivity of testing.

As a consequence of their biogenesis, EVs harbour a peculiar set of proteins, nucleic acids, and lipids that can be transferred from a parent to recipient cells, rendering these sub-micron structures unique sources and vehicles of biomarkers. Various analytical approaches including proteomics, transcriptomics, and metabolomics, although mostly focused on cancer-related conditions, are currently employed to study the content of EVs derived from different cell types and bodily fluids<sup>[94]</sup>. Nonetheless, the cargo of EVs is now becoming an important research topic in severe malaria allowing us to both understand disease pathogenesis and identify novel biomarkers, with proteins and microRNA (miRNA) being the most studied components of this cargo.

EV-associated proteins can typically be studied using either untargeted proteomics, to characterise the whole protein content, or through a hypothesis-driven targeted approach, to investigate individual proteins or a selected set of proteins based on previous evidence. Compared to other parasitic diseases, high-throughput untargeted proteomics - the leading technique for the discovery of new protein markers - has not been widely applied to investigate malaria-associated EVs yet, but has been explored in the last couple of years. The first report dates back to 2011 when exosomes from *P. yoelii*-infected BALB/c mice were analysed and revealed to contain both classical exosomal markers as well as parasite proteins<sup>[40]</sup>. Interestingly, 30 parasite proteins belonging to two major classes, proteins associated with RBCs membrane and proteins involved in parasite invasion into RBCs, were identified within iRBCs exosomes. Then, the presence of *Plasmodium* proteins within EVs

from human and mice malaria infection was confirmed by a number of proteomics-based studies<sup>[40,51,58,82,95]</sup>. Although the majority of these studies did not have as their main objective the identification of biomarkers, they all contributed to prove the presence of parasite-derived proteins with antigenic and immunomodulatory properties, or as potential virulence factors within EVs that, in the future, might be found useful for the development of novel diagnostic and prognostic tests.

Only a few studies have focused on EVs as a novel source of markers for severe malaria. In our group, we used high-throughput proteomics to characterise the protein cargo of MVs released during ECM in *P. berghei* infected mice<sup>[96]</sup>. The vast majority of identified proteins were host-derived and only a couple were from *P. berghei*. The protein content of MVs released during severe disease was significantly altered compared to that released upon early infection or in uninfected mice. Network analysis showed that proteins with altered abundance during ECM were associated with CM pathogenesis. Two of these proteins, carbonic anhydrase I and S100A8 were verified to be associated with CM MV in both murine and clinical samples, highlighting the importance of MV protein content to understand the role of EVs both in severe malaria and as a source of protein markers<sup>[96]</sup>. The protein cargo of MVs obtained from *P. falciparum*-infected individuals was later investigated by Antwi-Baffour and colleagues<sup>[97]</sup>, although cases with severe malaria were not investigated. The study identified several different host-derived proteins in infected and non-infected human subjects, as well as parasite-derived proteins in infected samples. Nonetheless, the results remained primarily descriptive and no diagnostic marker was actually proposed. More recently, proteomics was applied to identify novel potential biomarkers of *P. vivax* liver stage infection<sup>[98]</sup>. By taking advantage of a human liver-chimeric mouse model, plasma EVs obtained after *P. vivax* infection were studied to identify potential liver-stage expressed parasite proteins that could be indicative of infection. Among mouse and human proteins, they also identified parasite proteins showing variable distribution in abundance over different time points post-infection, indicating that parasite proteins contained within EVs vary with parasite developmental stages, supporting their potential role as a source of biomarkers<sup>[98]</sup>. In mice and human studies, there has been a consistent indication of EVs' importance in the role of malaria pathogenesis and their potential as markers for disease

severity; however, more research is required to confirm the potential of these EVs derived protein as biomarkers for severe malaria.

Within the groups of non-coding RNAs, miRNA are now considered promising biomarkers in many pathological conditions<sup>[99,100]</sup> due to their stability in various bodily fluids such as saliva, serum, plasma and CSF, and their role in gene expression regulation<sup>[101-106]</sup>. One of the advantages of studying EV-associated miRNAs is their particular stability as they are protected within a plasma membrane<sup>[107]</sup>. These short, non-coding RNA molecules display critical regulatory functions as they are involved in nearly all physiological processes such as cellular differentiation, proliferation, metabolism, development, and homeostasis<sup>[108,109]</sup>.

As previously mentioned, a large portion of EV miRNA studies are focused on cancers, which have shown the significance of identifying cargo miRNA. In a 2019 clinical cancer study, miRNA from whole plasma, EVs and EV-free plasma from lung adenocarcinoma and granuloma patients were evaluated. The study determined that whole plasma, EVs and EV-free plasma had differing miRNA expression profiles and the prediction performance of EVs was better than EV-free plasma. Plasma was the best predictor however, due to the lack of knowledge in storage and processing techniques of EVs<sup>[110]</sup>. Elevated levels of plasma EVs have since been observed in patients affected by various forms of cancer compared to healthy subjects and, interestingly, these levels decreased upon removal of the tumour, simultaneously decreasing tumour specific miRNA profiles within the plasma EVs<sup>[111,112]</sup>, which provides a further link between cancer and increased EV production. Similar results were demonstrated in patients with autoimmune, infectious and cardiovascular diseases, and neurological disorders<sup>[113-116]</sup>.

Next-generation sequencing technology is the recommended, standard approach when investigating the miRNA content of EVs for novel biomarker identification<sup>[117]</sup>. Accumulated sequencing data suggest the potential for miRNAs as diagnostic and prognostic markers, as well as for parasitic diseases caused by platyhelminths, arthropods, and protozoa, including *Plasmodium spp.*<sup>[118]</sup>. When analysing EVs derived from helminth parasites (*Trichuris muris*), the content was sequenced using the HiSeq 500 system, identifying 56 miRNA, 22 of which were novel<sup>[119]</sup>. A similar study looking at hookworms using the NextSeq 500 system identified

52 miRNA, many of which were found to be involved in inflammation regulation when mapped to mouse genes<sup>[120]</sup>.

One of the first studies on miRNA in *Plasmodium* infection suggested that this parasite did not have specific miRNAs but rather, takes advantage of the transcriptional machinery within RBCs for the activation and suppression of gene expression<sup>[121]</sup>. This study also identified miR-451 as highly expressed in iRBCs, although its accumulation was not associated with malaria infection<sup>[121]</sup>.

A study from Thailand observed, for the first time, lower expression of miR-451 and miR-16 in the plasma of adults infected with malaria, suggesting their role as biomarkers for malaria infection, especially in *Plasmodium vivax* infected individuals<sup>[122]</sup>. However, a large portion of transcriptomic studies have been performed using murine models focusing on the host's response to infection<sup>[123-125]</sup>, or using *in vitro* systems to target a specific cell-type. For instance, let-7i, miR-27a, and miR-150 were found to be over-expressed in the brain of CM-mice but not in non-CM animals<sup>[124]</sup>. Overexpression of these miRNA during infection may be essential for the instigation of neurological syndromes by regulating their downstream targets, thus having a potential regulatory role in the pathogenesis of severe malaria, as well as being targets for therapeutic intervention<sup>[124]</sup>.

Similar to iRBCs, EVs from iRBCs display higher levels of miR-451a and let-7b when compared to nRBCs, and once miR-451a within EVs is engulfed by endothelial cells, their gene expression and barrier properties are affected, which may then lead to vascular dysfunction, making the miRNA a possible target for therapeutic intervention<sup>[52]</sup>. Using a more complex model, our group analysed plasma EVs from mice with CM and found that the miRNAs from malaria EVs played a regulatory role in severe malaria pathogenesis. miR-146a levels were higher and miR-193b levels lower in plasma-derived EVs while miR-205, miR-215, and miR-467a were all elevated in brain tissue from CM mice when compared to non-infected or non-CM infected mice<sup>[126]</sup>. This difference in miRNA profiles suggests that miRNA present in circulation could have different functions from those present in tissues. Further investigation to verify the potential of these EVs derived miRNA as biomarkers for the cerebral syndrome using both experimental models and clinical samples will be necessary.

## **2.6 Conclusion**

*In vivo* and *ex vivo* studies point towards a role for EVs in the modulation of disease and the host response. No study has looked at the behaviour of EVs *in situ* however. Rather than passively transferred EVs, animal models utilising both transgenic parasites and transgenic host cells expressing tags that can be traced, combined with high-resolution imaging in the animal, will allow us to truly understand the complex involvement of EVs with their target cells. For instance, recent work used high-resolution microscopy to visualise circulating EVs in zebrafish embryos using a tissue-specific expression of genetically encoded markers of EVs. This approach will allow us to not only decipher the role of EVs in physiology including cargo delivery but also, to assess the effects of disease or treatment on EVs release and function<sup>[127]</sup>.

In addition, although evidence confirming the importance of EVs as a source of biomarkers are scattered, they also highlight a number of questions and unsolved problems. Indeed, most of the work performed so far still lack validation steps and clinical studies remain scarce. These limitations are such that most studies remain mainly descriptive and hamper the process of biomarker validation and implementation into clinical practice. In-depth investigations should also be carried out to understand the mechanisms of protein and miRNA packaging into EVs, as well as the signals involved in cell targeting. Deciphering these processes will contribute to the selection of highly specific biomarkers for larger validation studies. While biomarker studies applied to severe malaria and EVs are still in their infancy, there is hope for this field to provide novel strategies to fight severe malaria in the future.

## **Declarations**

### **Authors' contributions**

Conceived and designed the review: Cheng IS, Sealy BC, Tiberti N, Combes V

Made equal contribution to the writing of the sections: Cheng IS, Sealy BC

Provided feedback for manuscript revision: Cheng IS, Sealy BC

Read and approved the final manuscript: Cheng IS, Sealy BC, Tiberti N, Combes V

### **Availability of data and materials**

Not applicable.

### **Financial support and sponsorship**

Combes V was supported by the University of Technology, Faculty of Science grant. Cheng IS and Sealy BC were supported by the Australian Government Research Training Program Stipend. Tiberti N was supported by the Italian Ministry of Health "Fondi Ricerca Corrente - Linea 1 Progetto 3" to IRCCS. Sacro Cuore Don Calabria Hospital.

### **Conflicts of interest**

All authors declared that there are no conflicts of interest.

### **Ethical approval and consent to participate**

Not applicable.

### **Consent for publication**

Not applicable.

### **Copyright**

© The Author(s) 2020.

## **2.7 References**

1. Organization WH. World malaria report 2019. 2019. Available from <https://www.who.int/publications-detail/world-malaria-report-2019> [Last accessed on 6 May 2020]
2. Murray CJL, Rosenfeld LC, Lim SS, Andrews KG, Foreman KJ, et al. Global malaria mortality between 1980 and 2010: a systematic analysis. *Lancet* 2012;379:413-31.
3. Bangirana P, Opoka RO, Boivin MJ, Idro R, Hodges JS, et al. Severe malarial anemia is associated with long-term neurocognitive impairment. *Clin Infect Dis* 2014;59:336-44.
4. Storm J, Craig AG. Pathogenesis of cerebral malaria--inflammation and cytoadherence. *Front Cell Infect Microbiol* 2014;4:100.
5. Organization WH. Management of severe malaria: a practical handbook. [apps.who.int](https://apps.who.int/); 2012. Available from <https://apps.who.int/iris/handle/10665/79317> [Last accessed on 6 May 2020]
6. Jakeman GN, Saul A, Hogarth WL, Collins WE. Anaemia of acute malaria infections in non-immune patients primarily results from destruction of uninfected erythrocytes. *Parasitology* 1999;119:127-33.
7. Lamikanra AA, Brown D, Potocnik A, Casals-Pascual C, Langhorne J, et al. Malarial anemia: of mice and men. *Blood* 2007;110:18-28.
8. Vainieri ML, Blagborough AM, MacLean AL, Haltalli MLR, Ruivo N, et al. Systematic tracking of altered haematopoiesis during sporozoite-mediated malaria development reveals multiple response points. *Open Biol* 2016;6:160038.
9. Razakandrainibe R, Combes V, Grau GE, Jambou R. Crossing the wall: the opening of endothelial cell junctions during infectious diseases. *Int J Biochem Cell Biol* 2013;45:1165-73.
10. Dorovini-Zis K, Schmidt K, Huynh H, Fu W, Whitten RO, et al. The neuropathology of fatal cerebral malaria in malawian children. *Am J Pathol* 2011;178:2146-58.
11. Taylor TE, Fu WJ, Carr RA, Whitten RO, Mueller JS, et al. Differentiating the pathologies of cerebral malaria by postmortem parasite counts. *Nat Med* 2004;10:143-5.
12. Ponsford MJ, Medana IM, Prapansilp P, Hien TT, Lee SJ, et al. Sequestration and microvascular congestion are associated with coma in human cerebral malaria. *J Infect Dis* 2012;205:663-71.

13. Combes V, Guillemin GJ, Chan-Ling T, Hunt NH, Grau GER. The crossroads of neuroinflammation in infectious diseases: endothelial cells and astrocytes. *Trends Parasitol* 2012;28:311-9.
14. Dunst J, Kamena F, Matuschewski K. Cytokines and chemokines in cerebral malaria pathogenesis. *Front Cell Infect Microbiol* 2017;7:324.
15. Wassmer SC, Grau GER. Platelets as pathogenetic effectors and killer cells in cerebral malaria. *Expert Rev Hematol* 2016;9:515-7.
16. Chimalizeni Y, Kawaza K, Taylor T, Molyneux M. The platelet count in cerebral malaria, is it useful to the clinician? *Am J Trop Med Hyg* 2010;83:48-50.
17. Gérardin P, Rogier C, Ka AS, Jouvencel P, Brousse V, et al. Prognostic value of thrombocytopenia in African children with falciparum malaria. *Am J Trop Med Hyg* 2002;66:686-91.
18. Grau GE, Mackenzie CD, Carr RA, Redard M, Pizzolato G, et al. Platelet accumulation in brain microvessels in fatal pediatric cerebral malaria. *J Infect Dis* 2003;187:461-6.
19. Wassmer SC, Taylor T, Maclennan CA, Kanjala M, Mukaka M, et al. Platelet-induced clumping of Plasmodium falciparum-infected erythrocytes from Malawian patients with cerebral malaria-possible modulation in vivo by thrombocytopenia. *J Infect Dis* 2008;197:72-8.
20. Barbier M, Faille D, Loriod B, Textoris J, Camus C, et al. Platelets alter gene expression profile in human brain endothelial cells in an in vitro model of cerebral malaria. *PLoS One* 2011;6:e19651.
21. Wassmer SC, Combes V, Candal FJ, Juhan-Vague I, Grau GE. Platelets potentiate brain endothelial alterations induced by Plasmodium falciparum. *Infect Immun* 2006;74:645-53.
22. McMorran BJ, Wiczorski L, Drysdale KE, Chan JA, Huang HM, et al. Platelet factor 4 and Duffy antigen required for platelet killing of Plasmodium falciparum. *Science* 2012;338:1348-51.
23. Peyron F, Polack B, Lamotte D, Kolodie L, Ambroise-Thomas P. Plasmodium falciparum growth inhibition by human platelets in vitro. *Parasitology* 1989;99:317-22.
24. Aggrey AA, Srivastava K, Ture S, Field DJ, Morrell CN. Platelet induction of the acute-phase response is protective in murine experimental cerebral malaria. *J Immunol* 2013;190:4685-91.



25. Medana IM, Turner GDH. Human cerebral malaria and the blood-brain barrier. *Int J Parasitol* 2006;36:555-68.
26. Medana IM, Day NP, Hien TT, Mai NTH, Bethell D, et al. Axonal injury in cerebral malaria. *Am J Pathol* 2002;160:655-66.
27. Adams S, Brown H, Turner G. Breaking down the blood-brain barrier: signaling a path to cerebral malaria? *Trends Parasitol* 2002;18:360-6.
28. Beare NAV, Harding SP, Taylor TE, Lewallen S, Molyneux ME. Perfusion abnormalities in children with cerebral malaria and malarial retinopathy. *J Infect Dis* 2009;199:263-71.
29. Kampondeni SD, Birbeck GL, Seydel KB, Beare NA, Glover SJ, et al. Noninvasive measures of brain edema predict outcome in pediatric cerebral malaria. *Surg Neurol Int* 2018;9:53.
30. Seydel KB, Kampondeni SD, Valim C, Potchen MJ, Milner DA, et al. Brain swelling and death in children with cerebral malaria. *N Engl J Med* 2015;372:1126-37.
31. Schindler SM, Little JP, Klegeris A. Microparticles: a new perspective in central nervous system disorders. *Biomed Res Int* 2014;2014:756327.
32. Schofield L, Grau GE. Immunological processes in malaria pathogenesis. *Nat Rev Immunol* 2005;5:722-35.
33. Doyle LM, Wang MZ. Overview of extracellular vesicles, their origin, composition, purpose, and methods for exosome isolation and analysis. *Cells* 2019;8:727.
34. Mantel PY, Marti M. The role of extracellular vesicles in Plasmodium and other protozoan parasites. *Cell Microbiol* 2014;16:344-54.
35. Torrecilhas AC, Schumacher RI, Alves MJM, Colli W. Vesicles as carriers of virulence factors in parasitic protozoan diseases. *Microbes Infect* 2012;14:1465-74.
36. Combes V, Taylor TE, Juhan-Vague I, Mège JL, Mwenechanya J, et al. Circulating endothelial microparticles in malawian children with severe falciparum malaria complicated with coma. *JAMA* 2004;291:2542-4.
37. Campos FMF, Franklin BS, Teixeira-Carvalho A, Filho ALS, de Paula SCO, et al. Augmented plasma microparticles during acute Plasmodium vivax infection. *Malar J* 2010;9:327.
38. Nantakomol D, Dondorp AM, Krudsood S, Udomsangpetch R, Pattanapanyasat K, et al. Circulating red cell-derived microparticles in human malaria. *J Infect Dis* 2011;203:700-6.
39. Pankoui Mfonkeu JB, Gouado I, Fotso Kuate H, Zambou O, Amvam Zollo PH, et al. Elevated cell-specific microparticles are a biological marker for cerebral dysfunctions in human severe malaria. *PLoS One* 2010;5:e13415.

40. Martin-Jaular L, Nakayasu ES, Ferrer M, Almeida IC, Del Portillo HA. Exosomes from Plasmodium yoelii-infected reticulocytes protect mice from lethal infections. *PLoS One* 2011;6:e26588.
41. Bridges DJ, Bunn J, van Mourik JA, Grau G, Preston RJS, et al. Rapid activation of endothelial cells enables Plasmodium falciparum adhesion to platelet-decorated von Willebrand factor strings. *Blood* 2010;115:1472-4.
42. El-Assaad F, Wheway J, Mitchell AJ, Lou J, Hunt NH, et al. Cytoadherence of Plasmodium berghei-infected red blood cells to murine brain and lung microvascular endothelial cells in vitro. *Infect Immun* 2013;81:3984-91.
43. Jambou R, El-Assaad F, Combes V, Grau GE. In vitro culture of Plasmodium berghei-ANKA maintains infectivity of mouse erythrocytes inducing cerebral malaria. *Malar J* 2011;10:346.
44. Khaw LT, Ball HJ, Golenser J, Combes V, Grau GE, et al. Endothelial cells potentiate interferon- $\gamma$  production in a novel tripartite culture model of human cerebral malaria. *PLoS One* 2013;8:e69521.
45. Wassmer SC, Lépolard C, Traoré B, Pouvelle B, Gysin J, et al. Platelets reorient Plasmodium falciparum-infected erythrocyte cytoadhesion to activated endothelial cells. *J Infect Dis* 2004;189:180-9.
46. Canfield SG, Stebbins MJ, Morales BS, Asai SW, Vatine GD, et al. An isogenic blood-brain barrier model comprising brain endothelial cells, astrocytes, and neurons derived from human induced pluripotent stem cells. *J Neurochem* 2017;140:874-88.
47. Cho H, Seo JH, Wong KHK, Terasaki Y, Park J, et al. Three-dimensional blood-brain barrier model for in vitro studies of neurovascular pathology. *Sci Rep* 2015;5:15222.
48. Helms HC, Abbott NJ, Burek M, Cecchelli R, Couraud PO, et al. In vitro models of the blood-brain barrier: an overview of commonly used brain endothelial cell culture models and guidelines for their use. *J Cereb Blood Flow Metab* 2016;36:862-90.
49. Faille D, Combes V, Mitchell AJ, Fontaine A, Juhan-Vague I, et al. Platelet microparticles: a new player in malaria parasite cytoadherence to human brain endothelium. *FASEB J* 2009;23:3449-58.
50. Wassmer SC, Combes V, Grau GER. Platelets and microparticles in cerebral malaria: the unusual suspects. *Drug Discov Today Dis Mechanisms* 2011;8:e15-23.

51. Sampaio NG, Emery SJ, Garnham AL, Tan QY, Sisquella X, et al. Extracellular vesicles from early stage *Plasmodium falciparum*-infected red blood cells contain PfEMP1 and induce transcriptional changes in human monocytes. *Cell Microbiol* 2018;20:e12822.
52. Mantel PY, Hjelmqvist D, Walch M, Kharoubi-Hess S, Nilsson S, et al. Infected erythrocyte-derived extracellular vesicles alter vascular function via regulatory Ago2-miRNA complexes in malaria. *Nat Commun* 2016;7:12727.
53. Wang Z, Xi J, Hao X, Deng W, Liu J, et al. Red blood cells release microparticles containing human argonaute 2 and miRNAs to target genes of *Plasmodium falciparum*. *Emerg Microbes Infect* 2017;6:e75.
54. Couper KN, Barnes T, Hafalla JCR, Combes V, Ryffel B, et al. Parasite-derived plasma microparticles contribute significantly to malaria infection-induced inflammation through potent macrophage stimulation. *PLoS Pathog* 2010;6:e1000744.
55. Mantel PY, Hoang AN, Goldowitz I, Potashnikova D, Hamza B, et al. Malaria-infected erythrocyte-derived microvesicles mediate cellular communication within the parasite population and with the host immune system. *Cell Host Microbe* 2013;13:521-34.
56. Sisquella X, Ofir-Birin Y, Pimentel MA, Cheng L, Abou Karam P, et al. Malaria parasite DNA-harboring vesicles activate cytosolic immune sensors. *Nat Commun* 2017;8:1985.
57. Yu X, Cai B, Wang M, Tan P, Ding X, et al. Cross-regulation of two type I interferon signaling pathways in plasmacytoid dendritic cells controls anti-malaria immunity and host mortality. *Immunity* 2016;45:1093-107.
58. Demarta-Gatsi C, Rivkin A, Di Bartolo V, Peronet R, Ding S, et al. Histamine releasing factor and elongation factor 1 alpha secreted via malaria parasites extracellular vesicles promote immune evasion by inhibiting specific T cell responses. *Cell Microbiol* 2019;21:e13021.
59. Regev-Rudzki N, Wilson DW, Carvalho TG, Sisquella X, Coleman BM, et al. Cell-cell communication between malaria-infected red blood cells via exosome-like vesicles. *Cell* 2013;153:1120-33.
60. Wheway J, Latham SL, Combes V, Grau GER. Endothelial microparticles interact with and support the proliferation of T cells. *J Immunol* 2014;193:3378-87.
61. Gasser O, Schifferli JA. Activated polymorphonuclear neutrophils disseminate anti-inflammatory microparticles by ectocytosis. *Blood* 2004;104:2543-8.

62. Rhys HI, Dell'Accio F, Pitzalis C, Moore A, Norling LV, et al. Neutrophil microvesicles from healthy control and rheumatoid arthritis patients prevent the inflammatory activation of macrophages. *EBioMedicine* 2018;29:60-9.
63. Wen B, Combes V, Bonhoure A, Weksler BB, Couraud PO, et al. Endotoxin-induced monocytic microparticles have contrasting effects on endothelial inflammatory responses. *PLoS One* 2014;9:e91597.
64. Riggle BA, Manglani M, Maric D, Johnson KR, Lee MH, et al. CD8+ T cells target cerebrovasculature in children with cerebral malaria. *J Clin Invest* 2020;130:1128-38.
65. Poh CM, Howland SW, Grotenbreg GM, Rénia L. Damage to the blood-brain barrier during experimental cerebral malaria results from synergistic effects of CD8+ T cells with different specificities. *Infect Immun* 2014;82:4854-64.
66. Swanson PA, Hart GT, Russo MV, Nayak D, Yazew T, et al. CD8+ T cells induce fatal brainstem pathology during cerebral malaria via luminal antigen-specific engagement of brain vasculature. *PLoS Pathog* 2016;12:e1006022.
67. Combes V, Souza JBD, Rénia L, Hunt NH, Grau GE. Cerebral malaria: which parasite? Which model? *Drug Discov Today Dis Models* 2005;2:141-7.
68. Craig AG, Grau GE, Janse C, Kazura JW, Milner D, et al. The role of animal models for research on severe malaria. *PLoS Pathog* 2012;8:e1002401.
69. de Souza JB, Hafalla JCR, Riley EM, Couper KN. Cerebral malaria: why experimental murine models are required to understand the pathogenesis of disease. *Parasitology* 2010;137:755-72.
70. El-Assaad F, Combes V, Grau GE. Experimental models of microvascular immunopathology: the example of cerebral malaria. *J Neuroinfect Dis* 2014;5.
71. Riley EM, Couper KN, Helmby H, Hafalla JCR, de Souza JB, et al. Neuropathogenesis of human and murine malaria. *Trends Parasitol* 2010;26:277-8.
72. Amante FH, Stanley AC, Randall LM, Zhou Y, Haque A, et al. A role for natural regulatory T cells in the pathogenesis of experimental cerebral malaria. *Am J Pathol* 2007;171:548-59.
73. Claser C, Malleret B, Gun SY, Wong AYW, Chang ZW, et al. CD8+ T cells and IFN- $\gamma$  mediate the time-dependent accumulation of infected red blood cells in deep organs during experimental cerebral malaria. *PLoS One* 2011;6:e18720.

74. Franke-Fayard B, Janse CJ, Cunha-Rodrigues M, Ramesar J, Büscher P, et al. Murine malaria parasite sequestration: CD36 is the major receptor, but cerebral pathology is unlinked to sequestration. *Proc Natl Acad Sci U S A* 2005;102:11468-73.
75. Strangward P, Haley MJ, Shaw TN, Schwartz JM, Greig R, et al. A quantitative brain map of experimental cerebral malaria pathology. *PLoS Pathog* 2017;13:e1006267.
76. Combes V, Coltel N, Alibert M, van Eck M, Raymond C, et al. ABCA1 gene deletion protects against cerebral malaria: potential pathogenic role of microparticles in neuropathology. *Am J Pathol* 2005;166:295-302.
77. El-Assaad F, Wheway J, Hunt NH, Grau GER, Combes V. Production, fate and pathogenicity of plasma microparticles in murine cerebral malaria. *PLoS Pathog* 2014;10:e1003839.
78. Penet MF, Abou-Hamdan M, Coltel N, Cornille E, Grau GE, et al. Protection against cerebral malaria by the low-molecular-weight thiol pantethine. *Proc Natl Acad Sci U S A* 2008;105:1321-6.
79. Kuhn SM, McCarthy AE. Paediatric malaria: what do paediatricians need to know? *Paediatr Child Health* 2006;11:349-54.
80. White NJ, Pukrittayakamee S, Hien TT, Faiz MA, Mokuolu OA, et al. Malaria. *Lancet* 2014;383:723-35.
81. Shrivastava SK, Dalko E, Delcroix-Genete D, Herbert F, Cazenave PA, et al. Uptake of parasite-derived vesicles by astrocytes and microglial phagocytosis of infected erythrocytes may drive neuroinflammation in cerebral malaria. *Glia* 2017;65:75-92.
82. Martín-Jaular L, de Menezes-Neto A, Monguió-Tortajada M, Elizalde-Torrent A, Díaz-Varela M, et al. Spleen-dependent immune protection elicited by CpG adjuvanted reticulocyte-derived exosomes from malaria infection is associated with changes in T cell subsets' distribution. *Front Cell Dev Biol* 2016;4:131.
83. Nantakomol D, Chhima P, Day NP, Dondorp AM, Combes V, et al. Quantitation of cell-derived microparticles in plasma using flow rate based calibration. *Southeast Asian J Trop Med Public Health* 2008;39:146-53.
84. Babatunde KA, Yesodha Subramanian B, Ahoudi AD, Martinez Murillo P, Walch M, et al. Role of extracellular vesicles in cellular cross talk in malaria. *Front Immunol* 2020;11:22.
85. Sahu PK, Satpathi S, Behera PK, Mishra SK, Mohanty S, et al. Pathogenesis of cerebral malaria: new diagnostic tools, biomarkers, and therapeutic approaches. *Front Cell Infect Microbiol* 2015;5:75.

86. Varo R, Crowley VM, Siteo A, Madrid L, Serghides L, et al. Adjunctive therapy for severe malaria: a review and critical appraisal. *Malar J* 2018;17:47.
87. Adukpo S, Kusi KA, Ofori MF, Tetteh JKA, Amoako-Sakyi D, et al. High plasma levels of soluble intercellular adhesion molecule (ICAM)-1 are associated with cerebral malaria. *PLoS One* 2013;8:e84181.
88. Casals-Pascual C, Idro R, Gicheru N, Gwer S, Kitsao B, et al. High levels of erythropoietin are associated with protection against neurological sequelae in African children with cerebral malaria. *Proc Natl Acad Sci U S A* 2008;105:2634-9.
89. Conroy AL, Lafferty EI, Lovegrove FE, Krudsood S, Tangpukdee N, et al. Whole blood angiopoietin-1 and -2 levels discriminate cerebral and severe (non-cerebral) malaria from uncomplicated malaria. *Malar J* 2009;8:295.
90. Thakur K, Vareta J, Carson K, Taylor T, Sullivan D. Performance of cerebrospinal fluid (CSF) plasmodium falciparum histidine-rich protein-2 (pfHRP-2) in prediction of death in cerebral malaria (I10-2.005) 2014. Available from [https://n.neurology.org/content/82/10\\_Supplement/I10-2.005](https://n.neurology.org/content/82/10_Supplement/I10-2.005) [Last accessed on 6 May 2020]
91. Antwi-Baffour S, Malibha-Pinchbeck M, Stratton D, Jorfi S, Lange S, et al. Plasma mEV levels in Ghanaian malaria patients with low parasitaemia are higher than those of healthy controls, raising the potential for parasite markers in mEVs as diagnostic targets. *J Extracell Vesicles* 2020;9:1697124.
92. Hede MS, Fjelstrup S, Lötsch F, Zoleko RM, Klicpera A, et al. Detection of the malaria causing plasmodium parasite in saliva from infected patients using topoisomerase I activity as a biomarker. *Sci Rep* 2018;8:4122.
93. Krampa FD, Aniweh Y, Awandare GA, Kanyong P. Recent progress in the development of diagnostic tests for malaria. *Diagnostics (Basel)* 2017;7:54.
94. Choi DS, Kim DK, Kim YK, Gho YS. Proteomics, transcriptomics and lipidomics of exosomes and ectosomes. *Proteomics* 2013;13:1554-71.
95. Abdi A, Yu L, Goulding D, Rono MK, Bejon P, et al. Proteomic analysis of extracellular vesicles from a Plasmodium falciparum Kenyan clinical isolate defines a core parasite secretome. [version 2; peer review: 2 approved, 1 approved with reservations]. *Wellcome Open Res* 2017;2:50.

96. Tiberti N, Latham SL, Bush S, Cohen A, Opoka RO, et al. Exploring experimental cerebral malaria pathogenesis through the characterisation of host-derived plasma microparticle protein content. *Sci Rep* 2016;6:37871.
97. Antwi-Baffour S, Adjei JK, Agyemang-Yeboah F, Annani-Akollor M, Kyeremeh R, et al. Proteomic analysis of microparticles isolated from malaria positive blood samples. *Proteome Sci* 2016;15:5.
98. Gualdrón-López M, Flannery EL, Kangwanrangsang N, Chuenchob V, Fernandez-Orth D, et al. Characterization of plasmodium vivax proteins in plasma-derived exosomes from malaria-infected liver-chimeric humanized Mice. *Front Microbiol* 2018;9:1271.
99. Hanna J, Hossain GS, Kocerha J. The Potential for microRNA therapeutics and clinical research. *Front Genet* 2019;10:478.
100. Saliminejad K, Khorram Khorshid HR, Soleymani Fard S, Ghaffari SH. An overview of microRNAs: biology, functions, therapeutics, and analysis methods. *J Cell Physiol* 2019;234:5451-65.
101. Chen SY, Wang Y, Telen MJ, Chi JT. The genomic analysis of erythrocyte microRNA expression in sickle cell diseases. *PLoS One* 2008;3:e2360.
102. Chen X, Ba Y, Ma L, Cai X, Yin Y, et al. Characterization of microRNAs in serum: a novel class of biomarkers for diagnosis of cancer and other diseases. *Cell Res* 2008;18:997-1006.
103. Hammond SM. An overview of microRNAs. *Adv Drug Deliv Rev* 2015;87:3-14.
104. Mitchell PS, Parkin RK, Kroh EM, Fritz BR, Wyman SK, et al. Circulating microRNAs as stable blood-based markers for cancer detection. *Proc Natl Acad Sci U S A* 2008;105:10513-8.
105. Reid G, Kirschner MB, van Zandwijk N. Circulating microRNAs: association with disease and potential use as biomarkers. *Crit Rev Oncol Hematol* 2011;80:193-208.
106. Wang W, Li R, Meng M, Wei C, Xie Y, et al. MicroRNA profiling of CD3+ CD56+ cytokine-induced killer cells. *Sci Rep* 2015;5:9571.
107. Babatunde KA, Mbagwu S, Hernández-Castañeda MA, Adapa SR, Walch M, et al. Malaria infected red blood cells release small regulatory RNAs through extracellular vesicles. *Sci Rep* 2018;8:884.
108. Bartel DP. MicroRNAs: genomics, biogenesis, mechanism, and function. *Cell* 2004;116:281-97.

109. Wang J, Sen S. MicroRNA functional network in pancreatic cancer: from biology to biomarkers of disease. *J Biosci* 2011;36:481-91.
110. Chen X, Jin Y, Feng Y. Evaluation of plasma extracellular vesicle microRNA signatures for lung adenocarcinoma and granuloma with monte-carlo feature selection method. *Front Genet* 2019;10:367.
111. Sartori MT, Della Puppa A, Ballin A, Saggiorato G, Bernardi D, et al. Prothrombotic state in glioblastoma multiforme: an evaluation of the procoagulant activity of circulating microparticles. *J Neurooncol* 2011;104:225-31.
112. Zwicker JI, Liebman HA, Neuberg D, Lacroix R, Bauer KA, et al. Tumor-derived tissue factor-bearing microparticles are associated with venous thromboembolic events in malignancy. *Clin Cancer Res* 2009;15:6830-40.
113. da Silva EFR, Fonseca FAH, França CN, Ferreira PRA, Izar MCO, et al. Imbalance between endothelial progenitors cells and microparticles in HIV-infected patients naive for antiretroviral therapy. *AIDS* 2011;25:1595-601.
114. Pelletier F, Garnache-Ottou F, Angelot F, Biichlé S, Vidal C, et al. Increased levels of circulating endothelial-derived microparticles and small-size platelet-derived microparticles in psoriasis. *J Invest Dermatol* 2011;131:1573-6.
115. Stępień E, Stankiewicz E, Zalewski J, Godlewski J, Zmudka K, et al. Number of microparticles generated during acute myocardial infarction and stable angina correlates with platelet activation. *Arch Med Res* 2012;43:31-5.
116. Xue S, Cai X, Li W, Zhang Z, Dong W, et al. Elevated plasma endothelial microparticles in Alzheimer's disease. *Dement Geriatr Cogn Disord* 2012;34:174-80.
117. Bondar G, Xu W, Elashoff D, Li X, Faure-Kumar E, et al. Comparing NGS and NanoString platforms in peripheral blood mononuclear cell transcriptome profiling for advanced heart failure biomarker development. *J Biol Methods* 2020;7:e123.
118. Manzano-Román R, Siles-Lucas M. MicroRNAs in parasitic diseases: potential for diagnosis and targeting. *Mol Biochem Parasitol* 2012;186:81-6.
119. Eichenberger RM, Talukder MH, Field MA, Wangchuk P, Giacomini P, et al. Characterization of *Trichuris muris* secreted proteins and extracellular vesicles provides new insights into host-parasite communication. *J Extracell Vesicles* 2018;7:1428004.



120. Eichenberger RM, Ryan S, Jones L, Buitrago G, Polster R, et al. Hookworm secreted extracellular vesicles interact with host cells and prevent inducible colitis in mice. *Front Immunol* 2018;9:850.
121. Xue X, Zhang Q, Huang Y, Feng L, Pan W. No miRNA were found in Plasmodium and the ones identified in erythrocytes could not be correlated with infection. *Malar J* 2008;7:47.
122. Chamnanchanunt S, Kuroki C, Desakorn V, Enomoto M, Thanachartwet V, et al. Downregulation of plasma miR-451 and miR-16 in Plasmodium vivax infection. *Exp Parasitol* 2015;155:19-25.
123. Capuccini B, Lin J, Talavera-López C, Khan SM, Sodenkamp J, et al. Transcriptomic profiling of microglia reveals signatures of cell activation and immune response, during experimental cerebral malaria. *Sci Rep* 2016;6:39258.
124. El-Assaad F, Hempel C, Combes V, Mitchell AJ, Ball HJ, et al. Differential microRNA expression in experimental cerebral and noncerebral malaria. *Infect Immun* 2011;79:2379-84.
125. Lin JW, Sodenkamp J, Cunningham D, Deroost K, Tshitenge TC, et al. Signatures of malaria-associated pathology revealed by high-resolution whole-blood transcriptomics in a rodent model of malaria. *Sci Rep* 2017;7:41722.
126. Cohen A, Zinger A, Tiberti N, Grau GER, Combes V. Differential plasma microvesicle and brain profiles of microRNA in experimental cerebral malaria. *Malar J* 2018;17:192.
127. Verweij FJ, Hyenne V, Van Niel G, Goetz JG. Extracellular vesicles: catching the light in zebrafish. *Trends Cell Biol* 2019;29:770-6.

**Chapter Three:**

**Characterising extracellular  
vesicle microRNAs from Thai  
malaria patients**

## Chapter 3: Characterising extracellular vesicle microRNAs from Thai malaria patients

### Chapter overview

Extracellular vesicles are widely known to carry biomolecules such as RNA, which have the potential to act as markers for disease. The field of extracellular vesicles as biomarkers for malaria infections is still in its infancy. This chapter sought to develop methodology for RNA isolation from EVs isolated from the plasma of Thailand adult patients infected with malaria. Then using real time quantitative polymerase chain reaction (RT-qPCR) a select number of microRNAs significant to malaria, as stated in previous studies, were measured to determine if microRNA abundance varied depending on *Plasmodium* species.

### Authors' contributions

Author	Concept	Investigation	Methodology	Data curation	Formal Analysis	Writing-original draft	Writing-review & editing	Signature
Iris S. Cheng	X	X	X	X	X		X	Production Note: Signature removed prior to publication.
Nutpakal Ketprasit	X			X	X	X	X	Production Note: Signature removed prior to publication.
Fiona Deutsch		X	X				X	Production Note: Signature removed prior to publication.
Nham Tran			X				X	Production Note: Signature removed prior to publication.
Mallika Imwong	X							Production Note: Signature removed prior to publication.
Valery Combes	X				X		X	Production Note: Signature removed prior to publication.
Duangdao Palasuwan	X						X	Production Note: Signature removed prior to publication.

**Publication status:** Published

Cheng, I.S., Ketprasit, N., Deutsch, F. et al. The characterization of extracellular vesicles-derived microRNAs in Thai malaria patients. *Malar J* 19, 285 (2020).

**Link to publication:**





<https://doi.org/10.1186/s12936-020-03360-z>

RESEARCH

Open Access



# The characterization of extracellular vesicles-derived microRNAs in Thai malaria patients

Iris Simone Cheng<sup>1†</sup>, Nutpakal Ketprasit<sup>1,2†</sup>, Fiona Deutsch<sup>3</sup>, Nham Tran<sup>3</sup>, Mallika Imwong<sup>4</sup>, Valery Combes<sup>1\*\*</sup> and Duangdao Palasuwan<sup>5††</sup>

## Abstract

**Background:** Extracellular vesicles (EVs) have been broadly studied in malaria for nearly a decade. These vesicles carry various functional biomolecules including RNA families such as microRNAs (miRNA). These EVs-derived microRNAs have numerous roles in host-parasite interactions and are considered promising biomarkers for disease severity. However, this field lacks clinical studies of malaria-infected samples. In this study, EV specific miRNAs were isolated from the plasma of patients from Thailand infected with *Plasmodium vivax* and *Plasmodium falciparum*. In addition, it is postulated that these miRNAs were differentially expressed in these groups of patients and had a role in disease onset through the regulation of specific target genes.

**Methods:** EVs were purified from the plasma of Thai *P. vivax*-infected patients (n = 19), *P. falciparum*-infected patients (n = 18) and uninfected individuals (n = 20). EV-derived miRNAs were then prepared and abundance of hsa-miR-15b-5p, hsa-miR-16-5p, hsa-let-7a-5p and hsa-miR-150-5p was assessed in these samples. Quantitative polymerase chain reaction was performed, and relative expression of each miRNA was calculated using hsa-miR-451a as endogenous control. Then, the targets of up-regulated miRNAs and relevant pathways were predicted by using bioinformatics. Receiver Operating Characteristic with Area under the Curve (AUC) was then calculated to assess their diagnostic potential.

**Results:** The relative expression of hsa-miR-150-5p and hsa-miR-15b-5p was higher in *P. vivax*-infected patients compared to uninfected individuals, but hsa-let-7a-5p was up-regulated in both *P. vivax*-infected patients and *P. falciparum*-infected patients. Bioinformatic analysis revealed that these miRNAs might regulate genes involved in the malaria pathway including the adherens junction and the transforming growth factor- $\beta$  pathways. All up-regulated miRNAs could potentially be used as disease biomarkers as determined by AUC; however, the sensitivity and specificity require further investigation.

\*Correspondence: valery.combes@uts.edu.au; nantadao@gmail.com

<sup>†</sup>Iris Simone Cheng and Nutpakal Ketprasit are co-first authors

<sup>††</sup>Valery Combes and Duangdao Palasuwan are co-senior authors

<sup>1</sup> Malaria and Microvesicles Research Group, School of Life Sciences, Faculty of Sciences, University Technology of Sydney, Ultimo, Sydney, NSW 2007, Australia

<sup>5</sup> Oxidation in Red Cell Disorders Research Unit, Department of Clinical Microscopy, Faculty of Allied Health Sciences, Chulalongkorn University, 154 Rama 1 Road, Pathumwan, Bangkok 10330, Thailand

Full list of author information is available at the end of the article



© The Author(s) 2020. This article is licensed under a Creative Commons Attribution 4.0 International License, which permits use, sharing, adaptation, distribution and reproduction in any medium or format, as long as you give appropriate credit to the original author(s) and the source, provide a link to the Creative Commons licence, and indicate if changes were made. The images or other third party material in this article are included in the article's Creative Commons licence, unless indicated otherwise in a credit line to the material. If material is not included in the article's Creative Commons licence and your intended use is not permitted by statutory regulation or exceeds the permitted use, you will need to obtain permission directly from the copyright holder. To view a copy of this licence, visit <http://creativecommons.org/licenses/by/4.0/>. The Creative Commons Public Domain Dedication waiver (<http://creativecommons.org/publicdomain/zero/1.0/>) applies to the data made available in this article, unless otherwise stated in a credit line to the data.

**Conclusion:** An upregulation of hsa-miR-150-5p and hsa-miR-15b-5p was observed in *P. vivax*-infected patients while hsa-let-7a-5p was up-regulated in both *P. vivax*-infected and *P. falciparum*-infected patients. These findings will require further validation in larger cohort groups of malaria patients to fully understand the contribution of these EVs miRNAs to malaria detection and biology.

**Keywords:** Malaria, Patients, *Plasmodium falciparum*, *Plasmodium vivax*, Extracellular vesicles, microRNAs

### 3.1 Background

According to the World Health Organization (WHO) World Malaria Report 2019, there were an estimated 405,000 deaths, and 228 million cases were reported globally [1]. *Plasmodium vivax* has the highest prevalence and is known to cause relapse infection [2], whereas *P. falciparum* is the most virulent species causing severe syndromes. Malaria appears to be more devastating worldwide as the emergence of artemisinin-resistant malaria parasites [3, 4]. To overcome the disease, novel drug development is essential. On the other hand, in-depth understanding of the parasite biology and mechanisms underlying the disease is also urgently needed.

Extracellular vesicles (EVs), which are small membrane-bound vesicles, have been explored in malaria for the last decade. Classification of EVs is based on their cellular origin, size, and biological functions [5]. Two major types of EVs have been studied broadly including microvesicles (previously named microparticles) and exosomes. Another type of EVs are the apoptotic bodies which are released during the apoptotic process [6]. Microvesicles are vesicles that bleb from the cell membrane whereas exosomes are released from multivesicular bodies (MVBs) through an exocytotic process in the endolysosomal pathway [7].

Typically, EVs can be detected in very low numbers in healthy individuals. However, upon activation which is triggered by various pathological conditions [8–11], the number of EVs present in biological fluids increases. Various biomolecules were identified in EVs such as proteins, lipids, and nucleic acids [12]. Such biomolecules entrapped in EVs play many important roles in intercellular communication in numerous diseases, including malaria [13, 14].

EVs numbers have been shown to increase during malaria infection both in patients and in experimental malaria models [10, 11, 15–18]. They are associated with either protective [19] or enhanced pathogenicity of malaria infection [11, 16–18, 20, 21]. The most common feature demonstrated in malaria is that EVs can act as immunomodulators. EVs from infected-erythrocytes can stimulate innate immune cells including macrophages [22], natural killer cells [23], monocytes and neutrophils [24]. Interestingly, EVs participate in cell–cell communication between parasites and parasites or host

cells. Exosome-like vesicles have played a role in gametocytogenesis, which is crucial for malaria transmission, and these small membrane-bound vesicles could transfer drug-resistance markers to drug-sensitive parasites [25]. Additionally, EVs which cargo *P. falciparum* lactate dehydrogenase (PfLDH) could control parasite density in vitro [26]. One study also showed that EVs enriched with the parasite's genomic DNA, released from infected red blood cells could be internalized by monocytes and elicited an innate immune response [27].

As mentioned above, EVs carry many kinds of biomolecules including microRNAs (miRNAs). EVs were shown to protect the miRNAs from RNases-mediated degradation and EVs-entrapped miRNAs were also demonstrated to have regulatory functions [28–30]. MiRNAs are members of the non-coding RNAs family which were first discovered in *Caenorhabditis elegans* [31]. Malaria parasites do not express specific miRNAs [32, 33], as Dicer or Argonaute encoding genes are not found in these parasites [34–36]. However, several studies showed that miRNAs could translocate to *P. falciparum* [37, 38]. A pioneer investigation by Lamonte et al. showed interaction between human miRNAs and *P. falciparum*, where the expression of hsa-miR-451a and hsa-let-7i were increased in sickle cells. These miRNAs could inhibit parasitic protein translation resulting in low proliferation of parasites [38]. In other studies, expression of miRNAs in heart and brain tissues from mice with cerebral malaria were shown to be dysregulated when compared to non-cerebral malaria [39, 40].

MiRNAs, human Argonaute protein and RISC complex could be detected in the parasites [37] as well as in EVs released by infected erythrocytes [41, 42]. EVs carried Argonaute-miRNAs complex affecting recipient cells that have been demonstrated to alter vascular function [41] or the parasite's *var* gene expression [43]. These studies strengthen the roles of EVs-derived miRNAs in malaria pathogenesis. There are only three studies that have analysed miRNAs in malaria-infected patients. In human plasma samples, the expression of hsa-miR-451a and hsa-miR-16 in *P. vivax*-infected patients were lower than those in *P. falciparum*-infected patients. Moreover, hsa-miR-451a and hsa-miR-16 had a negative relationship with parasitaemia [44]. In a post-mortem study, the expression of various

miRNAs were found to be differentially expressed between malaria and non-malaria deaths [45]. Furthermore, hsa-miR-146a was newly predicted to play a role in innate immunity in pregnancy malaria [46]. Taken together, these studies highlight the potential roles of miRNAs in malaria infection.

Despite the fact that the presence of EVs-derived miRNAs has been demonstrated both in vitro and in experimental cerebral malaria [47], according to the literatures available, no study has analysed EVs-derived miRNAs in human plasma. Thus, this present study examined the relative expression of selected miRNAs isolated from human plasma EVs. In the present study, the relative expression among three biological groups was compared, i.e., *P. vivax*-infected or *P. falciparum*-infected patients and uninfected individuals. The whole population of circulating EVs, namely microvesicles together with exosomes were analysed to gain a better understanding of the whole EV-bound miRNA population and to not restrict this analysis to one sub-population. By studying the EV compartment as a whole the chances of finding differences in miRNA expression between the groups would be increased. Five miRNAs were selected based on previous in vitro, animal model, or clinical studies that suggested these miRNAs had a potential involvement in malaria, namely: hsa-miR-451a, hsa-miR-150-5p, hsa-miR-15b-5p, hsa-let-7a, and hsa-miR-16-5p [37–39, 41–44, 48]. This study provides novel insight about circulating EVs-derived miRNAs in human malaria.

## 3.2 Methods

### 3.2.1 Human samples collection and preparation

Malaria patients with *P. falciparum* or *P. vivax* were confirmed by microscopic examination by medical laboratory scientists at Buntharik district hospital in Ubon Rachathani. (Ethics approval by Ethics committee of the Faculty of Tropical Medicine, Mahidol University, MUTM 2012-046-05). Parasite species were identified and parasitaemia of each sample was calculated by counting the number of malaria-infected erythrocytes over the number of normal erythrocytes per thousand cells. Uninfected donors were recruited, and venipuncture was performed for all donors using tri-potassium ethylenediaminetetraacetic acid (K3EDTA) as an anticoagulant. K3EDTA blood samples were then centrifuged at  $1500\times g$  for 15 min.

Then, platelet-free plasma samples were prepared by centrifugation at  $13,000\times g$  for 2 min at room temperature (RT) [17]. Supernatants were collected and stored at  $-80\text{ }^{\circ}\text{C}$  for further isolation of EVs. Samples were then shipped to the University of Technology Sydney where all experiments were performed.

### 3.2.2 Extracellular vesicles isolation from human plasma

500  $\mu\text{L}$  of supernatants were mixed with 200  $\mu\text{L}$  of sodium citrate and 300  $\mu\text{L}$  of phosphate buffered saline (PBS) and then centrifuged at  $150,000\times g$  for 3 h at  $15\text{ }^{\circ}\text{C}$ . Supernatants were discarded and pellets were resuspended in 100  $\mu\text{L}$  sodium citrate and 900  $\mu\text{L}$  PBS and subjected to centrifugation at  $150,000\times g$  for 3 h at  $15\text{ }^{\circ}\text{C}$ .

### 3.2.3 Total RNA extraction

Pellets obtained after centrifugation were homogenized with 1 mL of RNAzol (Molecular Research Center, Inc) and 400  $\mu\text{L}$  of UltraPure™ DNase/RNase-Free distilled water (Invitrogen™). After a five-minute incubation at RT, they were centrifuged for 15 min at  $12,000\times g$  at  $4\text{ }^{\circ}\text{C}$ . Supernatants were transferred to new tubes with 800  $\mu\text{L}$  isopropanol and 5  $\mu\text{L}$  glycogen (5 mg/mL) then gently mixed. They were then placed at  $-30\text{ }^{\circ}\text{C}$  overnight and spun for 10 min at  $12,000\times g$  at  $4\text{ }^{\circ}\text{C}$  the next day. Pellets were kept and washed with cold 75% ethanol to remove excess isopropanol, spun at  $9000\times g$  for 3 min at  $4\text{ }^{\circ}\text{C}$ , the supernatant was discarded, and these steps were repeated twice. Later, excess ethanol was removed by spinning at  $12,000\times g$  for 30 s. RNA pellets were resolubilized with 10  $\mu\text{L}$  of UltraPure™ DNase/RNase-Free distilled water and heated for 5 min at  $55\text{ }^{\circ}\text{C}$ . Lastly, they were vortexed and briefly spun down.

### 3.2.4 Total RNA concentration measurement and cleaning

RNA concentration was measured using the NanoDrop One Microvolume UV–Vis Spectrophotometer (Thermo Scientific™). If the quality of total RNA in the samples was not optimal, i.e., the Nanodrop flagged the result as phenol contamination or Absorbance 260/230 < 1.7, a sodium acetate (NaOAc), a cleaning step was performed. Briefly, 5  $\mu\text{L}$  of glycogen (5 mg/mL) and 2.5  $\mu\text{L}$  of sodium acetate (3 M pH5.5) were added to samples and mixed comprehensively. The mixture was supplemented with 110  $\mu\text{L}$  of absolute ethanol and incubated overnight in  $-30\text{ }^{\circ}\text{C}$ . Later, washing steps were performed as mentioned in the RNA extraction with RNAzol above.

### 3.2.5 Primers for miRNAs detection

All primers in this study was purchased from Thermo Fisher Scientific.

Five human miRNAs were used to perform quantitative polymerase chain reaction as described in Table 3.1.

### 3.2.6 Reverse transcriptase quantitative polymerase chain reaction (RT-qPCR)

As the NanoDrop was not sensitive enough to measure the RNA concentration, fixed volumes of RNA for

**Table 3.1 Primers used for quantitative PCR**

miRNAs	NCBI accession number	Mature miRNAs sequences
hsa-miR-451a	MI0001729	AAACCGUUACCAUUACUGAGUU
hsa-miR-15b-5p	MI0000438	UAGCAGCACAUCAUGGUUUACA
hsa-miR-16-5p	MI0000070	UAGCAGCACGUAAAUAUUGGCG
hsa-let-7a-5p	MI0000060	UGAGGUAGUAGGUUGUAUAGUU
hsa-miR-150-5p	MI0000479	UCUCCCAACCCUUGUACCAGUG

cDNA synthesis were used. To analyse miRNAs expression, 0.5  $\mu$ L of total RNA was used for cDNA synthesis. RT-qPCR was performed as per manufacturer protocol using TaqMan<sup>®</sup> fast advanced master mix and TaqMan<sup>®</sup> advanced miRNA assay. Quantitative PCR (qPCR) was run on the QuantStudio 6 flex system (Applied Biosystem) in triplicate together with distilled water as negative control.

### 3.2.7 Relative expression analysis

Only samples that had not been already freeze-thawed were included in the study to avoid RNA degradation. Comparative threshold cycle or quantification cycle  $C_q$  (as described in [49]) method was used to analyse the qPCR data. Each sample was run in triplicates. Then, the average  $C_q$  from the three  $C_q$  values of those samples was calculated. To select one miRNA as an endogenous control, mean, standard deviation and variance for each miRNA analysed were calculated.  $\Delta C_q$  was then calculated using the following equation  $\Delta C_q = C_q$  of miRNA –  $C_q$  of endogenous control and relative expression was calculated by  $2^{(-\Delta\Delta C_q)}$  [50].

### 3.2.8 Target prediction and pathway involvement of dysregulated miRNAs

To predict possible targets of up-regulated miRNAs, the miRNAs of interest was submitted to Targetscan Release 7.2 and the predicted target genes were retrieved [51]. Then, the targets that overlapped genes involved in

malaria pathway were obtained from the Kyoto Encyclopedia of Genes and Genomes (KEGG) [52]. In order to identify the pathways for individual and combined analysis of miRNAs, DIANA-mirPath v3.0 was used, with a 5% false discovery rate (FDR) [53]. Fisher's exact test (Hypergeometric distribution) was applied for enrichment analysis. The potential pathways were considered based on their  $p$  value ( $p < 0.05$ ).

### 3.2.9 Evaluation of potential EVs-derived miRNA as biomarker

Mean of Delta Cq for each miRNA was used in this analysis following the previous study [54]. The receiver operating characteristic (ROC) was calculated to propose the potential use of miRNAs as diagnostic tools. Area under the curve (AUC) was analysed to show the accuracy of the test with  $p$ -value of each analysis.

### 3.2.10 Statistical analysis

For the samples, demographic, mean age of each group was presented by average and standard deviation. All data was tested for their normality by using Kolmogorov–Smirnov or Shapiro–Wilk tests and a non-parametric statistical analysis method was chosen. Comparison of parasitaemia percentage was achieved by the Mann–Whitney U Test. Kruskal–Wallis test was used for comparison of relative expression of miRNAs in each biological group followed by post hoc analysis using Dunn's test. Statistical significance for all tests was considered significant for  $\alpha = 0.05$ . All statistical tests were analysed by Prism 8. All figures shown in this article were created by Prism 8 software for Mac, GraphPad Software, La Jolla California USA, <https://www.graphpad.com>.

## 3.3 Results

### 3.3.1 Patient's characteristics

57 plasma samples were included in this study divided into three groups; *P. vivax*-infected patients ( $n = 19$ ), *P. falciparum*-infected patients ( $n = 18$ ), and uninfected community individuals ( $n = 20$ ) as per Table 3.2. The average age of malaria patients (Mean  $\pm$  SD) was

**Table 3.2 Sample characteristic**

Characteristics	PV-infected patients	PF-infected patients	Uninfected
Total number of patients	19	18	20
Gender			
Male	16	17	11
Female	3	1	9
Age (Mean $\pm$ SD)*	31.6 $\pm$ 9.59	33.4 $\pm$ 11.91	21.8 $\pm$ 0.89
% Parasitaemia (Mean $\pm$ SD)**	0.35 $\pm$ 0.28	1.29 $\pm$ 1.48	

\* Mean and SD of age *P. vivax*-infected patients was calculated from 10 patients, Mean and SD of age of PF-infected patients was calculated from 15 patients

\*\* %parasitaemia of *P. vivax*-infected patients calculated from 16 patients. %parasitaemia of PF-infected patients calculated from 14 patients



32.68 ± 11.08 years, *P. vivax*-infected patients was 31.6 ± 9.59, and *P. falciparum*-infected patients was 33.4 ± 11.91. The average age of uninfected individuals (21.8 ± 0.89 years) was significantly lower than both *P. vivax*-infected patients or *P. falciparum*-infected patients ( $p = 0.018$ ,  $p = 0.001$ , respectively). Percentage of parasitaemia (% Parasitaemia) of *P. vivax*-infected patients was 0.35 ± 0.28 while *P. falciparum*-infected patients was 1.29 ± 1.48. Overall parasitaemia was higher in *P. falciparum*-infected patients than *P. vivax*-infected patients ( $p = 0.0115$ ) as shown in Fig. 3.1a.

### 3.3.2 Relative expression of miRNAs in three biological groups

Total RNA was extracted from EVs pellets and analysed hsa-miR-451a, hsa-miR-15b-5p, hsa-miR-16-5p, hsa-let-7a-5p and hsa-miR-150-5p among *P. vivax*-infected patients, *P. falciparum*-infected patients and uninfected individuals. The average  $C_q$  was calculated from triplicate run (Fig. 3.1b). Hsa-miR-451a had the lowest  $C_q$  with the minimum standard deviation compared to the other miRNAs, at 26.36 ± 2.33 (Mean ± SD). A Kruskal–Wallis

test was undertaken to compare the  $C_q$  values in each biological group and showed that the values were not statistically different. These results indicated that this miRNA was the most stable among three biological groups and could be used as internal control. Moreover, previous studies demonstrated that hsa-miR-451a was highly expressed in both uninfected and parasitized red blood cells [32] and its expression was independent on the intra-erythrocytic development of the malaria parasite [33].

In the present study, EVs were isolated from Thai patients presenting with uncomplicated malaria and demonstrated that miRNAs can be detected in these EVs. Descriptive statistics of  $C_q$  values are presented in Table 3.3. The relative expression of each miRNA was calculated using hsa-miR-451a as endogenous control using the  $2^{(-\Delta\Delta C_q)}$  method [50]. The relative expressions of hsa-miR-15b-5p, hsa-miR-16-5p, hsa-let-7a-5p and hsa-miR-150-5p were compared between malaria-infected (regardless of the parasite species) and uninfected individuals (Fig. 3.2). Hsa-miR-150-5p ( $p = 0.0054$ ),

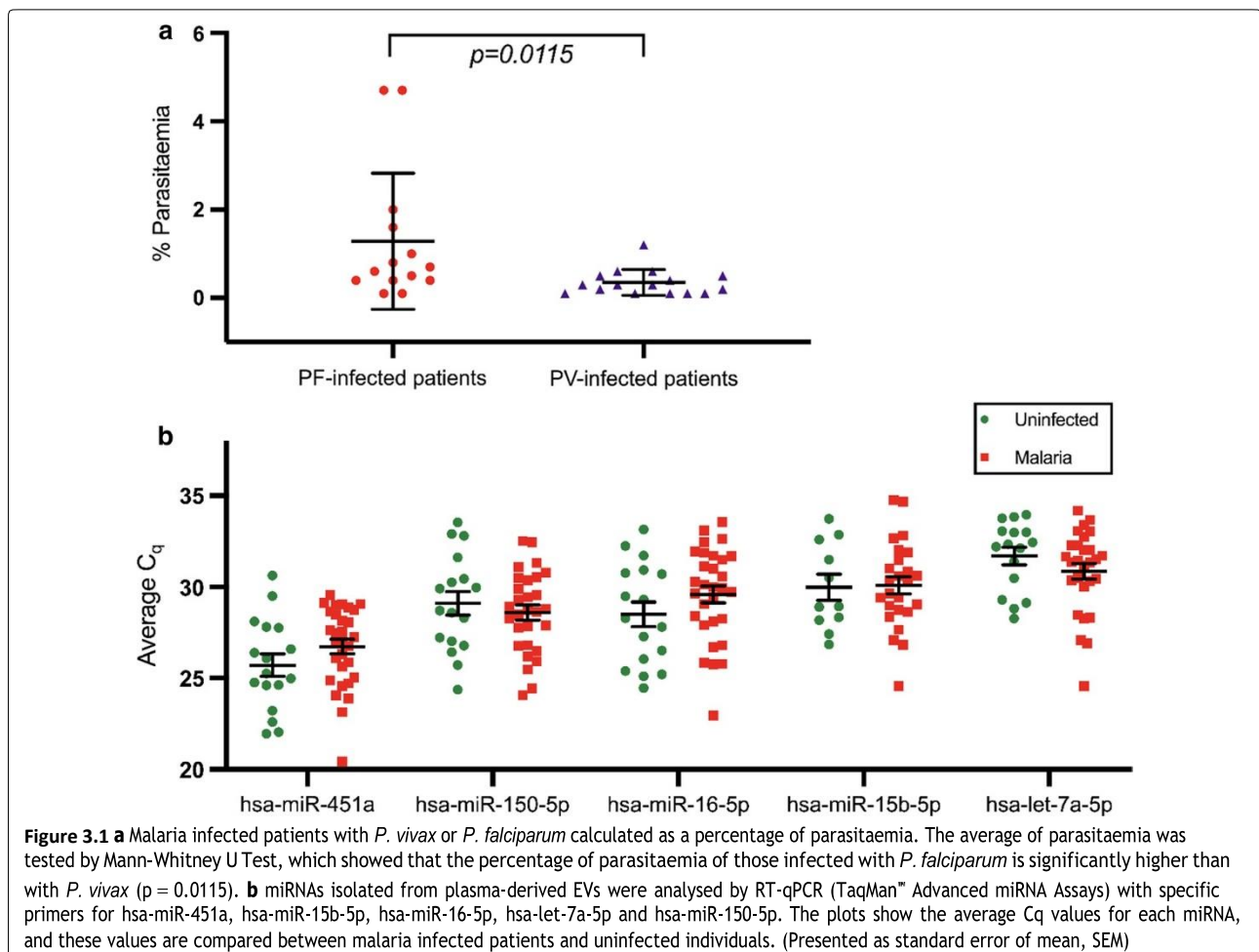




**Table 3.3** Descriptive statistics of quantification cycle (C<sub>q</sub>) values

miRNAs	Min C <sub>q</sub>	Max C <sub>q</sub>	Mean ± SD	Coefficient of variation(%)
hsa-miR-451a	20.43	30.63	26.36 ± 2.33	8.84
hsa-miR-15b-5p	24.57	34.77	30.06 ± 2.34	7.77
hsa-miR-16-5p	22.96	33.57	29.20 ± 2.65	9.09
hsa-let-7a-5p	24.57	34.19	31.17 ± 2.15	6.91
hsa-miR-150-5p	24.07	33.54	28.78 ± 2.37	8.24

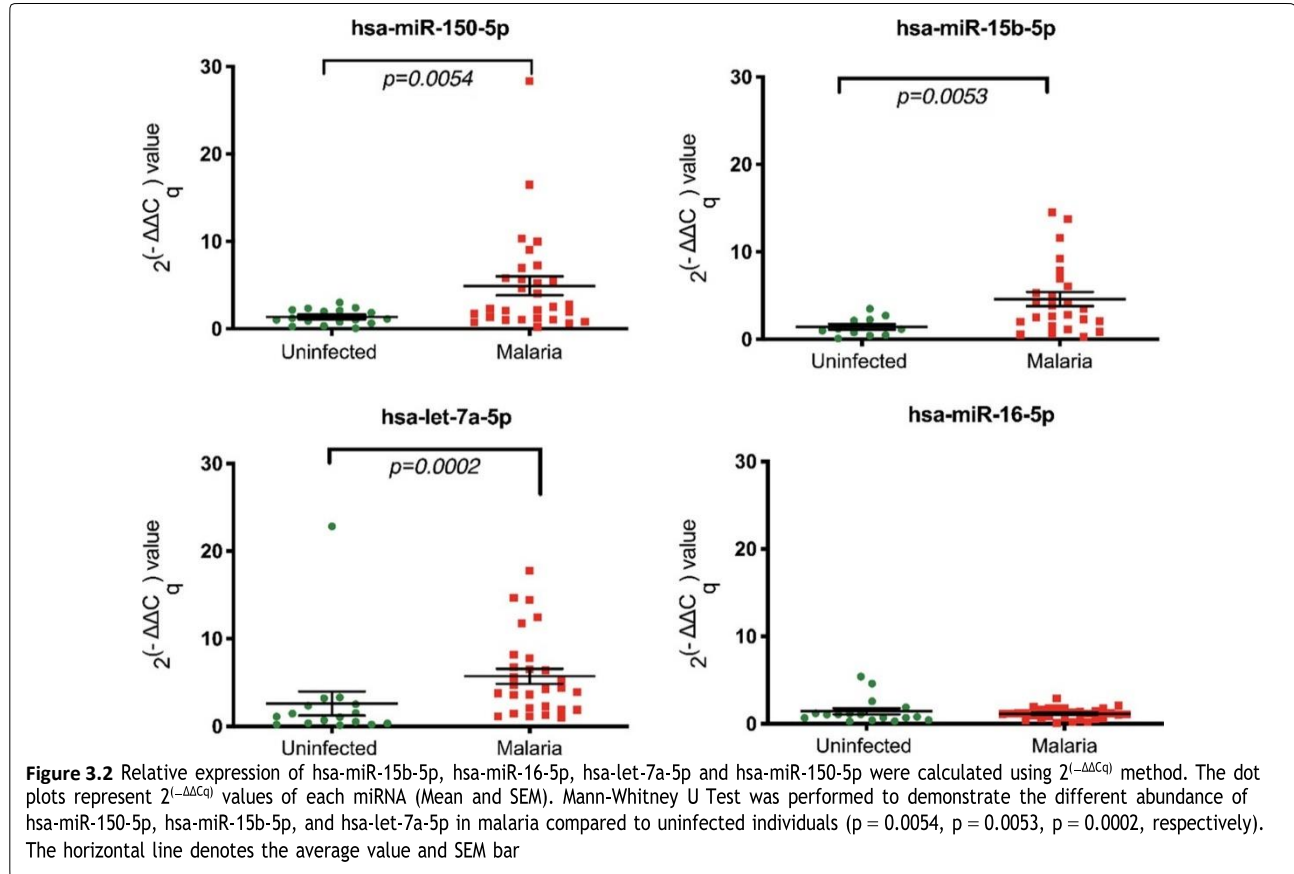
hsa-miR-15b-5p (p = 0.0053) and hsa-let-7a-5p (p = 0.0002) were significantly up-regulated in EVs from malaria-infected patients comparing to the uninfected group. However, the relative expression of hsa-miR-16-5p between infected and non-infected individuals was not different.

Next, the changes in the abundance of these miRNAs were examined among the three biological groups (Fig. 3.3). An up-regulation of hsa-miR-150-5p (p = 0.0119) and hsa-miR-15b-5p (p = 0.0052) was observed in EVs

from *P. vivax*-infected patients. Remarkably, hsa-let-7a-5p expression was higher in both *P. vivax*-infected patients and *P. falciparum*-infected patients (p = 0.0025, p = 0.0145, respectively). When those parameters were compared between *P. vivax*-infected patients and *P. falciparum*-infected patients, there was no difference. The descriptive analysis of each miRNA in each group is presented in Table 3.4.

**3.3.3 Target prediction and KEGG Pathway analysis of hsa-miR150-5p and hsa-miR-15b-5p**

In order to study the possible roles of up-regulated miRNAs in malaria patients, the prediction was made using Targetscan. These targets were later overlapped with genes involved in the biological pathways that are relevant to malaria. There were 15, 5, and 6 targets of hsa-miR-150-5p, hsa-miR-15b-5p, and hsa-let-7a-5p, respectively as shown in Additional file 1: Table S3.1. Some targets were regulated by more than one miRNA of interest. Hepatocyte growth factor (HGF) encoding gene was regulated by all up-regulated miRNAs. Toll-like receptor 4 (TLR4), interleukin 10, and thrombospondin-1 were found regulated by hsa-miR-150-5p and hsa-let-7a-5p.



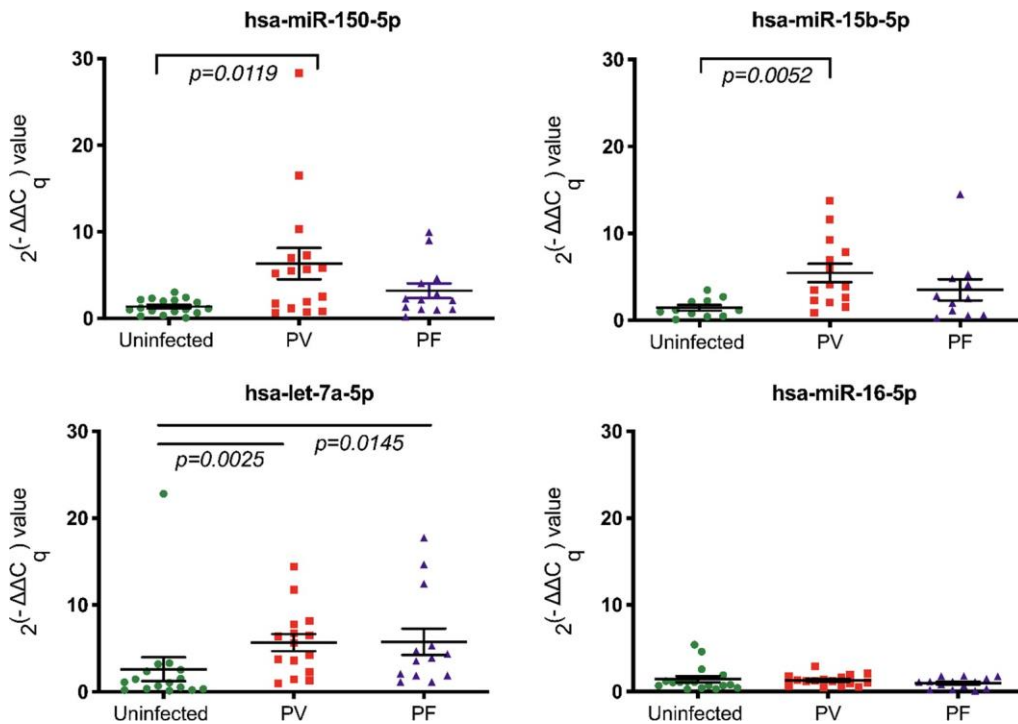


**Figure 3.3** This dot plot demonstrates the miRNAs expression values in 3 biological groups (Uninfected, *P. vivax*-infected patients or *P. vivax*, and *P. falciparum*-infected patients or *P. falciparum*). The Kruskal-Wallis was tested and followed by post hoc analysis using Dunn's test. hsa-miR-150-5p, hsa-miR-15b-5p were significantly up-regulated in *P. vivax* ( $p=0.0119$ ,  $p=0.0052$ , respectively). Relative expression of hsa-let-7a-5p was higher in both *P. vivax* and *P. falciparum* ( $p=0.0025$ ,  $p=0.0145$ , respectively). The horizontal line denotes the average value and SEM bar

**Table 3.4** Relative expression analysis of miRNAs

	$\Delta C_q$ (Mean $\pm$ SD)	$2^{(-\Delta\Delta C_q)}$ Mean (Mean $\pm$ SD)
<b>hsa-let-7a-5p</b>		
Uninfected	6.23 $\pm$ 1.91	1.28 $\pm$ 1.10
PV	4.09 $\pm$ 1.17	5.68 $\pm$ 3.85
PF	4.26 $\pm$ 1.32	5.76 $\pm$ 5.52
<b>hsa-miR-15b-5p</b>		
Uninfected	5.34 $\pm$ 1.49	1.43 $\pm$ 1.07
PV	3.29 $\pm$ 1.17	5.45 $\pm$ 3.96
PF	4.33 $\pm$ 1.68	3.51 $\pm$ 4.04
<b>hsa-miR-16-5p</b>		
Uninfected	2.79 $\pm$ 1.22	1.44 $\pm$ 1.47
PV	2.56 $\pm$ 0.72	1.31 $\pm$ 0.64
PF	3.21 $\pm$ 1.32	1.00 $\pm$ 0.60
<b>hsa-miR-150-5p</b>		
Uninfected	3.39 $\pm$ 1.44	1.37 $\pm$ 0.86
PV	1.54 $\pm$ 1.64	6.32 $\pm$ 7.23
PF	2.33 $\pm$ 1.49	3.20 $\pm$ 3.07

Next, to get insight into these up-regulated miRNAs, a KEGG pathway analysis was performed using DIANA-mirPath v3.0 that searches against experimentally validated miRNAs targets on Tarbase v7.0. The pathway analysis revealed 10, 22, and 32 pathways that were statistically overrepresented by targeted genes of hsa-miR-150-5p, hsa-miR-15b-5p, and hsa-let-7a-5p, respectively. When the combined analysis of up-regulated miRNAs was determined, there were 44 enriched pathways. Of those enrichment pathways, the overlapped pathways included adherens junction (5th in the list,  $p=2.52E^{-10}$ ) as well as TGF-beta signaling pathway (11th in the list,  $p=1.64E^{-7}$ ). Other important pathways that might engage in malaria were extracellular matrix (ECM)-receptor interaction (14th in the list,  $p=0.0005$ ), FoxO signaling pathway (29th in the list,  $p=0.0332$ ) and HIF-1 signaling pathway (30th in the list,  $p=0.0353$ ). In Fig. 3.4, the top 10 enriched pathways analysis were presented according to their ranks based on p-value.

### 3.3.4 Evaluation of the diagnostic potential of extracellular vesicles-derived miRNAs

In addition, this study aimed to investigate whether the EVs-bound miRNAs could be used as putative diagnostic

(See figure on next page.)

**Figure 3.4** Pathway enrichment analysis of up-regulated miRNAs were carried out by DIANA-mirPath v3.0 which searching against experimentally validated miRNAs targets on Tarbase v7.0. The combinatorial effect of up-regulated miRNAs was determined. Of those enriched pathways, the malaria-relevant pathways was found including adherens junction and TGF-beta signaling pathway. The bar chart presents with top 10 enriched pathway. The horizontal lines present -log<sub>10</sub> p-values

markers. The ROC was used, and the AUC was calculated for each miRNA in both *P. falciparum*-infected patients and *P. vivax*-infected patients. Three miRNAs showed a statistical significance in the *P. vivax*-infected patients. hsa-miR-150-5p AUC was 0.7794 ( $p = 0.0062$ ), hsa-miR-15b-5p AUC was 0.8766 ( $p = 0.0015$ ) and hsa-let-7a was 0.8375 ( $p = 0.0014$ ). In the *P. falciparum*-infected patients, only hsa-let-7a-5p was statistically significant with AUC 0.8221 ( $p = 0.0033$ ). Area under the ROC was shown with 95% confidence interval value (Fig. 3.5).

### 3.4 Discussion

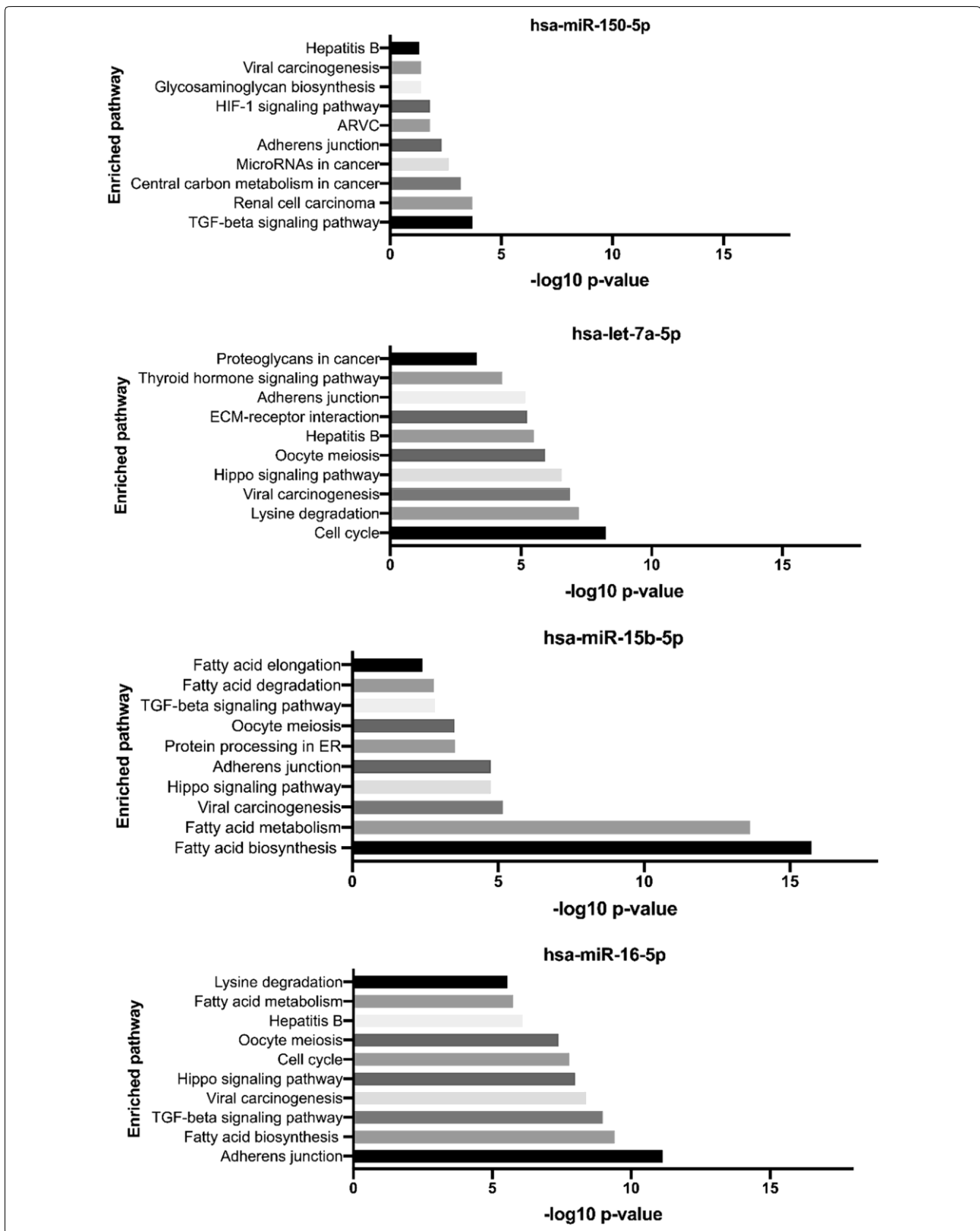
The present study, demonstrated that miRNAs can be detected in EVs were isolated from the blood of both Thai patients presenting with uncomplicated malaria and healthy donors. The miRNAs selected included hsa-miR-451a, hsa-miR-15b-5p, hsa-miR-16-5p, hsa-let-7a-5p and hsa-miR-150-5p that were previously analysed in the context of malaria [37–39, 41–44, 48]. As mentioned earlier, hsa-miR-451a was selected as endogenous control as its Cq values were the most stable among three groups. In contrast, Chamnanchanunt et al. found that hsa-miR-451a was down-regulated in *P. vivax*-infected patient plasma [44]. Other studies demonstrated that EVs cargo hsa-miR-451a could be internalized to target the parasites and diminish the parasite burden [38, 43]. Furthermore, in an in vitro study, red blood cell derived EVs containing hsa-miR-451a and human argonaute 2 (Ago2) were shown to be internalized by endothelial cells. This miR-Ago2 could down-regulate the expression of CAV-1 and ATF2 resulting in endothelial cells alteration which is a plausible factor contributing vascular dysfunction in cerebral malaria [42]. As various studies showed that EVs that cargo hsa-miR-451a could be taken up by various cells in the context of malaria, it would, therefore, be interesting to enumerate the number of EVs and compare it with the change in abundance of hsa-miR-451a.

The hsa-miR-15b-5p and hsa-miR-150-5p were up-regulated in the plasma-derived EVs from *P. vivax*-infected patients but not in the *P. falciparum*-infected patients. An analysis of miRNAs from whole blood of adult imported falciparum malaria showed a down regulation of hsa-miR-150-5p [48]. Kaur et al. have identified a potential biomarker for differential diagnosis between uncomplicated and complicated *P. vivax* malaria infection, hsa-miR-7977. In addition, an increase in this

miRNA was predicted to be involved in malaria pathogenesis through the transforming growth factor beta (TGF- $\beta$ ) signaling pathway [48]. Recently, a study in non-human primate (*Aotus lemurinus lemurinus*) confirmed that bone marrow is an important reservoir for gametocytogenesis and proliferation of *P. vivax* [55]. A study in bone marrow aspirate of human diagnosed with *P. vivax* showed an aberrant expression of miRNAs in CD71 positive erythroid cells during infection, hsa-miR-150 and hsa-miR-16 were down-regulated while hsa-miR-144 was increased. However, hsa-miR-451a, the most abundant erythroid miRNA, remained stable [56]. In experimental cerebral malaria (ECM), an investigation in brain tissue found a higher expression of miR-150 while microvesicles from ECM mice showed non statistically different change of miR-150 expression [39, 47]. Nonetheless, this present study only investigated the plasma from the patients before drug administration and the clinical manifestation after treatment were not followed. Taken together, these data suggest that hsa-miR-150-5p might be an essential miRNA involved in malaria infection.

The relative expression of hsa-miR-15b-5p was higher in EVs from *P. vivax*-infected patients. To date, there is no evidence about the altered expression of this miRNA which might link to *P. vivax* malaria. However, this miRNA is present in *P. falciparum* in vitro and its abundance was decreased following infection. Also, it was potentially predicted to form a chimeric fusion with ring-infected erythrocyte surface antigen (RESA) [38]. Even though the relative expression of this miRNA was not statistically significant in *P. falciparum*-infected patients, it was noticed in this study that it was slightly higher when this miRNA was compared with the uninfected group.

Next, the relative expression of hsa-let-7a, which was found in infected erythrocytes [33], was determined. The relative abundance of hsa-let-7a was significantly increased in both *P. vivax*-infected patients and *P. falciparum*-infected patients compared to uninfected controls. These results are in accordance with previous studies showing that this miRNA could be detected in EVs and might be derived from parasitized red blood cells [41, 42]. It is noteworthy that the overall expression of this miRNA is higher in the malaria patients (regardless of the parasite) than in uninfected donors. Several studies demonstrated that hsa-let-7a plays a role in host-parasite interaction [37, 41]. This miRNA in complex



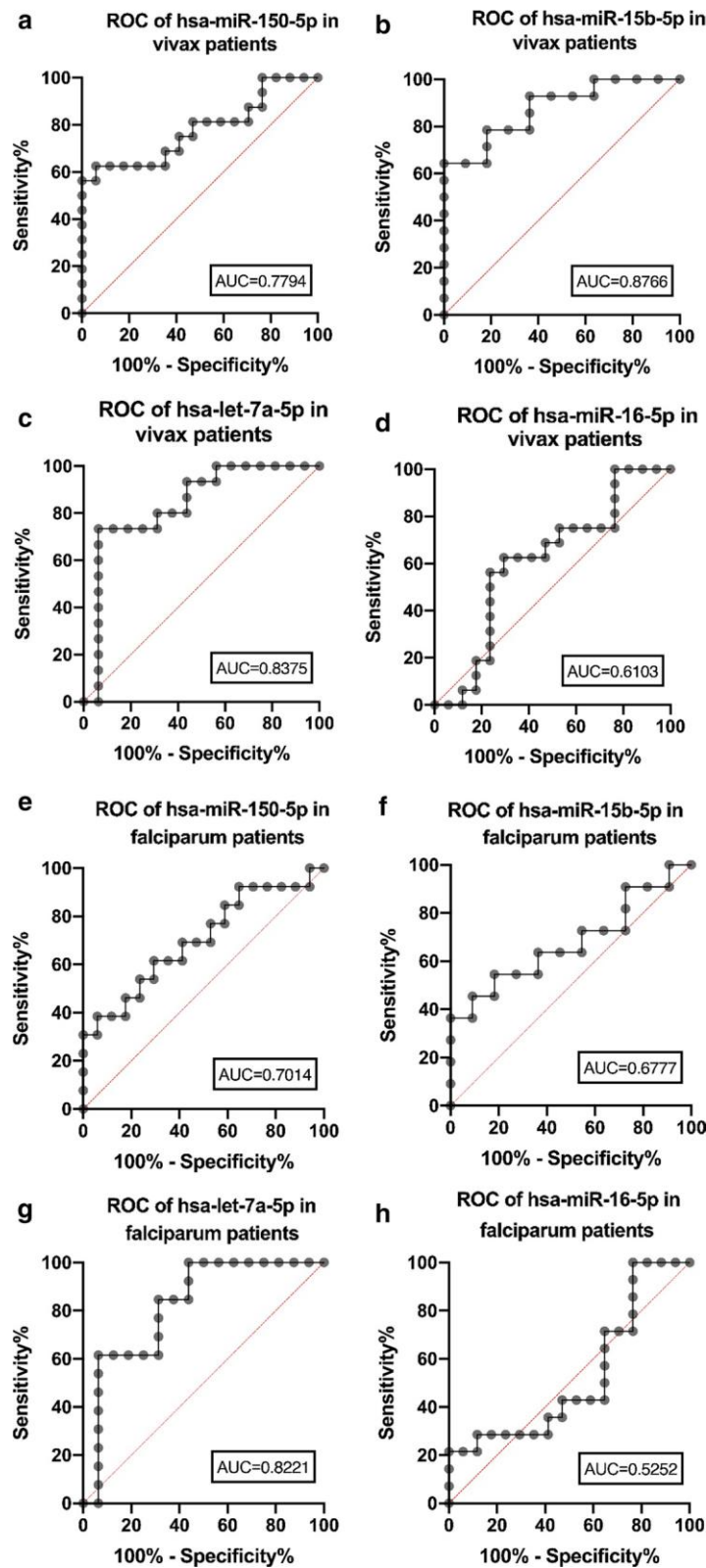


**Figure 3.5** Area Under the Receiver Operating Characteristic (ROC) curve (AUC) analysis. The AUC of each tests presents with the maximum AUC. In *P. vivax*-infected patients, hsa-miR-150-5p AUC was 0.7794 ( $p = 0.0062$ ), hsa-miR-15b-5p AUC was 0.8766 ( $p = 0.0015$ ), and hsa-let-7a was 0.8375 ( $p = 0.0014$ ). For the *P. falciparum*-infected patients, there was the hsa-let-7a-5p that was statistically significant with AUC 0.8221 ( $p = 0.0033$ )



with Ago2 [41] could be detected in *P. falciparum* and potentially targets the *Plasmodium* gene: Rad54 [37]. In addition, hsa-let-7a expression was low in erythrocyte-derived EVs in a *P. falciparum* in vitro experiment but another member in the let7 family: hsa-let-7b was higher in the EVs fraction compared to infected or uninfected erythrocytes. Interestingly, miRNAs profiling from in vitro *P. falciparum* infected erythrocyte-derived EVs also showed that hsa-let-7a, hsa-let-7i, hsa-let-7 g and hsa-let-7f were highly expressed [42]. Some of these miRNAs might derive from parasitized red blood cells as they were found highly enriched in previous analyses [33]. In addition, a study in experimental cerebral malaria demonstrated an increased expression of let-7i in brain tissues which might link to cerebral malaria pathogenesis [39]. This implies that miRNAs within the let-7 family might play a role in the parasite biology, malaria pathogenesis and further studies should be performed to elucidate their functions.

Furthermore, the relative expression of hsa-miR-16-5p was analysed. There was no change in the abundance both in *P. vivax*-infected patients and *P. falciparum*-infected patients when compared to uninfected individuals. This is consistent with two previous studies showing that hsa-miR-16-5p is highly expressed in both *P. falciparum*-infected erythrocytes and normal erythrocytes. Thus, the relative expression of this miRNA might not be modulated during infection. However, these results differ from a study that found down-regulation of hsa-miR-16-5p in *P. vivax*-infected patients [44]. Interestingly, a previous study using an ECM model (*P. berghei* strain ANKA) found an up-regulation of miR-16 in plasma-derived microvesicles [47] suggesting that further studies are needed to elucidate the expression of this miRNA during complicated and uncomplicated malaria infection.

Several pathways might be important in the context of malaria. Importantly, the adherens junction and the transforming growth factor (TGF)- $\beta$  were found enriched by the targeted genes of 3 dysregulated miRNAs. Adherens junctions are possibly regulated by hsa-miR-150-5p, hsa-miR-15b-5p and hsa-let-7a-5p. The blood-brain barrier (BBB) is a vital compartment of central nervous system as it separates the CNS from surrounding environment. Adherens junctions in endothelial cells participate to the forming and maintaining of the integrity of the BBB. A number of studies also showed that some miRNAs might regulate this type of junction. For example, the down regulation of vascular endothelium cadherin (VE-Cadherin) was affected by overexpression of miR-101 and this lead to HIV-associated neurological disorder [57]. Also, the overexpression of miR-142-3p repressed the expression of VE-Cadherin and impaired vascular integrity in zebrafish [58]. Similarly, in ECM, the

authors postulated the roles of overexpressed miR-19a-3p and miR-19b-5p in this pathway as well [40]. Knowing the roles of miRNAs in the context of malaria particularly cerebral malaria pathogenesis is paramount as it might lead to the development of an adjunctive therapy. For instance, inhibition of miR-27 could prevent vascular leakage associated with ischaemia [59]. However, no study of the dysregulated miRNAs analysed in this work, which are in association with this pathway, has been performed in human malaria. More studies are therefore needed to fill this gap.

Circulating miRNAs have been studied and proposed as diagnostic biomarkers in many infectious diseases including malaria. Most studies on infectious diseases have detected human miRNAs such as those in tuberculosis [60], hepatitis B [61], schistosomiasis [62] while some studies investigated microbial miRNAs as biomarkers as well [54, 63–65]. Despite the fact that *Plasmodium spp.* lack RNA interference machinery and its own miRNAs [32, 36], human derived miRNAs were demonstrated as promising biomarkers [44, 48]. For example, in human malaria, hsa-miR-16 and hsa-miR-451a were proposed to be biomarkers for *P. vivax* infection diagnosis [44]. In the present study, the potential of miRNAs isolated from EVs in malaria patients was evaluated for the first time. The calculated p-values from AUC analysis indicated that hsa-miR-150-5p, hsa-miR-15b-5p might be used as biomarkers for *P. vivax* malaria whereas hsa-let-7a-5p might be used to test for both *P. vivax* and *P. falciparum* malaria. However, the sensitivity and specificity were not much higher. Therefore, further analysis of these miRNAs is recommended because the number of patient samples were relatively low in this study. Furthermore, as mentioned earlier, this study selected the miRNAs based on previous studies that investigated these miRNAs in the context of malaria. A more in-depth study is needed to develop new biomarkers. For instance, profiling miRNA using microarrays or next-generation sequencing will allow an evaluation of all miRNAs present in the EVs. Also, these miRNAs should be analysed in the patients after they recover from the disease. It might be useful in the context of *P. vivax* malaria as this species can cause relapse infection. In addition, these markers should be further analysed and compared in the different groups of *P. falciparum* malaria patients such as uncomplicated and severe malaria. These will be useful if patients can be early predicted the chance of developing severe malaria beforehand.

### 3.5 Conclusion

This novel study explored hsa-miR-150-5p, hsa-miR-15b-5p, hsa-let-7a-5p, and hsa-miR-16-5p which were isolated from EVs from Thai malaria patient's plasma.

The relative expression of hsa-miR-150-5p and hsa-miR-15b-5p were significantly higher in *P. vivax*-infected patients where hsa-let-7a-5p was significantly up-regulated in both *P. vivax*-infected patients and *P. falciparum*-infected patients. Targets prediction and pathways enrichment analysis also provided the possible roles of these up-regulated miRNAs in the context of malaria, especially the TGF- $\beta$  pathway, which need further investigation to elucidate their exact roles in the malaria biology and the disease pathogenesis.

As this current study only evaluated those miRNAs from EVs of uncomplicated malaria patients, it is therefore encouraging to analyse in the future the EVs-derived miRNAs in those patients with severe complications.

### Supplementary information

**Supplementary information** accompanies this paper at <https://doi.org/10.1186/s12936-020-03360-z>.

**Additional file 1: Table S3.1.** Individual target prediction of up-regulated miRNAs and genes involved in malaria pathway.

### Acknowledgements

The authors acknowledge Assistant Professor Tewarit Sarachana and Miss Surangrat Thongkorn for their invaluable advice in the data analysis.

### Authors' contributions

NK, ISC, MI, VC and DP designed and conceived the study. ISC, FD and NT designed the qPCR assays for the paper. ISC and FD performed the experimental studies. NK, ISC and VC contributed to the data analysis. NK performed bioinformatic analysis, interpreted and wrote the manuscript. All authors provided advice in figure preparation and manuscript revision. All authors read and approved the final manuscript.

### Funding

This research was funded by Chulalongkorn University and Thailand Science Research Innovation (TSRI), RTA6280006. Nutpakal Ketprasit was financially supported both tuition fees and monthly stipend by the scholarship from Graduate School, Chulalongkorn University to commemorate the 72nd Anniversary of his Majesty King Bhumibol Adulyadej of 2016 academic year. For research expense, Nutpakal was funded by the 90th Anniversary Chulalongkorn University Fund (Ratchadaphiseksomphot Endowment Fund: GCU-GR1125602095M) of 2016 academic year and Overseas research scholarship of 2016 academic year supported by Graduate school and Faculty of Allied Health Sciences, Chulalongkorn University. Iris Simone Cheng is supported by the Australian Government Research Training Program Stipend.

### Availability of data and materials

The datasets used and/or analysed during the current study are available from the corresponding authors on reasonable request.

### Ethical approval

Ethics approval by Ethics committee of the Faculty of Tropical Medicine, Mahidol University, MUTM 2012-046-05. Ethics approval for the University of Technology Sydney, UTS HREC ETH18-2756.

### Consent for publication

All authors reviewed and consented the final manuscript for publication.

### Competing interests

All authors declare no competing interests, no personal or professional conflicts of interest, and no financial support from the companies that produce and/or distribute the devices, or materials described in this report.

### Author details

<sup>1</sup> Malaria and Microvesicles Research Group, School of Life Sciences, Faculty of Sciences, University Technology of Sydney, Ultimo, Sydney, NSW 2007, Australia. <sup>2</sup> Graduate Programme in Clinical Hematology Sciences, Department of Clinical Microscopy, Faculty of Allied Health Sciences, Chulalongkorn University, Bangkok, Thailand. <sup>3</sup> Non-coding RNA Cancer Group, School of Biomedical Engineering, Faculty of Engineering and IT, University Technology of Sydney, Sydney, NSW, Australia. <sup>4</sup> Department of Molecular Tropical Medicine and Genetics, Faculty of Tropical Medicine, Mahidol University, Bangkok, Thailand. <sup>5</sup> Oxidation in Red Cell Disorders Research Unit, Department of Clinical Microscopy, Faculty of Allied Health Sciences, Chulalongkorn University, 154 Rama 1 Road, Pathumwan, Bangkok 10330, Thailand.

Received: 21 March 2020 Accepted: 5 August 2020

Published online: 10 August 2020

### 3.6 References

- World Health Organization. World malaria report 2019. Geneva: WorldHealth Organization; 2019.
- White NJ. Malaria. In: Manson's Tropical Diseases, 23rd Edn. Farrar J, Hotez P, Thomas Junghanss T, Kang G, Lalloo D, White NJ, Eds. Saunders Ltd Publ.; 2014.
- Ashley EA, Dhorda M, Fairhurst RM, Amaratunga C, Lim P, Suon S, et al. Spread of artemisinin resistance in *Plasmodium falciparum* malaria. *N Engl J Med*. 2014;371:411–23.
- Hamilton WL, Amato R, van der Pluijm RW, Jacob CG, Quang HH, Thuy-Nhien NT, et al. Evolution and expansion of multidrug-resistant malaria in southeast Asia: a genomic epidemiology study. *Lancet Infect Dis*. 2019;19:943–51.
- Andaloussi SE, Mäger I, Breakefield XO, Wood MJ. Extracellular vesicles: biology and emerging therapeutic opportunities. *Nat Rev Drug Discov*. 2013;12:347–57.
- Caruso S, Poon IKH. Apoptotic cell-derived extracellular vesicles: more than just debris. *Front Immunol*. 2018;9:1486.
- György B, Szabó TG, Pásztói M, Pál Z, Misják P, Aradi B, et al. Membrane vesicles, current state-of-the-art: emerging role of extracellular vesicles. *Cell Mol Life Sci*. 2011;68:2667–88.
- Hugel B, Martínez MC, Kunzelmann C, Freyssinet J-M. Membrane micro-particles: two sides of the coin. *Physiology*. 2005;20:22–7.
- Hugel B, Socié G, Vu T, Toti F, Gluckman E, Freyssinet J-M, et al. Elevated levels of circulating procoagulant microparticles in patients with paroxysmal nocturnal hemoglobinuria and aplastic anemia. *Blood*. 1999;93:3451–6.
- Nantakomol D, Dondorp AM, Krudsood S, Udomsangpetch R, Pattanapanyasat K, Combes V, et al. Circulating red cell-derived microparticles in human malaria. *J Infect Dis*. 2011;203:700–6.
- Combes V, Taylor TE, Juhan-Vague I, Mege JL, Mwenechanya J, Tembo M, et al. Circulating endothelial microparticles in malawian children with severe falciparum malaria complicated with coma. *JAMA*. 2004;291:2542–4.
- Iraci N, Leonardi T, Gessler F, Vega B, Pluchino S. Focus on extracellular vesicles: physiological role and signalling properties of extracellular membrane vesicles. *Int J Mol Sci*. 2016;17:171.
- Schorey JS, Cheng Y, Singh PP, Smith VL. Exosomes and other extracellular vesicles in host–pathogen interactions. *EMBO Rep*. 2015;16:24–43.
- Shah R, Patel T, Freedman JE. Circulating extracellular vesicles in human disease. *N Engl J Med*. 2018;379:958–66.
- Mfonkeu JBP, Gouado I, Kuate HF, Zambou O, Zollo PHA, Grau GER, et al. Elevated cell-specific microparticles are a biological marker for cerebral dysfunctions in human severe malaria. *PLoS ONE*. 2010;5:e13415.
- El-Assaad F, Wheway J, Hunt NH, Grau GE, Combes V. Production, fate and pathogenicity of plasma microparticles in murine cerebral malaria. *PLoS Pathog*. 2014;10:e1003839.
- Combes V, Coltel N, Alibert M, Van Eck M, Raymond C, Juhan-Vague I, et al. ABCA1 gene deletion protects against cerebral malaria: potential pathogenic role of microparticles in neuropathology. *The American journal of pathology*. 2005;166(1):295–302.

18. Campos FMF, Franklin BS, Teixeira-Carvalho A, Filho ALS, de Paula SCO, Fontes CJ, et al. Augmented plasma microparticles during acute *Plasmodium vivax* infection. *Malar J*. 2010;9:327.
19. Martin-Jaular L, Nakayasu ES, Ferrer M, Almeida IC, del Portillo HA. Exosomes from *Plasmodium yoelii*-infected reticulocytes protect mice from lethal infections. *PLoS ONE*. 2011;6:e26588.
20. Sahu U, Sahoo PK, Kar SK, Mohapatra BN, Ranjit M. Association of TNF level with production of circulating cellular microparticles during clinical manifestation of human cerebral malaria. *Hum Immunol*. 2013;74:713–21.
21. Tiberti N, Latham SL, Bush S, Cohen A, Opoka RO, John CC, et al. Exploring experimental cerebral malaria pathogenesis through the characterisation of host-derived plasma microparticle protein content. *Sci Rep*. 2016;6:37871.
22. Couper KN, Barnes T, Hafalla JCR, Combes V, Ryffel B, Secher T, et al. Parasite-derived plasma microparticles contribute significantly to malaria infection-induced inflammation through potent macrophage stimulation. *PLoS Pathog*. 2010;6:e1000744.
23. Ye W, Chew M, Hou J, Lai F, Leopold SJ, Loo HL, et al. Microvesicles from malaria-infected red blood cells activate natural killer cells via MDA5 pathway. *PLoS Pathog*. 2018;14:e1007298.
24. Mantel P-Y, Hoang Anh N, Goldowitz I, Potashnikova D, Hamza B, Vorobjev I, et al. Malaria-infected erythrocyte-derived microvesicles mediate cellular communication within the parasite population and with the host immune system. *Cell Host Microbe*. 2013;13:521–34.
25. Regev-Rudzki N, Wilson DW, Carvalho TG, Sisquella X, Coleman BM, Rug M, et al. Cell-cell communication between malaria-infected red blood cells via exosome-like vesicles. *Cell*. 2013;153:1120–33.
26. Correa R, Coronado L, Caballero Z, Faral P, Robello C, Spadafora C. Extracellular vesicles carrying lactate dehydrogenase induce suicide in increased population density of *Plasmodium falciparum* *in vitro*. *Sci Rep*. 2019;9:5042.
27. Sisquella X, Ofir-Birin Y, Pimentel MA, Cheng L, Abou Karam P, Sampaio NG, et al. Malaria parasite DNA-harboring vesicles activate cytosolic immune sensors. *Nat Commun*. 2017;8:1985.
28. Cheng L, Sharples RA, Scicluna BJ, Hill AF. Exosomes provide a protective and enriched source of miRNA for biomarker profiling compared to intracellular and cell-free blood. *J Extracell Vesicles*. 2014. <https://doi.org/10.3402/jev.v3.23743>.
29. Vojtech L, Woo S, Hughes S, Levy C, Ballweber L, Sauteraud RP, et al. Exosomes in human semen carry a distinctive repertoire of small non-coding RNAs with potential regulatory functions. *Nucleic Acids Res*. 2014;42:7290–304.
30. Valadi H, Ekström K, Bossios A, Sjöstrand M, Lee JJ, Lötvall JO. Exosome-mediated transfer of mRNAs and microRNAs is a novel mechanism of genetic exchange between cells. *Nat Cell Biol*. 2007;9:654.
31. Lee RC, Feinbaum RL, Ambros V. The *C. elegans* heterochronic gene *lin-4* encodes small RNAs with antisense complementarity to *lin-14*. *Cell*. 1993;75:843–54.
32. Rathjen T, Nicol C, McConkey G, Dalmay T. Analysis of short RNAs in the malaria parasite and its red blood cell host. *FEBS Lett*. 2006;580:5185–8.
33. Xue X, Zhang Q, Huang Y, Feng L, Pan W. No miRNA were found in *Plasmodium* and the ones identified in erythrocytes could not be correlated with infection. *Malar J*. 2008;7:47.
34. Coulson RMR, Hall N, Ouzounis CA. Comparative genomics of transcriptional control in the human malaria parasite *Plasmodium falciparum*. *Genome Res*. 2004;14:1548–54.
35. Hall N, Karras M, Raine JD, Carlton JM, Kooij TW, Berriman M, et al. A comprehensive survey of the *Plasmodium* life cycle by genomic, transcriptomic, and proteomic analyses. *Science*. 2005;307:82–6.
36. Baum J, Papenfuss AT, Mair GR, Janse CJ, Vlachou D, Waters AP, et al. Molecular genetics and comparative genomics reveal RNAi is not functional in malaria parasites. *Nucleic Acids Res*. 2009;gkp239.
37. Dandewad V, Vindu A, Joseph J, Seshadri V. Import of human miRNA-RISC complex into *Plasmodium falciparum* and regulation of the parasite gene expression. *J Biosci*. 2019;44:50.
38. LaMonte G, Philip N, Reardon J, Lacsina JR, Majoros W, Chapman L, et al. Translocation of sickle cell erythrocyte microRNAs into *Plasmodium falciparum* inhibits parasite translation and contributes to malaria resistance. *Cell Host Microbe*. 2012;12:187–99.
39. El-Assaad F, Hempel C, Combes V, Mitchell AJ, Ball HJ, Kurtzhals JA, et al. Differential microRNA expression in experimental cerebral and non-cerebral malaria. *Infect Immun*. 2011;79:2379–84.
40. Martin-Alonso A, Cohen A, Quispe-Ricalde MA, Foronda P, Benito A, Berzosa P, et al. Differentially expressed microRNAs in experimental cerebral malaria and their involvement in endocytosis, adherens junctions, FoxO and TGF- $\beta$  signalling pathways. *Sci Rep*. 2018;8:11277.
41. Mantel PY, Hjelmqvist D, Walch M, Kharoubi-Hess S, Nilsson S, Ravel D, et al. Infected erythrocyte-derived extracellular vesicles alter vascular function via regulatory Ago2-miRNA complexes in malaria. *Nat Commun*. 2016;7:12727.
42. Babatunde KA, Mbagwu S, Hernandez-Castaneda MA, Adapa SR, Walch M, Filgueira L, et al. Malaria infected red blood cells release small regulatory RNAs through extracellular vesicles. *Sci Rep*. 2018;8:884.
43. Wang Z, Xi J, Hao X, Deng W, Liu J, Wei C, et al. Red blood cells release microparticles containing human argonaute 2 and miRNAs to target genes of *Plasmodium falciparum*. *Emerg Microbes Infect*. 2017;6:e75.
44. Chamnanchanunt S, Kuroki C, Desakorn V, Enomoto M, Thanachartwet V, Sahassananda D, et al. Downregulation of plasma miR-451 and miR-16 in *Plasmodium vivax* infection. *Exp Parasitol*. 2015;155:19–25.
45. Prapansilp Panote TG. MicroRNA in malaria. *MicroRNAs in medicine*. Lawrie CH, Ed. Wiley; 2013:183–97.
46. van Loon W, Gai PP, Hamann L, Bedu-Addo G, Mockenhaupt FP. miRNA-146a polymorphism increases the odds of malaria in pregnancy. *Malar J*. 2019;18:7.
47. Cohen A, Zinger A, Tiberti N, Grau GE, Combes V. Differential plasma microvesicle and brain profiles of microRNA in experimental cerebral malaria. *Malar J*. 2018;17:192.
48. Kaur H, Sehgal R, Kumar A, Sehgal A, Bansal D, Sultan AA. Screening and identification of potential novel biomarker for diagnosis of complicated *Plasmodium vivax* malaria. *J Transl Med*. 2018;16:272.
49. de Ronde MWJ, Ruijter JM, Moerland PD, Creemers EE, Pinto-Sietsma SJ. Study design and qPCR data analysis guidelines for reliable circulating miRNA biomarker experiments: a Review. *Clin Chem*. 2018;64:1308–18.
50. Livak KJ, Schmittgen TD. Analysis of relative gene expression data using real-time quantitative PCR and the 2<sup>-Delta-Delta C(T)</sup> Method. *Meth Ods*. 2001;25:402–8.
51. Agarwal V, Bell GW, Nam J-W, Bartel DP. Predicting effective microRNA target sites in mammalian mRNAs. *eLife*. 2015;4:e05005.
52. Kanehisa M, Goto S. KEGG: Kyoto encyclopedia of genes and genomes. *Nucleic Acids Res*. 2000;28:27–30.
53. Vlachos IS, Zagganas K, Paraskevopoulou MD, Georgakilas G, Karagkouni D, Vergoulis T, et al. DIANA-miRPath v3.0: deciphering microRNA function with experimental support. *Nucleic Acids Res*. 2015;43:W460–6.
54. Meninger T, Lerman G, Regev-Rudzki N, Gold D, Ben-Dov IZ, Sidi Y, et al. Schistosomal microRNAs isolated from extracellular vesicles in sera of infected patients: a new tool for diagnosis and follow-up of human schistosomiasis. *J Infect Dis*. 2016;215:378–86.
55. Obaldia N, Meibalan E, Sa JM, Ma S, Clark MA, Mejia P, et al. Bone marrow is a major parasite reservoir in *Plasmodium vivax* infection. *mBio*. 2018;9:e00625–718.
56. Baro B, Deroost K, Raiol T, Brito M, Almeida AC, de Menezes-Neto A, et al. *Plasmodium vivax* gametocytes in the bone marrow of an acute malaria patient and changes in the erythroid miRNA profile. *PLoS Negl Trop Dis*. 2017;11:e0005365.
57. Mishra R, Singh SK. HIV-1 Tat C modulates expression of miRNA-101 to suppress VE-cadherin in human brain microvascular endothelial cells. *J Neurosci*. 2013;33:5992–6000.
58. Lalwani MK, Sharma M, Singh AR, Chauhan RK, Patowary A, Singh N, et al. Reverse genetics screen in zebrafish identifies a role of miR-142a-3p in vascular development and integrity. *PLoS ONE*. 2012;7:e52588.
59. Young JA, Ting KK, Li J, Moller T, Dunn L, Lu Y, et al. Regulation of vascular leak and recovery from ischemic injury by general and VE-cadherin-restricted miRNA antagonists of miR-27. *Blood*. 2013;122:2911–9.
60. Qi Y, Cui L, Ge Y, Shi Z, Zhao K, Guo X, et al. Altered serum microRNAs as biomarkers for the early diagnosis of pulmonary tuberculosis infection. *BMC Infect Dis*. 2012;12:384.
61. Zhang X, Zhang Z, Dai F, Shi B, Chen L, Zhang X, et al. Comparison of circulating, hepatocyte specific messenger RNA and microRNA as bio-markers for chronic hepatitis B and C. *PLoS ONE*. 2014;9:e92112.



62. He X, Sai X, Chen C, Zhang Y, Xu X, Zhang D, et al. Host serum miR-223 is a potential new biomarker for *Schistosoma japonicum* infection and the response to chemotherapy. *Parasit Vectors*. 2013;6:272.
63. Alizadeh Z, Mahami-Oskouei M, Spotin A, Kazemi T, Ahmadpour E, Cai P, et al. Parasite-derived microRNAs in plasma as novel promising biomarkers for the early detection of hydatid cyst infection and post-surgery follow-up. *Acta Trop*. 2019;202:105255.
64. Quintana JF, Makepeace BL, Babayan SA, Ivens A, Pfarr KM, Blaxter M, et al. Extracellular *Onchocerca*-derived small RNAs in host nodules and blood. *Parasit Vectors*. 2015;8:58.
65. Tritten L, Burkman E, Moorhead A, Satti M, Geary J, Mackenzie C, et al. Detection of circulating parasite-derived MicroRNAs in filarial infections. *PLoS Negl Trop Dis*. 2014;8:e2971.

### Publisher's Note

Springer Nature remains neutral with regard to jurisdictional claims in published maps and institutional affiliations.

## Additional file

**Supplementary Table 3.1** Individual target prediction of up-regulated miRNAs and genes involved in malaria pathway

Up-regulated miRNAs	Predicted target genes
<b>hsa-miR-150-5p</b>	<i>SDC2, LRP1, HGF, GYPC, MYD88, TLR4, IL10, TGFB1</i> <i>TNF, IL18, CSF3, KLRC4, CD36, THBS1, ITGAL</i>
<b>hsa-miR-15b-5p</b>	<i>HGF, TLR4, TGFB2, THBS2, CD40</i>
<b>hsa-let-7a-5p</b>	<i>HGF, TLR4, IL10, IL6, VCAM1, THBS1</i>

**Abbreviation** *SDC2*: Syndecan-2, *LRP1*: Low density lipoprotein receptor-related protein 1, *HGF*: Hepatocyte growth factor, *GYPC*: Glycophorin C, *MYD88*: Myeloid differentiation primary response 88, *TLR4*: Toll Like Receptor 4, *IL10*: Interleukin 10, *TGFB1*: Transforming Growth Factor Beta 1, *TNF*: Tumor necrosis factor, *IL18*: Interleukin 18, *CSF3*: Colony Stimulating Factor 3, *KLRC4*: Killer Cell Lectin Like Receptor C4, *CD36*: cluster of differentiation 36 or platelet glycoprotein 4, *THBS1*: *Thrombospondin 1*, *ITGAL*: Integrin alpha L chain, *TGFB2*: Transforming growth factor-beta 2, *THBS2*: *Thrombospondin-2*, *CD40*: Cluster of differentiation 40, *IL6*: Interleukin 6, *VCAM*: *vascular cell adhesion molecule 1*

**Chapter Four:**

**Extracellular vesicle microRNA  
biomarker discovery in children  
with severe malaria**

## Chapter 4: Extracellular vesicle miRNAs in plasma as biomarkers for disease severity and neurocognitive impairment in children with severe malaria

### Chapter overview

Accurate and reliable prognostic biomarkers of severe malaria and its outcomes are necessary to help treat patients with poor outcomes earlier to decrease the duration of neurological dysfunction or prevent mortality. This chapter focuses on high-throughput transcriptomic analysis of plasma extracellular vesicle cargo from children with severe malaria via next-generation sequencing. The transcriptomic profiles were compared among severe malaria outcomes to discover potential microRNAs with predictive potential. After identifying differentially expressed microRNAs of interest and performing gene ontology analysis, the microRNAs were validated using a new cohort of children with severe malaria via RT-qPCR. This allowed the identification of 5 microRNAs with high prognostic potential, particularly when observing cerebral malaria outcomes.

### Authors' contributions

Author	Concept	Investigation	Methodology	Data curation	Formal Analysis	Writing-original draft	Writing-review & editing	Signature
Iris S. Cheng	X	X	X	X	X	X	X	Production Note: Signature removed prior to publication.
Robert O. Opoka							X	Production Note: Signature removed prior to publication.
Raïssa L. Gill				X				Production Note: Signature removed prior to publication.
Paul Bangirana							X	Production Note: Signature removed prior to publication.
Chandy C. John							X	Production Note: Signature removed prior to publication.
Valery Combes	X						X	Production Note: Signature removed prior to publication.

**Publication status:** In submission process

## **Extracellular vesicle miRNAs in plasma as biomarkers for disease severity and neurocognitive impairment in children with severe malaria**

[Iris S. Cheng](#)<sup>1</sup>, [Robert O. Opoka](#)<sup>2</sup>, [Raissa L. Gill](#)<sup>3</sup>, [Paul Bangirana](#)<sup>2,4</sup>, [Chandy C. John](#)<sup>5</sup>, [Valery Combes](#)<sup>1</sup>

<sup>1</sup>Malaria and Microvesicles Research Group, School of Life Sciences, Faculty of Sciences, University of Technology Sydney, Ultimo, Sydney, New South Wales, 2007, Australia

<sup>2</sup>Global Health Uganda, Kampala, Uganda

<sup>3</sup>Climate Change Cluster, School of Life Sciences, Faculty of Sciences, University of Technology Sydney, Ultimo, Sydney, New South Wales, 2007, Australia

<sup>4</sup>Department of Psychiatry, Makerere University College of Health Sciences, Kampala, Uganda

<sup>5</sup>Ryan White Center for Infectious Diseases and Global Health, Department of Pediatrics, Indiana University, Indianapolis, USA

Corresponding authors

Valery Combes, Email: [valery.combes@uts.edu.au](mailto:valery.combes@uts.edu.au)

Word Count: 8614

## **Abstract**

Cerebral malaria (CM) and severe malarial anaemia (SMA) are two major complications of *Plasmodium falciparum* severe malaria. Severe malaria results in hundreds of thousands of deaths in children under age five, with survivors at risk of developing significant motor and neurocognitive impairment (NCI). Pathogenesis of severe malaria is not entirely understood, though, among other cellular and soluble factors, increased extracellular vesicle (EV) levels are associated with disease severity in individuals with CM. Currently, there are no reliable markers for early assessment of disease severity; however, recent interest in EV cargo, such as proteins and microRNA, has identified potential biomarkers. This study investigates, for the first time, the complete microRNA profile of plasma EVs by next-generation sequencing (NGS), in children with severe malaria ( $n_{\text{total}}=20$ ,  $n=4/\text{group}$ : CM with full recovery (FR), CM with fatal outcome (FO), CM with NCI, SMA with FR, and SMA with NCI) and asymptomatic community control children (CC) ( $n=3$ ). This unbiased approach identified 92 differentially expressed microRNAs and 13 microRNAs of interest. Five miRNAs of interest, hsa-miR-1-3p, hsa-miR-19a, hsa-miR-30, hsa-miR-4516, and hsa-miR-590-3p were verified via real-time quantitative polymerase chain reaction (RT-qPCR) on an additional 25 ( $n=5/\text{group}$ ) children with severe malaria and 5 community children, as differentiating one or more of the 5 disease groups from another and/or from CC. Four out of the five microRNAs have high prognostic potential especially when differentiating the outcomes of CM, specifically children that developed neurocognitive impairment and survived from those with fatal outcomes. All five miRNAs have high sensitivity and specificity for the groups they can differentiate and, when combined into a panel, have greater potential as prognostic biomarkers.

**Keywords:** Extracellular vesicles (EVs), microRNA (miRNA), plasma, malaria, biomarker, next-generation sequencing (NGS), paediatric, cerebral malaria, severe malarial anaemia, neurocognitive impairment

## **4.1 Introduction**

Severe malaria is one of the leading causes of neurological disability and child mortality<sup>1</sup>. In 2021 World Health Organisation (WHO) estimated 247 million malaria cases occurred globally, 95% of which were in the WHO African Region, leading to 619,000 deaths worldwide, of which 77% were in children under five<sup>2,3</sup>. *Plasmodium falciparum* is the most prevalent and deadly malaria parasite, accounting for 99.7% of malaria cases in the WHO African Region<sup>3,4</sup>. *P. falciparum* infection can quickly progress to severe illness within 24 hours, causing the most severe and fatal forms of malaria<sup>3</sup>. Approximately 1% of *P. falciparum*-infected patients who experience uncomplicated malaria advance into severe malaria (SM), and can potentially progress to lethal complications<sup>5</sup>.

Features of *P. falciparum* that contribute to severe disease pathogenesis include induction of host inflammatory response, exponential parasite growth, mature infected red blood cells (iRBCs) adhering to blood vessel walls blocking the microvasculature and activating the endothelium<sup>6</sup>. Complications such as cerebral malaria (CM), severe malarial anaemia (SMA), metabolic complications such as hypoglycaemia and acidosis, acute respiratory distress syndrome, renal failure, and pulmonary oedema can occur in combination or independently and rapidly progress, becoming fatal within hours or days<sup>7,8</sup>. CM, caused by an uncontrolled systemic inflammatory response that induces the production of pro-inflammatory cytokines and iRBCs sequestration in brain microvasculature and organ walls<sup>5,9</sup>, is among the deadliest complications of malaria, while SMA, caused by a decrease of RBCs in circulation and altered haematopoiesis<sup>7</sup> is the most common complication. Children who survive CM and SMA can develop motor and cognitive impairment, termed neurological sequelae or neurocognitive impairment (NCI). Mortality rates are exceptionally high in African children with SM, and if patients are treated successfully and survive, there is a 10-30% risk of suffering long-term NCI<sup>10</sup>. There is currently a dearth of alternative functional or neuropsychological markers for NCI prognosis<sup>11,12</sup>. Recently, a handful of potential biomarkers for neurocognitive impairment in paediatric severe malaria have been investigated. Concentrations of CSF tau during a CM have been shown to potentially identify children at risk of developing long-term neurocognitive impairment and elevated plasma tau was associated with lasting NCI and mortality in CM and SMA children<sup>13,12</sup>. Plasma levels of angiopoietin-2 have also

demonstrated associations with disease severity and worse neurocognitive outcomes during severe malaria<sup>14,15</sup>.

Increased levels of extracellular vesicles (EVs) circulating in patients are a significant feature of malaria<sup>16–18</sup>. Submicron EVs are potentially released by all host cell types and comprise three main groups if defined according to size: exosomes (50 nm – 100 nm), microvesicles (100 nm – 1000 nm) and apoptotic bodies (1000 nm – 5000 nm), although other parameters can also differentiate various EV subpopulations<sup>19</sup>. EVs contain nucleic acids, lipids, and cytosolic proteins from the parent cell and are recognised as a source of potential biomarkers<sup>20,21</sup>. The transfer of EVs cargo to a target cell contributes to intercellular communication, exchange of biological information and disease pathogenesis, for many diseases including malaria<sup>22–28</sup>.

Early detection and adequate treatment of malaria are essential, as initial infection can quickly progress into life-threatening SM<sup>29</sup>. Biomarkers have long functioned as prognostic and diagnostic mappers of the progression and outcome of chronic disease<sup>30</sup>. Although the search for biomarkers to distinguish severe forms of malaria has only recently begun, the absence of reliable biomarkers that identify malaria patients at risk of death or NCI drives research progression.

Most of the identified potential biomarkers for SM are proteins, such as erythropoietin, von Willebrand factor, angiopoietin-2, *Plasmodium falciparum* histidine-rich protein 2 (PfHRP2), and intercellular adhesion molecule 1 (ICAM-1), elevated levels of which indicate severe disease<sup>31–35</sup>. In addition to EVs' importance in disease pathogenesis and their cargo's biomarker potential, the EVs themselves can act as biomarkers for disease severity. An increase in EV production is strongly related to disease severity, demonstrated in cancers, cardiovascular disease, autoimmune diseases, parasitic (including malaria), bacterial or viral infections and neurological disorders<sup>16,17,36–39</sup>. Concurrently there is still a lack of reliable biomarkers that can predict morbidity and mortality, and the adjunctive therapies designed to aid anti-malarial drugs have been so far ineffective<sup>40</sup>.

MicroRNAs (miRNA) are a class of small non-coding RNAs (RiboNucleic Acids, 17-25 nucleotides) that regulate a third of the genes within the genome and are known to control cellular differentiation, development, metabolism and homeostasis<sup>41–43</sup>. Extracellular miRNAs have been identified in various biological fluids such as serum, plasma, cerebrospinal fluid, saliva, urine, breast milk, peritoneal fluid, pleural fluid, amniotic fluid, and tears<sup>44,45</sup>. RNA



molecules are highly unstable; however, miRNAs have been shown to be resistant to RNase, extreme pH, long durations at room temperature, and multiple freeze-thaw cycles<sup>46–48</sup>. Though, for reproducible and consistent results, the stability of miRNA is highly dependent on the collection, preparation, handling and storage of biological fluids, significantly impacting their potential to be used as non-invasive biomarkers<sup>49,50</sup>. In addition to delivering miRNA to target cells with high efficiency, EVs act as an additional protection layer rendering more stable miRNAs than freely circulating miRNAs<sup>51–54</sup>. Due to the lipid bilayer, EVs are more stable and thus have the potential of having a long-lasting effect on the immune response<sup>23,55</sup>. In parasites, miRNAs are catalogued with argonaute and dicers (critical players in miRNA biogenesis); however, not for unicellular parasites such as *Plasmodium* spp., *Trypanosoma cruzi*, *Cryptosporidium* spp., and some *Leishmania* species that are, to the best of our knowledge, devoid of RNA interference machinery<sup>56</sup>. The interest in miRNA in the malaria field is in its infancy, and there is only a handful of studies on human samples. One of the first studies was conducted on adults and found significantly lower hsa-miR-451 and hsa-miR-16 expression levels in *Plasmodium vivax*-infected patient plasma compared to healthy controls<sup>57</sup>. Another study showed that hsa-miR-7977, hsa-miR-28-3p, hsa-miR-378-5p, hsa-miR-194-5p, and hsa-miR-3667-5p were significantly upregulated in complicated *P. vivax* infected patients<sup>58</sup>. Our group recently investigated miRNA expression in Thai malaria patients and found hsa-miR-150-5p, hsa-miR-15b-5p, hsa-let-7a-5p upregulated in the whole blood of *P. vivax* infected patients, and hsa-let-7a-5p also upregulated in *P. falciparum*-infected patients compared to healthy individuals<sup>59</sup>. More recent research showed that hsa-miR-4497 expression levels were higher in the plasma of children with SM than those with uncomplicated malaria<sup>60</sup>. In a CM mouse model, increased expressions of miR-27a, miR-150 and let-7i were observed in brain tissue, reflecting disease severity<sup>61</sup>. In another study, miR-146a expression was higher, and miR-193b expression was lower in EVs from CM mice than in non-infected and non-cerebral malaria (non-CM) mice<sup>22</sup>. The study also observed elevated levels of miR-205, miR-215 and miR-467a in the brain tissue of CM mice compared to non-infected and non-CM mice<sup>22</sup>. These findings suggest that EV-associated miRNA and tissue miRNA have different miRNA profiles and potentially different functions.

Various studies have investigated the role of EVs derived from single-cell types such as RBCs, platelets, or endothelial cells; however, the study of all circulating EVs from various vascular cells is still in its infancy. We hypothesise that the analysis of miRNAs derived from malaria-

infected patient plasma EVs could permit the identification of new biomarkers of disease outcome to aid in early medical intervention. An RNA next-generation sequencing (NGS) study was conducted on Ugandan paediatric plasma EV samples of CC, CM and SMA (Figure 4.1). Patients who fully recovered from CM or SMA without complications were compared to those who survived CM or SMA but developed NCI and those who succumbed to complications. Differentially expressed miRNAs were confirmed in another set of plasma from the same cohort of children using TaqMan® real-time quantitative polymerase chain reaction (RT-qPCR). This study is the first to assess the entire miRNA profile of malaria patient EVs with a detailed clinical and biological profile in addition to their neurological status (with or without NCI).

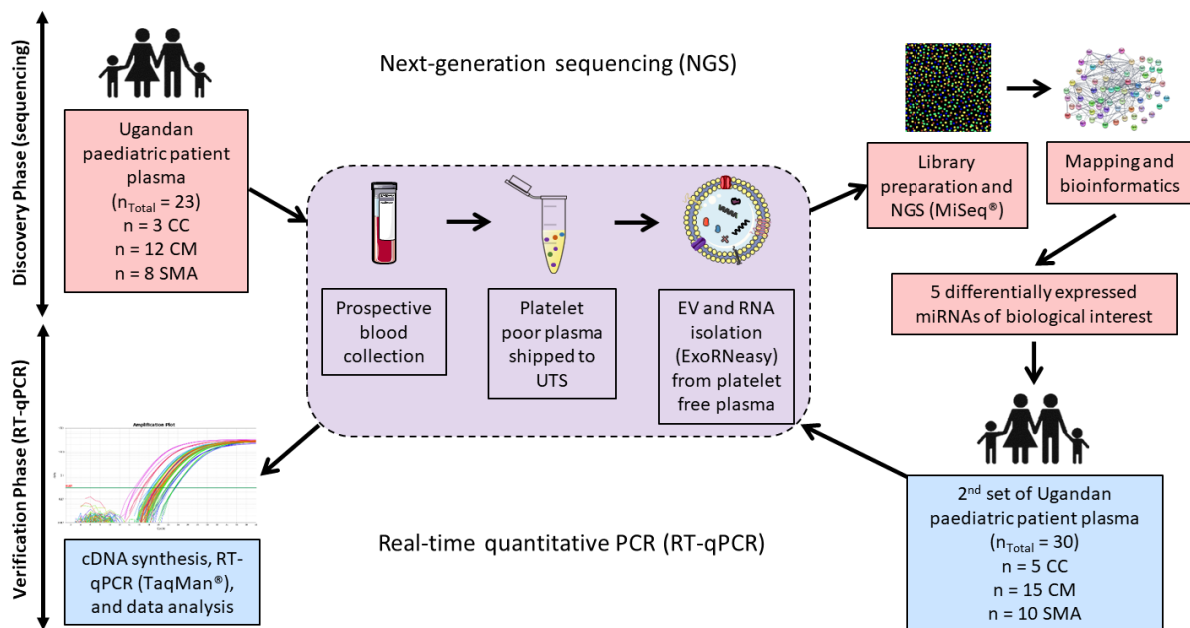


**Figure 4.1** Study pipeline summarising the patient groups, EV and RNA purification from human paediatric samples and bioinformatics. Abbreviations: CC, community children; CM, cerebral malaria; EV, extracellular vesicles; SMA, severe malarial anaemia; UTS, University of Technology Sydney

## **4.2 Materials and methods**

### **4.2.1 Study Participants**

Children between 18 months and 12 years of age were recruited between 2008 and 2012 to assess long-term neurocognitive outcomes following severe malaria. Samples were collected prospectively from community children or patients with CM and SMA enrolled in the Acute Care Unit of Mulago National Referral and Teaching Hospital, Kampala, Uganda. Community control children (CC) were children without symptomatic malaria or a history of SM in the nuclear family, extended family, or neighbouring families of children with SM, and enrolled to be in the same age range as the children with SM.

CM was defined as *Plasmodium falciparum* (Pf) present on a blood smear, coma, and no other known cause of coma on testing. Lumbar punctures to rule out meningitis were performed as part of routine clinical care on children with suspected CM in whom the procedure was not contraindicated and whose caregivers consented to the procedure, and children with an elevated CSF WBC count ( $\geq 5$  WBC/ $\mu$ L) or positive CSF culture for a meningitis pathogen were excluded from the study. SMA was defined as Pf present on blood smear and a haemoglobin level of  $\leq 5$  g/dL in children. Clinical testing included routine clinical tests (complete blood counts and blood levels of glucose and lactate) and serum/plasma levels of creatine, glucose, sodium, and bilirubin. Neurological tests performed included seizure frequency, coma duration, and coma scores (coma defined by Blantyre coma score  $< 3$  or Glasgow coma score  $< 8$ ) to assess impaired consciousness levels in children  $< 5$  years old and  $\geq 5$  years old, respectively. All study participants (children with CM, SMA or CC) received neurocognitive testing at baseline, 6 and 12 months later. Accordingly, clinical, biological, and neurological data, as well as the clinical outcome (i.e., survival, death, and NCI at 0, 6, and 12 months), are available for all patient groups. Inclusion and exclusion criteria and neurological, biological and clinical data have been previously reported<sup>11,62</sup>.

### **4.2.2 Informed consent and ethical approval**

Parents or guardians provided written informed consent for study participants. All procedures in the present study have received human ethics (UTS HREC 2015000382) and biosafety (2015-08-R-GPCA) approvals from the University of Technology Sydney. Ethical approval was

also granted by the Institutional Review Boards for human studies at Makerere University School of Medicine (Study # 2008-033), the University of Minnesota (Study # 0802M27022) and the Uganda National Council for Science and Technology (Study # HS 432). Experiments were all performed in agreement with applicable guidelines and regulations.

#### 4.2.3 Experimental design

From the recruited paediatric Ugandan cohort, following specific demographics selection guidelines (Table 4.1), six groups were selected for NGS ( $n_{\text{total}}=23$ ): community control ( $n=3$ ), fully recovered CM (CM FR,  $n=4$ ) and SMA (SMA FR,  $n=4$ ) patients, CM (CM NCI,  $n=4$ ) and SMA (SMA NCI,  $n=4$ ) patients who developed NCI, and CM patients who succumbed to complications (CM FO,  $n=4$ ). An additional 30 patients ( $n=5$  per group) were selected for RT-qPCR verification, utilising the same demographic selection guidelines (Table 4.1).

#### 4.2.4 Neuropsychological/Cognitive tests

Trained neuropsychology testers performed age-appropriate neurocognitive testing on all study children. The tests used have been validated for Ugandan children and used in multiple studies<sup>10,11,62–64</sup>. Tests were standardized by creating of an age-adjusted z-score for the test from the scores of the community children, as previously published<sup>11</sup>. For the present study, the primary focus was on overall cognition, and cognitive impairment was defined by an age-adjusted z-score of  $<-1.5$  at 1 or more time points (0, 6 or 12 month follow-up) in the overall cognition score. Because of the wide age range of children studied, cognitive testing that covered the full age range was required. Overall cognition was therefore assessed by the early learning composite score of the Mullen Scales of Early Learning for children 18 months to 4 years of age, and the mental processing index of the Kaufman Assessment Battery for Children (Second Edition) for children 5-12 years of age. The neurocognitive examination results have been previously published<sup>11</sup>.

**Table 4.1** Characteristics of paediatric patient group baseline demographics and clinical findings

Demographic and clinical findings							
Next-Generation Sequencing paediatric patient group	CC (n = 3)	CM FR (n = 4)	CM NCI (n = 4)	CM FO (n = 4)	SMA FR (n = 4)	SMA NCI (n = 4)	P Value <sup>a</sup>
Age, y, mean (SD)	3.17 (0.87)	3.18 (0.72)	3.50 (0.34)	3.15 (0.77)	3.26 (0.57)	2.16 (0.36)	.22
Sex, male:female, No.	3:0	4:0	1:3	4:0	4:0	4:0	
Plasma volume, $\mu$ L, mean (SD)	182 (4.73)	185 (2.65)	178 (6.98)	179 (12.50)	179 (6.25)	176 (10.72)	.54
Blantyre coma scale <sup>§</sup> , mean		2	1	1	5	5	
Coma duration, hours, median (IQR)	0	72.50 (40.62-97.50)	82.00 (14-151.4)	0	0	0	0.0006
Haemoglobin, g/dL, mean (SD)	12.27 (1.25)	7.25 (1.24)	5.98 (1.56)	8.80 (2.01)	3.68 (0.33)	3.78 (0.38)	.0015 <sup>c</sup>
Platelet count, $\times 10^9$ /L, median (IQR)	503 (493-522)	114 (50-140)	108 (24-273)	61 (12-314) <sup>#</sup>	98 (56-130)	170 (163-176)	.05
Hypoxia Y:N/# (O <sub>2</sub> saturation <95%)	0:3	0:4	1:3	1:3	2:2	0:4	
Lactic acidosis Y:N/# (lactate >5 mmol/L)	0:3	1:3	2:2	2:2	2:2	1:3	
Plasmodium falciparum peripheral blood density, parasites/ $\mu$ L, median (IQR)	0	202 840 (149 160-260 975)*	32 590 (7225-614 680)*	404 940 (340 770-443 000)** <sup>#</sup>	37 740 (6555-166 485)	29 900 (11 375-69 110)	.065 <sup>d</sup>
PfHRP-2 level, ng/mL, median (IQR)	4.8 (4.8-12)	2008 (479-4859)	584 (115- 624)	5992 (1236-7505)	3186 (1666-3757)	499 (326-1079)	.05
RT-qPCR paediatric patient group							
RT-qPCR paediatric patient group	CC (n = 5)	CM FR (n = 5)	CM NCI (n = 5)	CM FO (n = 5)	SMA FR (n = 5)	SMA NCI (n = 5)	P Value <sup>a</sup>
Age, y, mean (SD)	6.85 (1.40)	6.42 (1.21)	7.38 (0.94)	6.17 (1.63)	5.95 (0.66)	5.86 (3.15)	.35
Sex, male:female, No.	5:0	5:0	3:2	3:2	3:2	4:1	
Plasma volume, $\mu$ L, mean (SD)	176 (3.38)	186 (2.79)	178 (3.60)	176 (3.49)	184 (5.95)	175 (4.22)	.02 <sup>e</sup>
Coma duration, hours, median (IQR)	0	19.00 (15.25-60)	75.00 (34.17-108.5)	0	0	0	<0.0001
Haemoglobin, g/dL, mean (SD)	11.42 (1.94)	7.48 (1.72)	8.38 (2.31)	8.70 (2.96)	4.12 (0.40)	3.58 (0.64)	.0005 <sup>c</sup>
Platelet count, $\times 10^9$ /L, median (IQR)	261 (196-356)	35 (28-63)	79 (26-436)	16 (8-36) <sup>#</sup>	90 (32-156)	153 (130-180)	.0049 <sup>f</sup>
Hypoxia Y:N/# (O <sub>2</sub> saturation <95%)	0:5	0:5	2:3	0:5	0:5	2:3	
Lactic acidosis Y:N/# (lactate >5 mmol/L)	0:5	0:5	3:2	0:5	0:5	1:4	
Plasmodium falciparum peripheral blood density, parasites/ $\mu$ L, median (IQR)	0	786 160 (375 380-1 144 430)***	21 360 (4280-30 380)	74 840 (13 860-651 110)*	23 860 (10 390-63 980)	47 020 (6390-151 030)	.0305 <sup>g</sup>
PfHRP-2 level, ng/mL, median (IQR)	4.8 (4.8-4.8)	5311 (539-19 759)	5767 (3404-17 983)	5800 (3839-28 475)	2790 (933-6646)	140 (85-877)	.0012 <sup>h</sup>

Abbreviations: CC, community children; CM, cerebral malaria; FO, fatal outcome; FR, full recovery; IQR, Interquartile Range; NCI, neurocognitive impairment; SD, standard deviation; SMA, severe malarial anaemia

<sup>a</sup> P Value based on one-way ANOVA Kruskal-Wallis

<sup>b</sup> CM NCI group differs from SMA FR and SMA NCI groups

<sup>c</sup> CC group differs from SMA FR and SMA NCI groups

<sup>d</sup> No significant difference between the malaria patient groups

<sup>e</sup> Blantyre coma scale for preverbal children <5 years of age; minimum score: 0 (poor), maximum score: 5 (good), abnormal score  $\leq$  4; <sup>f</sup> Missing information for 1 patient; \* One patient with hyperparasitaemia (parasite > 250000/ $\mu$ L, n); \*\* Three patients with hyperparasitaemia (missing information for one patient); \*\*\* Four patients with hyperparasitaemia

<sup>e</sup> CM FR group slightly differs from SMA NCI

<sup>f</sup> CC group differs from CM FO

<sup>g</sup> CM FR group differs from CM NCI

<sup>h</sup> CC group differs from CM NCI and CM FO

#### 4.2.5 Blood collection and platelet-free plasma preparation and storage

Whole blood ( $\leq 5.5$  mL) was collected from each child via sodium citrate venipuncture at admission. The whole blood samples were centrifuged at 1,500 g for 15 min at room temperature for this EV study. The supernatant (platelet-poor plasma) was centrifuged at 13,000 g for 3 min at room temperature to remove cell debris and any remaining platelets. Supernatants (platelet-free plasma (PFP) containing EVs) were collected and stored at  $-80$  °C until EV isolation. Samples were then shipped to the University of Technology Sydney, where all the experiments were performed.

#### 4.2.6 Isolation of extracellular vesicles

This study will focus on Extracellular vesicles that fall into the exosome and microvesicle size categories and will be collectively termed EVs, as we aim to identify circulating biomarkers of disease severity rather than studying subpopulations of EVs. The PFP samples ( $\sim 180$   $\mu$ L) were thawed at room temperature and centrifuged at 13,000 g for 2 min to remove potential aggregates formed through the freezing process. Following the manufacturer's protocol,  $\sim 180$   $\mu$ L of PFP was passed through a QIAgen® exoEasy membrane affinity spin column to isolate EVs 80 nm to 400 nm in size<sup>65</sup>. EVs were eluted from the column using XE buffer (QIAGEN®) and stored at  $-80$  °C for size and concentration verification.

#### 4.2.7 Extracellular vesicle concentration and size

The EVs were stored at  $-80$  °C and thawed just before analysis on the NanoSight NS300 (Malvern). Once thawed the EVs were vortexed for 15 seconds and then diluted with sterile PBS to the detectable range of the NanoSight, approximately  $10^6$  to  $10^9$  particles per mL or 20 to 100 particles per field of view to allow accurate particle tracking. After dilution, the EVs were vortexed for 15 seconds once more and then immediately analysed on the NanoSight NTA v3.2, 10 recordings for 60 seconds at 25 °C with camera level set to 11 and detection threshold set to 10, PBS washes were run in between samples.

#### 4.2.8 Total RNA extraction

For high-quality RNA, isolation was performed with the RNeasy portion of the exoRNeasy kit (Qiagen®), and all procedures were time monitored to avoid RNA degradation during the isolation process. Once the EVs were isolated, QIAzol was added directly to the exoEasy column and chloroform was added for phase separation. The aqueous phase was recovered and transferred to a mini elute spin column where total RNA binds to the column. The spin column was washed 3 times, and the total RNA was eluted with 14 µL of ultra-pure water, then stored as 2 x 7 µL aliquots flash-frozen with liquid nitrogen and stored at -80 °C. The RNA samples were never thawed more than once to avoid RNA degradation. NanoDrop One spectrophotometer (Thermo Scientific) was used to monitor solvent contamination such as phenol, protein, ethylenediaminetetraacetic acid (EDTA) and guanidinium isothiocyanate (GITC).

#### 4.2.9 miRNA library preparation

The miRNA library was prepared with a QIAseq™ miRNA Library Kit (Cat No.: 331502, Qiagen) and QIAseq™ miRNA 12 Index IL (Cat No.: 331592, Qiagen). Following the manufacturer's protocol, 5 µL of RNA was used for complementary DNA (cDNA) synthesis (miRNA library preparation). Using a thermal cycler, the 3' and 5' adapters were ligated to mature miRNAs. Reverse transcription primers and Unique molecular indices (UMIs) were then used to reverse transcribe the ligated miRNAs to cDNA and UMI assignment. The cDNA was cleaned with magnetic beads, and then library amplification (22 cycles) was performed with universal forward primers and indexing reverse primers. A final library clean-up was completed with magnetic beads to remove any possible primer dimerisation. The library was eluted with 20 µL of nuclease-free water, flash-frozen with liquid nitrogen as 4 x 5 µL aliquots, stored at -80 °C, and never thawed more than twice.

#### 4.2.10 Quality Control before NGS

All library concentrations were determined using the Qubit™ 1 X dsDNA high-sensitivity assay kit (Cat No.: Q33230, Invitrogen™). The length of the cDNA in the library was measured with a high-sensitivity DNA Bioanalyzer kit (P/No.: 5067-4626, Agilent High Sensitivity Kit). From

the library, 2  $\mu\text{L}$  was used for Qubit™ measurements, 1  $\mu\text{L}$  for bioanalyser analysis, and 1  $\mu\text{L}$  for library dilution. Using both measures, the molarity of each library was determined using the equation,  $\frac{X \text{ ng}/\mu\text{L} * 10^6}{\text{bp} * \text{MW}} = Y \text{ nM}$ ,

and then diluted to 4 nM and equally pooled into one tube. The concentration and size of the pooled library were measured, and the molarity was calculated and adjusted to 4 nM based on the acquired values by diluting with nuclease-free water when necessary.

#### 4.2.11 Denaturing, diluting, and sequencing the library

The 4nM library was denatured by mixing 5  $\mu\text{L}$  of 4 nM library with 5  $\mu\text{L}$  of 0.2 N NaOH and incubating it at 30 °C for 5 min. Then 900  $\mu\text{L}$  of cold hybridisation buffer was added to the tube, resulting in 1 mL of a 20 pM denatured library. The denatured library was further diluted to 10 pM, and the PhiX denatured library control was then added to the denatured library for a final concentration of 5% for maximum read output. The MiSeq® v3 reagent tray (Ref No.: 15043894, Illumina®) was defrosted in water, and the MiSeq® flow cell was rinsed with Milli-Q® water. The denatured library was loaded onto the MiSeq® v3 reagent tray (150 cycles, 2 x 75 base pairs), and deep sequencing was performed using the MiSeq® system from Illumina®. BaseSpace Sequence Hub Illumina® was used to monitor the runs quality control, flow cell, % pass filter and % Q30 (Phred quality score of 30 to a base). Experiments including EV and RNA isolation, library preparation, and sequencing were performed at the University of Technology Sydney and the UTS Core Sequencing Facility.

#### 4.2.12 Mapping and expression analysis

Initial quality control was done with the FASTQC system to ensure the run went smoothly. The sequences were then run through Qiagen® Geneglobe to align and map against the human genome. Quality filtering and adapter trimming were applied when necessary, and a nucleotide (nt) cut-off was at 16 nt. The raw sequences were also processed using CLC Genomics Workbench (CLC-GWB) 21 (Qiagen®, RRID: SCR\_011853) using the workflows in Supplementary Figure 4.1. The FASTQ files exported after sequencing were run through a QC and trim workflow (Supplementary Figure 4.1A). The QC workflow reports typical library



characteristics such as distributions of sequence lengths, base qualities, and nucleotide compositions. The trim workflow removed sequences based on sequence quality, adapter contamination and sequences shorter than 15 nt. The QC and trimmed sequences were then run through the miRNA quantification workflow (Supplementary Figure 4.1B) with miRNA length set at 15-55 nt and minimum supporting count (read threshold) set to 10 reads (minimum reads for a miRNA to be considered expressed). The occurrence of UMI tags extracted from reads was counted and mapped against 2654 mature miRNA listed in the miRBase v22 database<sup>66</sup>. The mapped mature miRNAs were run through the miRNA differential expression workflow, which used the Trimmed Mean of M-values normalisation method (Supplementary Figure 4.1C), producing a list of differentially expressed miRNA and their common functional role. Following a defined selection criterion, miRNAs of interest were selected according to their ability to differentiate the patient groups. Heatmaps of the differentially expressed miRNA were created using the program Clustergrammer to cluster the samples and visualise miRNA of interest.

#### 4.2.13 Verification via RT-qPCR

After selecting miRNA of biological interest, new patients ( $n_{\text{total}}=30$ ,  $n=5$  per group) from the same cohort were chosen using the same criteria for NGS (Table 4.1). The EV and RNA isolation process is as stated above. As per manufacturer protocol, the cDNA templates were prepared using 2  $\mu\text{L}$  of total RNA and the TaqMan<sup>®</sup> Advanced miRNA cDNA Synthesis Kit (Cat No.: A28007, Applied Biosystems<sup>™</sup>). The epMotion<sup>®</sup> 5073 was used to distribute TaqMan<sup>®</sup> Advanced miRNA Assay (Cat No.: A25576, Applied Biosystems<sup>™</sup>) and cDNA templates into 384-well PCR plates, the plates were then run on the QuantStudio<sup>™</sup> 12K Flex Real-Time PCR System (Cat No.: 4471087, Applied Biosystems<sup>™</sup>) in quadruplicates.

The NGS read counts were used to select an endogenous control (EC) for RT-qPCR analysis, and the following criterion was used, co-efficient variation ( $< 5\%$ ), base mean ( $\geq 3000$ ), standard deviation ( $< 1$ ), and fold change ( $< 1$ ).<sup>60</sup> After selecting the EC, miRNA relative expression levels were determined by using the cycle threshold (Ct) to calculate the  $2^{-\Delta\Delta\text{Ct}}$ , where  $\Delta\text{Ct} = \text{Ct}_{\text{miRNA}} - \text{Ct}_{\text{endogenous control}}$  and  $\Delta\Delta\text{Ct} = \Delta\text{Ct} - \text{average } \Delta\text{Ct}_{\text{control group}}$ .

#### 4.2.14 RT-qPCR statistical analysis

All statistical analyses for RT-qPCR were performed using statistical software R version 4.1.2 and GraphPad Prism version 8. The  $2^{-\Delta\Delta Ct}$  of biologically significant comparisons were analysed via Kruskal-Wallis and Planned Dunn's test with Bonferroni adjustment and a Mann-Whitney test to compare CC vs SM. Receiver operating characteristic (ROC) curves were generated to assess the predictive performance of the miRNAs of interest by analysing the clinical sensitivity and specificity for every possible cut-off. Sensitivity refers to the rate of true positive patients correctly identified, and specificity refers to the rate of true negative patients correctly identified. An area under the curve (AUC) of 1 means the test 100% accurately and correctly identifies the positive and negative patients.

Methods sections 4.2.1, 4.2.2, 4.2.4, and 4.2.5 are also used in Chapter 5, as the samples are from the same cohort. Methods section 4.2.2 is also used in Chapter 6, where the same consent and ethical approvals were used.

To decrease repetitiveness, these sections will not be repeated in the following chapters, please refer to this chapter (4) for the details.

## **4.3 Results**

### **Discovery Phase**

#### 4.3.1 Nanoparticle tracking analysis profile of platelet-free plasma extracellular vesicle

The nanoparticle tracking analysis detected that EVs between 15-715nm were isolated from the paediatric PFP using exoEasy membrane affinity spin columns, with the majority of the EVs being 220nm. All three patient groups, CC, CM FR and SMA FR had similar EV profiles, with averages of  $3.2 \times 10^8$ ,  $2.7 \times 10^8$ , and  $2.0 \times 10^8$  EVs in 180  $\mu$ L of PFP (Figure 4.2A and 4.2B).

### 4.3.2 Extracellular vesicle RNA population profile

The libraries were confirmed to be devoid of primer dimer contamination (150 bp) individually and when pooled (Figure 4.2C). The concentration of cDNA ranged from 2.76 ng/ $\mu$ L to 23.70 ng/ $\mu$ L, with the CC patients having the lowest amount of cDNA and CM NCI patients having the highest amount of cDNA (Figure 4.2D). The bioanalyser readout cDNA sizes ranged from 162 bp to 172 bp and the pooled cDNA library was 170 bp, as expected for the cDNA (Figure 4.2C and 4.2D).

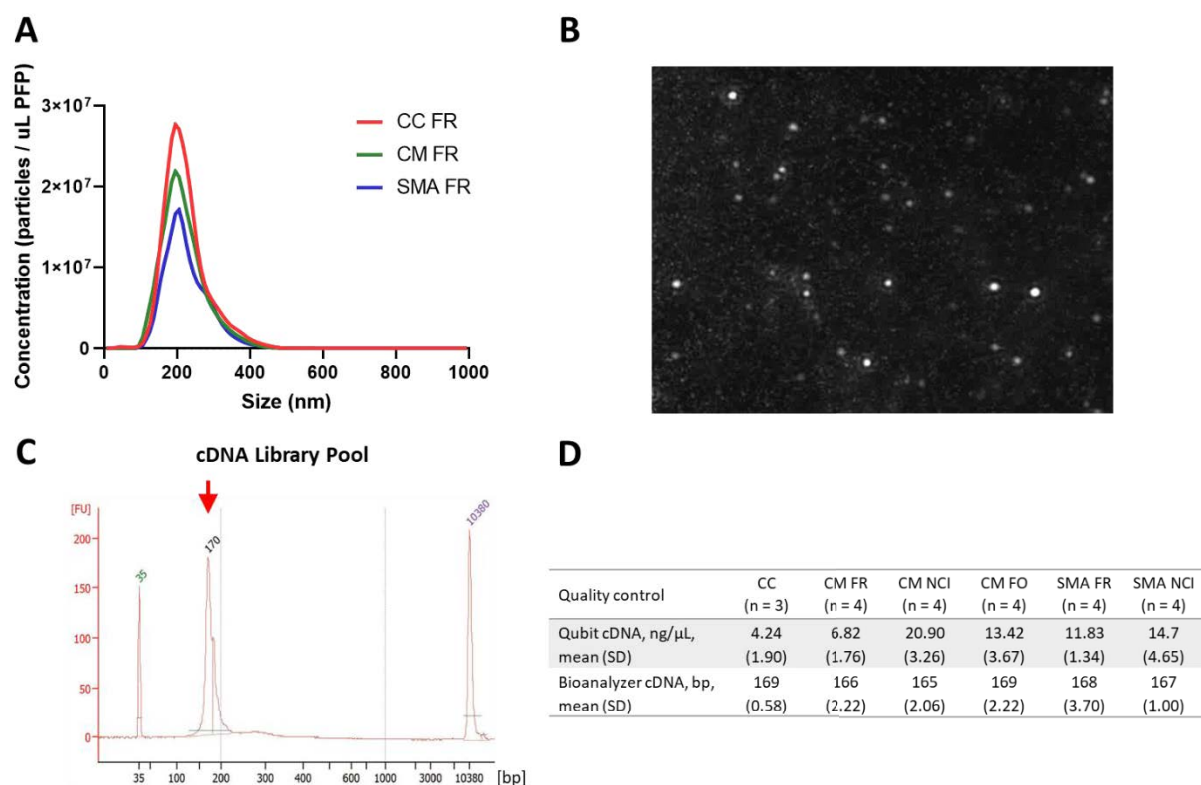


**Figure 4.2** Quality control for library size and length, and extracellular vesicle size and concentration. (A) particle concentration and size measured using NanoSight 300, extracellular vesicle population distribution is similar for the three main patient groups (B) NanoSight 300 image of extracellular vesicles (C) Pooled cDNA library run on a high sensitivity cDNA bioanalyzer, shows the absence of primer dimers (150 bp) and major microRNA looping prior to sequencing (D) Qubit concentrations and bioanalyzer cDNA sizes measured for each individual sample before dilutions for sequencing, group averages presented in the table. CC had the lowest cDNA concentration at 4.24 ng/ $\mu$ L and CM NCI had the highest concentration at 20.90 ng/ $\mu$ L. The cDNA sizes were not significantly different, ranging between 162 – 172 bp. Abbreviations: CC, community children; CM, cerebral

malaria; FO, fatal outcome; FR, full recovery; NCI, neurocognitive impairment; SMA, severe malarial anaemia

The sequenced patient plasma EV-RNA gave a total of > 116 million (SD 1.10) reads that passed through the filter, with an average of 5 million reads per sample successfully identified without over-clustering the flow cell. The reads were then mapped against the human genome using Geneglobe to identify small biotypes of RNA (miRNA, rRNA, tRNA, mRNA, piRNA, hairpin RNA and other small RNA). For the six experimental groups, Geneglobe identified an average of  $2.12 \pm 0.04$ ,  $1.88 \pm 0.20$ ,  $2.33 \pm 0.10$ ,  $3.15 \pm 0.20$ ,  $2.65 \pm 0.09$ , and  $2.59 \pm 0.03$  million reads ( $10^6$ ) for CC, CM FR, CM NCI, CM FO, SMA FR and SMA NCI respectively (Table 4.2). Total good quality mapped reads for CC, CM FR, CM NCI, CM FO, SMA FR and SMA NCI were  $0.45 \pm 0.04$ ,  $0.36 \pm 0.20$ ,  $0.51 \pm 0.10$ ,  $0.64 \pm 0.10$ ,  $0.58 \pm 0.09$ , and  $0.46 \pm 0.04$  million reads ( $10^6$ ), respectively (Table 4.2). Across all samples, miRNA took up a larger percentage of the RNA profile; 22-65% of the RNA population comprised mature miRNAs, at an average of 43%, followed by 18% rRNA, 5.5% tRNA, 2.7% mRNA, 1.3% piRNA, 0.08% hairpin, 1.97% other RNA, and 28% not characterised but mappable RNA (Figure 4.3A).

#### 4.3.3 Differential expression analysis between the clinical groups

Using CLC-GWB, the threshold stringency was increased during the analysis of the six experimental groups giving an average of  $0.34 \pm 0.03$ ,  $0.49 \pm 0.29$ ,  $0.27 \pm 0.15$ ,  $0.35 \pm 0.13$ ,  $0.42 \pm 0.14$ , and  $0.33 \pm 0.12$  million reads mapped ( $10^6$ ) for CC, CM FR, CM NCI, CM FO, SMA FR and SMA NCI respectively (Table 4.2). After trimming and filtering, the sequences were run through the miRNA quantification workflow in CLC-GWB. An average of 39% of the patient groups' mature miRNA sequences matched the miRBase database, and 61% did not match any sequence in miRBase (Table 4.2). The clinical groups all had a lower average percentage of miRNA matched to the miRBase sequences, ranging from 27% to 44%. In contrast, the CC group was the only group with more matched miRNA than not matched (Table 4.2).

Differential expression analysis was then performed with CLC-GWB, and multiple read cut-offs were tested. A read cut-off of 1 resulted in 1126 mature miRNAs, and a read cut-off of 5 resulted in 314 mature miRNAs. A read cut-off of 10 was used to avoid false identifications,

and 234 mature miRNAs were identified from all groups. Individually, 154, 189, 199, 176, 174 and 180 mature miRNAs were mapped in CC, CM GO, CM NCI, CM FO, SMA GO and SMA NCI groups, respectively (Figure 4.3B). The mature miRNAs identified via NGS were compared using a six-way Venn diagram to identify the similarities between the groups<sup>67</sup>. The 6 subgroups had 125 miRNAs in common, all malaria patients had 17 miRNAs in common, the CM groups had 3 miRNAs in common, and the SMA groups had 2 miRNAs in common (Figure 4.3B). The mapped mature miRNAs were plotted on a principal component analysis scatter plot to identify any extreme outliers within the groups. There was strong grouping among the patients in the CC (Figure 4.3C, red) and SMA FR (Figure 4.3C, blue) groups, moderate clustering in the CM FO (Figure 4.3C, dark yellow) and SMA NCI (Figure 4.3C, orange) groups and a broader spread in the CM FR (Figure 4.3C, green) and CM NCI (Figure 4.3C, purple) groups, CM FR having the most significant distance between patients.

By analysing this unique group of miRNAs, the expression levels of the top 20 most abundant miRNAs in the plasma EVs were compared across all 6 patient subgroups (Table 4.3, Figure 4.3D). The top 5 most expressed miRNAs were hsa-miR-16-5p, hsa-miR-126-3p, hsa-miR-223-3p, hsa-let-7a-5p, and hsa-let-7b-5p, making up 19% of all mature miRNAs present in the samples (Table 4.3, Figure 4.3D). Hsa-miR-16-5p is the most abundant miRNA in all the samples and the most consistently present across all patients (Supplementary Table 4.1). The top 5 most expressed miRNA seed sequences made up 22% of all seed sequences mapped (Supplementary Table 4.2). A large portion of the mature miRNA did not match to sequences listed in miRBase; the top 5 most abundant novel seed sequences include 'GTAAAGT', 'AGAGAGA', 'TTAAGTG', 'GTTGGTC', and 'TAGGTCA' (Supplementary Table 4.3).

Five clinically relevant comparisons were examined, CM FO vs CM FR, CM NCI vs CM FR, CM FO vs CM NCI, CM NCI vs SMA NCI, and SMA FR vs SMA NCI, identifying 14, 47, 42, 19, and 11 differentially expressed mature miRNA respectively (Figures 4.4 and 4.5, Supplementary Table 4.4). Using a log<sub>2</sub> fold change of < -1 and > 1 and a p-value of < 0.05, volcano plots were generated, and 92 differentially expressed miRNAs were identified amongst the six patient subgroups (Figure 4.4). Heatmaps were generated using Clustergrammer<sup>68</sup>, and clustering was based on Cosine distance and average linkage. There was a clear distinction between CM FR and CM NCI, CM FO and CM NCI, CM NCI and SMA NCI, and SMA FR and SMA NCI, and to a lesser degree, CM FO and CM FR (Figure 4.5). Pairwise comparisons were used for cluster

analysis, and miRNA candidates were selected by their presence in  $\geq 50\%$  of patients, Log2 fold change  $< -3$  and  $> 3$ , and p-value  $< 0.05$ .

**Table 4.2** Genomic mapping of different small RNA species from Ugandan paediatric patient plasma EVs

Genomic mapping via Geneglobe												
RNA profile	CC (n = 3)		CM FR (n = 12)		CM NCI (n = 4)		CM FO (n = 4)		SMA FR (n = 4)		SMA NCI (n = 4)	
	Avg	SD	Avg	SD	Avg	SD	Avg	SD	Avg	SD	Avg	SD
Total reads, x10 <sup>6</sup>	2.12	0.04	1.88	0.20	2.33	0.10	3.15	0.20	2.65	0.09	2.59	0.03
Total good quality mapped reads, x10 <sup>6</sup>	0.45	0.04	0.36	0.20	0.51	0.10	0.64	0.10	0.58	0.09	0.46	0.04
Reads percentage (%)												
miRNA	39.59	4.06	36.12	11.66	51.65	7.74	33.50	9.47	48.01	7.34	46.78	2.33
rRNA	16.19	3.91	20.92	4.53	17.29	5.58	19.98	4.04	15.86	4.73	16.15	1.82
tRNA	9.50	5.88	4.47	2.45	3.79	0.66	4.48	2.53	5.00	1.19	5.79	2.01
mRNA	1.20	0.08	2.23	0.64	2.67	0.77	3.64	1.51	2.72	0.52	3.63	0.83
piRNA	1.20	0.25	1.09	0.25	1.60	0.25	1.27	0.70	1.12	0.05	1.31	0.09
Hairpin	0.04	0.02	0.07	0.04	0.08	0.03	0.09	0.06	0.07	0.05	0.14	0.09
Other small RNA	2.75	0.59	1.76	1.19	1.66	0.42	2.57	1.55	1.30	0.22	1.75	0.33
Not characterised but mappable RNA	29.53	4.35	33.34	13.45	21.27	4.54	34.46	16.37	25.91	5.05	24.44	1.48
Genomic mapping via CLC genomic workbench												
Mature miRNA profile												
Total good quality reads, x10 <sup>6</sup>	0.34	0.03	0.49	0.29	0.27	0.15	0.35	0.13	0.42	0.14	0.33	0.12
miRNA matched in miRBase												
Reads, x10 <sup>6</sup> (SD)	0.18	0.03	0.09	0.05	0.09	0.04	0.15	0.12	0.18	0.06	0.14	0.05
Percentage (%) (SD)	54	4	27	17	32	6	36	28	43	8	44	5
miRNA not matched in miRBase												
Reads, x10 <sup>6</sup> (SD)	0.15	0.002	0.40	0.32	0.18	0.11	0.20	0.10	0.24	0.09	0.19	0.07
Percentage (%) (SD)	46	4	73	17	68	6	64	28	57	8	56	5

The sequences were processed through Qiagen® Geneglobe where low-quality reads were filtered, and all short < 16 nucleotide sequences were removed. The total reads between groups are consistent, with the total RNA consisting largely of miRNA, ranging between 22-65% per individual patient with CM FO (33.50%, SD 9.47) being the lowest and CM NCI (51.65%, SD 7.74) being the highest. Many not-characterised but mappable RNA were also identified, opening the door for novel miRNA discovery. Mapping was also done using CLC genomic workbench, sequences were trimmed and sequences shorter than 15 nucleotides were filtered out, miRNA length was set to 15-55 nucleotides, and a threshold of 10 reads. An average of 39% of the miRNA matched the miRBase database and 61% of the miRNA did not match sequences in miRBase.

Abbreviations: CC, community children; CM, cerebral malaria; FO, fatal outcome; FR, full recovery; NCI, neurocognitive impairment; SD, standard deviation; SMA, severe malarial anaemia; miRNA, microRNA; rRNA, ribosomal RNA; tRNA, transfer RNA; mRNA, messenger RNA; piRNA, P-Element induced wimpy testis (Piwi)-interacting RNAs

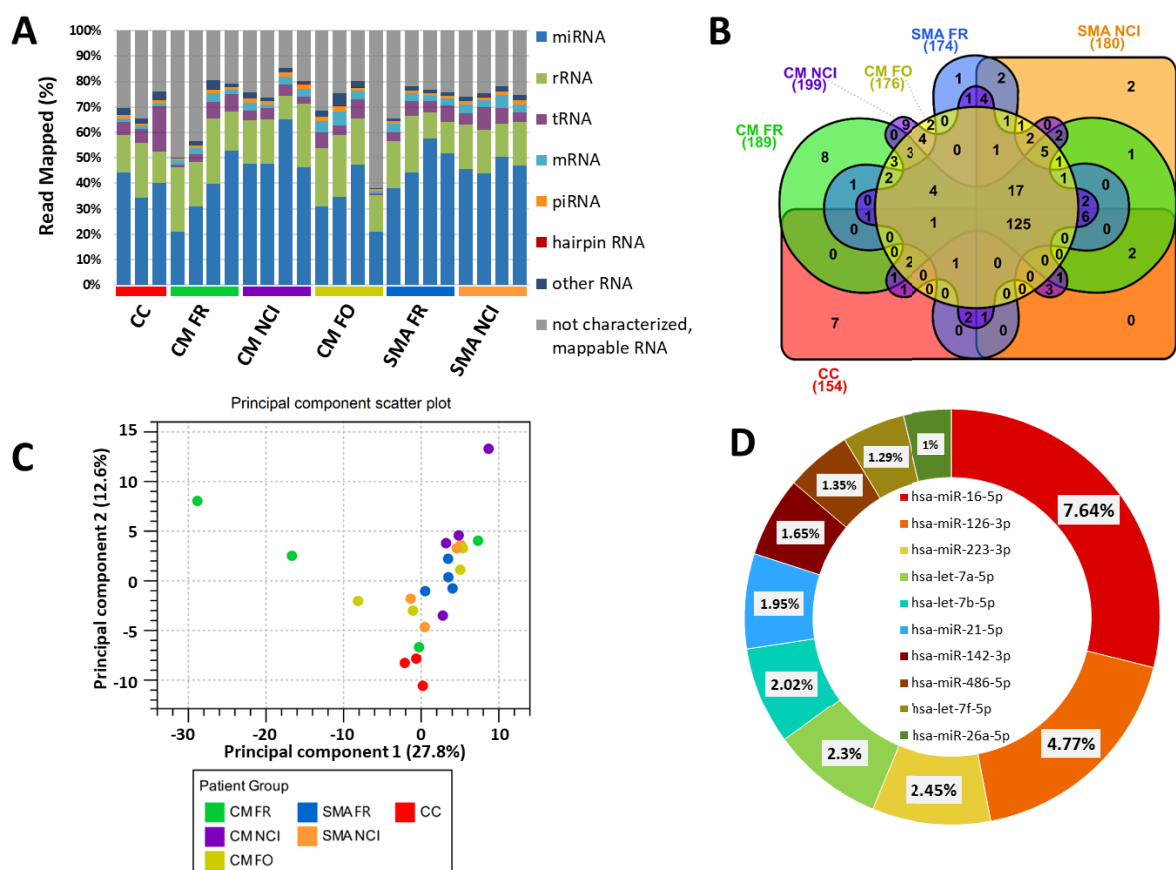


**Figure 4.3** MircorRNA characterisation in malaria-infected Ugandan paediatric patient plasma EVs using next-generation sequencing. (A) Distribution of RNA biotypes identified in individual patient plasma EV transcriptome during NGS analysis using Geneglobe. (B) Venn diagram of patient group-specific mature mapped miRNA created using InteractiVenn. (C) Principal component analysis plot of the miRNA population identified in each patient. (D) The average percentage for the top 10 most expressed mature miRNAs. Abbreviations: CC, community children; CM, cerebral malaria; FO, fatal outcome; FR, full recovery; NCI, neurocognitive impairment; SMA, severe malarial anaemia; miRNA, microRNA; rRNA, ribosomal RNA; tRNA, transfer RNA; mRNA, messenger RNA; piRNA, P-Element induced wimpy testis (Piwi)-interacting RNAs



**Table 4.3** Top 20 most abundant mature miRNA sequences identified in Ugandan paediatric plasma-derived EVs

Mature miRNA counts x10 <sup>4</sup>	Avg %	CC (n = 3)		CM FR (n = 12)		CM NCI (n = 4)		CM FO (n = 4)		SMA FR (n = 4)		SMA NCI (n = 4)	
		Avg	SD	Avg	SD	Avg	SD	Avg	SD	Avg	SD	Avg	SD
hsa-miR-16-5p	7.64	4.07	1.42	1.49	0.43	2.00	0.97	2.59	1.99	3.16	0.98	3.22	1.53
hsa-miR-126-3p	4.77	2.20	0.14	1.21	0.91	1.06	0.65	1.87	1.36	2.08	1.02	1.95	1.21
hsa-miR-223-3p	2.45	1.27	0.10	0.62	0.41	0.62	0.43	0.54	0.38	1.60	0.89	0.89	0.75
hsa-let-7a-5p	2.3	1.15	0.35	0.51	0.25	0.48	0.14	0.73	0.64	1.09	0.36	0.85	0.23
hsa-let-7b-5p	2.02	0.81	0.30	0.38	0.12	0.71	0.27	0.56	0.43	0.93	0.26	0.79	0.47
hsa-miR-21-5p	1.95	0.79	0.12	0.46	0.43	0.16	0.14	1.52	2.29	0.79	0.40	0.51	0.08
hsa-miR-142-3p	1.65	0.82	0.20	0.53	0.35	0.24	0.07	0.40	0.32	0.85	0.28	0.56	0.07
hsa-miR-486-5p	1.35	0.57	0.23	0.20	0.08	0.40	0.18	0.65	0.45	0.46	0.20	0.61	0.33
hsa-let-7f-5p	1.29	0.67	0.12	0.32	0.19	0.17	0.04	0.45	0.37	0.60	0.18	0.45	0.09
hsa-miR-26a-5p	1	0.48	0.05	0.30	0.22	0.21	0.14	0.32	0.22	0.51	0.20	0.33	0.09
hsa-let-7i-5p	0.89	0.37	0.08	0.20	0.08	0.21	0.07	0.32	0.27	0.46	0.11	0.29	0.07
hsa-miR-146a-5p	0.74	0.18	0.007	0.15	0.05	0.13	0.05	1.19	1.52	0.27	0.11	0.17	0.05
hsa-miR-26b-5p	0.57	0.29	0.03	0.17	0.12	0.07	0.03	0.24	0.20	0.28	0.10	0.18	0.04
hsa-miR-126-5p	0.49	0.28	0.07	0.21	0.07	0.12	0.06	0.22	0.20	0.30	0.12	0.19	0.10
hsa-miR-150-5p	0.41	0.23	-	0.17	0.08	0.14	0.08	0.10	0.07	0.35	0.16	0.15	0.01
hsa-miR-342-3p	0.33	0.20	-	0.13	0.07	0.11	0.07	0.11	-	0.25	0.12	0.14	0.03
hsa-miR-191-5p	0.33	0.17	0.0004	0.11	0.08	0.14	0.05	0.12	0.02	0.24	0.15	0.16	0.03
hsa-miR-92a-3p	0.26	0.18	0.002	0.08	0.04	0.11	0.03	0.10	0.07	0.14	-	0.15	0.06
hsa-miR-451a	0.26	0.22	0.07	0.06	0.03	0.11	0.08	0.42	-	0.16	0.03	0.20	0.09
hsa-miR-30d-5p	0.25	0.12	-	0.07	0.03	0.15	0.03	0.13	0.05	0.18	0.05	0.09	0.01

Abbreviations: CC, community children; CM, cerebral malaria; FO, fatal outcome; FR, full recovery; NCI, neurocognitive impairment; SD, standard deviation; SMA, severe malarial anaemia

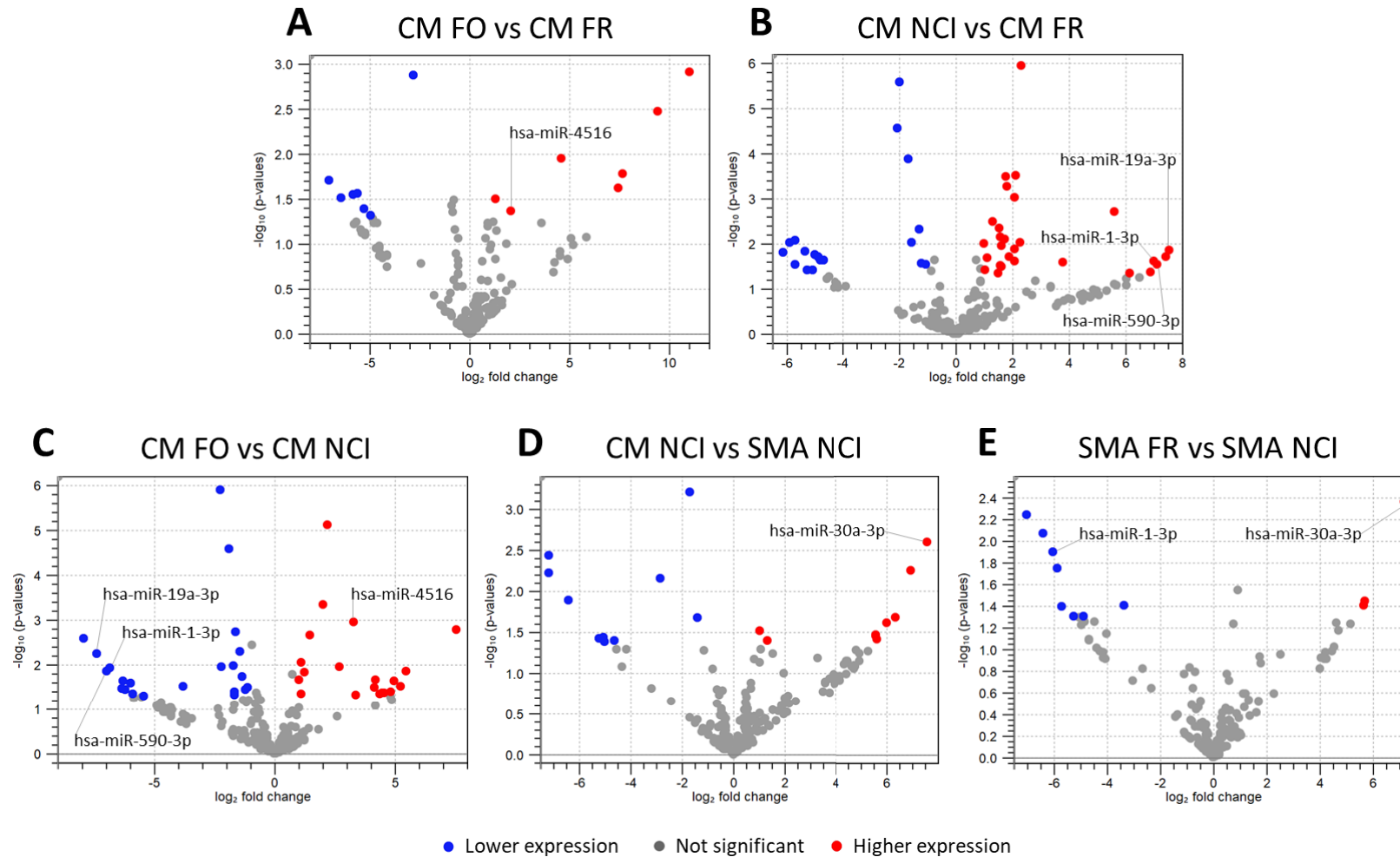


**Figure 4.4** Volcano plots of the mature microRNAs in the 5 comparisons of biological interest,  $|\text{Log}_2\text{Fold Change}| > 1$ ,  $P\text{-value} < 0.05$ . (A-E) respectively show 14, 47, 42, 19, and 11 differentially expressed microRNAs, a total of 92 differentially expressed microRNAs were discovered between the six subgroups of paediatric patients. MicroRNA named on the volcano plots were selected for RT-qPCR validation. Abbreviations: CC, community children; CM, cerebral malaria; FO, fatal outcome; FR, full recovery; NCI, neurocognitive impairment; SMA, severe malarial anaemia



#### 4.3.4 Pathway analysis on miRNAs of interest

Within the clinical groups, 22 differentially expressed miRNA were identified with the stringent selection criteria, and pathway analysis was performed with Metascape to generate the GO terms (Figure 4.6A). The miRNA-predicted target genes were generated using the miRDB database, capping the target score at  $\geq 60$ . The top 20 GO terms involve the head, neuron, and motor development (Figure 4.6A). When the analysis was expanded to the top 50 GO terms, there was further support for the central nervous system, muscle, and sensory organ development, as well as regulation of the cell junction, cell adhesion and vesicle-mediated transport (Supplementary Figure 4.2A). The 22 miRNAs were then compared to the miRNAs known to regulate genes in the *Homo sapiens* malaria KEGG pathway and 13 matched, i.e., hsa-miR-1260a, hsa-miR-1290, hsa-miR-1-3p, hsa-miR-152-3p, hsa-miR-19a-3p, hsa-miR-206, hsa-miR-30a-3p, hsa-miR-335-5p, hsa-miR-339-5p, hsa-miR-424-5p, hsa-miR-4488, hsa-miR-4516, and hsa-miR-590-3p (Table 4.4). By cross-referencing with the *Homo sapiens* malaria KEGG pathway, the 13 miRNAs were found to regulate 13 genes that encode for these 13 proteins, LFA1, HGF, MCP1, MET, HSPG, IL1, GCSF, CD40, NKC, VCAM1, CR1, LRP, and INF $\gamma$  (Figure 4.7, Table 4.4). Of the 13 miRNAs, has-miR-590-3p regulates the most genes: five of the thirteen malaria-related genes, affecting proteins CD40, VCAM1, CR1, LRP, and INF $\gamma$ . Then followed by hsa-miR-1-3p, which regulates three of the thirteen malaria-related genes, affecting proteins HGF, MCP1, and MET; hsa-miR-30a-3p, which regulates HGF and IL1, and hsa-miR-4516 that regulates NKC and LRP.

Five miRNAs of interest were selected by choosing miRNAs that can differentiate more than one comparison, regulate the most genes within the human malaria KEGG pathway, and miRNAs with the most significant GO pathways. These criteria allowed the selection of hsa-miR-1-3p, hsa-miR-19a-3p, hsa-miR-30a-3p, hsa-miR-4516, and hsa-miR-590-3p (Figures 4.4-4.6), which regulate 11 out of the 13 proteins, HGF, MCP1, MET, HSPG, IL1, CD40, NKC, VCAM1, CR1, LRP, and INF $\gamma$ . Pathway analysis was implemented in the same manner as described above, and the top 20 GO terms showed that these 5 miRNAs significantly regulated mRNA metabolic processes, cell-cell adhesion, cellular localisation, endosome membrane, and head and neuron development (Figure 4.6B). Compared to the 22 miRNAs GO heatmap, the 5 miRNAs GO heatmap has many more pathways involved in the head, neuron, and motor development (Figure 4.6). Likewise, the top 50 GO terms for the 5 miRNAs of interest have

approximately double the amount of pathways involved in neuronal and motor development, cell junction, cell adhesion, protein transport, behaviour, and regulation of vesicle-mediated transport (Supplementary Figure 4.2B). In addition, there were also pathways involving the morphogenesis of epithelium and regulation of epithelial cell proliferation. The top 20 GO terms for the 5 miRNAs of interest primarily consist of biological processes and cellular component pathways (Supplementary Figure 4.2B). All five miRNAs are involved in regulating 80% of the pathways identified (Supplementary Table 4.5).

**Table 4.4** MicroRNAs that regulate proteins from the malaria KEGG pathway

CM FR vs CM FO	CM NCI vs CM FR	CM NCI vs CM FO	SMA FR vs SMA NCI
hsa-miR-4488 ↓ 5	hsa-miR-1-3p ↑ 2, 3, 4	hsa-miR-1-3p ↑ 2, 3, 4	hsa-miR-1-3p ↓ 2, 3, 4
hsa-miR-4516 ↓ 9, 12	hsa-miR-19a-3p ↑ 5	hsa-miR-19a-3p ↑ 5	hsa-miR-30a-3p ↑ 2, 6
	hsa-miR-206 ↑ 3, 4	hsa-miR-152-3p ↑ 4	hsa-miR-1290 ↓ 2
	hsa-miR-339-5p ↓ 7	hsa-miR-335-5p ↑ 4	
	hsa-miR-424-5p ↑ 8	hsa-miR-4516 ↓ 9, 12	
CM NCI vs SMA NCI	hsa-miR-590-3p ↑ 8, 10, 11, 12, 13	hsa-miR-590-3p ↑ 8, 10, 11, 12, 13	
hsa-miR-30a-3p ↑ 2, 6		hsa-miR-1260a ↓ 1, 11	

13 genes controlled by 13 microRNA listed above (KEGG pathway malaria)

1:LFA1; 2: HGF; 3:MCP1; 4:MET; 5:HSPG; 6:IL1; 7:GCSF; 8:CD40; 9:NKC; 10:VCAM1; 11:CR1; 12:LRP; 13:IFN $\gamma$

Abbreviations: CC, community children; CM, cerebral malaria; FO, fatal outcome; FR, full recovery; NCI, neurocognitive impairment; SMA, severe malarial anaemia

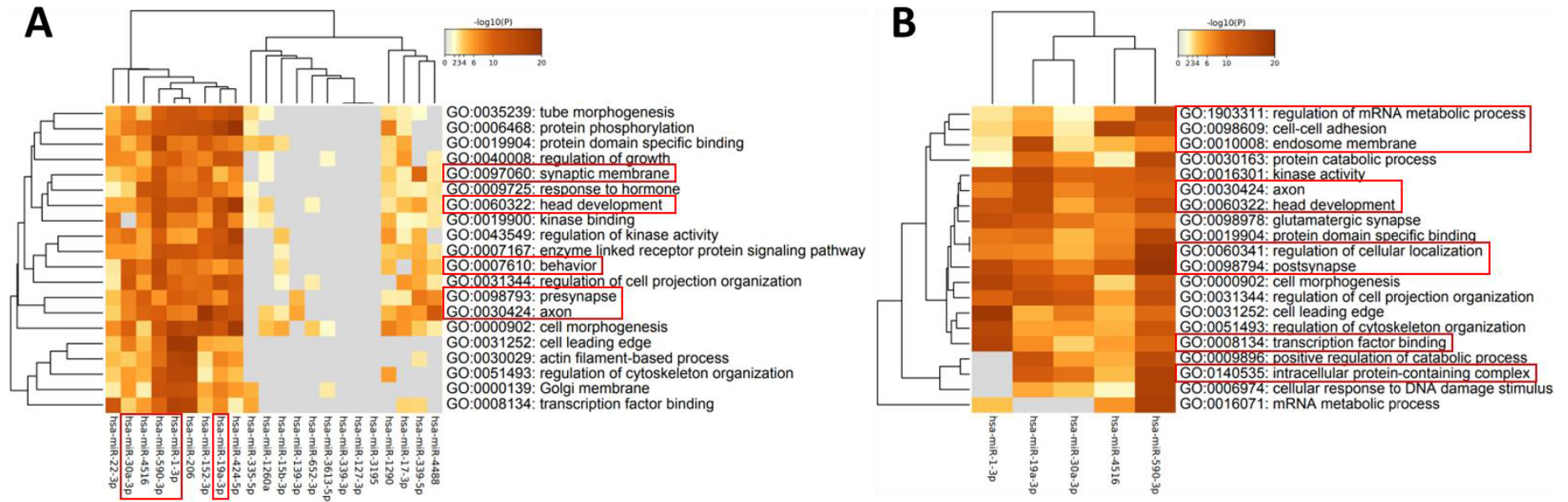


**Figure 4.6** Top 20 gene ontology terms for differentially expressed miRNA present in  $\geq 50\%$  of patients. (A) 22 differentially expressed miRNA. MiRNA in red boxes were selected for RT-qPCR validation. (B) Five miRNAs of interest.

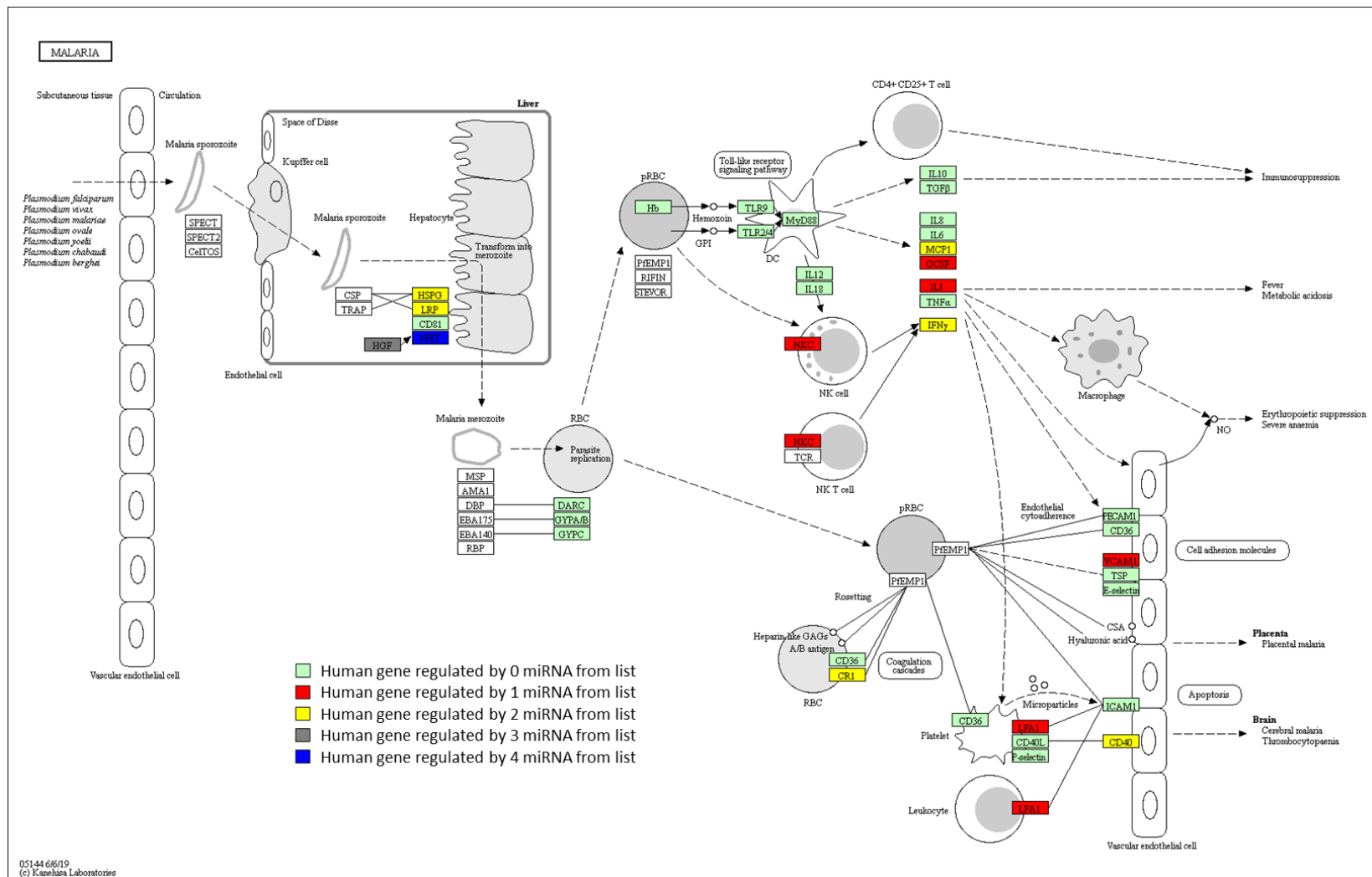


**Figure 4.7** Malaria KEGG pathway, hsa05144, 13 miRNAs of interest regulate 13 genes involved in malaria. Green boxes, Human genes not regulated by the miRNA in the list.

## Verification Phase

### 4.3.5 Selecting endogenous control for real-time quantitative PCR normalisation

Using RT-qPCR, the miRNAs identified via NGS were verified with a new series of patients (5 per group). Based on the miRNA's representation in the different groups and their significance in malaria pathogenesis, the 5 miRNAs of interest are hsa-miR-1-3p, hsa-miR-19a-3p, hsa-miR-30a-3p, hsa-miR-4516, and hsa-miR-590-3p. Using the NGS data, an endogenous control was selected; the selection criteria based on a previous publication<sup>60</sup> includes a coefficient of variation of < 5 % on normalised UMI counts across all samples, UMI count mean  $\geq 3000$ , standard deviation < 1, and  $\log_2$  fold change < 1. Using these criteria, hsa-miR-16-5p was identified as the best endogenous control for normalisation during RT-qPCR analysis. The relative expression was calculated using the  $2^{-\Delta\Delta C_t}$  method,  $\Delta C_t = C_t (\text{miRNA}) - C_t (\text{endogenous control})$ ,  $\Delta\Delta C_t = \Delta C_t (\text{patient group}) - \text{average } \Delta C_t (\text{control patient group, CC})$ .

### 4.3.6 MicroRNA verification via real-time quantitative PCR

A non-parametric Kruskal-Wallis test was applied to the normalised  $C_t$  values to compare the different groups of patients. If significant, a planned Dunn's contrast with Bonferroni adjustment analysis was performed on the 5 biologically significant comparisons (Figure 4.8A, Table 4.5). First the main disease groups, CC, CM and SMA were compared showing significantly lower expressions of hsa-miR-1-3p and hsa-miR-4516 in CC children than CM children (Figure 4.8A, top row). Similar expressions were found for CC children when compared to SMA children with the addition of hsa-miR-19a-3p levels also being significantly lower in CC children. The two main disease groups were then compared and showed hsa-miR-19a-3p and hsa-miR-590-3p expressions to be significantly lower in CM children compared to SMA children (Figure 4.8A, top row). All of the severe malaria patients were then combined and compared to the healthy children using a non-parametric Kruskal-Wallis test followed by a Mann-Whitney test. The analysis found significantly lower levels of hsa-miR-1-3p and hsa-miR-4516 in CC children compared to those with severe malaria (Figure 4.8A, top row).

Moving onto comparing the subgroups of severe malaria, there were no significant miRNA expression differences between CM children who made full recoveries and CM children who developed NCI. Then when compared to CM children that died, the CM children that fully



recovered had significantly lower expressions of hsa-miR-1-3p, hsa-miR-19a-3p, hsa-miR-30a-3p, and hsa-miR-4516 (Figure 4.8A, bottom row). Whereas only hsa-miR-1-3p, hsa-miR-19a-3p, and hsa-miR-4516 were under expressed in CM children who developed NCI compared to CM children that died (Figure 4.8A, bottom row). In contrast to the CM group comparisons, the SMA children that fully recovered had significantly higher levels of hsa-miR-30a-3p than the SMA children who developed NCI and none of the other miRNAs were differentially expressed. Lastly it was found that hsa-miR-19a-3p was the only miRNA that was significantly under expressed in CM children that developed NCI compared to SMA children that developed NCI (Figure 4.8A, bottom row).

#### 4.3.7 Differing miRNA expression profiles between sequencing and PCR analysis

The miRNA expression profiles between the RT-qPCR and NGS were different for many of the patient group comparisons (Table 4.5). When compared to CM children that died, NGS identified hsa-miR-4516 to be significantly less expressed in CM children that fully recovered without complications, whereas RT-qPCR identified all miRNA except hsa-miR-590-3p to be less expressed in CM FR children (Table 4.5). For the comparison between CM children that developed NCI verses CM children that fully recovered, NGS identified 3 out of the 5 miRNAs were significantly overexpressed in CM NCI; however, for RT-qPCR, none were differentially expressed (Table 4.5). Analysis via NGS found significantly higher levels of hsa-miR-1-3p and hsa-miR-19a-3p in CM children that developed NCI compared to CM children that died, however both miRNA levels were lower via RT-qPCR. For the same comparison, hsa-miR-4516 was significantly under expressed in CM NCI children for both RT-qPCR and NGS results, and hsa-miR-590-3p was significantly over expressed in CM NCI children in the NGS analysis, but no differences were identified via RT-qPCR. Both NGS and RT-qPCR analysis showed significantly higher levels of hsa-miR-30a-3p in SMA children that fully recovered compared to SMA children that developed NCI, and hsa-miR-1-3p levels were lower in SMA FR, only in the NGS analysis. Lastly, the NGS results showed hsa-miR-30a-3p to be over expressed in CM children that developed NCI compared to SMA children that developed NCI and hsa-miR-19a-3p to be less expressed in the CM NCI children via RT-qPCR analysis.

**Table 4.5** Comparison of next generation sequencing and RT-qPCR expression levels between severe malaria patient groups

Expression levels via Next Generation Sequencing					
MicroRNA	CLC Genomic Work Bench, Trimmed Mean of M (TMM) <sup>#</sup>				
	CM FR vs CM FO	CM NCI vs CM FR	CM NCI vs CM FO	CM NCI vs SMA NCI	SMA FR vs SMA NCI
hsa-miR-1-3p	-	↑ CM NCI (0.025)	↑ CM NCI (0.012)	-	↓ SMA FR (0.013)
hsa-miR-19a-3p	-	↑ CM NCI (0.014)	↑ CM NCI (0.006)	-	-
hsa-miR-30a-3p	-	-	-	↑ CM NCI (0.003)	↑ SMA FR (0.004)
hsa-miR-4516	↓ CM FR (0.043)	-	↓ CM NCI (0.001)	-	-
hsa-miR-590-3p	-	↑ CM NCI (0.028)	↑ CM NCI (0.014)	-	-

Relative Expression via RT-qPCR (5 biologically significant comparisons)								
MicroRNA	Planned Dunn's contrasts with Bonferroni adjustment <sup>#</sup>					Kruskal-Wallis Test		
	CM FR vs CM FO	CM NCI vs CM FR	CM NCI vs CM FO	CM NCI vs SMA NCI	SMA FR vs SMA NCI	χ <sup>2</sup>	df	P value
hsa-miR-1-3p	↓ CM FR (10 x 10 <sup>9</sup> )	0.688	↓ CM NCI (0.007)	0.073	1.000	50.377	5	1 x 10 <sup>9</sup>
hsa-miR-19a-3p	↓ CM FR (0.021)	1.000	↓ CM NCI (1 x 10 <sup>4</sup> )	↓ CM NCI (0.008)	0.285	37.582	5	5 x 10 <sup>7</sup>
hsa-miR-30a-3p	↓ CM FR (0.039)	1.000	0.187	0.133	↑ SMA FR (0.020)	14.762	5	0.011
hsa-miR-4516	↓ CM FR (4 x 10 <sup>6</sup> )	0.683	↓ CM NCI (0.002)	0.218	0.979	33.523	5	3 x 10 <sup>6</sup>
hsa-miR-590-3p	1.000	0.701	0.778	0.117	0.754	10.058	5	0.074

Relative Expression via RT-qPCR (3 main patient groups)									
MicroRNA	Mann-Whitney <sup>#</sup>	Kruskal-Wallis Test		Planned Dunn's contrasts with Bonferroni adjustment <sup>#</sup>			Kruskal-Wallis Test		
	CC vs SM	χ <sup>2</sup>	P value	CC vs CM	CC vs SMA	CM vs SMA	χ <sup>2</sup>	df	P value
hsa-miR-1-3p	↓ CC (8 x 10 <sup>10</sup> )	77	7 x 10 <sup>10</sup>	↓ CC (3 x 10 <sup>7</sup> )	↓ CC (6 x 10 <sup>10</sup> )	0.146	40.683	2	1 x 10 <sup>9</sup>
hsa-miR-19a-3p	0.232	603	0.232	1.000	↓ CC (0.017)	↓ CM (8 x 10 <sup>4</sup> )	13.437	2	0.001
hsa-miR-30a-3p	0.264	651	0.264	0.165	1.000	0.143	4.036	2	0.133
hsa-miR-4516	↓ CC (1 x 10 <sup>5</sup> )	126	1 x 10 <sup>5</sup>	↓ CC (6 x 10 <sup>4</sup> )	↓ CC (8 x 10 <sup>6</sup> )	0.235	21.371	2	2 x 10 <sup>5</sup>
hsa-miR-590-3p	0.883	564	0.883	0.366	0.291	↓ CM (9 x 10 <sup>3</sup> )	7.517	2	0.023

Abbreviations: CC, community children; CM, cerebral malaria; df, degrees of freedom; FO, fatal outcome; FR, full recovery; IQR, Interquartile Range; NCI, neurocognitive impairment; SMA, severe malarial anaemia

<sup>#</sup> P value

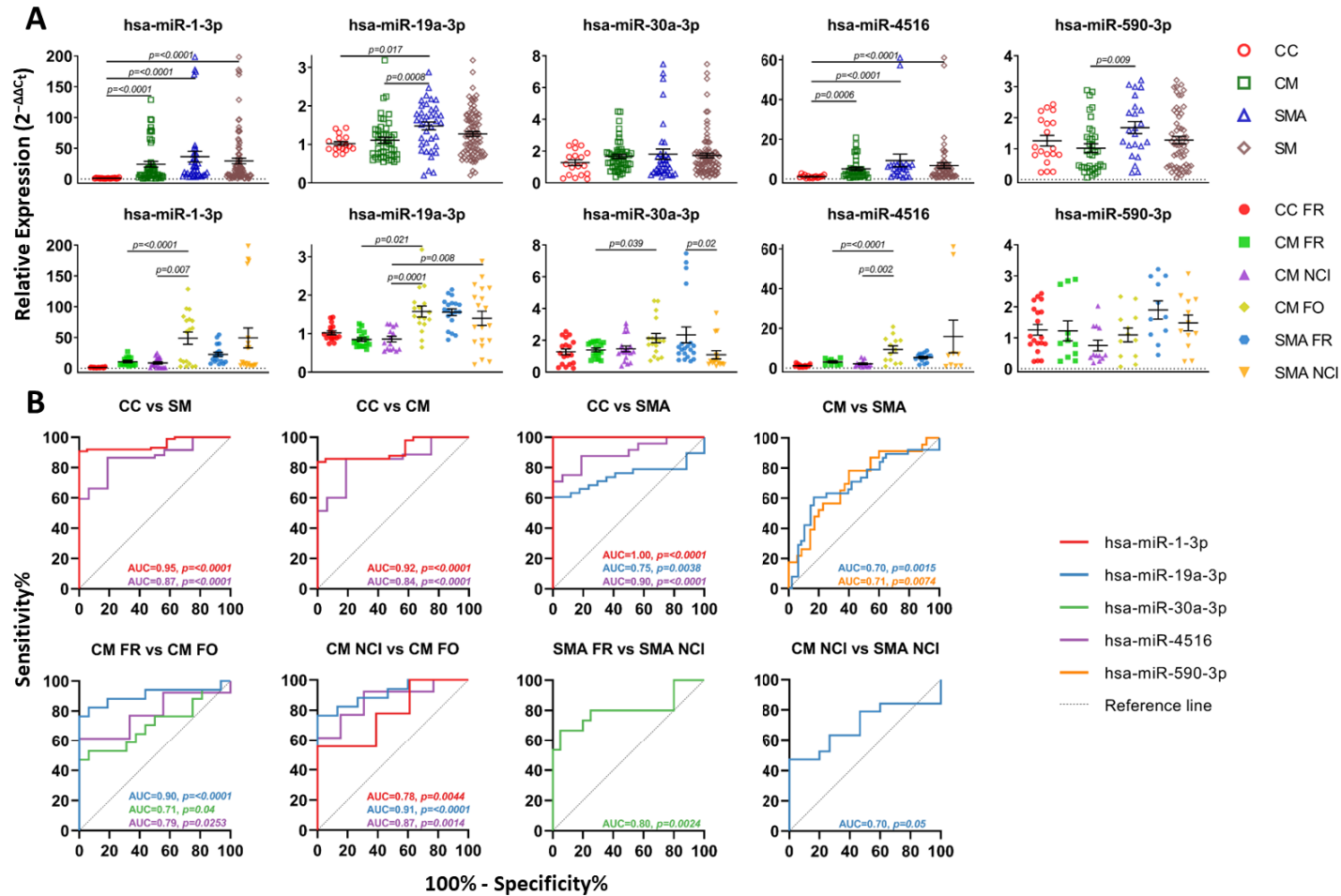


Figure 4.8 Validation of microRNA expression via RT-qPCR. (A) Relative expression of the five microRNA of interest across all groups. (B) Receiver operator curve for the prognostic value of each microRNA of interest within relative biological comparisons. Abbreviations: CC, community children; CM, cerebral malaria; FO, fatal outcome; FR, full recovery; NCI, neurocognitive impairment; SMA, severe malarial anaemia

#### 4.3.8 Receiver operator curves identified numerous miRNAs with prognostic potential

To determine the prognostic performance of the miRNAs of interest, ROC curves were generated for the miRNAs that could significantly differentiate two patient groups (Figure 4.8B). The healthy CC children can be accurately and correctly distinguished from severe malaria children (SM, CM, and SMA) with the use of hsa-miR-1-3p (AUC > 0.92, p-value < 0.0001, for all three comparisons) and hsa-miR-4156 (AUC > 0.84, p-value < 0.0001, for all three comparisons) (Figure 4.8B, top row). Interestingly, for the comparison between CC children and SMA children, hsa-miR-1-3p had an AUC of 1.00 and p-value < 0.0001, meaning the sensitivity and specificity are both 100%; therefore, hsa-miR-1-3p can accurately and correctly identify the CC patients from the SMA patients 100% of the time with no false negatives. Hsa-miR-19a-3p was also a significant miRNA for differentiating CC children from SMA children but to a lesser degree as the AUC was 0.75 with a p-value of 0.0038 (Figure 4.8B, top row). Two miRNA, hsa-miR-19a-3p (AUC=0.70, p-value=0.0015) and hsa-miR-590-3p (AUC=0.71, p-value=0.0074) were candidates for distinguishing CM children from SMA children, although they had a lower AUC value, they were still at an acceptable level for discriminating the groups (Figure 4.8B, top row).

For the subgroup outcome comparisons, the CM FR vs CM FO children could be discerned with hsa-miR-19a-3p (AUC > 0.90, p-value < 0.0001), hsa-miR-30a-3p (AUC > 0.71, p-value=0.04), and hsa-miR-4516 (AUC > 0.79, p-value=0.0253) (Figure 4.8B, bottom row). Similarly, the CM NCI vs CM FO children could be differentiated with hsa-miR-1-3p (AUC > 0.78, p-value=0.0044), hsa-miR-19a-3p (AUC=0.91, p-value < 0.0001) and hsa-miR-4516 (AUC > 0.87, p-value=0.0014) (Figure 4.8B, bottom row). Then when comparing SMA FR to SMA NCI children hsa-miR-30a-3p was the only miRNA with a good ROC curve of AUC=0.08 and p-value=0.024 (Figure 4.8B, bottom row). Lastly, the CM NCI and SMA NCI children could be distinguished with hsa-miR-19a-3p, with an AUC=0.70 and p-value=0.05, although the p-value is on the boarder of significance (Figure 4.8B, bottom row).

## **4.4 Discussion**

Currently, there is an absence of reliable markers predicting malaria mortality and morbidity, especially which patients with severe malaria are at risk of NCI. The discovery of prognostic malaria biomarkers is crucial for patients with severe malaria. It would enable physicians to implement appropriate adjunctive therapies and medical interventions to increase the chances of survival and decrease the risk of long-term sequelae in children, minimising the effect of learning and behaviour problems on the quality of life. In this study, we report the first genome-wide miRNA gene expression profile of plasma EVs from children infected with malaria. A group of Ugandan children was closely monitored, from hospital admission to mortality or discharge, and with follow-up through 12 months for NCI. To the best of our knowledge, no study has identified the unique expression profiles and signatures of plasma EV miRNAs from severe malaria patients and compared the different disease states and healthy controls. Although there were many challenges, this study identified the miRNAs packaged into EVs during the early response to malaria infection and discovered potential prognostic miRNA biomarkers for severe malaria. High-throughput and high-content data analysis techniques have advanced to allow exponential growth in molecular data related to EVs<sup>69,70</sup>. In addition to highly specific and sensitive assays, biomarker discovery could become relatively straightforward; however, a standardised methodology is crucial.

A main challenge faced when working with paediatric patients was the small sample volume (~180 µL of plasma per patient) collected from paediatric patients. The sample processing workflow was established to ensure high-quality RNA was isolated from the EVs without RNA loss during processing. Numerous methodologies and isolation kits were tested, and the Qiagen® serum plasma miRNA isolation kit collected the cleanest RNA. Consistency in RNA isolation speed between batches was also crucial; the longer it took to complete the isolation, the more nucleotide degradation was detected in both NGS and RT-qPCR. However, the nucleotide degradation rate was miRNA specific, which was consistent with research that linked miRNA sequence properties to miRNA stability<sup>54</sup>. The study observed that miRNA half-life correlated with GC content, where miRNAs with high GC content were more stable. In addition to the standardised isolation methods, small RNA QC was performed to monitor quality and size. Similarly, the cDNA library was monitored and checked to ensure all primer dimers were removed before sequencing. The standardisation of sample processing, isolation

methods, and QC contributes to consistency throughout the study, providing reliable results intra-assay and between techniques.

An issue with sequencing several samples in one batch is over-clustering the flow cell; therefore, we split our samples into two runs, 11 samples in the first run and 12 samples in the second run. Splitting into two runs allowed the MiSeq® Illumina® system to identify an average of 5 million reads per sample without over-clustering the flow cell. Sample variation can also be a problem with human samples, which can be reduced with large sample sizes or, in this case, the closely matched clinical and biological history between patients. Another method of monitoring sample variation was the use of a PCA plot; our study identified two CM FR patients with lower amounts of identified reads and miRNAs than other groups (Figure 4.3C). Neither CM FR child was excluded from the analysis as they did not skew the data (analysis not shown). Overall, the CM patients (CM FR, CM NCI, and CM FO) had a wider spread than the SMA and CC patients, and the CM NCI and SMA NCI patient groups clustered together, potentially indicating similar RNA profiles.

This study provides the first evidence of paediatric plasma EV miRNA prognostic biomarkers for distinct disease outcomes of severe malaria. Across all the samples, miRNA was attributed to the main percentage of RNA, followed by not characterised but mappable RNA. When analysing the percentage of matched miRNA to the percentage of not matched miRNA, community control children had the highest percentage of matched miRNA, and all the disease groups had less. There is a vast potential for novel miRNA discovery within our clinical groups as 56 to 73% of the miRNAs have not been matched to any mature miRNA in the miRbase database (Table 4.2). Among the 6 patient groups, 234 mature miRNAs were identified, of which 92 were differentially expressed, and 13 were of clinical interest. Five miRNAs were selected based on their relevance to malaria and coverage of genes matched in the malaria KEGG pathway. The eleven genes play essential roles in malaria infection, such as regulating endothelial junctions at the blood-brain barrier, malaria parasite elimination, monocyte and macrophage migration, memory CD8 T cells recruitment to the liver, and regulation of pathophysiological syndromes<sup>71-76</sup>.

Comparisons between the different outcomes of CM had the most amount of differentiating miRNA for both NGS and RT-qPCR analysis (Table 4.5). This could indicate that pathogenically the children have different pathways that are being expressed or suppressed which led to a

certain outcome of CM. The NGS and RT-qPCR analysis showed similarities between the two cohorts of children, as CM survivors (with or without NCI) had lower levels of hsa-miR-4516 compared to CM fatal outcomes, and SMA survivors without NCI had higher amounts of hsa-miR-30a-3p than those with NCI (Table 4.5). There were also differences between the results obtained in the NGS and the RT-PCR. As all pre-analytic parameters (demographics and clinical findings, EV and RNA isolation) were the same and tightly controlled, the only major difference that could explain this discrepancy was the age differences between the cohorts used for each analysis, i.e., NGS: mean 3.1 years old and RT-PCR: mean 6.4 years old. The expression of miRNAs in children with CM suffering from neurocognitive impairment was opposite between NGS and RT-qPCR, which could indicate that children two to four years old (average 3.1 years old) with CM NCI package more disease specific miRNA into plasma EVs than five to ten years old (average 6.4 years old).

The four miRNAs upregulated in CM NCI from the NGS results were hsa-miR-1-3p, hsa-miR-19a-3p, hsa-miR-30a-3p, and hsa-miR-590-3p, these miRNAs are involved in neurological pathways; however, no studies were found relating them to neurological syndromes in malaria. GO analysis showed that these four miRNAs regulate developmental growth, head development, epithelial cell proliferation, presynaptic, and postsynaptic pathways (Supplementary Figure 4.2B). When paired together as a panel, these miRNAs could potentially act as functional or neuropsychological prognostic markers for severe malaria children who fully recovered without complications, fully recovered but developed neurocognitive impairment and those who died due to complications.

The ROC analysis for the verification cohort confirmed the prognostic performance of the miRNAs of interest amongst the disease groups. This study found that hsa-miR-1-3p and hsa-miR-4516 could best distinguish children with severe malaria (CM and/or SMA) from CC (Figure 4.8B). In contrast, hsa-miR-19a-3p and hsa-miR-590-3p could differentiate children with CM from SMA. Fatal outcomes in CM compared to survivors (with or without NCI) were predictively differentiated by hsa-miR-19a-3p and hsa-miR-4516. Hsa-miR-30a-3p was also able to distinguish survivors from fatal outcomes in CM prognostically but with less accuracy. Similarly, hsa-miR-1-3p could differentiate CM survivors with NCI from fatal outcomes with less precision. Survivors of SMA with NCI compared to those without, were prognostically

discriminate with hsa-miR-30a-3p. Lastly, when comparing children with NCI in CM to those with NCI in SMA, hsa-miR-19a-3p had good prognostic capacity.

As mentioned above, hsa-miR-1-3p can accurately distinguish healthy children from children with severe malaria, as well as CM survivors with NCI from CM fatal outcomes. MiR-1-3p is one of the more extensively studied miRNAs; it has been associated with muscle development, epithelial cell differentiation, and ischemic neurological disorders, though it has not been investigated in the context of malaria infection<sup>77,78</sup>. When infected with malaria, normal and infected red blood cells sequester and interact with endothelial cells that line the microvasculature<sup>79</sup>. This interaction could lead to increased abundance of hsa-miR-1-3p, affecting cellular function.

Hsa-miR-19a-3p is a good candidate for differentiating CM from SMA, as well as the survivors (with or without NCI) of CM from fatal outcomes in CM. Compared to the four other miRNAs miR-19a-3p has been investigated in mice with CM and found to be up-regulated in the brains of CM mice compared to non-infected or non-CM mice<sup>80</sup>. The study also illustrated miR-19a-3p's significant role in CM pathways such as TGF- $\beta$  and endocytosis. In our study, children between 2-4 years old who eventually develop CM NCI had an increase in miR-19a-3p compared to children that died due to CM. This could indicate miR-19a-3p as an important regulator during cerebral malaria especially in the brain, regulating endothelial cell development, growth, adhesion, and organisation. MiR-19a-3p levels may increase during CM NCI in children 2-4 years old due to local ischemia caused by red blood cell sequestration. However, our study showed miR-19a-3p levels were higher in CM fatal outcomes for the older cohort of children, this could be due to severe brain swelling which ultimately causes death. MiR-19a has also been found to be upregulated in rats with traumatic brain injury (TBI) and possibly negatively regulate TBI-altered genes<sup>81</sup>. They also related increased expression of miR-19a to dying neurons.

Comparing CM survivors without NCI to CM children that died, hsa-miR-30a-3p can prognostically distinguish the outcomes, it can also differentiate SMA survivors with and without NCI (Figure 4.8B bottom row). Although miR-30a has not been studied in malaria, it has been investigated in other diseases and has been found to regulate epithelial cell proliferation and differentiation, repress neural cell adhesion molecules, impede cortical development and maturation in the prefrontal cortex, and neuroinflammation<sup>82-85</sup>. Similar to



the other miRNA, miR-30a-3p levels are higher in CM fatal outcomes than CM survivors for the older children (5-10 years old), which could be linked to severe brain swelling and break down of the blood brain barrier, leading to increased production of EVs. MiR-30a-3p was also higher in SMA survivors compared to SMA survivors with NCI for both age groups, which could indicate normal brain development as the miRNA is not present to impede developmental pathways.

Comparable to hsa-miR-1-3p, hsa-miR-4516 can distinguish healthy children from severe malaria children, as well as survivors of CM (with or without NCI) from CM fatal outcomes. Hsa-miR-4516 has not been studied in malaria, though it has been in cancers and viral infections, where it has been described to damage airway epithelial adhesion<sup>86,87</sup>. Pathway analysis showed that hsa-miR-4516 is more involved in cell response to hormones and cell-cell adhesion, which is tightly related to haemorrhages<sup>88</sup>. This is similar to our findings where hsa-miR-4516 is higher in CM children that died compared to CM survivors, which could indicate a role in the disruption of cell-cell adhesion in the blood brain barrier.

Lastly, our findings showed that hsa-miR-590-3p could be used to differentiate children with CM from SMA. MiR-590 has not been investigated in malaria EVs but has been studied in various cancerous and non-cancerous cell lines and shown to regulate cell proliferation, epithelial cell proliferation and differentiation, and mitigate neuron damage<sup>89-92</sup>. Serum levels of miR-590 have been shown to be lower in Alzheimer's disease patients at mild, moderate, and severe stages when compared to healthy patients<sup>92</sup>. The same study also found lower levels of miR-590 in mice cerebral cortex tissue, hippocampal tissue, and serum from an Alzheimer's disease model. Our study found miR-590 to be more abundant in children ages 2-4 years who survived CM but developed NCI compared to CM survivors and fatal outcomes in CM; however, no significant differences were detected in the older children, mean age of 6.4 years old. This could indicate miR-590 being more active in younger children, as well as having a more tissue-specific effect in older children to adults.

Investigating the role of miRNA in pathogenic infections such as malaria is essential for understanding the mechanisms and pathways involved in pathogenesis<sup>93,94</sup>. For instance, several non-coding RNAs demonstrated functions in the regulation of virulence and antigenic variation during malaria infection<sup>95-97</sup>. The study of miRNAs in human malaria pathogenesis and therapy is still in its infancy; therefore, there is a great need for more studies and

improvements in high-throughput sequencing. In addition to prognostic biomarkers, diagnostic biomarker research may increase in importance as the number of *P. falciparum* parasites with deletions of PfHRP2 and 3 increases, rendering the parasites undetectable by rapid diagnostic tests<sup>98</sup>.

## **4.5 Conclusion**

Severe malaria can lead to severe complications that can have lasting effects on children's well-being and education. The treatments for these complications are readily available, but due to late implementation, they are inefficient. By utilising deep sequencing techniques, biomarkers of disease severity can be identified, and physicians can plan and carry out early treatment with adjunctive therapies. This study shows that miR-1-3p, miR-19a-3p, miR-30a-3p, and miR-4516 can distinguish CM patients that will fully recover or develop NCI from CM patients that will die due to the complications. These 4 miRNAs can be combined into a miRNA panel to further increase sensitivity and specificity for future investigations. There is also the potential to distinguish which patient will develop a certain type of NCI, as miR-19a-3p can differentiate CM NCI from SMA NCI; however, it has lower sensitivity and specificity, which may go up once in a panel. It is also shown that miR-1-3p, miR-19a-3p, miR-4516, and miR-590-3p levels are differentially expressed in healthy children compared to children with severe malaria and between CM and SMA children. These differences in expression could provide further information regarding the mechanisms of pathogenesis, as currently there is still much to uncover for CM and SMA disease development and progression. These prognostic biomarkers would allow patients who have already been diagnosed with malaria to employ earlier treatment decreasing the chance of complications and long-term neurological complications in CM thus preventing hospital readmissions in SMA patients. Predictive tests of the miRNA panel on a different larger cohort would be the next step to ensure reliable, accurate, and reproducible diagnostic predictions; however, this is the peak of the iceberg and a lot more research is required.

## **Acknowledgements**

We are grateful to the children and their parents or guardians who participated in this study. We thank the study teams at Mulago Hospital, Makerere University, and the University of Minnesota for their commitment to treating the children and collecting the data. We would also like to thank Kay Anantanawat for providing her expertise in next-generation sequencing.

## **Authors' contributions**

**Iris S. Cheng:** conceptualisation; investigation; methodology; data curation; formal analysis; validation; software; writing-original draft; writing-review & editing. **Raissa L. Gill:** RT-qPCR statistics. **Robert O. Opoka:** writing-review & editing. **Paul Bangirana:** writing-review & editing. **Chandy C. John:** writing-review & editing. **Valery Combes:** conceptualisation; funding acquisition; project administration; supervision; visualization; writing-review & editing.

## **Competing interests**

The authors declare no competing interests.

## **Availability of data and material**

The data that support the findings of this study are available from the corresponding author upon reasonable request.

## **4.6 References**

1. Idro, R. *et al.* Cerebral malaria is associated with long-term mental health disorders: a cross sectional survey of a long-term cohort. *Malar. J.* 15, 184 (2016).
2. United Nations International Children’s Emergency Fund, World Health Organisation, World Bank Group & United Nations. *Levels and trends in child mortality 2020*. 56 <https://www.unicef.org/reports/levels-and-trends-child-mortality-report-2020> (2020).
3. World Health Organization. *World malaria report 2022*. Geneva: World Health Organization; Licence:CC BY-NC-SA 3.0 IGO. <https://www.who.int/publications/i/item/9789240064898> (2022).
4. World Health Organization. *World malaria report 2019*. Geneva: World Health Organization; Licence:CC BY-NC-SA 3.0 IGO. <https://www.who.int/publications/i/item/9789241565721> (2019).
5. Storm, J. & Craig, A. G. Pathogenesis of cerebral malaria--inflammation and cytoadherence. *Front. Cell. Infect. Microbiol.* 4, 100 (2014).
6. Wassmer, S. C. *et al.* Investigating the Pathogenesis of Severe Malaria: A Multidisciplinary and Cross-Geographical Approach. *Am. J. Trop. Med. Hyg.* 93, 42–56 (2015).
7. White, N. J. *et al.* Malaria. *Lancet* 383, 723–735 (2014).
8. Wassmer, S. C. & Grau, G. E. R. Severe malaria: What’s new on the pathogenesis front? *International journal for parasitology* 47, 145–152 (2017).
9. Combes, V. *et al.* Microvesiculation and cell interactions at the brain-endothelial interface in cerebral malaria pathogenesis. *Prog. Neurobiol.* 91, 140–151 (2010).
10. Bangirana, P. *et al.* Malaria with neurological involvement in Ugandan children: effect on cognitive ability, academic achievement and behaviour. *Malar. J.* 10, 334 (2011).
11. Bangirana, P. *et al.* Severe malarial anemia is associated with long-term neurocognitive impairment. *Clin. Infect. Dis.* 59, 336–344 (2014).

12. Datta, D. *et al.* Association of Plasma Tau With Mortality and Long-term Neurocognitive Impairment in Survivors of Pediatric Cerebral Malaria and Severe Malarial Anemia. *JAMA Netw. Open* 4, e2138515 (2021).
13. Datta, D. *et al.* Elevated Cerebrospinal Fluid Tau Protein Concentrations on Admission Are Associated With Long-term Neurologic and Cognitive Impairment in Ugandan Children With Cerebral Malaria. *Clin. Infect. Dis.* 70, 1161–1168 (2020).
14. Ouma, B. J. *et al.* Endothelial activation, acute kidney injury, and cognitive impairment in pediatric severe malaria. *Crit. Care Med.* 48, e734–e743 (2020).
15. Ouma, B. J. *et al.* Plasma angiopoietin-2 is associated with age-related deficits in cognitive subscales in Ugandan children following severe malaria. *Malar. J.* 20, 17 (2021).
16. Combes, V. *et al.* Circulating endothelial microparticles in malawian children with severe falciparum malaria complicated with coma. *JAMA* 291, 2542–2544 (2004).
17. Pankoui Mfonkeu, J. B. *et al.* Elevated cell-specific microparticles are a biological marker for cerebral dysfunctions in human severe malaria. *PLoS ONE* 5, e13415 (2010).
18. Langfitt, J. T. *et al.* Neurodevelopmental impairments 1 year after cerebral malaria. *Pediatrics* 143, (2019).
19. György, B. *et al.* Detection and isolation of cell-derived microparticles are compromised by protein complexes resulting from shared biophysical parameters. *Blood* 117, e39-48 (2011).
20. Palviainen, M. *et al.* Extracellular vesicles from human plasma and serum are carriers of extravesicular cargo-Implications for biomarker discovery. *PLoS ONE* 15, e0236439 (2020).
21. Babatunde, K. A. *et al.* Malaria infected red blood cells release small regulatory RNAs through extracellular vesicles. *Sci. Rep.* 8, 884 (2018).
22. Cohen, A., Zinger, A., Tiberti, N., Grau, G. E. R. & Combes, V. Differential plasma microvesicle and brain profiles of microRNA in experimental cerebral malaria. *Malar. J.* 17, 192 (2018).
23. Babatunde, K. A. *et al.* Role of extracellular vesicles in cellular cross talk in malaria. *Front. Immunol.* 11, 22 (2020).

24. Opadokun, T. & Rohrbach, P. Extracellular vesicles in malaria: an agglomeration of two decades of research. *Malar. J.* 20, 442 (2021).
25. Regev-Rudzki, N. *et al.* Cell-cell communication between malaria-infected red blood cells via exosome-like vesicles. *Cell* 153, 1120–1133 (2013).
26. Sampaio, N. G., Cheng, L. & Eriksson, E. M. The role of extracellular vesicles in malaria biology and pathogenesis. *Malar. J.* 16, 245 (2017).
27. Kioko, M. *et al.* Extracellular vesicles could be a putative posttranscriptional regulatory mechanism that shapes intracellular RNA levels in *Plasmodium falciparum*. *Nat. Commun.* 14, 6447 (2023).
28. Khowawisetsut, L. *et al.* Differential Effect of Extracellular Vesicles Derived from *Plasmodium falciparum*-Infected Red Blood Cells on Monocyte Polarization. *Int. J. Mol. Sci.* 24, (2023).
29. Trampuz, A., Jereb, M., Muzlovic, I. & Prabhu, R. M. Clinical review: Severe malaria. *Crit. Care* 7, 315–323 (2003).
30. Al-Hadlaq, S. M., Balto, H. A., Hassan, W. M., Marraiki, N. A. & El-Ansary, A. K. Biomarkers of non-communicable chronic disease: an update on contemporary methods. *PeerJ* 10, e12977 (2022).
31. Casals-Pascual, C. *et al.* High levels of erythropoietin are associated with protection against neurological sequelae in African children with cerebral malaria. *Proc Natl Acad Sci USA* 105, 2634–2639 (2008).
32. Bridges, D. J. *et al.* Rapid activation of endothelial cells enables *Plasmodium falciparum* adhesion to platelet-decorated von Willebrand factor strings. *Blood* 115, 1472–1474 (2010).
33. Conroy, A. L. *et al.* Whole blood angiopoietin-1 and -2 levels discriminate cerebral and severe (non-cerebral) malaria from uncomplicated malaria. *Malar. J.* 8, 295 (2009).
34. Thakur, K., Vareta, J., Carson, K., Taylor, T. & Sullivan, D. Performance of Cerebrospinal Fluid (CSF) *Plasmodium Falciparum* Histidine-Rich Protein-2 (pfHRP-2) in Prediction of Death in Cerebral Malaria (I10-2.005). (2014).

35. Adukpo, S. *et al.* High plasma levels of soluble intercellular adhesion molecule (ICAM)-1 are associated with cerebral malaria. *PLoS ONE* 8, e84181 (2013).
36. Corcoran, C., Friel, A. M., Duffy, M. J., Crown, J. & O'Driscoll, L. Intracellular and extracellular microRNAs in breast cancer. *Clin. Chem.* 57, 18–32 (2011).
37. Walenta, K. *et al.* Circulating microparticles as indicators of peripartum cardiomyopathy. *Eur. Heart J.* 33, 1469–1479 (2012).
38. Boilard, E. *et al.* Platelets amplify inflammation in arthritis via collagen-dependent microparticle production. *Science* 327, 580–583 (2010).
39. Mobarrez, F. *et al.* Microparticles and microscopic structures in three fractions of fresh cerebrospinal fluid in schizophrenia: case report of twins. *Schizophr. Res.* 143, 192–197 (2013).
40. Varo, R. *et al.* Adjunctive therapy for severe malaria: a review and critical appraisal. *Malar. J.* 17, 47 (2018).
41. Hammond, S. M. An overview of microRNAs. *Adv. Drug Deliv. Rev.* 87, 3–14 (2015).
42. Wang, W. *et al.* MicroRNA profiling of CD3<sup>+</sup> CD56<sup>+</sup> cytokine-induced killer cells. *Sci. Rep.* 5, 9571 (2015).
43. Bartel, D. P. MicroRNAs: genomics, biogenesis, mechanism, and function. *Cell* 116, 281–297 (2004).
44. Weber, J. A. *et al.* The microRNA spectrum in 12 body fluids. *Clin. Chem.* 56, 1733–1741 (2010).
45. El-Mogy, M. *et al.* Diversity and signature of small RNA in different bodily fluids using next generation sequencing. *BMC Genomics* 19, 408 (2018).
46. Gilad, S. *et al.* Serum microRNAs are promising novel biomarkers. *PLoS ONE* 3, e3148 (2008).
47. Mitchell, P. S. *et al.* Circulating microRNAs as stable blood-based markers for cancer detection. *Proc Natl Acad Sci USA* 105, 10513–10518 (2008).
48. Chen, X. *et al.* Characterization of microRNAs in serum: a novel class of biomarkers for diagnosis of cancer and other diseases. *Cell Res.* 18, 997–1006 (2008).

49. Glinge, C. *et al.* Stability of Circulating Blood-Based MicroRNAs - Pre-Analytic Methodological Considerations. *PLoS ONE* 12, e0167969 (2017).
50. Kirschner, M. B. *et al.* The Impact of Hemolysis on Cell-Free microRNA Biomarkers. *Front. Genet.* 4, 94 (2013).
51. Taylor, D. D. & Gercel-Taylor, C. The origin, function, and diagnostic potential of RNA within extracellular vesicles present in human biological fluids. *Front. Genet.* 4, 142 (2013).
52. Cheng, L., Sharples, R. A., Scicluna, B. J. & Hill, A. F. Exosomes provide a protective and enriched source of miRNA for biomarker profiling compared to intracellular and cell-free blood. *J. Extracell. Vesicles* 3, (2014).
53. López de Las Hazas, M.-C. *et al.* Dietary bovine milk miRNAs transported in extracellular vesicles are partially stable during GI digestion, are bioavailable and reach target tissues but need a minimum dose to impact on gene expression. *Eur. J. Nutr.* 61, 1043–1056 (2022).
54. Coenen-Stass, A. M. L. *et al.* Extracellular microRNAs exhibit sequence-dependent stability and cellular release kinetics. *RNA Biol.* 16, 696–706 (2019).
55. Yim, K. H. W., Borgoni, S. & Chahwan, R. Serum extracellular vesicles profiling is associated with COVID-19 progression and immune responses. *J of Extracellular Bio* 1, e37 (2022).
56. Manzano-Román, R. & Siles-Lucas, M. MicroRNAs in parasitic diseases: potential for diagnosis and targeting. *Mol. Biochem. Parasitol.* 186, 81–86 (2012).
57. Chamnanchanunt, S. *et al.* Downregulation of plasma miR-451 and miR-16 in *Plasmodium vivax* infection. *Exp. Parasitol.* 155, 19–25 (2015).
58. Kaur, H. *et al.* Screening and identification of potential novel biomarker for diagnosis of complicated *Plasmodium vivax* malaria. *J. Transl. Med.* 16, 272 (2018).
59. Ketprasit, N. *et al.* The characterization of extracellular vesicles-derived microRNAs in Thai malaria patients. *Malar. J.* 19, 285 (2020).
60. Gupta, H. *et al.* Plasma MicroRNA Profiling of *Plasmodium falciparum* Biomass and Association with Severity of Malaria Disease. *Emerging Infect. Dis.* 27, 430–442 (2021).



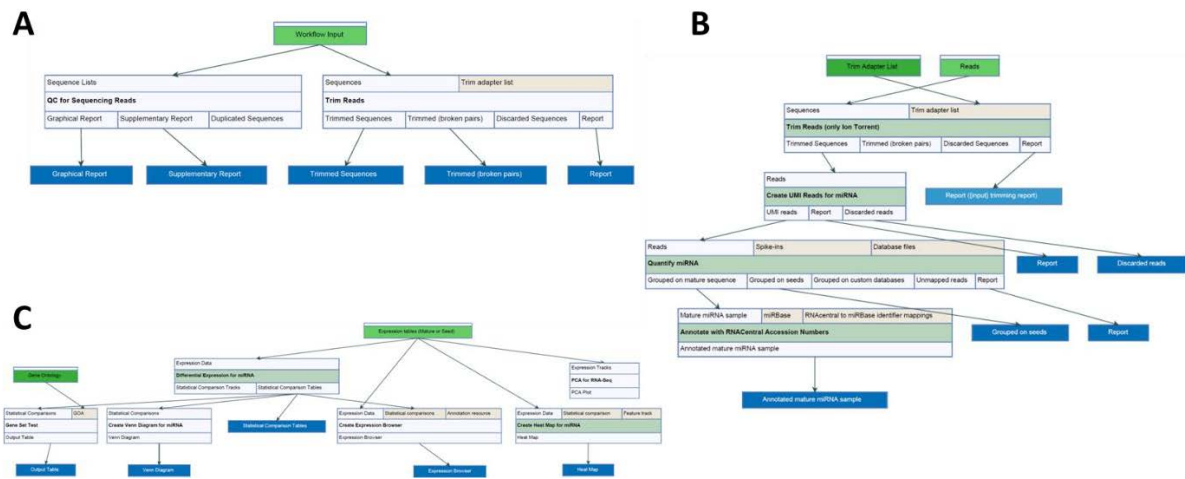
61. El-Assaad, F. *et al.* Differential microRNA expression in experimental cerebral and noncerebral malaria. *Infect. Immun.* 79, 2379–2384 (2011).
62. Shabani, E. *et al.* High plasma erythropoietin levels are associated with prolonged coma duration and increased mortality in children with cerebral malaria. *Clin. Infect. Dis.* 60, 27–35 (2015).
63. John, C. C. *et al.* Cerebral malaria in children is associated with long-term cognitive impairment. *Pediatrics* 122, e92-9 (2008).
64. Idro, R., Marsh, K., John, C. C. & Newton, C. R. J. Cerebral malaria: mechanisms of brain injury and strategies for improved neurocognitive outcome. *Pediatr. Res.* 68, 267–274 (2010).
65. Buschmann, D. *et al.* Evaluation of serum extracellular vesicle isolation methods for profiling miRNAs by next-generation sequencing. *J. Extracell. Vesicles* 7, 1481321 (2018).
66. Kozomara, A., Birgaoanu, M. & Griffiths-Jones, S. miRBase: from microRNA sequences to function. *Nucleic Acids Res.* 47, D155–D162 (2019).
67. Heberle, H., Meirelles, G. V., da Silva, F. R., Telles, G. P. & Minghim, R. InteractiVenn: a web-based tool for the analysis of sets through Venn diagrams. *BMC Bioinformatics* 16, 169 (2015).
68. Fernandez, N. F. *et al.* Clustergrammer, a web-based heatmap visualization and analysis tool for high-dimensional biological data. *Sci. Data* 4, 170151 (2017).
69. Zhou, J. *et al.* High-throughput single-EV liquid biopsy: Rapid, simultaneous, and multiplexed detection of nucleic acids, proteins, and their combinations. *Sci. Adv.* 6, (2020).
70. Tanasi, I., Adamo, A., Kanga, P. T., Bazzoni, R. & Krampera, M. High-throughput analysis and functional interpretation of extracellular vesicle content in hematological malignancies. *Comput. Struct. Biotechnol. J.* 18, 2670–2677 (2020).
71. Armah, H. *et al.* Cytokines and adhesion molecules expression in the brain in human cerebral malaria. *Int. J. Environ. Res. Public Health* 2, 123–131 (2005).
72. Inoue, S.-I. *et al.* Enhancement of dendritic cell activation via CD40 ligand-expressing  $\gamma\delta$  T cells is responsible for protective immunity to Plasmodium parasites. *Proc Natl Acad Sci USA* 109, 12129–12134 (2012).

73. Royo, J. *et al.* Changes in monocyte subsets are associated with clinical outcomes in severe malarial anaemia and cerebral malaria. *Sci. Rep.* 9, 17545 (2019).
74. King, T. & Lamb, T. Interferon- $\gamma$ : The Jekyll and Hyde of Malaria. *PLoS Pathog.* 11, e1005118 (2015).
75. Lefebvre, M. N. *et al.* Expeditious recruitment of circulating memory CD8 T cells to the liver facilitates control of malaria. *Cell Rep.* 37, 109956 (2021).
76. Hansen, D. S. *et al.* The natural killer complex regulates severe malarial pathogenesis and influences acquired immune responses to Plasmodium berghei ANKA. *Infect. Immun.* 73, 2288–2297 (2005).
77. Safa, A. *et al.* miR-1: A comprehensive review of its role in normal development and diverse disorders. *Biomed. Pharmacother.* 132, 110903 (2020).
78. Talebi, A., Rahnema, M. & Bigdeli, M. R. The Positive Effect of MiR1 Antagomir on Ischemic Neurological Disorders Via Changing the Expression of Bcl-w and Bad Genes. *Basic Clin. Neurosci.* 11, 811–820 (2020).
79. Storm, J. *et al.* Cerebral malaria is associated with differential cytoadherence to brain endothelial cells. *EMBO Mol. Med.* 11, (2019).
80. Martin-Alonso, A. *et al.* Differentially expressed microRNAs in experimental cerebral malaria and their involvement in endocytosis, adherens junctions, FoxO and TGF- $\beta$  signalling pathways. *Sci. Rep.* 8, 11277 (2018).
81. Boone, D. K. *et al.* Evidence linking microRNA suppression of essential prosurvival genes with hippocampal cell death after traumatic brain injury. *Sci. Rep.* 7, 6645 (2017).
82. Peck, B. C. E. *et al.* miR-30 Family Controls Proliferation and Differentiation of Intestinal Epithelial Cell Models by Directing a Broad Gene Expression Program That Includes SOX9 and the Ubiquitin Ligase Pathway. *J. Biol. Chem.* 291, 15975–15984 (2016).
83. Wang, Z. *et al.* MiR-30a-5p is induced by Wnt/ $\beta$ -catenin pathway and promotes glioma cell invasion by repressing NCAM. *Biochem. Biophys. Res. Commun.* 465, 374–380 (2015).

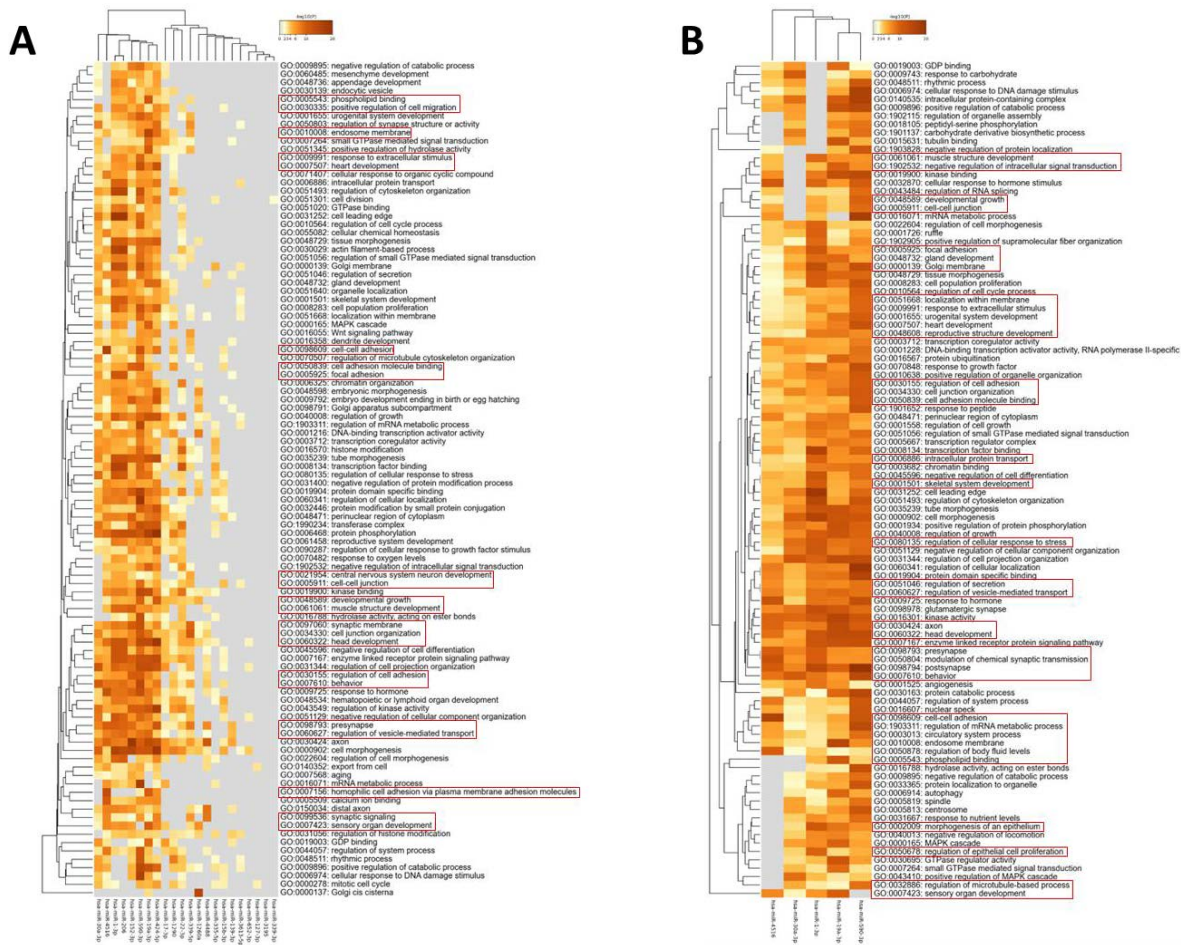
84. Mellios, N., Huang, H.-S., Grigorenko, A., Rogaev, E. & Akbarian, S. A set of differentially expressed miRNAs, including miR-30a-5p, act as post-transcriptional inhibitors of BDNF in prefrontal cortex. *Hum. Mol. Genet.* 17, 3030–3042 (2008).
85. Choi, H.-R., Ha, J. S., Kim, E.-A., Cho, S.-W. & Yang, S.-J. MiR-30a-5p and miR-153-3p regulate LPS-induced neuroinflammatory response and neuronal apoptosis by targeting NeuroD1. *BMB Rep.* (2022).
86. Jin, X.-H., Lu, S. & Wang, A.-F. Expression and clinical significance of miR-4516 and miR-21-5p in serum of patients with colorectal cancer. *BMC Cancer* 20, 241 (2020).
87. Hu, Y. *et al.* microRNA-4516 Contributes to Different Functions of Epithelial Permeability Barrier by Targeting Poliovirus Receptor Related Protein 1 in Enterovirus 71 and Coxsackievirus A16 Infections. *Front. Cell. Infect. Microbiol.* 8, 110 (2018).
88. Lyimo, E. *et al.* In Vivo Imaging of the Buccal Mucosa Shows Loss of the Endothelial Glycocalyx and Perivascular Hemorrhages in Pediatric Plasmodium falciparum Malaria. *Infect. Immun.* 88, (2020).
89. Mou, K. *et al.* miR-590-5p inhibits tumor growth in malignant melanoma by suppressing YAP1 expression. *Oncol. Rep.* 40, 2056–2066 (2018).
90. Liu, T., Wu, Y., Huang, T., Zhang, X. & Cai, Y. miR-590 promotes the proliferation of HUMSCs and induces ECM synthesis by targeting Smad7. *Oncol. Lett.* 14, 3941–3946 (2017).
91. Guan, H. *et al.* MicroRNA-590 inhibits migration, invasion and epithelial-to-mesenchymal transition of esophageal squamous cell carcinoma by targeting low-density lipoprotein receptor-related protein 6. *Oncol. Rep.* 44, 1385–1392 (2020).
92. Shang, L. *et al.* miR-590-5p Overexpression Alleviates  $\beta$ -Amyloid-Induced Neuron Damage via Targeting Pellino-1. *Anal Cell Pathol (Amst)* 2022, 7657995 (2022).
93. Shirahama, S., Miki, A., Kaburaki, T. & Akimitsu, N. Long non-coding RNAs involved in pathogenic infection. *Front. Genet.* 11, 454 (2020).
94. Tribolet, L. *et al.* MicroRNA biomarkers for infectious diseases: from basic research to biosensing. *Front. Microbiol.* 11, 1197 (2020).

95. Chakrabarti, K. *et al.* Structural RNAs of known and unknown function identified in malaria parasites by comparative genomics and RNA analysis. *RNA* 13, 1923–1939 (2007).
96. Mourier, T. *et al.* Genome-wide discovery and verification of novel structured RNAs in *Plasmodium falciparum*. *Genome Res.* 18, 281–292 (2008).
97. Raabe, C. A. *et al.* A global view of the nonprotein-coding transcriptome in *Plasmodium falciparum*. *Nucleic Acids Res.* 38, 608–617 (2010).
98. World Health Organization. *World malaria report 2021*. Geneva: World Health Organization; Licence:CC BY-NC-SA 3.0 IGO. <https://www.who.int/publications/i/item/9789240040496> (2021).

## 4.7 Supplementary data



**Supplementary Figure 4.1** CLC genomics workbench workflow. (A) QC and trimming of low-quality or adapter contaminated sequences. (B) MiRNA quantification, mapping trimmed sequences to mature miRNA listed in the miRBase database. (C) MiRNA differential expression analysis.



**Supplementary Figure 4.2** Top 50 gene ontology terms for differentially expressed miRNA present in  $\geq 50\%$  of patients. (A) 22 differentially expressed miRNA. (B) Five miRNAs of interest.

**Supplementary Table 4.1** Top 20 most abundant mature microRNA sequences identified in plasma-derived extracellular vesicles for each child

Sample	Avg %	CC			CM FR			CM NCI				CM FO				SMA FR				SMA NCI				
		400	484	429	196	577	675	469	312	372	538	801	99	357	678	756	236	238	409	438	56	173	252	523
hsa-miR-16-5p	7.64	60,091	26,395	35,612	14,459	7,986	17,810	19,160	28,684	24,549	23,191	3,469	56,229	27,571	19,008	979	33,143	32,236	16,683	44,236	58,197	27,676	19,703	23,330
hsa-miR-126-3p	4.77	23,751	20,321	22,067	11,712	1,760	26,514	8,503	21,248	8,798	8,306	3,861	28,228	34,885	11,110	520	31,135	14,432	7,401	30,364	40,085	11,666	16,017	10,249
hsa-miR-223-3p	2.45	13,166	11,268	13,615	5,845	2,034	12,842	4,222	12,430	4,830	6,765	591	8,275	9,651	3,398	89	17,391	9,551	7,149	30,057	21,163	2,782	9,074	2,610
hsa-let-7a-5p	2.3	15,313	6,909	12,181	6,135	1,433	8,335	4,478	6,690	5,160	4,446	2,903	6,259	17,778	4,728	434	15,521	9,714	5,838	12,413	11,461	8,412	5,062	9,077
hsa-let-7b-5p	2.02	11,881	4,502	7,887	3,870	1,878	5,262	4,358	10,752	8,377	5,926	3,405	4,022	12,375	5,431	532	10,925	5,920	7,907	12,470	15,678	6,028	3,380	6,348
hsa-miR-21-5p	1.95	6,581	7,499	9,493	4,891	533	11,568	1,520	3,970	770	998	837	54,855	4,070	1,688	130	8,865	12,909	1,650	8,275	3,738	5,529	5,614	5,366
hsa-miR-142-3p	1.65	7,269	6,321	10,970	6,746	968	10,189	3,451	3,167	2,749	2,465	1,254	6,797	7,420	1,467	177	11,141	10,130	3,945	8,693	6,421	5,130	4,686	6,154
hsa-miR-486-5p	1.35	8,631	2,904	5,410	1,184	2,135	1,398	3,331	5,788	4,547	4,831	947	12,724	5,041	7,905	221	2,441	4,115	4,168	7,835	8,000	10,513	2,150	3,649
hsa-let-7f-5p	1.29	7,530	4,949	7,533	4,238	753	5,782	2,107	1,928	2,201	1,799	1,039	6,866	9,245	1,762	151	7,271	7,759	3,069	5,918	3,680	5,482	3,497	5,198
hsa-miR-26a-5p	1	4,208	5,472	4,568	2,738	521	6,416	2,210	4,258	1,696	1,961	365	5,243	5,358	1,994	60	5,078	4,786	2,416	8,026	4,235	2,448	4,187	2,502
hsa-let-7i-5p	0.89	4,588	2,726	3,729	1,874	859	2,944	2,319	2,553	2,571	2,409	866	7,326	3,803	1,589	122	3,980	4,492	3,589	6,354	4,002	3,022	1,932	2,814
hsa-miR-146a-5p	0.74	1,780	1,808	1,936	1,267	-	2,253	1,081	1,781	867	-	-	33,337	2,372	-	23	2,381	4,327	1,241	2,921	-	2,466	1,283	1,465
hsa-miR-26b-5p	0.57	2,499	3,247	2,861	1,834	309	3,676	1,156	-	931	867	209	4,855	3,724	908	46	3,087	2,955	1,167	3,874	2,069	1,410	2,337	1,538
hsa-miR-126-5p	0.49	3,813	2,175	2,451	1,346	-	2,753	-	1,813	-	-	536	4,650	3,381	845	79	4,628	1,828	-	2,585	3,689	1,329	1,698	1,053
hsa-miR-150-5p	0.41	-	-	2,338	1,663	441	1,993	2,620	1,512	2,690	884	465	-	1,631	1,183	62	-	1,635	3,270	5,583	1,678	1,380	-	1,375
hsa-miR-342-3p	0.33	-	-	2,027	1,184	299	2,132	1,736	2,101	1,351	834	176	-	-	1,075	-	1,042	2,143	2,351	4,303	1,704	1,433	-	1,006
hsa-miR-191-5p	0.33	-	1,650	1,657	832	270	2,458	812	2,060	868	1,383	-	-	1,463	1,004	-	1,137	2,273	1,400	4,941	1,821	-	1,278	-
hsa-miR-92a-3p	0.26	1,771	-	1,727	826	394	-	1,260	-	1,222	1,239	679	-	1,620	1,376	126	-	-	1,413	-	2,076	1,778	-	732
hsa-miR-451a	0.26	2,953	1,536	-	-	248	-	914	2,438	808	847	178	4,194	-	-	-	1,285	1,886	-	-	2,938	-	1,112	-
hsa-miR-30d-5p	0.25	-	1,159	-	733	268	-	1,114	1,876	1,422	1,258	-	-	1,751	787	-	1,307	1,543	1,750	2,737	-	-	953	753

Abbreviations: CC, community children; CM, cerebral malaria; FO, fatal outcome; FR, full recovery; NCI, neurocognitive impairment; SMA, severe malarial anaemia

**Supplementary Table 4.2** Top 20 most abundant seed sequences identified in plasma-derived extracellular vesicles for each individual patient sample

Sample	CC			CM FR			CM NCI				CM FO				SMA FR				SMA NCI						
	400	484	429	196	577	675	469	312	372	538	801	99	357	678	756	236	238	409	438	56	173	252	523		
Seeds	e.g. mature miRNA	Avg %																							
AGCAGCA	hsa-miR-16-5p	7.6	59,231	26,410	35,314	14,363	7,983	17,942	19,069	28,600	24,242	23,017	3,448	56,891	27,338	18,941	969	32,815	32,157	16,583	44,268	57,580	27,360	19,806	23,025
GAGGTAG	hsa-let-7a-5p	6.85	41,380	20,160	32,933	16,983	5,143	23,815	14,141	23,374	18,939	15,176	8,561	26,159	45,327	14,335	1,263	39,184	29,514	21,193	40,012	36,921	24,076	14,686	24,681
CGTACCG	hsa-miR-126-3p	3.71	18,344	15,635	17,196	9,211	1,404	20,415	6,596	16,771	6,662	6,521	3,139	21,315	27,280	8,804	423	24,454	10,697	5,682	23,642	31,966	8,935	12,351	8,150
GTCAGTT	hsa-miR-223-3p	2.3	12,285	10,726	12,671	5,663	1,913	12,262	3,955	11,458	4,585	6,422	562	8,086	9,295	3,204	-	16,087	8,855	6,684	28,299	19,927	2,593	8,561	2,437
AGCTTAT	hsa-miR-21-5p	1.95	6,546	7,467	9,384	4,868	-	11,451	1,520	4,011	770	1,010	837	55,441	4,067	1,688	130	8,841	12,780	1,661	8,226	3,707	5,489	5,587	5,324
TCAAGTA	hsa-miR-1297	1.59	6,666	8,798	7,382	4,575	830	10,153	3,354	5,501	2,640	2,845	574	10,311	9,030	2,897	106	8,155	7,766	3,580	11,958	6,316	3,872	6,577	4,011
GTAGTGT	hsa-miR-142-3p	1.52	6,811	5,854	10,098	6,291	902	9,591	3,138	2,892	2,495	2,271	1,127	5,939	6,912	1,349	165	10,298	9,430	3,490	7,875	5,919	4,789	4,393	5,690
CCTGTAC	hsa-miR-486-5p	1.34	8,519	2,868	5,322	1,184	2,135	1,398	3,312	5,726	4,522	4,809	947	12,612	4,983	7,850	221	2,422	4,076	4,144	7,796	7,919	10,354	2,135	3,600
GAGAACT	hsa-miR-146a-5p	0.87	2,139	2,396	2,347	1,573	-	3,733	1,164	2,411	922	733	-	34,433	2,650	824	-	2,734	5,625	1,377	3,984	-	2,614	1,782	1,583
GTAACA	hsa-miR-30a-5p	0.7	3,139	2,677	3,203	1,486	-	2,763	1,869	3,728	2,126	1,947	180	6,569	3,624	1,327	-	2,948	3,040	2,501	5,135	3,388	1,901	2,097	1,593
ATTGCAC	hsa-miR-25-3p	0.62	3,674	1,812	2,880	1,179	-	1,544	1,807	2,385	1,829	1,880	759	4,816	2,399	1,940	155	1,923	2,364	2,076	4,389	3,752	2,860	1,296	1,331
ATTATTA	hsa-miR-126-5p	0.51	3,741	2,151	2,411	1,321	-	2,703	768	1,792	695	646	536	4,578	3,310	845	-	4,555	1,799	-	2,555	3,631	1,312	1,667	1,042
CTCCAA	hsa-miR-150-5p	0.41	-	1,122	2,294	1,639	-	1,963	2,594	-	2,666	884	465	-	1,601	1,183	-	-	1,615	3,234	5,530	1,666	1,361	-	1,357
GCAGCAT	hsa-miR-103a-3p	0.37	1,917	1,904	1,907	855	-	1,911	-	-	822	996	-	5,377	1,920	886	-	1,068	2,168	1,004	2,871	-	1,276	1,499	758
AACGGAA	hsa-miR-191-5p	0.37	1,391	1,829	1,671	866	-	2,626	817	2,157	896	1,406	-	-	1,483	1,065	-	1,153	2,402	1,378	5,128	1,837	836	1,402	-
CTCACAC	hsa-miR-342-3p	0.34	-	-	1,995	1,194	-	2,118	1,740	2,139	1,349	850	176	-	1,156	1,081	-	1,076	2,170	2,322	4,294	1,685	1,444	-	1,031
AACCGTT	hsa-miR-451a	0.31	3,039	1,580	1,057	706	-	-	941	2,520	850	895	178	4,255	-	-	-	1,325	1,981	-	-	3,087	852	1,140	808
AGCACCA	hsa-miR-29a-3p	0.27	-	-	1,067	-	-	1,205	-	1,806	-	-	-	15,496	-	-	-	-	1,656	-	3,757	-	-	814	-
AAAGTGC	hsa-miR-106a-5p	0.21	1,970	1,110	1,734	524	-	-	758	-	809	-	-	2,065	1,405	-	-	-	1,567	884	2,083	-	1,271	829	-
GAGGGGC	hsa-miR-3184-5p	0.19	1,793	-	-	-	-	-	834	-	1,164	1,082	171	-	-	-	851	-	-	1,164	-	1,082	1,515	-	-

Abbreviations: CC, community children; CM, cerebral malaria; FO, fatal outcome; FR, full recovery; NCI, neurocognitive impairment; SMA, severe malarial anaemia



**Supplementary Table 4.3** Top 20 most abundant novel seed sequences identified in plasma-derived extracellular vesicles for each patient sample

Sample	CC			CM FR				CM NCI				CM FO			SMA FR				SMA NCI				
	400	484	429	196	577	675	469	312	372	538	801	99	357	678	756	236	238	409	438	56	173	252	523
Seeds																							
GTAAAGT	23	-	17	-	-	-	17	13	17	8	13	-	-	15	10	-	10	17	-	14	14	-	10
AGAGAGA	7	6	9	-	-	-	-	59	-	-	-	-	-	14	-	7	63	-	20	49	29	-	-
TTAAGTG	14	-	14	-	-	-	10	11	12	7	9	-	-	12	8	-	10	8	-	12	14	-	12
GTTGGTC	8	8	8	8	-	8	-	8	-	8	7	8	7	8	-	8	8	6	-	8	8	8	8
TAGGTCA	10	5	10	-	-	-	9	9	9	6	8	-	-	8	8	-	7	9	-	10	9	-	8
TTGACCT	9	7	7	8	-	10	8	13	8	5	6	-	12	8	-	8	7	-	-	8	-	7	6
TCAGTTT	10	8	9	8	-	9	-	-	7	7	-	9	8	7	-	11	7	8	12	10	-	8	-
GAAAGTA	7	-	7	6	-	-	-	-	7	5	6	-	-	7	7	-	7	6	-	7	7	5	7
GAGAGAG	-	-	-	-	-	-	-	48	-	6	-	-	-	10	-	-	37	-	-	29	12	-	-
CCGAATT	-	12	8	15	-	13	-	-	6	-	-	-	15	-	-	16	-	-	-	-	-	11	-
GTACCGT	9	8	8	-	-	10	-	8	-	5	-	10	9	-	-	9	-	-	9	11	-	7	5
AAAGTAG	7	6	7	-	-	-	-	-	6	6	6	-	-	7	-	-	6	7	-	7	7	-	6
AACTGAA	7	-	11	-	-	-	-	-	-	-	6	-	-	-	8	-	7	-	-	-	6	-	6
TGAAAGT	7	-	-	-	-	-	-	-	7	5	6	-	-	-	-	-	7	6	-	-	6	-	6
GCGACCT	-	7	-	-	10	8	-	-	-	6	-	6	-	-	-	-	7	-	14	7	8	6	-
CCCTGTA	6	8	-	-	-	6	-	8	-	-	-	6	-	-	-	9	-	-	8	8	-	8	5
CCATAAA	-	7	-	-	-	8	-	-	-	-	-	11	-	-	-	7	11	-	10	-	-	7	5
CCACAGG	-	8	-	-	-	8	-	9	-	-	-	10	8	-	-	-	8	-	10	-	-	7	-
AAGTAGG	-	-	7	-	-	-	-	-	6	-	5	-	-	7	-	-	-	6	-	-	6	-	6
GTAGGTC	6	-	9	-	-	-	-	-	6	-	5	-	-	-	-	-	-	5	-	-	6	-	5

Abbreviations: CC, community children; CM, cerebral malaria; FO, fatal outcome; FR, full recovery; NCI, neurocognitive impairment; SMA, severe malarial anaemia



**Supplementary Table 4.5** Top 20 GO term clusters with the corresponding miRNA of interest

Regulating miRNA	GO	Category	Description	Count	%	Log10(P)	Log10(q)
	GO:0098794	GO Cellular Components	postsynapse	120	5.23	-21.76	-17.41
	GO:0060341	GO Biological Processes	regulation of cellular localization	136	5.93	-19.02	-14.97
	GO:0031252	GO Cellular Components	cell leading edge	49	6.47	-18.62	-14.75
	GO:0030424	GO Cellular Components	axon	72	6.73	-17.77	-13.42
	GO:0016071	GO Biological Processes	mRNA metabolic process	110	4.79	-17.09	-13.35
	GO:0016301	GO Molecular Functions	kinase activity	77	7.2	-16.87	-12.97
	GO:0031344	GO Biological Processes	regulation of cell projection organization	71	6.64	-16.75	-12.97
	GO:0140535	GO Cellular Components	intracellular protein-containing complex	125	5.45	-16.7	-13.06
	GO:0006974	GO Biological Processes	cellular response to DNA damage stimulus	121	5.27	-16.58	-13.01
	GO:0060322	GO Biological Processes	head development	80	7.48	-16.54	-12.89
	GO:0098609	GO Biological Processes	cell-cell adhesion	63	5.89	-16.23	-12.79
	GO:0000902	GO Biological Processes	cell morphogenesis	59	7.79	-16.06	-12.72
	GO:0008134	GO Molecular Functions	transcription factor binding	55	7.27	-16.03	-12.72
	GO:0098978	GO Cellular Components	glutamatergic synapse	47	4.39	-16.01	-12.51
	GO:0019904	GO Molecular Functions	protein domain specific binding	116	5.05	-15.57	-12.33
	GO:0010008	GO Cellular Components	endosome membrane	62	5.56	-15.11	-12.01
	GO:0051493	GO Biological Processes	regulation of cytoskeleton organization	50	6.61	-15.1	-12.01
	GO:0030163	GO Biological Processes	protein catabolic process	115	5.01	-14.88	-11.84
	GO:0009896	GO Biological Processes	positive regulation of catabolic process	92	4.01	-14.6	-11.61
	GO:1903311	GO Biological Processes	regulation of mRNA metabolic process	65	2.83	-14.53	-11.57

"Count" is the number of genes in the user-provided lists with membership in the given ontology term. "%" is the percentage of all of the user-provided genes that are found in the given ontology term (only input genes with at least one ontology term annotation are included in the calculation). "Log10(P)" is the p-value in log base 10. "Log10(q)" is the multi-test adjusted p-value in log base 10.

- hsa-miR-1-3p
- hsa-miR-19a-3p
- hsa-miR-30a-3p
- hsa-miR-4516
- hsa-miR-590-3p

**Chapter Five:**

**Extracellular vesicle protein  
biomarker discovery in children  
with severe malaria**

## Chapter 5: Proteomic analysis of paediatric plasma extracellular vesicles for the identification of prognostic biomarkers for severe malaria outcomes

### Chapter overview

Semi-quantitative proteomic analysis is used to compare plasma extracellular vesicle cargo from children with severe malaria. This allowed for the detection of potential plasma EV protein biomarkers that could predict which children would develop neurocognitive impairment or mortality. The differentially expressed proteins were then mapped and compare to literature using Ingenuity Pathway Analysis. This allowed for a better understanding of which pathways and mechanisms the proteins were associated with, and if it coincided with previous malaria studies. A total of 94 proteins of interest were identified, two of which were *Plasmodium falciparum* proteins.

### Authors' contributions

Author	Concept	Investigation	Methodology	Data curation	Formal Analysis	Writing-original draft	Writing-review & editing	Signature
Iris S. Cheng	X	X	X	X	X	X	X	Production Note: Signature removed prior to publication.
Robert O. Opoka							X	Production Note: Signature removed prior to publication.
Natalia Tiberti							X	Production Note: Signature removed prior to publication.
Paul Bangirana							X	Production Note: Signature removed prior to publication.
Chandy C. John							X	Production Note: Signature removed prior to publication.
Valery Combes	X						X	Production Note: Signature removed prior to publication.

**Publication status:** In submission process

# Proteomic analysis of paediatric plasma extracellular vesicles for the identification of prognostic biomarkers for severe malaria outcomes

[Iris S. Cheng](#)<sup>1</sup>, [Robert O. Opoka](#)<sup>2</sup>, [Natalia Tiberti](#)<sup>3</sup>, [Paul Bangirana](#)<sup>2,4</sup>, [Chandy C. John](#)<sup>5</sup>, [Valery Combes](#)<sup>1</sup>

<sup>1</sup>Malaria and Microvesicles Research Group, School of Life Sciences, Faculty of Sciences, University of Technology Sydney, Ultimo, Sydney, New South Wales, 2007, Australia

<sup>2</sup>Global Health Uganda, Kampala, Uganda

<sup>3</sup>Department of Infectious, Tropical Diseases and Microbiology, IRCCS Sacro Cuore Don Calabria Hospital, Negrar di Valpolicella, Italy

<sup>4</sup>Department of Psychiatry, Makerere University College of Health Sciences, Kampala, Uganda

<sup>5</sup>Ryan White Center for Infectious Diseases and Global Health, Department of Pediatrics, Indiana University, Indianapolis, USA

Corresponding authors

Valery Combes, Email: [valery.combes@uts.edu.au](mailto:valery.combes@uts.edu.au)

Word Count: 8441

## **Abstract**

As the status of malaria remains a significant health problem in many developing tropical and subtropical countries, the need for accurate and reliable prognostic biomarkers is high. Extracellular vesicles (EVs) are subcellular components released by all cell types and are found in healthy people and individuals suffering from various diseases; however, numbers are increased in diseases such as malaria. Different *in vitro* studies on malaria have investigated the protein contents of EVs from specific cell types, though only a few have assessed the protein content of circulating EVs and their relationship to disease signs and symptoms. This study aimed to compare proteomic profiles of plasma EVs from children with differing severe malaria outcomes to discover predictive biomarkers. The protein profiles for plasma EVs of 5 healthy children and 20 malaria patients were obtained using mass spectrometry. In total, 1622 proteins were identified: 74 were specific to the healthy control children's plasma EVs, 924 were specific to EVs from severe malaria children, and 624 were shared. Three hundred eighteen proteins were differentially expressed (DEPs) among all the children (healthy and ill). Using Ingenuity pathway analysis, 34 plasma EV DEPs were identified when comparing children with severe malarial anaemia (SMA) and cerebral malaria (CM) who fully recovered without complications. Among children with CM, 31 plasma EV DEPs were identified between those who fully recovered without complication and those who succumbed to the disease. Lastly, 48 plasma EV DEPs were found when comparing SMA children who fully recovered to those who recovered but developed neurocognitive impairment. Many DEPs, such as S100 calcium-binding, aggrecan, apolipoprotein A4, serum amyloid A2, and immunoglobulin proteins, were associated with the immune response and inflammatory pathways through cell signalling and activation. The majority of the DEPs identified had higher relative abundance in children with SMA who developed neurocognitive impairment or children with CM who died.

**Keywords:** Extracellular vesicles (EVs), proteomic, plasma, malaria, paediatric, cerebral malaria, severe malarial anaemia, neurocognitive impairment

## **5.1 Introduction**

Malaria is a complex disease caused in humans by five species of the unicellular *Plasmodium* parasite, transmitted through the bite of female *Anopheles* mosquitoes. Malaria is a primary global health concern as approximately half of the people worldwide are at risk of infection; it is endemic in a total of 84 countries<sup>1</sup>. An estimated 247 million malaria cases and 619,000 deaths were reported in 2021 by WHO; 95% of the cases occurred in sub-Saharan Africa, and approximately half a million deaths (77%) were of children under five years old<sup>1</sup>. Most people infected with malaria are asymptomatic; however, people with naïve immune systems without clinical immunity develop flu-like symptoms and if treatment is delayed or not appropriate, ~4.5% will worsen, becoming uncontrolled and developing into severe malaria<sup>2-4</sup>.

Two common manifestations of severe malaria are severe malarial anaemia (SMA), which is associated with altered haematopoiesis and increased clearance of all red blood cells, and cerebral malaria (CM), which is associated with malaria-infected RBC (iRBC) sequestration in the vasculature of most organs, including the brain<sup>5-7</sup>. Both complications are linked to high mortality rates and can also lead to neurocognitive impairment (NCI), which can last for many years after the initial infection<sup>7,8</sup>.

Significant clinical differences are seen in African children, with the blood-brain barrier breakdown observed in CM. Still, disruption is limited for children with SMA, which contributes to the complex pathogenesis involved in NCI<sup>6,9</sup>. After treatment for severe malaria, approximately 25% of survivors develop NCI<sup>10</sup>. Deficits in attention, cognitive ability, associative memory, and behaviour have been documented in CM patients who developed NCI. In contrast, SMA might affect the patient's overall cognitive ability for visual reception, fine motor scales, and receptive and expressive language. This may suggest differences in the mechanism of NCI in these two syndromes<sup>11,12</sup>. These deficits associated with NCI affect the child's long-term development, academic achievement and eventually socioeconomic status<sup>8,13</sup>. The developmental challenges lead to less education and lower incomes, which in turn contributes to household vulnerability to malaria, continuing the cycle of poverty<sup>14</sup>.

Once infected with malaria, the disease can quickly progress into severe malaria and become life-threatening; therefore, proper treatment and early detection are essential<sup>15</sup>. Prognostic biomarkers for severe malaria complications would allow for earlier detection and treatment,



though biomarker research has only recently begun to distinguish the severe forms of malaria. Currently, only a few potential biomarkers have been identified for severe malaria, the majority being proteins, such as von Willebrand factor, angiotensin-1 and 2, intercellular adhesion molecule 1 (ICAM-1), erythropoietin, and *Plasmodium falciparum* histidine-rich protein 2 (PfHRP2), most of which are elevated during severe disease<sup>16-24</sup>. Although these proteins have shown potential, they lacked accuracy across different countries or were differentiating severe malaria (CM or SMA) from healthy patients, which is not required as reliable diagnostic techniques already exist. Therefore, there is a need for predictive biomarkers of severe malaria outcomes, allowing early identification of children who may develop NCI or are at risk of lethal complications, as many children have already progressed to severe malaria upon hospitalisation<sup>25</sup>.

Tau is a well-known protein associated with neurodegenerative disorders and traumatic brain injury and has been linked to neurological disruption<sup>26-29</sup>. Tau protein is a potential cerebrospinal fluid (CSF) and plasma biomarker for Alzheimer's disease, and soluble tau has also been investigated in severe malaria<sup>30</sup>. In a 2007 retrospective study, elevated levels of Tau protein were found in the CSF of children with CM; however, follow-up for long-term NCI was not reported<sup>31</sup>. Recently, a study involving Uganda children with severe malaria found elevated tau protein concentrations in CSF and plasma at admission related to long-term NCI in children recovering from CM<sup>32,33</sup>. Although plasma levels were elevated in children hospitalised with SMA, there was no association with NCI, possibly indicating different mechanisms of NCI for children with SMA<sup>33</sup>. Elevated levels of tau in the CSF of Uganda children with CM at the time of hospitalisation were also associated with acute kidney injury, indicating potential mechanisms that link kidney injury with brain injury<sup>34</sup>.

Angiotensin has previously been associated with severe malaria. Recently, a study in Central India showed that plasma levels of angiotensin-2 and ratios of angiotensin-2/angiotensin-1 in patients (83% adults, 16% children) at time of admission could distinguish CM patients who do not survive from those with CM but survived (only angiotensin-2), non-CM and mild malaria<sup>35</sup>. After 48 hours of treatment, the ratios of angiotensin-2/angiotensin-1 decreased in mild malaria, non-CM, and CM survivor cases but did not in CM patients who died<sup>35</sup>. In a Ugandan cohort of children (18 months to 12 years old), angiotensin-2 and the ratio of angiotensin-2/angiotensin-1 were associated with worsened cognition and neurodevelopmental injury<sup>36</sup>. In a prospective, longitudinal study of the same cohort of

children with CM and SMA, increased angiopoietin-2 was associated with worse neurocognitive function in children under five years old but not in children five years or older<sup>37</sup>. By bridging the knowledge gap, reliable prognostic biomarkers for severe malaria morbidity and mortality could allow for earlier interventions with adjunctive therapies, as they have so far been ineffective due to late administrations<sup>38</sup>. Identifying patients at risk of severe complications would permit timely treatment, possibly lowering the risk of long-term deficits.

Extracellular vesicles (EVs) are a heterogeneous mix of submicron particles released by all host cell types during cellular processes such as proliferation, senescence, and apoptosis<sup>39</sup>. EVs carry protein, lipids, and nucleic acids from their cell of origin and act as vessels in intercellular communication and the exchange of biological information, supporting their involvement in disease pathogenesis<sup>40–48</sup>. EVs have been shown to provide valuable information on the status and progression of a disease or condition<sup>40</sup>. EVs are notable sources of biomarkers, and EVs themselves have also demonstrated biomarker potential in multiple studies where elevated numbers of EVs, mainly platelet-, endothelial-, and RBC-derived microvesicles, were measured circulating in human patients with CM<sup>41,49–51</sup>. The potential of EVs as biomarkers for severe malaria is still in its infancy, as in-depth studies are required to establish their prognostic value. This study aims to identify potential prognostic biomarkers that can differentiate the different outcomes of severe malaria in children from Uganda by comparing their proteome profiles (Figure 5.1).

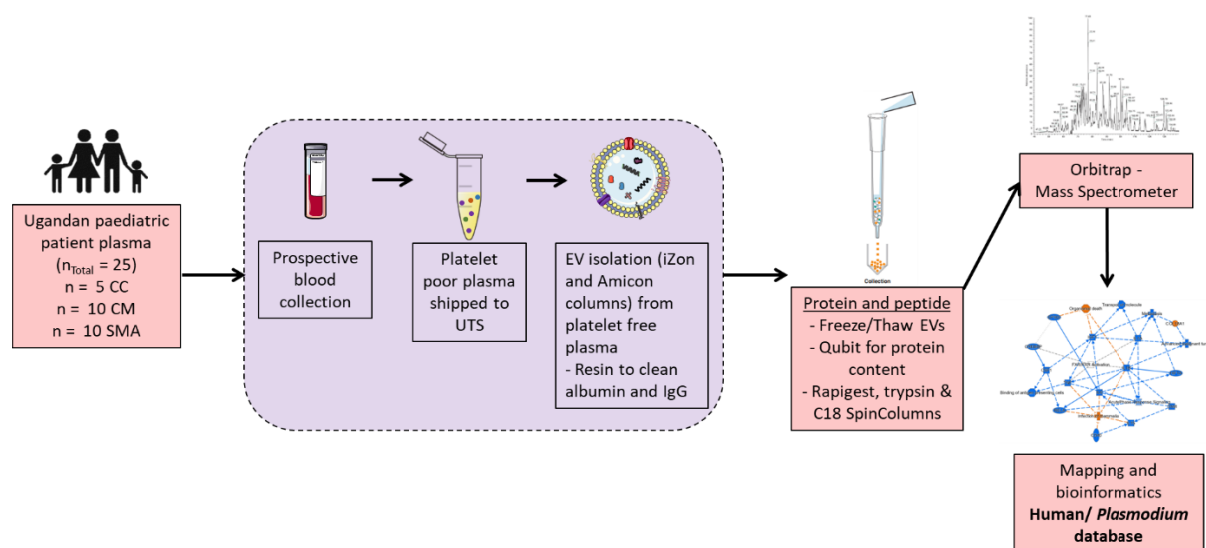


**Figure 5.1** Study pipeline depicting the patient groups, sample collection and processing, protein purification from paediatric samples and bioinformatics.

Abbreviations: CC, community children; CM, cerebral malaria; EV, extracellular vesicles; SMA, severe malarial anaemia; UTS, University of Technology Sydney

## **5.2 Materials and methods**

### **5.2.1 Study Participants**

Please refer to section 4.2.1 for study participant details and 4.2.4 for patient group classification. Table 5.1 presents the demographics of the patient cohort.

### **5.2.2 Ethical approval and informed consent**

Please refer to section 4.2.2 for information regarding ethical approvals and guardian consent.

### **5.2.3 Study design**

By comparing the clinical, biological, and neurological data, 25 children were selected for five patient sub-groups: community controls (n=5), children who fully recovered from CM (CM FR, n=5) or SMA (SMA FR, n=5), children with fatal outcomes of CM (CM FO, n=5), and children who survived SMA but developed NCI (SMA NCI, n=5). Three sets of clinically significant comparisons were performed: 1) among children with CM, those who fully recover (FR) were compared to those with fatal outcomes (FO); 2) among children with SMA, those who FR were compared to those who survived but developed NCI; and 3) among those who fully recovered the children with CM and SMA were compared. Appropriate comparisons between the CC group and severe malaria patients were performed to develop a baseline of activity within the children.

### **5.2.4 Platelet-free plasma preparation and storage**

Please refer to section 4.2.5 regarding blood collection, storage, preparation and transportation.

<b>Table 5.1</b> Characteristics of paediatric patient group baseline demographics and clinical findings						
Demographic and clinical findings						
Mass spectrometry paediatric patient group	CC (n = 5)	CM FR (n = 5)	CM FO (n = 5)	SMA FR (n = 5)	SMA NCI (n = 5)	P Value <sup>a</sup>
Age, y, mean (SD)	3.00 (0.45)	3.33 (0.46)	3.12 (0.63)	2.62 (0.30)	2.48 (0.83)	.32
Sex, male:female, No.	5:0	2:3	4:1	5:0	5:0	
Plasma volume, µL, mean (SD)	175 (5.5)	168 (5.9)	177 (8.5)	179 (5.3)	170 (6.1)	.43
Blantyre coma scale <sup>5</sup> , mean		1	1	5	5	
Coma duration, hours, median (IQR)	0	90.50 (50-132.3)	0	0	0	.0001
Haemoglobin, g/dL, mean (SD)	11.6(1.35)	5.43 (0.87)	6.95 (1.10)	4.02 (0.95)	3.64 (0.59)	.002
Platelet count, x10 <sup>9</sup> /L, median (IQR)	471 (362-597)	82 (40-138)	54 (41-76)	101 (107-185)	141 (132-153)	.03
Hypoxia Y:N/# (O <sub>2</sub> saturation <95%)	0:5	0:5	1:4	2:3	0:5	
Lactic acidosis Y:N/# (lactate >5 mmol/L)	0:5	1:4	1:4	1:4	1:4	
Plasmodium falciparum peripheral blood density, parasites/µL, median (IQR)	0	206 600 (52 305-230 550)	204 555 (63 522-301 500)*	65 000 (11 320-103 020)	49 200 (29 630-230 620)	.006
PfHRP-2 level, ng/mL, median (IQR)	4.8 (4.8-4.8)	5063 (6991- 9287)	8238 (658-12758)	2665 (987-4251)	506 (95-785_)	.051

Abbreviations: CC, community children; CM, cerebral malaria; FO, fatal outcome; FR, full recovery; IQR, Interquartile Range; NCI, neurocognitive impairment; SD, standard deviation; SMA, severe malarial anaemia

<sup>a</sup> P Value based on one-way ANOVA Kruskal-Wallis

<sup>5</sup> Blantyre coma scale for preverbal children <5 years of age; minimum score: 0 (poor), maximum score: 5 (good), abnormal score ≤ 4

\* One patients with hyperparasitaemia

### 5.2.5 EV isolation, size measurement, and serum protein removal

EVs from ~180  $\mu$ L of PFP were collected using iZON qEV 75 nm -1000 nm singles to ensure high EV recovery yield and purity. Fractions 6-10 were eluted with PBS and then concentrated with an Amicon Ultra 0.5 mL Ultracel 3k following the manufacturer's protocol. EVs were stored at -80 °C for later size confirmation via nanoparticle tracking analysis using the NanoSight NS300 (Malvern). To remove excess contaminating serum albumin and IgG from the EV samples, Proteome Purify™ 2, human serum protein immunodepletion resin, was used at 1:8 (EV: resin). After combining the two solutions, the mixture was mixed on a roller mixer for an hour at 300 rpm. The EV-resin mixture was then transferred to Spin-X Filter Units and centrifuged for 30 mins at 14,000 g at 18 °C. The immunodepleted EVs were temporarily stored at -30 °C for two days until protein digestion.

The EVs were thawed and vortexed for 15 seconds and then diluted with sterile PBS to  $\sim 10^6$  to  $10^9$  particles per mL to measure the size and concentration with the NanoSight. After dilution, the EVs were vortexed for another 15 seconds and immediately analysed with NTA v3.2 for ten recordings, 60 seconds each at 25 °C, with the camera level set to 11 and detection threshold at 10. PBS was used to flush the NanoSight between each run.

### 5.2.6 Protein digestion and tandem mass spectrometry analyses

The EVs were freeze-thawed five times to extract the proteins, alternating between liquid nitrogen for 30 seconds and 50 °C for 2 mins, followed by sonication for 5 minutes<sup>56,57</sup>. Protein concentrations were measured using a Qubit protein assay to normalise the protein concentration for digestion. The protein was digested following a modified version of a previously reported protocol<sup>56</sup> by adding 100  $\mu$ L of 0.1% RapiGest™ SF surfactant (Waters) to each sample, followed by incubation at 100 °C for 5 min. The samples were then left to cool down for a few minutes and sonicated for 30 seconds. Next, 2  $\mu$ L of 50 mM tris(2-carboxyethyl)phosphine (TCEP) was added to each sample as the reducing agent to break the disulphide bonds between and within proteins, followed by incubation at 60 °C for 20 min. Once the sample cooled down, trifluoroacetic acid (TFA) was added to reach a desired pH of <2 for RapiGest™ cleavage, TFA concentrations being approximately 0.5-1% of the total volume in the tube. The samples were kept at 37 °C for 35 mins and then centrifuged at 16,000 g for 10 mins at RT to recover the supernatant. Micro SpinColumns (Harvard Apparatus) were

used to desalt and clean the samples. Before use, the micro SpinColumns were washed by adding 150  $\mu$ L of 100% acetonitrile (AcN) to the columns and letting them sit for 10 mins, followed by centrifuging twice for 1 min at 1000 g. This was followed by two more rinses, once with 150  $\mu$ L of 50% AcN / 0.1% Formic Acid (FA) and a spin for 1 min at 1000 g, then 150  $\mu$ L of 5% AcN / 0.1% FA and a spin for 1 min at 1000 g. After discarding the eluted wash solution used to rinse the column, the sample was passed through the column by centrifuging for 1 min at 1000 g. The column was washed with 150  $\mu$ L of 5% AcN / 0.1% FA and spun for 1 min at 1000 g. The peptides were then eluted with 150  $\mu$ L of 50% AcN / 0.1% FA and centrifuged for 1 min at 1000 g. The last elution step was repeated to ensure all peptides were collected from the column and the elution was pooled. The elution collected in lo-bind tubes was concentrated using the Savant™ DNA SpeedVac™ Concentrator (Thermo Scientific™) for 2.5 hours on high heat; once dried, the pellets were stored at -80 °C.

Tandem mass spectrometry was performed on a QExactive Orbitrap Plus (Thermo Electron) equipped with an Ultimate 3000 HPLC and autosampler system (Dionex). The peptides were reconstituted with 2% AcN + 0.1% TFA for a 2  $\mu$ g / 5  $\mu$ L concentration. The peptides were run at a gradient of 140 min at the Mass Spectrometry Facility at the University of Technology Sydney, Australia. MS/MS data were analysed using PEAKS Studio X pro to generate protein lists by mapping against the UniProt Knowledgebase and plasmODB genome database for the genus *Plasmodium*. Differential expression analysis was also performed using PEAKS Studio X pro using the PEAKQ normalisation method, and the base sample was set to average with cut-offs, FDR  $\leq$ 1%, used at least one peptide, and fold change  $\geq$ 1 when comparing all five subgroups together and fold change  $\geq$ 2 when comparing the three clinically significant comparisons. Venn diagrams were made using InteractiVenn<sup>58</sup> and Venny 2.1<sup>59</sup>. The volcano plots were created using GraphPad Prism 10.1.0, and heatmaps were then made using Clustergrammer<sup>60</sup>. The rows and columns were hierarchically clustered using cosine distance and average linkage of the log<sub>2</sub> ratios of the abundance of each sample relative to the average abundance. The conditions in different samples were clustered based on a similar expression trend across the proteins.

### 5.2.7 Mapping and bioinformatics

The list of proteins identified using PEAKS Studio X pro was then run through QIAGEN® Ingenuity Pathway Analysis (IPA) Fall Release (2023) with stricter thresholds (FDR  $\leq$  1%, fold change 2, unique peptides  $\geq$ 1, p-value  $<$ 0.01 when comparing all five sub-groups and FDR  $\leq$  1%,  $|\text{Log}_2\text{Fold Change}| > 1$ , unique peptides  $\geq$ 2, p-value  $<$ 0.001 when analysing the three clinically significant comparisons) to identify proteins of interest<sup>61</sup>. This generated canonical pathways, disease and functional analyses, and networks for all the comparisons. The significance when associating the data set and canonical pathways was calculated in two ways: 1) a ratio of the number of molecules from the data set that map to the pathway divided by the total number of molecules that map to the canonical pathway is displayed; and 2) a right-tailed Fisher's Exact Test was used to calculate a p-value determining the probability that the association between the genes in the dataset and the canonical pathway is explained by chance alone. In many cases, a z-score was calculated to indicate the likelihood of activation or inhibition of that pathway.

The diseases and functions analysis identified the most significant biological functions and diseases from the data set. A right-tailed Fisher's Exact Test was used to calculate a p-value, determining the probability that each biological function and disease assigned to that data set is due to chance alone. A z-score was calculated to indicate the likelihood of an increase or decrease in that disease or function.

The data set containing protein identifiers and corresponding data measurement values was uploaded into the application. Each identifier was mapped to its corresponding entity in QIAGEN's Knowledge Base. These molecules, called Network Eligible molecules, were overlaid onto a global molecular network developed from information in the QIAGEN Knowledge Base. Networks of Network Eligible Molecules were then algorithmically generated based on their connectivity.

## **5.3 Results**

### **5.3.1 EV size and concentration**

The EVs were purified using iZON columns, followed by concentration with Amicon filters to collect them. The size and concentration of the isolated EVs were measured via nanoparticle tracking analysis (Nanosight 300). The EV sizes ranged from 15 nm to 1000 nm, and the average EV size was ~200 nm (Figure 5.2A-C). The three main groups of patients had similar EV distribution profiles, with a prominent peak around 150 nm followed by a smaller peak at 200 nm. Community control children had the lowest amount of EVs ( $5.0 \times 10^9$  EVs in 180  $\mu$ L of PFP), followed by SMA patients ( $11.9 \times 10^9$  EVs in 180  $\mu$ L of PFP), and closely CM patients ( $16.2 \times 10^9$  EVs in 180  $\mu$ L of PFP).

### **5.3.2 Technical reproducibility**

An MS-based semi-quantitative proteomics strategy was used for a proteome-wide comparison between 5 healthy children (CC) and 20 malaria-infected children (CM and SMA). The 25 samples were analysed using technical duplicates, and similar numbers of proteins were identified. One of the technical replicates failed for a CC patient, and that sample was excluded from the analysis. The percentage of similar proteins for the patient technical replicates was an average of 65% (48 - 80%) (Table 5.2). A Pearson correlation was calculated for each technical replicate pair, and the average r-value was 0.997 (range 0.990-0.999) for all the patient replicates (Figure 5.2D, Supplementary Figure 5.1). High values of R (0.90-0.98) indicated highly reproducible label-free quantification between technical replicates.



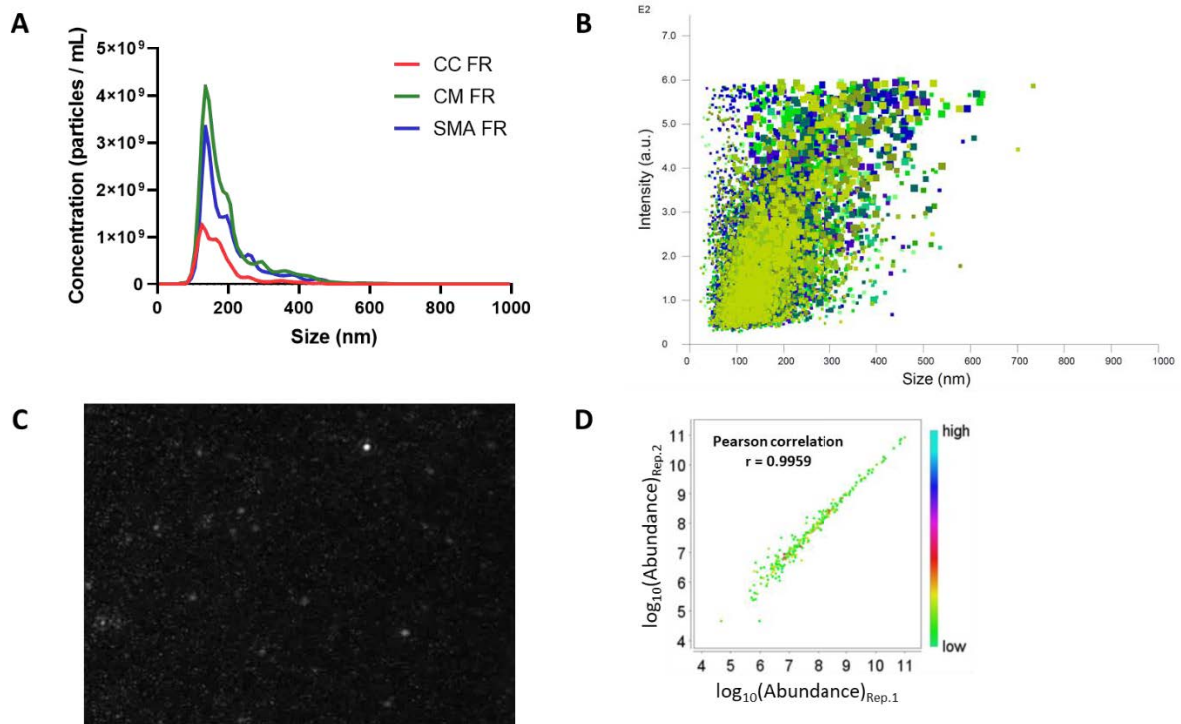


**Figure 5.2** Measurement of size and concentration of extracellular vesicles using nanoparticle tracking analysis. (A) Compared to malaria patients the community control samples had fewer extracellular vesicles, whereas the size distribution was approximately the same for all patients. (B) Representative scatter plot depicting the correlation between technical replicates. (C) Recording of extracellular vesicles using the NS300 nanoparticle tracker. (D) The Pearson correlation coefficient value of relative protein abundance between two analytical replicates of a representative sample reflecting the reproducibility of label-free quantitation,  $r = 0.9959$ .

**Table 5.2** Percentage similarity between patient technical replicates and number of proteins identified in each patient

Patient Groups	Sample ID	All Proteins			Proteins only in Technical Replicate 1		Proteins only in Technical Replicate 2		Proteins in both Technical Replicates	
		Tech Rep 1	Tech Rep 2	Tech Rep 1+2	# of Protein	% of total	# of Protein	% of total	# of Protein	% of total
CC FR	559	356	309	449	140	31%	93	21%	216	48%
CC FR	748	317	255	332	77	23%	15	5%	240	72%
CC FR	348	298	299	372	73	20%	74	20%	225	61%
CC FR	459	241	203	259	56	22%	18	7%	185	71%
CM FR	769	567	584	694	110	16%	127	18%	457	66%
CM FR	564	368	351	457	106	23%	89	20%	262	57%
CM FR	290	462	383	502	119	24%	40	8%	343	68%
CM FR	450	267	254	306	52	17%	39	13%	215	70%
CM FR	416	455	424	522	98	19%	67	13%	357	68%
CM FO	240	411	364	474	110	23%	63	13%	301	64%
CM FO	239	614	554	703	149	21%	89	13%	465	66%
CM FO	203	320	300	385	85	22%	65	17%	235	61%
CM FO	530	480	424	556	132	24%	76	14%	348	63%
CM FO	716	521	466	588	112	21%	67	11%	399	68%
SMA FR	590	310	304	365	61	17%	55	15%	249	68%
SMA FR	695	507	421	605	184	30%	98	16%	323	53%
SMA FR	180	289	286	344	58	17%	55	16%	231	67%
SMA FR	368	410	418	516	98	19%	106	21%	312	61%
SMA FR	430	327	308	353	45	13%	26	7%	282	80%
SMA NCI	189	383	313	440	127	29%	57	13%	256	58%
SMA NCI	113	335	328	389	61	16%	54	14%	274	70%
SMA NCI	149	507	384	560	176	31%	53	10%	331	59%
SMA NCI	467	383	365	444	79	18%	61	14%	304	69%
SMA NCI	232	467	418	550	132	24%	83	15%	335	61%

Abbreviations: CC, community children; CM, cerebral malaria; FO, fatal outcome; FR, full recovery; NCI, neurocognitive impairment; SMA, severe malarial anaemia

### 5.3.3 Proteomic analysis

A total of 1622 plasma EV proteins were identified across all patients (Figure 5.3A). Four hundred and twenty (420) proteins were common to all malaria patients and community controls (CC) (Figure 5.3A). Comparatively, fewer proteins were detected in the CC group compared to the malaria patient groups, CC, CM FR, CM FO, SMA FR and SMA NCI, presented with 520, 717, 777, 602, and 670 proteins, respectively (Table 5.3). Likewise, the number of protein groups (collection of proteins identified by a set of peptides) identified was also lower in the CC group compared to malaria patients; CC, CM FR, CM FO, SMA FR and SMA NCI had 180, 265, 283, 226, and 248, respectively (Table 5.3). Variations between human plasma samples can occur due to the complexity of the sample. To minimise variation, clinical and biological data for all samples in each group were matched during sample selection, allowing at least 80% of proteins to be shared between at least two patients in a group (Figure 5.3B-F). When comparing the controls to the severe malaria patients, 624 proteins were common, with 74 proteins exclusively present in CC and 924 proteins exclusively present in severe malaria patients (Figure 5.4A). By comparing the three main groups, CC, CM and SMA, 263 plasma EV proteins were exclusive to CM, and 216 proteins were exclusive to SMA (Figure 5.4B). When comparing the proteins detected in each clinical outcome (FR and FO for CM and FR and NCI for SMA), i.e., SMA FR vs CM FR, CM FO vs CM FR, and SMA FR vs SMA NCI, all three comparisons had approximately 700 proteins in common per individual comparison (Figure 5.4C-E). Each sub-group had 200-300 proteins exclusive to that patient group (Figure 5.4C-E).

Of the 1622 plasma EV proteins identified, 44 were *P. falciparum* proteins, 34 were exclusively found in CM patients, one in SMA patients, and eight were common to both CM and SMA (Figure 5.5A and B). When comparing the sub-groups, 11 and 8 proteins were uniquely present in CM FR and CM FO, respectively, and none were identified in SMA FR or SMA NCI (Figure 5.5C). One malaria protein was shared between CC and severe malaria; however, this protein fragment was eventually eliminated in the downstream analysis (Figure 5.5A).

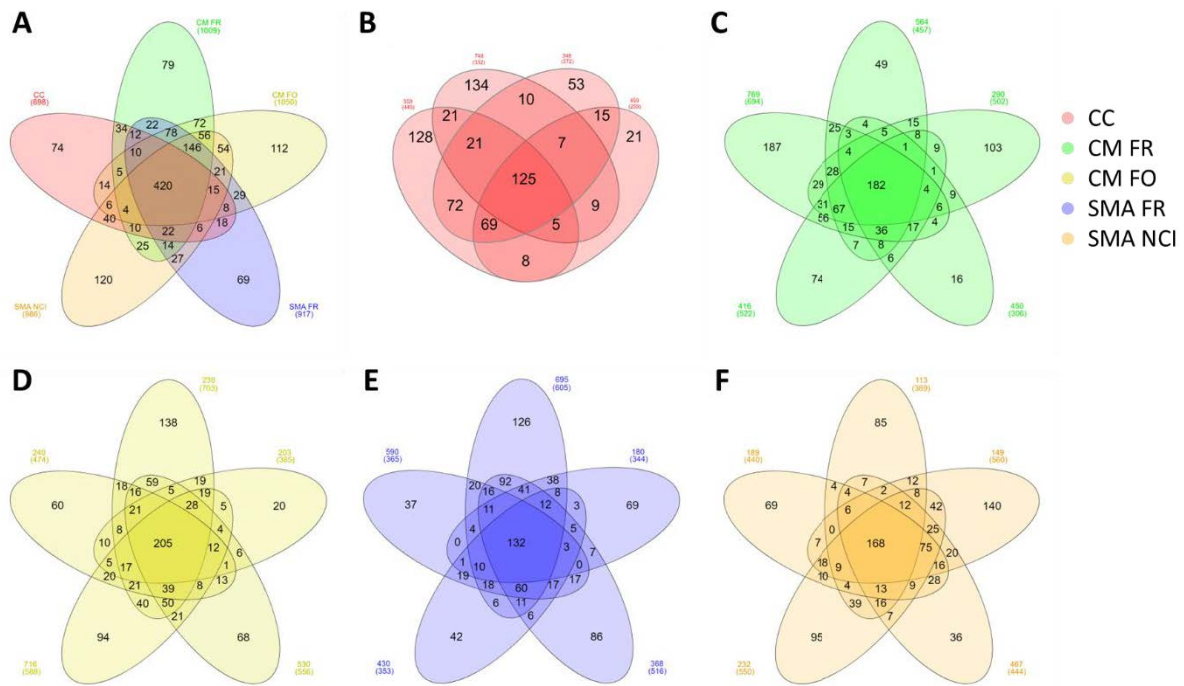


**Figure 5.3** Venn diagram comparing the plasma EV proteins identified in each patient and malaria subgroup. (A) Comparison of all proteins (1622) identified in the patient groups, 698, 1009, 1050, 917, and 986 proteins in CC, CM FR, CM FO, SMA FR, and SMA NCI, respectively, 420 proteins were in common to all five sub-groups. (B) Proteins identified in the four CC, 125 proteins were common to all four patients. (C-F) Comparison of all proteins identified in the CM FR, CM FR, SMA FR, and SMA NCI sub-groups, respectively 182, 205, 132, and 168 proteins were common to all 5 patients within the group. Abbreviations: CC, community children; CM, cerebral malaria; FO, fatal outcome; FR, full recovery; NCI, neurocognitive impairment; SMA, severe malarial anaemia

**Table 5.3** Number of proteins and protein groups identified in each patient group via mass spectroscopy

	CC (n=4)	CM FR (n=5)	CM FO (n=5)	SMA FR (n=5)	SMA NCI (n=5)
<b>Average # of proteins</b>	520	717	777	602	670
<b>Range</b>	388-608	498-1006	574-1072	497-767	531-951
<b>Average # of protein groups</b>	180	265	283	226	248
<b>Range</b>	131-232	184-357	194-337	175-275	195-319

Abbreviations: CC, community children; CM, cerebral malaria; FO, fatal outcome; FR, full recovery; NCI, neurocognitive impairment; SMA, severe malarial anaemia

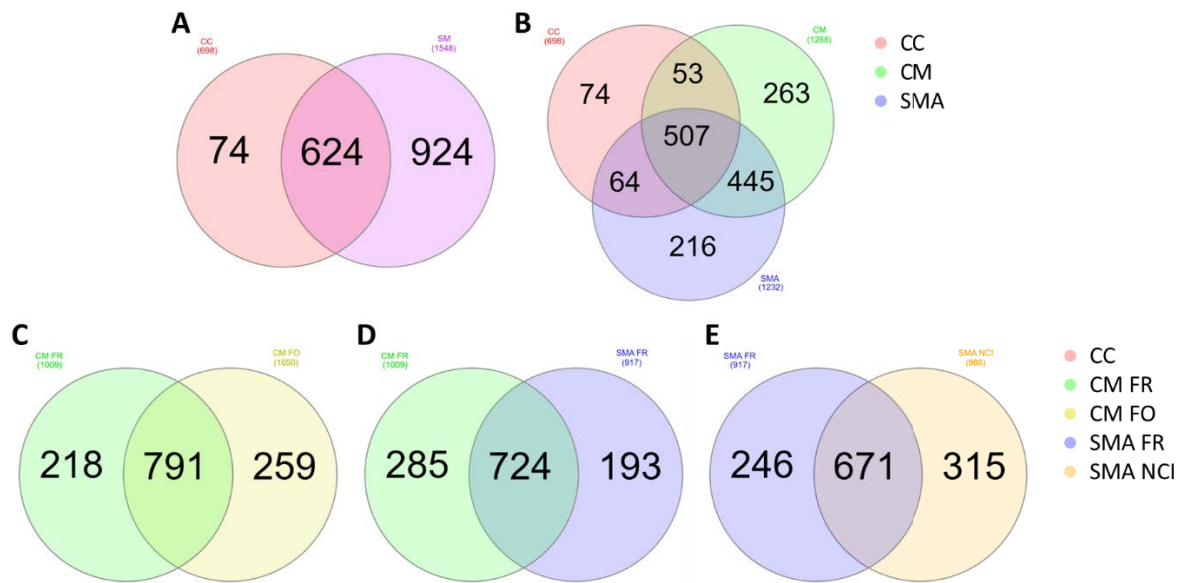


**Figure 5.4** Comparison of proteins identified in the three main groups of children. (A) Comparison of healthy and infected children, 624 proteins were common, with only 74 exclusive to CC. (B) Comparison of the three main groups of children and malaria patients, 507 proteins were common, followed by 445 protein common between children with CM and SMA. (C-E) Comparison of the clinically relevant sub-groups of severe malaria outcomes, CM FO vs CM FR, SMA FR vs CM FR, and SMA FR vs SMA NCI, the comparisons had respectively, 791, 724, and 671 proteins in common, and approximately 200 to 300 proteins exclusive to the individual groups. Abbreviations: CC, community children; CM, cerebral malaria; FO, fatal outcome; FR, full recovery; NCI, neurocognitive impairment; SMA, severe malarial anaemia

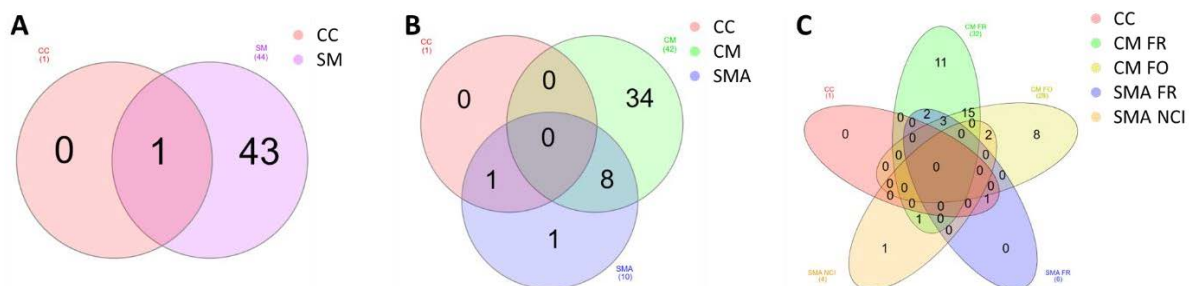


**Figure 5.5** Comparison of *Plasmodium falciparum* proteins identified in all the patients. (A) 44 malaria proteins were identified in all the patients, one was found in common with the CC group; however, this was a fragment of a protein which was later eliminated during downstream analysis. (B) Majority of the proteins were in the CM group with 34 proteins, 8 proteins were in common between CM and

SMA patients. (C) The CM FR sub-group had 11 proteins exclusive to that group, followed by 8 proteins in the CM FO group, 15 proteins were common to CM FR and CM FO. Abbreviations: CC, community children; CM, cerebral malaria; FO, fatal outcome; FR, full recovery; NCI, neurocognitive impairment; SM; severe malaria; SMA, severe malarial anaemia

#### 5.3.4 Expression and pathway analysis for 5 sub-groups (community controls and malaria patients)

Differential expression analysis was performed using PEAKS X pro to compare the five sub-groups (CC, CM FR, CM FO, SMA FR, SMA NCI), represented in the heatmap (Figure 5.6A) 318 differentially expressed proteins (DEPs) were identified in the plasma EVs when a threshold of  $FDR \leq 1\%$ , unique peptides  $\geq 1$ , and  $p\text{-value} < 0.001$  was applied. The most considerable difference in protein profile is between the CC and SMA NCI patients, where most proteins' relative abundance is higher in the SMA NCI patient EVs (Figure 5.6A). Children with CM and SMA who fully recovered after treatment had a similar protein clustering (Figure 5.6A). The children with CM FO and SMA NCI also had similar clustering, where approximately two-thirds of the proteins had high relative abundance compared to the other groups (Figure 5.6A).

The number of DEPs was narrowed down using the following cut-offs  $FDR \leq 1\%$ , unique peptides  $\geq 2$ , and  $p\text{-value} < 0.001$  to curate a list of 227 proteins from the five sub-group comparisons to predict up- and downstream effects using IPA (Figure 5.7). IPA mapped 223 DEPs, which were then narrowed down to 183 DEPs by excluding duplicates. The pathway analysis indicated activation or inhibition of specific pathways by the proteins carried by the plasma EVs. This suggested that those specific pathways could be altered if a cell interacted with or took up these plasma EVs. The children in the CC group were also compared to the patient groups, and the results showed that the DEPs led to an overall inhibition of cell signalling, molecule transport, immunological processes, and inflammatory pathways (Figure 5.7A). Due to the inhibition of inflammatory proteins, an indirect relationship predicted the activation of the following pathways/themes: "Infection of Mammalia" disease, collagen, and organismal death in the CC group (Figure 5.7A). In severe malaria, DEPs from patients with CM FR were associated with inhibition of immunological pathways related to cell activation, recruitment, and migration, as well as inhibition of blood clots and adhesion of blood platelet pathways (Figure 5.7B and Supplementary Figure 5.2A-C). The DEPs from CM FO patients



were predicted to cause activation of the Liver X Receptor-Retinoid X Receptor (LXR/RXR) pathway, nuclear receptor subfamily 1 group H member 3 (NR1H3) receptor, positive regulatory domain containing 1, with zinc finger domain (PRDM1) receptor and glomerulonephritis, along with inhibition of cellular movement and infiltration and kidney damage (Figure 5.7C and Supplementary Figure 5.2D). The analysis also identified the activation of liver inflammation by DEPs from SMA FR patients and the inhibition of immune response pathways and immune cell activation (Figure 5.7D and Supplementary 5.2E). Inhibition of blood cell phagocytosis, endothelial cell death and development, inflammatory response, and vascular cell proliferation were also associated with these DEPs (Figure 5.7D and Supplementary Figure 5.2E-H). Lastly, DEPs from SMA NCI patients were associated with the activation of several pathways involved in immune cell recruitment, migration, activation, adhesion and death, blood cell proliferation, calcium ion flux, and kidney cell death (Figure 5.7E and Supplementary Figure 5.2I-M).

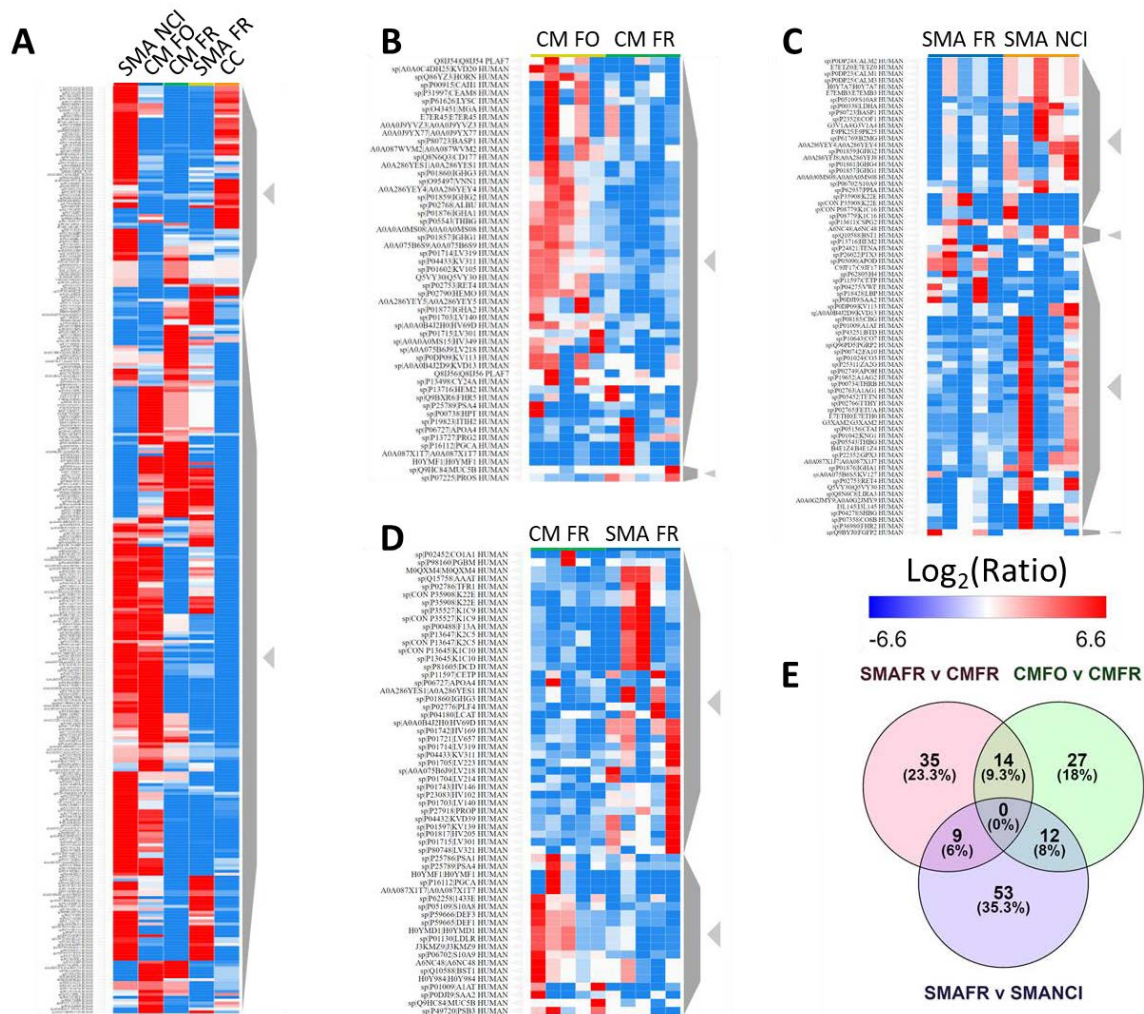


**Figure 5.6** Differentially expressed plasma extracellular vesicle proteins identified with PEAKS Xpro. (A) 318 proteins were differentially expressed in the 5 sub-groups, normalisation based on the average abundance, FDR  $\leq$  1%, PEAKSQ (p-value  $<0.001$ ), has at least 1 used peptide. (B-D) Comparison of the clinically relevant sub-groups, CM FO vs CM FR, and SMA FR vs SMA NCI, SMA FR vs CM FR, with 53, 74, and 58 differentially expressed proteins, respectively. Normalisation was based on average abundance, FDR  $\leq$  1%, Fold Change  $\geq$ 2, Significance method PEAKSQ (p-value  $<0.01$ ), has at least 1 used peptide. (E) Venn diagram representing differentially expressed proteins in the clinically relevant comparisons, there were no proteins common to all three comparisons and SMA FR vs SMA NCI had the most proteins exclusive to that group, 53 proteins. Abbreviations: CC, community children; CM, cerebral malaria; FO, fatal outcome; FR, full recovery; NCI, neurocognitive impairment; SMA, severe malarial anaemia



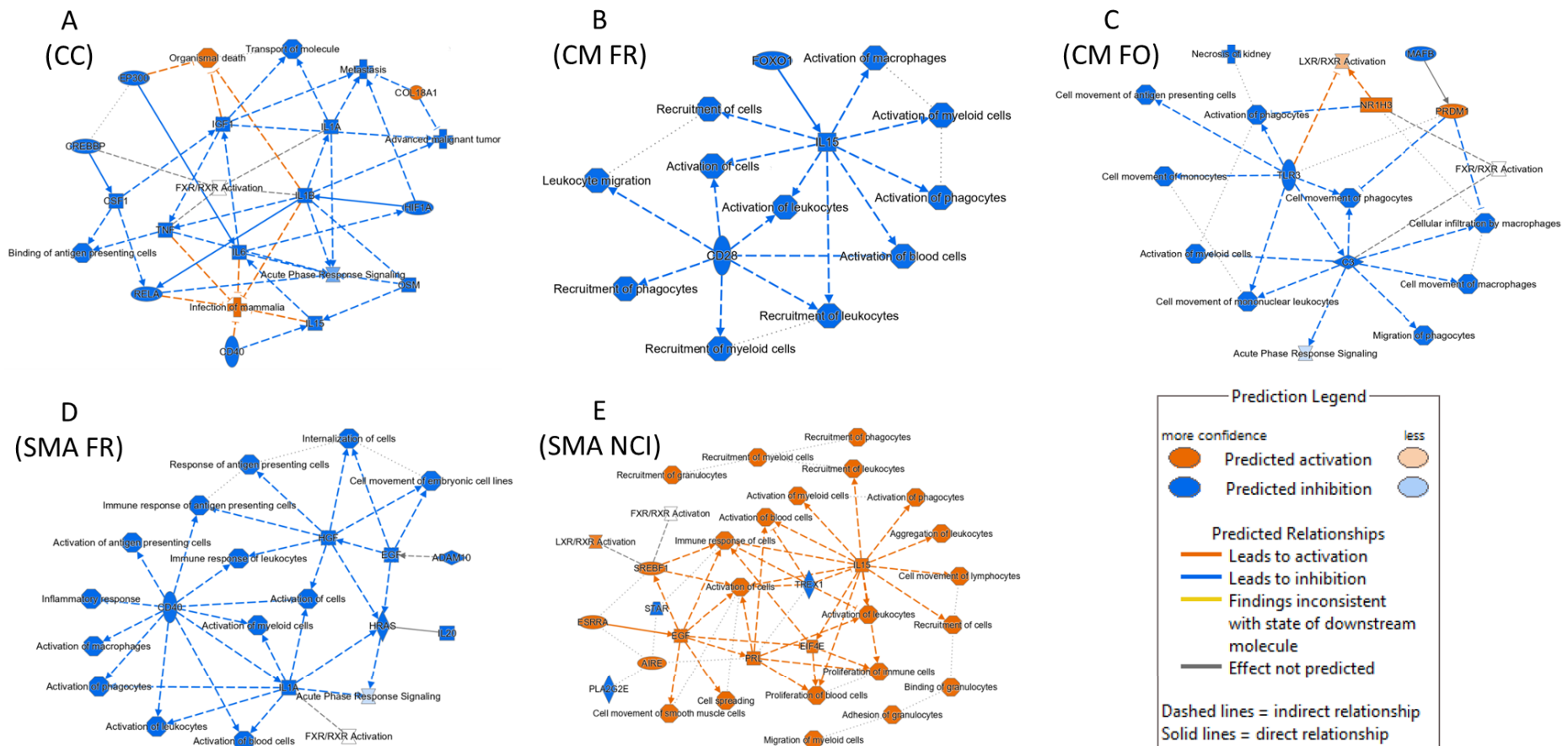


**Figure 5.7** Summary of the major biological themes identified using Ingenuity Pathway Analysis. Threshold cut-offs were set to FDR  $\leq$  1%, unique peptides  $\geq$  2, p-value  $<$  0.001. (A) The CC group overall had an inhibition of pathways, with indirect relationships causing the activation of ‘Organismal death’ and ‘Infection of Mammalia’. (B-D) CM FR, CM FO and SMA FR all had large amounts of pathway inhibition, CM FO also had an activation of the LXR/RXR pathway. Abbreviations: CC, community children; CM, cerebral malaria; FO, fatal outcome; FR, full recovery; NCI, neurocognitive impairment; SMA, severe malarial anaemia.

### 5.3.5 Expression analysis for the clinically relevant malaria comparisons

Differential expression analysis was then run pairwise using PEAKS Xpro for three biologically relevant comparisons: SMA FR vs CM FR, CM FR vs CM FO, and SMA FR vs SMA NCI. Volcano plots were used to graphically represent the differences between the patient groups using the significance ( $-\text{Log}_{10}(\text{p-value})$ ) versus the fold-change ( $\text{Log}_2(\text{fold-change})$ ) (Figure 5.8A-C). A total of 1117 proteins were plotted with 778, 908, and 775 proteins in SMA FR vs CM FR, CM FR vs CM FO, and SMA FR vs SMA NCI plots, respectively (Figure 5.8A-C). Out of all the proteins, only two differentially expressed were *P. falciparum* proteins, i.e., immunogenic merozoite surface protein 6 (MSP6) and glutamate-rich protein (GLURP)<sup>62,63</sup>, and both levels of relative abundance were significantly higher in CM FO than CM FR (Figures 5.8B).

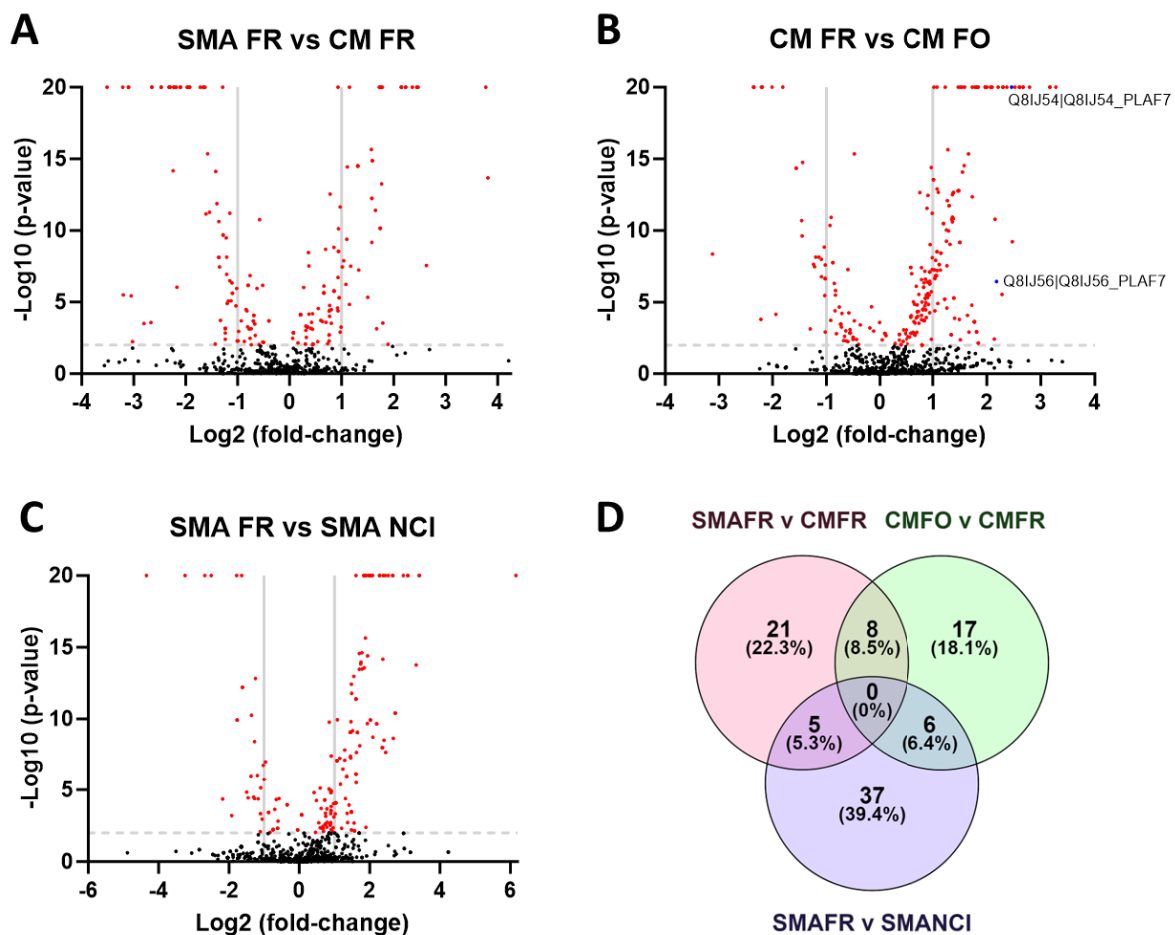


**Figure 5.8** Volcano plots of three clinically relevant comparisons of severe malaria outcomes. The cut-offs are shown with horizontal dotted lines and vertical solid lines, representing a  $\text{p-value} < 0.01$ , and  $|\text{Log}_2\text{Fold Change}| > 1$ . Proteins with very small  $\text{p-values}$  are plotted on  $-\text{Log}_{10}(\text{p-value}) = 20$ . (A-C) A total of 1117 proteins identified in the malaria patient samples are plotted, 778, 908, and 775 proteins

are plotted for SMA FR vs CM FR, CM FR vs CM FO, and SMA FR vs SMA NCI, respectively. (B) Two malaria proteins were found to be differentially expressed. (D) Using threshold cut-offs,  $FDR \leq 1\%$ ,  $|\text{Log}_2\text{Fold Change}| > 1$ , unique peptides  $\geq 2$ , and  $p\text{-value} < 0.001$  a list of proteins was created and analysed using Ingenuity pathway analysis. The analysis mapped 94 differentially expressed proteins with 34, 31, and 48 proteins in comparisons SMA FR vs CM FR, CM FO, vs CM FR, and SMA FR vs SMA NCI, respectively. Abbreviations: CM, cerebral malaria; FO, fatal outcome; FR, full recovery; NCI, neurocognitive impairment; SMA, severe malarial anaemia

### 5.3.6 Identification of biological processes and functional group networks

#### *5.3.6.1 Comparisons between the clinically relevant malaria sub-groups*

Next, IPA analysis was performed for the three clinically significant severe malaria comparisons with stricter thresholds ( $FDR \leq 1\%$ ,  $|\text{Log}_2\text{Fold Change}| > 1$ , unique peptides  $\geq 2$ ,  $p\text{-value} < 0.001$ ) to curate a list of 116 DEPs for all three comparisons to determine their role as potential prognostic biomarkers for severe malaria outcomes, i.e., full recovery, neurocognitive impairment, and death. After processing the DEPs list with the new thresholds, 109 passed the cut-offs implemented by the IPA software and were mapped, leaving only human proteins, all the malaria proteins being cut-off. IPA then filtered out duplicates, narrowing the list to 94 DEPs in total. Comparisons between SMA FR and CM FR, CM FO and CM FR, and SMA FR and SMA NCI showed 34, 31, and 48 DEPs, respectively (Figure 5.8D and Supplementary Table 5.1).

The top 10 differentiating plasma EV proteins in the dataset that passed the IPA core analysis cut-offs and mapped to the ingenuity knowledge base are listed in Table 5.4. Five defining proteins span two comparisons for SMA FR, calcium-binding protein (S100A8 and 9), keratin (KRT), and cholesteryl ester transfer protein (CETP), respectively lower, higher, and higher in SMA FR compared to CM FR and SMA NCI and serum amyloid A2 (SAA2) higher in CM FR and lower in SMA NCI compared to SMA FR (Table 5.4). As for CM FR, eight proteins, aggrecan (ACAN), apolipoprotein (APOA4) and five immunoglobulin (IG) proteins were respectively higher, higher, and lower in CM FR compared to SMA FR and CM FO and proteasome subunit alpha type-1 and 4 (PSMA4) was higher in CM FR compared to SMA FR and lower in CM FR compared to CM FO (Figure 5.6 and Table 5.4). Comparisons of SMA FR versus SMA NCI and CM FO versus CM FR shared 6 DEPs: brain acid soluble protein 1 (BASP1), three immunoglobulin (IG) proteins, retinol-binding protein 4 (RBP4), serum protease inhibitor,

clade A [alpha-1 antiproteinase, antitrypsin], and member 7 (SERPINA) and all had higher levels in the more severe outcome, that is in SMA NCI and CM FO.

**Table 5.4** Top 10 most highly dysregulated proteins for each severe malaria outcome comparison

SMA FR vs CM FR		CM FO vs CM FR		SMA FR vs SMA NCI	
<b>Expr Fold Change ↑</b>					
Molecules	Value	Molecules	Value	Molecules	Value
ACAN	↑ 1.770	ACAN	↑ 1.860	CFHR2	↑ 1.820
COL1A1	↑ 1.770	ALAD	↑ 1.650	KRT16	↑ 1.800
S100A8	↑ 1.690	CFHR5	↑ 1.640	IGHG4	↑ 1.740
APOA4	↑ 1.680	ITIH2	↑ 1.620	C8B	↑ 1.730
S100A9	↑ 1.670	APOA4	↑ 1.590	S100A8	↑ 1.730
DEFA1 (includes others)	↑ 1.640	PROS1	↑ 1.500	SERPINA6	↑ 1.730
SAA2	↑ 1.560			CFI	↑ 1.720
PSMA1	↑ 1.520			PGLYRP2	↑ 1.700
PSMA4	↑ 1.520			TTR	↑ 1.700
LDLR	↑ 1.510			CLEC3B	↑ 1.680
<b>Expr Fold Change ↓</b>					
Molecules	Value	Molecules	Value	Molecules	Value
PF4	↓ -6.667	IGKV3D-20	↓ -5.263	VWF	↓ -5.263
IGHV1-2	↓ -5.263	IGHG2	↓ -5.263	PTX3	↓ -3.704
LCAT	↓ -5.000	HP	↓ -4.167	SAA2	↓ -3.448
KRT9	↓ -5.000	IGHA1	↓ -3.846	CETP	↓ -2.778
F13A1	↓ -5.000	ALB	↓ -3.704	KRT2	↓ -2.703
KRT10	↓ -3.571	IGHG1	↓ -3.333	VCAN	↓ -2.439
IGLV3-21	↓ -3.333	IGLV2-18	↓ -3.226	TNC	↓ -2.381
SLC1A5	↓ -3.226	IGHV3-49	↓ -3.125	LBP	↓ -2.174
IGLV2-18	↓ -2.941	IGHG3	↓ -3.030	APOD	↓ -2.128
IGKV1D-39	↓ -2.857	HPX	↓ -2.632		

Abbreviations: CM, cerebral malaria; FO, fatal outcome; FR, full recovery; NCI, neurocognitive impairment; SMA, severe malarial anaemia

### 5.3.6.2 Pathways, disease, and functions altered by DEPs between SMA FR and CM FR

DEPs between SMA and CM patients that fully recovered without complication were found to activate cellular stress and injury, cellular immune response, and immune system canonical pathway categories in CM FR children (Figure 5.9A). Many proteins were shown to inhibit haemostasis, the immune system and vesicle-mediated transport canonical pathway categories in CM FR compared to SMA FR (Figure 5.9A). Some specific canonical pathways inhibited in CM FR compared to SM FR included binding and uptake of ligands by scavenger receptors, cell surface interactions at the vascular wall, phagocytosis, B cell receptor signalling, interactions between lymphoid and non-lymphoid cells, and neutrophil extracellular signalling (Supplementary Figure 5.3A). The specific canonical pathways activated in CM FR include Class I MHC-mediated antigen processing and presentation, neutrophil degranulation, and S100 family signalling (Supplementary Figure 5.3B).

The most significant diseases and disorders altered by the DEPs in CM FR patients compared to SMA FR patients included dermatological, immunological, and inflammatory disease, organismal injury and abnormalities, and inflammatory response (Table 5.5). The most significant molecular and cellular functions altered were lipid, vitamin, and mineral metabolism, molecular transport, small molecule biochemistry, and post-translational modifications (Table 5.5). The most significant physiological system development and functions that were influenced include the haematological system, immune cell trafficking, humoral immune response, embryonic development, and hair and skin development and function (Table 5.5). Some additional diseases and functions affected in CM FR compared to SMA FR patients were cellular signalling, movement, interaction, growth and proliferation, infectious and haematological diseases, neurological disease, skeletal and muscular system development, function and disorders, developmental disorder, protein trafficking, and nervous system development and function (Supplementary Figure 5.4).

The first network for comparing SMA FR and CM FR illustrated the activation of lipid metabolism, molecular transport, and small molecule biochemistry functions (Figure 5.9B). This activation (orange) occurred in CM FR children when compared to SMA FR due to the variation of 13 molecules, high (red) levels of aggrecan (ACAN), collagen type I alpha one chain (COL1A1), calcium-binding protein A8 and 9 (S100A8 and S100A9 or MRP8 and MRP14 respectively), apolipoprotein A-IV (APOA4), defensin, alpha 1 (DEFA1), serum amyloid A2 (SAA2), low-density lipoprotein receptor (LDLR) platelet factor 4 (PF4 or CXCL4), Lecithin

cholesterol acyltransferase (LCAT), and coagulation factor XIII A (F13A1)). This was accompanied by low (green) levels of cholesteryl ester transfer protein (CETP) and dermcidin (DCD) in CM FR when compared to SMA FR (Figure 5.9B). The second and third networks display inhibition (blue) of cancer, dermatological diseases, developmental disorders, and haematological disease in CM FR children compared to SMA FR due to lower levels of 11 molecules, the immunoglobulin (IG) proteins (IGHVs-5, IGHV1-2, IGHV1-69, IGHV1-69D, IGKV3-11, IGKV1-39, IGKV1D-39, IGLV1-40, IGLV2-18, IGLV3-21, and IGLV6-57 (Figure 5.9C and D). The fourth network showed inhibition of dermatological diseases and conditions, organismal injury and abnormalities, and post-translational modification in CM FR against SMA FR due to lower levels of 5 molecules, cornified envelope protein (CFP) and keratin proteins, KRT2, KRT5, KRT9, and KRT10 (Figure 5.9E). Lastly, the fifth network illustrated the inhibition of amino acid metabolism and molecular transport in CM FR when compared to SMA FR by lower levels of solute carrier family 1 member 5 (SLC1A5) and transferrin receptor (TFRC/CD71) and activation of small molecule biochemistry by higher levels of proteasome subunit alpha type-1 and 4 (PSMA1 and 4) (Figure 5.9F).



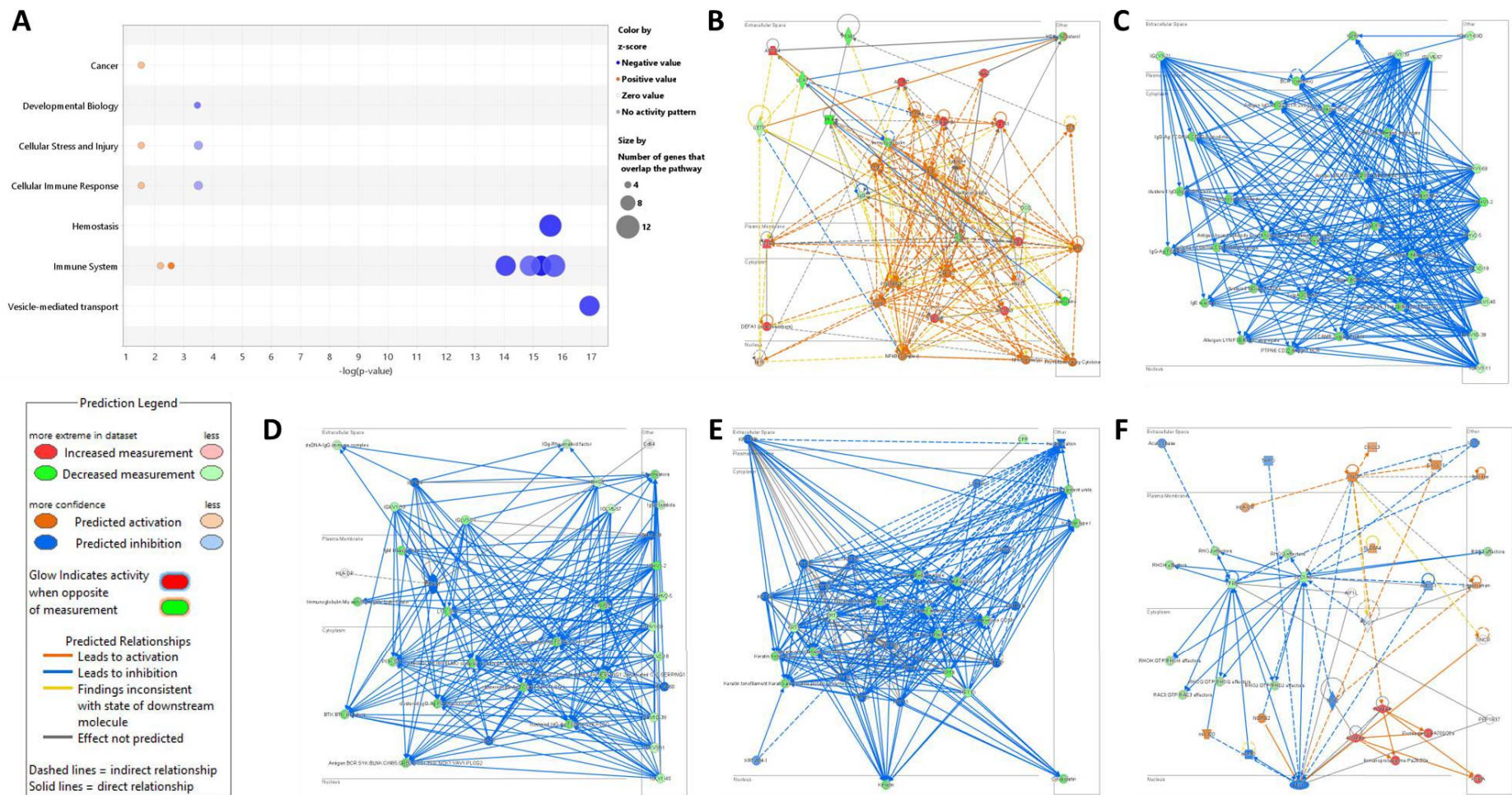


**Figure 5.9** Most significant canonical pathway categories and networks for the comparison between children with severe malarial anaemia and cerebral malaria who fully recovered without complications. Threshold cut-off:  $FDR \leq 1\%$ ,  $|\text{Log}_2\text{Fold Change}| > 1$ , unique peptides  $\geq 2$ , and  $p\text{-value} < 0.001$ . (A) Bubble chart of main canonical pathways. (B-F) Top function networks highlighting the protein expression and predicted activation or inhibition.

**Table 5.5** Top 5 diseases and biological functions that were significantly altered by the differentially expressed proteins

SMA FR vs CM FR			CM FO vs CM FR			SMA FR vs SMA NCI		
Diseases and Disorders								
Name	p-value range	# Molecules	Name	p-value range	# Molecules	Name	p-value range	# Molecules
Dermatological Diseases and Conditions	4.78E-02 - 6.22E-07	13	Inflammatory Response	5.00E-02 - 2.87E-06	14	Infectious Diseases	7.61E-03 - 2.26E-18	22
Immunological Disease	4.44E-02 - 6.22E-07	17	Cardiovascular Disease	4.48E-02 - 9.62E-06	12	Organismal Injury and Abnormalities	1.39E-02 - 2.26E-18	43
Inflammatory Disease	2.80E-02 - 6.22E-07	12	Organismal Injury and Abnormalities	5.00E-02 - 9.62E-06	20	Cardiovascular Disease	1.39E-02 - 1.47E-12	27
Organismal Injury and Abnormalities	4.78E-02 - 6.22E-07	23	Neurological Disease	5.00E-02 - 1.05E-05	15	Hematological Disease	1.28E-02 - 1.47E-12	28
Inflammatory Response	4.78E-02 - 7.25E-06	12	Metabolic Disease	4.87E-02 - 2.85E-05	13	Neurological Disease	1.28E-02 - 2.47E-11	31
<b>Molecular and Cellular Functions</b>			<b>Molecular and Cellular Functions</b>			<b>Molecular and Cellular Functions</b>		
Name	p-value range	# Molecules	Name	p-value range	# Molecules	Name	p-value range	# Molecules
Lipid Metabolism	4.86E-02 - 1.29E-06	5	Cell-To-Cell Signaling and Interaction	4.96E-02 - 2.22E-08	12	Cell-To-Cell Signaling and Interaction	1.39E-02 - 1.66E-13	22
Molecular Transport	4.86E-02 - 1.29E-06	11	Cellular Assembly and Organization	2.00E-02 - 7.65E-08	9	Lipid Metabolism	1.19E-02 - 8.53E-08	19
Small Molecule Biochemistry	4.86E-02 - 1.29E-06	8	Cell Death and Survival	5.00E-02 - 1.28E-06	7	Small Molecule Biochemistry	1.19E-02 - 8.53E-08	24
Vitamin and Mineral Metabolism	2.34E-02 - 3.48E-06	9	Cellular Compromise	3.31E-02 - 2.87E-06	8	Cellular Movement	1.23E-02 - 1.40E-07	18
Post-Translational Modification	1.72E-02 - 5.42E-06	3	Cellular Function and Maintenance	4.61E-02 - 2.87E-06	8	Cell Morphology	1.39E-02 - 2.04E-07	12
<b>Physiological System Development and Function</b>			<b>Physiological System Development and Function</b>			<b>Physiological System Development and Function</b>		
Name	p-value range	# Molecules	Name	p-value range	# Molecules	Name	p-value range	# Molecules
Hematological System Development and Function	4.78E-02 - 7.25E-06	10	Organismal Development	3.18E-02 - 1.05E-05	3	Hematological System Development and Function	1.39E-02 - 2.92E-11	18
Immune Cell Trafficking	4.78E-02 - 1.42E-05	7	Tissue Development	3.18E-02 - 1.05E-05	3	Immune Cell Trafficking	1.25E-02 - 2.92E-11	16
Humoral Immune Response	4.48E-02 - 1.87E-04	4	Hematological System Development and Function	4.96E-02 - 5.20E-05	5	Cardiovascular System Development and Function	1.23E-02 - 5.91E-08	15
Embryonic Development	3.72E-02 - 5.71E-04	8	Immune Cell Trafficking	4.96E-02 - 5.58E-04	5	Organismal Development	9.94E-03 - 5.91E-08	20
Hair and Skin Development and Function	3.72E-02 - 5.71E-04	5	Connective Tissue Development and Function	1.87E-02 - 1.35E-03	2	Organismal Functions	7.96E-03 - 5.29E-07	6

Abbreviations: CM, cerebral malaria; FO, fatal outcome; FR, full recovery; NCI, neurocognitive impairment; SMA, severe malarial anaemia



### 5.3.6.3 Pathways, disease, and functions altered by DEPs between CM FO and CM FR

The DEPs between CM children who died and CM children who fully recovered without complications were found to inhibit pathogen and cytokine signalling, cellular stress, injury, growth, proliferation, and development, cellular immune response, immune system, haemostasis, and vesicle-mediated transport canonical pathway categories in CM FR children (Figure 5.10A). There were only two activated canonical pathway categories, cytokine signalling and cellular immune response, for CM FR and CM FO comparisons (Figure 5.10A). Some specific inhibited canonical pathways in CM FR compared to CM FO included binding and uptake receptors, cell surface interactions at the vascular wall, Fc-gamma receptor-dependent phagocytosis, B cell receptor signalling, lymphoid and non-lymphoid cell interactions, neutrophil extracellular signalling pathway, neutrophil degranulation, and phagosome formation (Supplementary Figure 5.3B). There was only one activated canonical pathway in CM FR comparatively, IL-12 signalling and production in macrophages (Supplementary Figure 5.3B).

The top 5 most significant diseases and disorders predicted to be altered in CM FR compared to CM FO include inflammatory response, cardiovascular disease, organismal injury and abnormalities, neurological disease, and metabolic disease (Table 5.5). The topmost molecular and cellular functions altered in CM FR versus CM FO are cell-to-cell signalling and interaction, cellular assembly and organisation, cell death and survival, cellular compromise and cellular function and maintenance (Table 5.5). The most significant physiological system development and functions for CM FR compared to CM FO are haematological system development and function, immune cell trafficking, humoral immune response, embryonic development, and hair and skin development and function (Table 5.5). Additional significant diseases and functions affected by the DEPs between CM FO and CM FR include amino acid metabolism, psychological disorders, skeletal and muscular disorders, inflammatory disease, infectious diseases, developmental disorders, protein synthesis, cellular growth, proliferation, movement, and signalling, and nervous system development and function (Supplementary Figure 5.5).

There were three most significant networks, the first one illustrating 13 molecules with increased levels of apolipoprotein A-IV (APOA4) and complement factor H-related 5 (CFHR5) affecting neurological disease processes and lower levels of immunoglobulin proteins (IGHG1, IGHG2, IGHG3, IGKV3-11, IGLV2-18, and IGLV1-40), haptoglobin (HP), albumin (ALB),

hemopexin (HPX), lysozyme (LYZ), and retinol-binding protein 4 (RBP4) inhibit cellular assembly and organisation and organismal development in CM FR when compared to CM FO (Figure 5.10B). The second network displayed nine molecules causing some activation of cardiovascular disease, organismal injury and abnormalities, and endocrine system disorder due to the higher levels of aggrecan (ACAN), protein S 1 (PROS1), inter-alpha-trypsin 2 (ITIH2) and lower levels of immunoglobulin kappa variable 1-5 (IGKV1-5), carcinoembryonic antigen-related cell adhesion molecule 8 (CEACAM8), carbonic anhydrase 1 (CA1), neutrophil activation marker (CD177), brain acid soluble protein 1 (BASP1), serum protease inhibitor, clade A [alpha-1 antiproteinase, antitrypsin], member 7 (SERPINA7) in CM FR compared to CM FO (Figure 5.10C). The slight activation in CM FR could indicate that protein levels in CM FO cause more robust activation than CM FR (Figure 5.10C). The third network displayed eight molecules in CM FR when compared to CM FO that inhibited cell-to-cell signalling and interaction, cellular compromise, and cellular function and maintenance by higher levels of aminolevulinic acid dehydratase (ALAD) and lower levels of immunoglobulin proteins (IGKV3D-20, IGKV1-5, IGHA1, IGHA2, IGHV3-49, and IGHV1-69D), and proteasome subunit alpha type-4 (PSMA4) (Figure 5.10D).

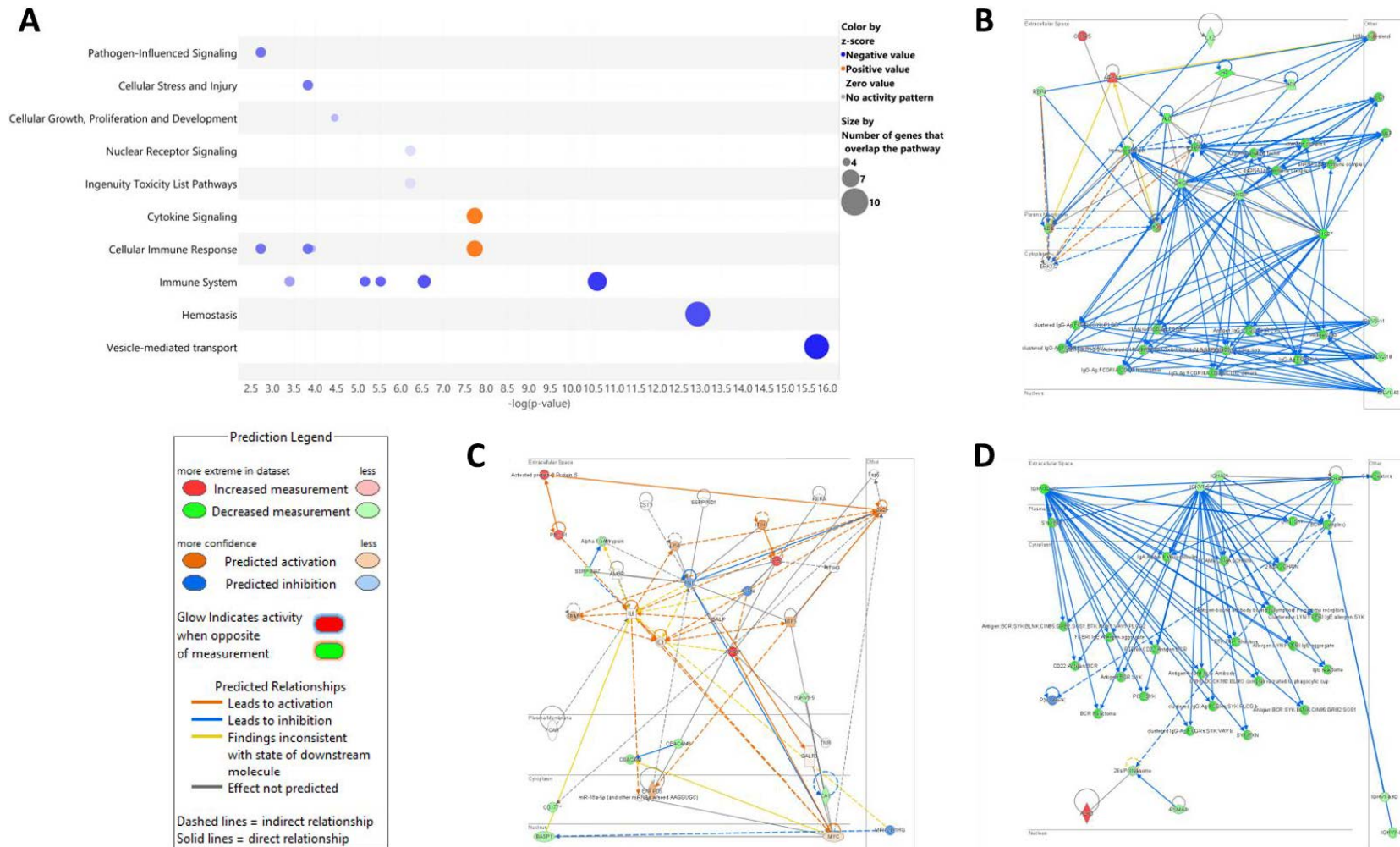


**Figure 5.10** Most significant canonical pathway categories and networks for the comparison between children with cerebral malaria who died and children with cerebral malaria who fully recovered without complications. Threshold cut-off:  $FDR \leq 1\%$ ,  $|\text{Log}_2\text{Fold Change}| > 1$ , unique peptides  $\geq 2$ , and  $p\text{-value} < 0.001$ . (A) Bubble chart of main canonical pathways. (B-D) Top function networks highlighting the protein expression and predicted activation or inhibition.

#### *5.3.6.4 Pathways, disease, and functions altered by DEPs between SMA FR and SMA NCI*

The comparison between SMA FR and SMA NCI showed activation of many pathways and processes in networks similar to the results illustrated above when comparing all five sub-groups. All canonical pathway categories listed for SMA NCI were activated compared to SMA FR, notably the immune response, immune system, haemostasis, cellular growth and development, and nuclear receptor signalling (Figure 5.11A). The inhibited canonical pathway categories include cellular immune response, cytokine signalling and ingenuity toxicity list pathways (Figure 5.11A). Some specific canonical pathways that were activated in SMA NCI when compared to SMA FR are LXR/RXR, DHCR24 signalling, elevated platelet cytosolic Ca<sup>2+</sup> response, complement cascade, neutrophil degranulation, and extracellular trap signalling, clotting cascade, Fcγ receptor-dependent phagocytosis, phagosome formation, S100 Family signalling, and dendritic cell maturation (Supplementary Figure 5.3C). Only two canonical pathways were inhibited: the acute phase response signalling and IL-12 signalling and production in macrophages (Supplementary Figure 5.3C).

Many DEPs that altered diseases and biological function were identified between SMA FR and SMA NCI (Table 5.5). The top 5 most statistically significant diseases and disorders affected by DEPs are infectious diseases, organismal injury and abnormalities, neurological disease, and metabolic disease (Table 5.5). The most significant molecular and cellular functions are cell-to-cell signalling and interaction, lipid metabolism, small molecule biochemistry, cellular movement, and cell morphology (Table 5.5). Lastly, the topmost physiological system development and functions are haematological system development and function, immune cell trafficking, cardiovascular system development and function, organismal development, and organismal function (Table 5.5). Additional diseases and functions affected in SMA NCI compared to SMA FR include haematological disease, skeletal and muscular disorders, psychological disorders, cellular movement, morphology, signalling, growth, proliferation, tissue development, molecular transport, connective tissue disorder, inflammatory and immunological disease, developmental disorder, ophthalmic disease, auditory disease, DNA replication, recombination, and repair, antigen presentation, behaviour, protein synthesis (Supplementary Figure 5.6). Many developments and functions were affected, such as the nervous, skeletal, muscular, respiratory, endocrine, hepatic, and visual systems (Supplementary Figure 5.6).

When compared to SMA FR, the DEPs in SMA NCI children resulted in four activated networks (Figure 5.11). The first network showed activation of infectious diseases, organismal injury and abnormalities, and haematological system development and function by 17 molecules (Figure 5.11B). This was due to higher levels of serum protease inhibitor, clade A [ $\alpha$ -1 antitrypsin, antitrypsin], members 6 and 7 (SERPINA6 and 7), cofilin 1 (CFI), coagulation factor X (F10), apolipoprotein H (APOH), complement C3 (C3), retinol-binding protein 4 (RBP4), kininogen 1 (KNG1), orosomucoid 1 and 2 (ORM1 and 2), transthyretin (TTR),  $\alpha$ -2-HS-glycoprotein (AHSG) in SMA NCI when compared to SMA FR (Figure 5.11B). This was also caused by lower levels of apolipoprotein D (APOD), cholesteryl ester transfer protein (CETP), lipopolysaccharide-binding protein (LBP), Serum amyloid A (SAA2), and versican (VCAN) in SMA NCI when compared to SMA FR (Figure 5.11B). The second network illustrated the activation of cardiovascular disease, organismal injury and abnormalities, cell-to-cell signalling and interaction by 9 DEPs in SMA NCI compared to SMA FR (Figure 5.11C). The activation was caused by higher levels of prothrombin/coagulation factor II (F2),  $\alpha$ -2-glycoprotein 1, zinc-binding (AZGP1), peptidoglycan recognition protein 2 (PGLYRP2), S100 calcium-binding protein A8 and 9 (S100A8 and S100A9), peptidylprolyl isomerase A (PPIA), calmodulin 1 (CALM1), Cofilin 1 (CFL1), and brain acid soluble protein 1 (BASP1) in SMA NCI when compared to SMA FR (Figure 5.11C). The third network interestingly depicts the activation of developmental disorders, hereditary disorders, and immunological disease by nine molecules (Figure 5.11D). This activation was due to higher levels of immunoglobulin proteins (IGKV1D-13 and IGHA1), glutathione peroxidase 3 (GPX3), C-type lectin domain family 3 member B (CLEC3B), complement factor H-related protein 2 (CFHR2), complement component 7 (C7), complement component C8 beta chain (C8b), lactate dehydrogenase A (LDHA) and lower levels of keratin 2 (KRT2) in SMA NCI children compared to SMA FR children (Figure 5.11D). As for the fourth network, cellular assembly and organisation, cell-to-cell signalling and interaction, and haematological system development and function were activated in SMA NCI compared to SMA FR due to 8 DEPs (Figure 5.11E). The activation was caused by increased levels of immunoglobulin proteins (IGHG1, IGHG2, and IGHG4), keratin 16 (KRT16), and  $\beta$ 2 microglobulin (B2M) in SMA NCI compared to SMA FR (Figure 5.11E). Activation was also due to decreased levels of pentraxin 3 (PTX3), tenascin C (TNC), and von Willebrand factor (VWF) in SMA NCI versus SMA FR (Figure 5.11E).

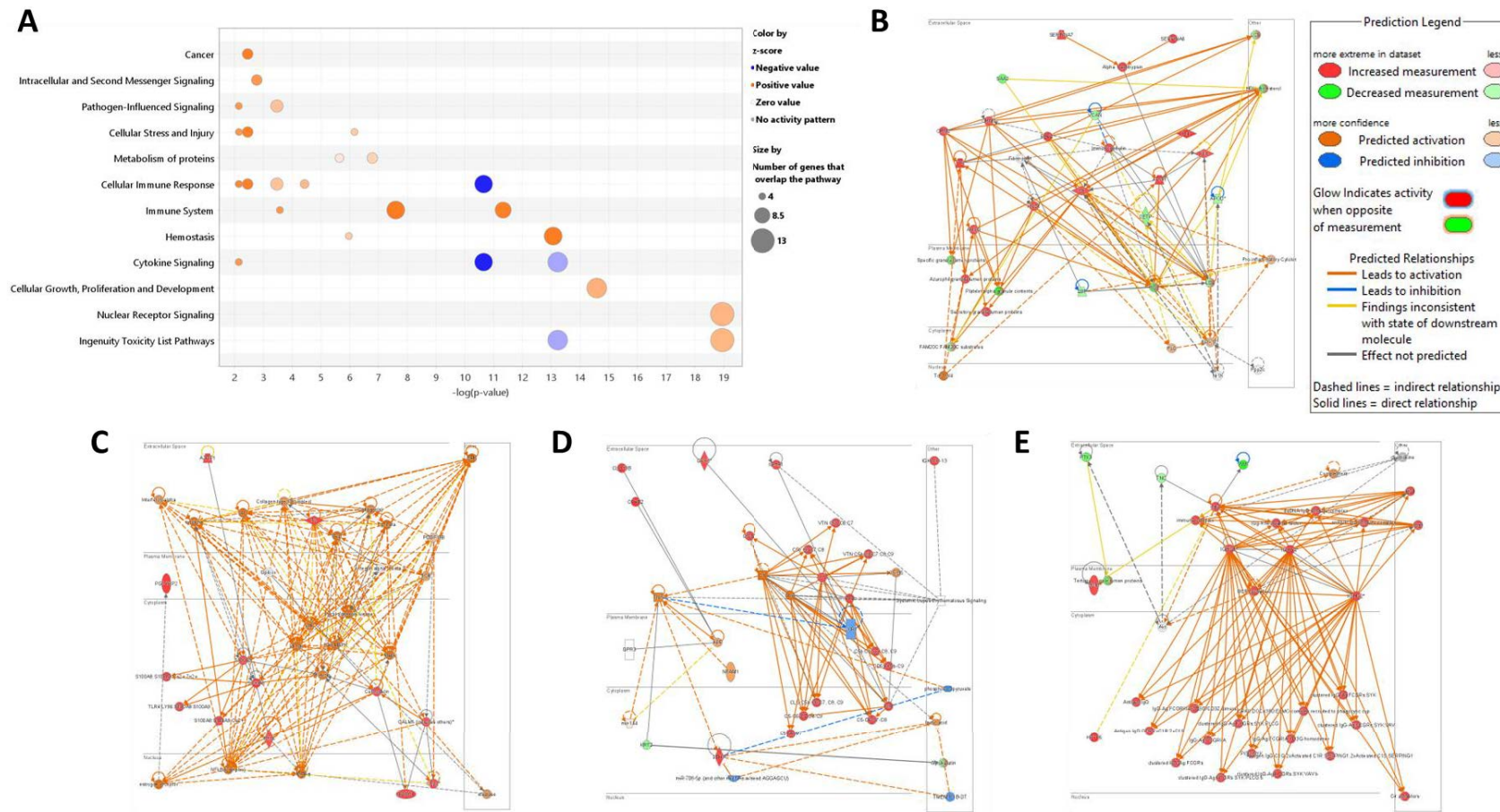


**Figure 5.11** Most significant canonical pathway categories and networks for the comparison between children with severe malarial anaemia who fully recovered without complications and children with severe malarial anaemia who survived but developed neurocognitive impairment. Threshold cut-off: FDR  $\leq 1\%$ ,  $|\text{Log}_2\text{Fold Change}| > 1$ , unique peptides  $\geq 2$ , and  $p\text{-value} < 0.001$ . (A) Bubble chart of main canonical pathways. (B-E) Top function networks highlighting the protein expression and predicted activation or inhibition.

## **5.4 Discussion**

Using high-throughput analysis, this study identified plasma EV proteins in the early stages of severe malaria infection in children for the first time and suggested proteins with prognostic biomarker potential for identifying children at risk of NCI and death. EVs were isolated from small volumes (180  $\mu$ L) of plasma per paediatric patient, and the proteins were isolated and digested for proteome-wide comparison. The technical replicates for all samples were consistent and similar based on the Pearson correlations. After filtering the proteins with specified cut-offs, 420 proteins were common to all patient groups (CC and severe malaria) and could potentially be involved in EV formation and packaging. Overall, more proteins were identified in the severe malaria groups than in the CC group, which could indicate that less activation occurs in the CC group. Interestingly, when comparing the CC group to children with severe malaria, 624 proteins were shared and could be involved in EV formation; only 74 proteins were specific to CC, and 924 were specific to severe malaria. When comparing the three main groups, CC, CM and SMA, the severe malaria groups each had 263 and 216 proteins exclusive to their group, respectively, indicating the possible involvement of pathogenic specific proteins for the individual severe malaria complications.

While identifying biomarkers carried by EVs, the biomolecule interaction was explored, providing insight into crucial roles during disease development. By comparing the proteomic profiles of each patient sub-group (CC, CM FR, CM FO, SMA FR, SMA NCI), 318 DEPs were identified; using stricter cut-offs and IPA mapping, this was narrowed down to 183 DEPs. By comparing children from the neighbouring community (CC), a baseline of activity can be established, and inhibition of immunological and inflammatory processes and proteins was identified (Figure 5.7A). This impairment of immunity has indirectly led to the activation of “infection of Mammalia” disease and organismal death (Figure 5.7A). It has been reported that immunity is weakened when exposed to stressful environments, and the body goes into a dysfunctional immune state, making the person more prone to infection, relapse, and reactivation of infection<sup>64</sup>. In this same study, RNA sequencing on blood samples showed consistent activation of “infection in Mammalia” in healthy adult males deployed in the harsh Antarctic station<sup>64</sup>. This could indicate that healthy children living in the community of malaria

endemic regions were exposed to a stressful environment, leading to a dysfunctional immune state.

The DEPs in patients with CM FR established inhibited immune cell activation, blood clots and platelet adhesion pathways, which could be linked to weakened immunity, allowing the initial infection to worsen in these patients via an increase in parasitaemia without as strong of a pro-inflammatory response compared to children who did not survive CM. Platelets have been shown to mediate iRBC cytoadherence to endothelial cells and enhance iRBC clumping, contributing to pathogenesis<sup>65-68</sup>. Platelets were also reported to induce malaria parasite killing for all major *Plasmodium* species for adult and child human patients naturally infected with malaria<sup>69,70</sup>. A study in Colombia showed that longer illness durations and younger age were associated with severe thrombocytopenia in severe malaria<sup>70</sup>. Thus, inhibiting these blood clot and platelet pathways would cause less sequestration in the microvasculature, leading to fewer haemorrhages and comas; inhibition also allows the parasite to persist and evade platelet killing.

The DEPs in patients with CM FO indirectly activated the LXR/RXR canonical pathway, NR1H3 nuclear receptor, PRDM1 transcriptional regulator, and glomerulonephritis. LXR/RXR system is a crucial regulator of cholesterol, glucose and fatty acid homeostasis and neuroprotection<sup>71-73</sup>. LXR is an inflammation regulator that suppresses inflammatory gene expression in macrophages<sup>74</sup>. When NR1H3, also known as LXRA, is together with LXRβ, they create a subfamily of nuclear receptors that regulate lipid homeostasis, innate immunity and inflammation at the genomic level<sup>75</sup>. PRDM1, conversely, regulates B and T cell differentiation, playing a critical role in immunosuppression, and studies have shown its prognostic values across many different cancer types<sup>76</sup>. In malaria, PRDM1/BLIMP1 is induced by IL-12 and is associated with Type 1 regulatory cell development. It is thought to prevent pathology while allowing parasite persistence by suppressing the Th1 response. It is also highly expressed in asymptomatic Ugandan children, providing protection once infected<sup>77-79</sup>. Glomerulonephritis was also predicted to occur, which can be triggered by Th1 or Th2 response<sup>80</sup>. The outcome of *Plasmodium* infection is determined by the balance between anti- and pro-inflammatory immune responses<sup>81</sup>. A weaker pro-inflammatory response can result in uncontrolled parasite replication and excessive pro-inflammatory response, leading to tissue damage and severe malaria syndromes such as CM and multi-organ failure<sup>81</sup>.



Likewise, the DEPs in patients with SMA FR were associated with an inhibited immune response, stopping phagocytosis in the vasculature, endothelial cell death and development, and vascular cell development, likely allowing the infection to persist. We also identified EV proteins involved in liver inflammation, which is commonly associated with severe malaria infection and allows for protection against the liver stage of malaria parasites<sup>82-84</sup>.

As mentioned above, the DEPs in EVs from patients with CM FR were associated with an inhibition of platelet adhesion; the opposite was found for the DEPs in EVs from patients with SMA NCI. The DEPs were related to immune response activation, vascular cell proliferation, platelet adhesion, calcium ion flux, and kidney cell death. The activation of blood platelet adhesion would allow for increased sequestration and kill parasites in circulation. Calcium ion activation is also essential as it is associated with parasite development, locomotion, fertilisation and host cell infection<sup>85</sup>. During severe malaria infection, apoptosis in cells from vital organs such as the kidneys has been documented, and during anaemia onset, an acute kidney injury, regardless of parasite load, provides a mechanism of iron-recycling salvage pathways<sup>86,87</sup>.

Three clinically significant comparisons of severe malaria outcomes include SMA FR vs CM FR, CM FO vs CM FR, and SMA FR vs SMA NCI, as our work aimed to identify prognostic biomarkers for the outcome of severe malaria. The comparison between patients with SMA who fully recovered and those who developed NCI had the highest number of DEPs, indicating unique pathways and functions occurring in SMA NCI children. Out of the total 94 DEPs, 19 proteins appeared to be of particular interest, as five proteins differentiated SMA FR from CM FR and SMA NCI, eight differentiated CM FR from SMA FR and CM FO, and six distinguished the more severe outcomes, SMA NCI and CM FO from SMA FR and CM FR, respectively.

Overall, the children with CM FR, based on their EV content, which can mirror the parent cell, had weaker immunity compared to children with SMA FR and CM FO as they had a less active immune system and response and vesicle-mediated transport for cellular communication caused by the GEPs: elevated relative abundance of ACAN and APOA4, and lower relative abundance of IGHG3, IGHV1-69D, IGKV3-11, IGLV1-40, IGLV2-18 in children with CM FR, and PSMA4 is relatively higher in children with CM FO and lower in children with SMA FR when compared to children who fully recovered without complications (Figure 5.6A, 5.6D, and 5.9-5.11A, and Supplementary Table 5.1). This indicates that the DEPs in CM FR are predicted to alter the immune and inflammatory responses. DEPs in plasma EVs from children with CM FR

were associated with the activation of the immune response, such as cytokine signalling, compared to CM FO, specifically macrophage production of IL-12 signalling (Figure 5.10A and Supplementary Figure 5.3B). IL-12 is a pro-inflammatory cytokine produced by dendritic cells, neutrophils and macrophages and is part of the adaptive immune response by stimulating the proliferation of Th1 cells. The levels of IL-12 are associated with systemic inflammation and vascular dysfunction and may be a predictor of acute malaria infection. However, there are conflicting findings regarding the abundance of IL-12 and severe malaria<sup>88</sup>.

The EVs from children with SMA FR had a more active immune response than CM FR but much less than SMA NCI, where many inflammatory pathways were activated (Figure 5.11A and Supplementary Figure 5.3C). These differences can potentially be set apart with five proteins: higher relative abundance of CETP and KRT2, lower relative abundance of S100A8 and S100A9, and relatively higher amounts of SAA2 in children with CM FR and relatively lower amounts in children with SMA NCI, both when compared to children with SMA FR. The alarmins S100A8 and S100A9 were associated with infection-mediated inflammation, and in malaria, they are expressed by monocytes and reduce the expression of MHC class II antigen-presenting molecules<sup>79</sup>. In a murine model of CM where plasma EVs were analysed, increased amounts of S100A8 were associated with CM infection, which is also seen here as S100A8 and 9 were both higher in CM FR and SMA NCI compared to SMA FR<sup>56</sup>.

Another area of interest was determining whether EVs carried proteins that could predict severe malaria outcomes such as NCI and death. This study found six proteins that could act as neurological or deadly malaria markers: BASP1, IGHA1, IGHG1, IGHG2, RBP4, and SERPINA7. All six proteins were involved with inflammatory and immune system activity. In the brain, BASP1 is involved in brain development; however, in disease, BASP1 has been associated with poor cancer prognosis and endothelial apoptosis in diabetes<sup>89-91</sup>. This could indicate BASP1 as a marker for host injury due to inflammation, as indicated by the IPA predictions.

Research has shown a close relation between apolipoproteins and tau in the modulation of neurological disruption in patients with Alzheimer's disease, with apolipoprotein also being a potential marker of Alzheimer's disease in CSF and plasma<sup>92-94</sup>. Across the three clinically relevant comparisons, differentially expressed apolipoproteins were identified, of which children with SMA NCI had significantly lower relative levels of apolipoprotein D and significantly higher relative levels of apolipoprotein H compared to children who fully

recovered from SMA. This could indicate an association between these two apolipoproteins and worse cognitive outcomes; however, much more research is required.

It is interesting to see these differences reflected in the plasma EV cargo during early responses to malaria infection, as this may indicate pre-determined outcomes of severe malaria early on in infection depending on the individual's pathological response to infection. This study identified many proteins with predictive potential for each sub-group of severe malaria outcomes. Due to the complex pathogenesis involved in malaria development, multiple proteins should be combined into a panel to work as functional prognostic biomarkers and used to predict severe malaria outcomes.

## **Acknowledgements**

We are grateful to the children and their parents or guardians who participated in this study. We thank the study teams at Mulago Hospital, Makerere University, and the University of Minnesota for their commitment to treating the children and collecting the data.

## **Authors' contributions**

**Iris S. Cheng:** conceptualisation; investigation; methodology; data curation; formal analysis; validation; software; writing-original draft; writing-review & editing. **Robert O. Opoka:** writing-review & editing. **Natalia Tiberti:** writing-review & editing. **Paul Bangirana:** writing-review & editing. **Chandy C. John:** writing-review & editing. **Valery Combes:** conceptualisation; funding acquisition; project administration; supervision; visualisation; writing-review & editing.

## **Competing interests**

The authors declare no competing interests.

## **Availability of data and material**

The data supporting this study's findings are available from the corresponding author upon reasonable request.

## 5.5 References

1. World Health Organization. *World malaria report 2022*. Geneva: World Health Organization; Licence:CC BY-NC-SA 3.0 IGO. <https://www.who.int/publications/i/item/9789240064898> (2022).
2. Winskill, P. *et al.* Estimating the burden of severe malarial anaemia and access to hospital care in East Africa. *Nat. Commun.* **14**, 5691 (2023).
3. Taylor, C., Namaste, S. M. L., Lowell, J., Useem, J. & Yé, Y. Estimating the Fraction of Severe Malaria among Malaria-Positive Children: Analysis of Household Surveys in 19 Malaria-Endemic Countries in Africa. *Am. J. Trop. Med. Hyg.* **104**, 1375–1382 (2021).
4. World Health Organization. *World malaria report 2019*. Geneva: World Health Organization; Licence:CC BY-NC-SA 3.0 IGO. <https://www.who.int/publications/i/item/9789241565721> (2019).
5. White, N. J. Anaemia and malaria. *Malar. J.* **17**, 371 (2018).
6. Severe malaria. *Trop. Med. Int. Health* **19 Suppl 1**, 7–131 (2014).
7. White, N. J. Severe malaria. *Malar. J.* **21**, 284 (2022).
8. Rosa-Gonçalves, P., Ribeiro-Gomes, F. L. & Daniel-Ribeiro, C. T. Malaria related neurocognitive deficits and behavioral alterations. *Front. Cell. Infect. Microbiol.* **12**, 829413 (2022).
9. Tunon-Ortiz, A. & Lamb, T. J. Blood brain barrier disruption in cerebral malaria: Beyond endothelial cell activation. *PLoS Pathog.* **15**, e1007786 (2019).
10. Bruneel, F. Human cerebral malaria: 2019 mini review. *Rev Neurol (Paris)* **175**, 445–450 (2019).
11. Bangirana, P. *et al.* Severe malarial anemia is associated with long-term neurocognitive impairment. *Clin. Infect. Dis.* **59**, 336–344 (2014).
12. Bangirana, P. *et al.* Neurocognitive domains affected by cerebral malaria and severe malarial anemia in children. *Learn. Individ. Differ.* **46**, 38–44 (2016).

13. Nakitende, A. J. *et al.* Severe malaria and academic achievement. *Pediatrics* **151**, (2023).
14. Kooko, R., Wafula, S. & Orishaba, P. Socio-economic determinants of malaria prevalence among under five children in Uganda: Evidence from 2018-19 Uganda malaria indicator survey. *J. Vector Borne Dis.* **0**, 0 (2022).
15. Okitawutshu, J. *et al.* Key factors predicting suspected severe malaria case management and health outcomes: an operational study in the Democratic Republic of the Congo. *Malar. J.* **21**, 274 (2022).
16. Dalko, E. *et al.* Erythropoietin Levels Increase during Cerebral Malaria and Correlate with Heme, Interleukin-10 and Tumor Necrosis Factor-Alpha in India. *PLoS ONE* **11**, e0158420 (2016).
17. Casals-Pascual, C. *et al.* High levels of erythropoietin are associated with protection against neurological sequelae in African children with cerebral malaria. *Proc Natl Acad Sci USA* **105**, 2634–2639 (2008).
18. Phiri, H. T. *et al.* Elevated plasma von Willebrand factor and propeptide levels in Malawian children with malaria. *PLoS ONE* **6**, e25626 (2011).
19. Hollestelle, M. J. *et al.* von Willebrand factor propeptide in malaria: evidence of acute endothelial cell activation. *Br. J. Haematol.* **133**, 562–569 (2006).
20. Bridges, D. J. *et al.* Rapid activation of endothelial cells enables Plasmodium falciparum adhesion to platelet-decorated von Willebrand factor strings. *Blood* **115**, 1472–1474 (2010).
21. Oluboyo, A. O., Chukwu, S. I., Oluboyo, B. O. & Odewusi, O. O. Evaluation of Angiopoietins 1 and 2 in Malaria-Infested Children. *J. Environ. Public Health* **2020**, 2169763 (2020).
22. Conroy, A. L. *et al.* Whole blood angiopoietin-1 and -2 levels discriminate cerebral and severe (non-cerebral) malaria from uncomplicated malaria. *Malar. J.* **8**, 295 (2009).
23. Thakur, K., Vareta, J., Carson, K., Taylor, T. & Sullivan, D. Performance of Cerebrospinal Fluid (CSF) Plasmodium Falciparum Histidine-Rich Protein-2 (pfHRP-2) in Prediction of Death in Cerebral Malaria (I10-2.005). (2014).
24. Adukpo, S. *et al.* High plasma levels of soluble intercellular adhesion molecule (ICAM)-1 are associated with cerebral malaria. *PLoS ONE* **8**, e84181 (2013).

25. Chiabi, A. *et al.* Severe malaria in Cameroon: Pattern of disease in children at the Yaounde Gynaeco-Obstetric and Pediatric hospital. *J. Infect. Public Health* **13**, 1469–1472 (2020).
26. Samudra, N., Lane-Donovan, C., VandeVrede, L. & Boxer, A. L. Tau pathology in neurodegenerative disease: disease mechanisms and therapeutic avenues. *J. Clin. Invest.* **133**, (2023).
27. Zhang, Y., Wu, K.-M., Yang, L., Dong, Q. & Yu, J.-T. Tauopathies: new perspectives and challenges. *Mol. Neurodegener.* **17**, 28 (2022).
28. Kiani, L. Disease-specific modifications of tau protein. *Nat. Rev. Neurol.* **19**, 459 (2023).
29. Zhang, X. *et al.* Tau pathology in parkinson's disease. *Front. Neurol.* **9**, 809 (2018).
30. Gonzalez-Ortiz, F. *et al.* Brain-derived tau: a novel blood-based biomarker for Alzheimer's disease-type neurodegeneration. *Brain* **146**, 1152–1165 (2023).
31. Medana, I. M., Idro, R. & Newton, C. R. J. C. Axonal and astrocyte injury markers in the cerebrospinal fluid of Kenyan children with severe malaria. *J. Neurol. Sci.* **258**, 93–98 (2007).
32. Datta, D. *et al.* Elevated Cerebrospinal Fluid Tau Protein Concentrations on Admission Are Associated With Long-term Neurologic and Cognitive Impairment in Ugandan Children With Cerebral Malaria. *Clin. Infect. Dis.* **70**, 1161–1168 (2020).
33. Datta, D. *et al.* Association of Plasma Tau With Mortality and Long-term Neurocognitive Impairment in Survivors of Pediatric Cerebral Malaria and Severe Malarial Anemia. *JAMA Netw. Open* **4**, e2138515 (2021).
34. Conroy, A. L. *et al.* Cerebrospinal fluid biomarkers provide evidence for kidney-brain axis involvement in cerebral malaria pathogenesis. *Front. Hum. Neurosci.* **17**, 1177242 (2023).
35. Jain, V., Thomas, T., Basak, S., Sharma, R. K. & Singh, N. Sequential dysregulated plasma levels of angiopoietins (ANG-2 and ratios of ANG-2/ANG-1) are associated with malaria severity and mortality among hospital admitted cases in South Bastar Region of Chhattisgarh, Central India. *Pathog. Glob. Health* **116**, 47–58 (2022).
36. Ouma, B. J. *et al.* Endothelial activation, acute kidney injury, and cognitive impairment in pediatric severe malaria. *Crit. Care Med.* **48**, e734–e743 (2020).

37. Ouma, B. J. *et al.* Plasma angiopoietin-2 is associated with age-related deficits in cognitive subscales in Ugandan children following severe malaria. *Malar. J.* **20**, 17 (2021).
38. Varo, R. *et al.* Adjunctive therapy for severe malaria: a review and critical appraisal. *Malar. J.* **17**, 47 (2018).
39. Doyle, L. M. & Wang, M. Z. Overview of extracellular vesicles, their origin, composition, purpose, and methods for exosome isolation and analysis. *Cells* **8**, (2019).
40. Liu, Y.-J. & Wang, C. A review of the regulatory mechanisms of extracellular vesicles-mediated intercellular communication. *Cell Commun. Signal.* **21**, 77 (2023).
41. Babatunde, K. A. *et al.* Role of extracellular vesicles in cellular cross talk in malaria. *Front. Immunol.* **11**, 22 (2020).
42. Opadokun, T. & Rohrbach, P. Extracellular vesicles in malaria: an agglomeration of two decades of research. *Malar. J.* **20**, 442 (2021).
43. Opadokun, T., Agyapong, J. & Rohrbach, P. Protein Profiling of Malaria-Derived Extracellular Vesicles Reveals Distinct Subtypes. *Membranes (Basel)* **12**, (2022).
44. Regev-Rudzki, N. *et al.* Cell-cell communication between malaria-infected red blood cells via exosome-like vesicles. *Cell* **153**, 1120–1133 (2013).
45. Abou Karam, P. *et al.* Malaria parasites release vesicle subpopulations with signatures of different destinations. *EMBO Rep.* **23**, e54755 (2022).
46. De Sousa, K. P. *et al.* Proteomic identification of the contents of small extracellular vesicles from in vivo *Plasmodium yoelii* infection. *Int. J. Parasitol.* **52**, 35–45 (2022).
47. Armijos-Jaramillo, V., Mosquera, A., Rojas, B. & Tejera, E. The search for molecular mimicry in proteins carried by extracellular vesicles secreted by cells infected with *Plasmodium falciparum*. *Commun. Integr. Biol.* **14**, 212–220 (2021).
48. Toda, H. *et al.* Plasma-derived extracellular vesicles from *Plasmodium vivax* patients signal spleen fibroblasts via NF- $\kappa$ B facilitating parasite cytoadherence. *Nat. Commun.* **11**, 2761 (2020).



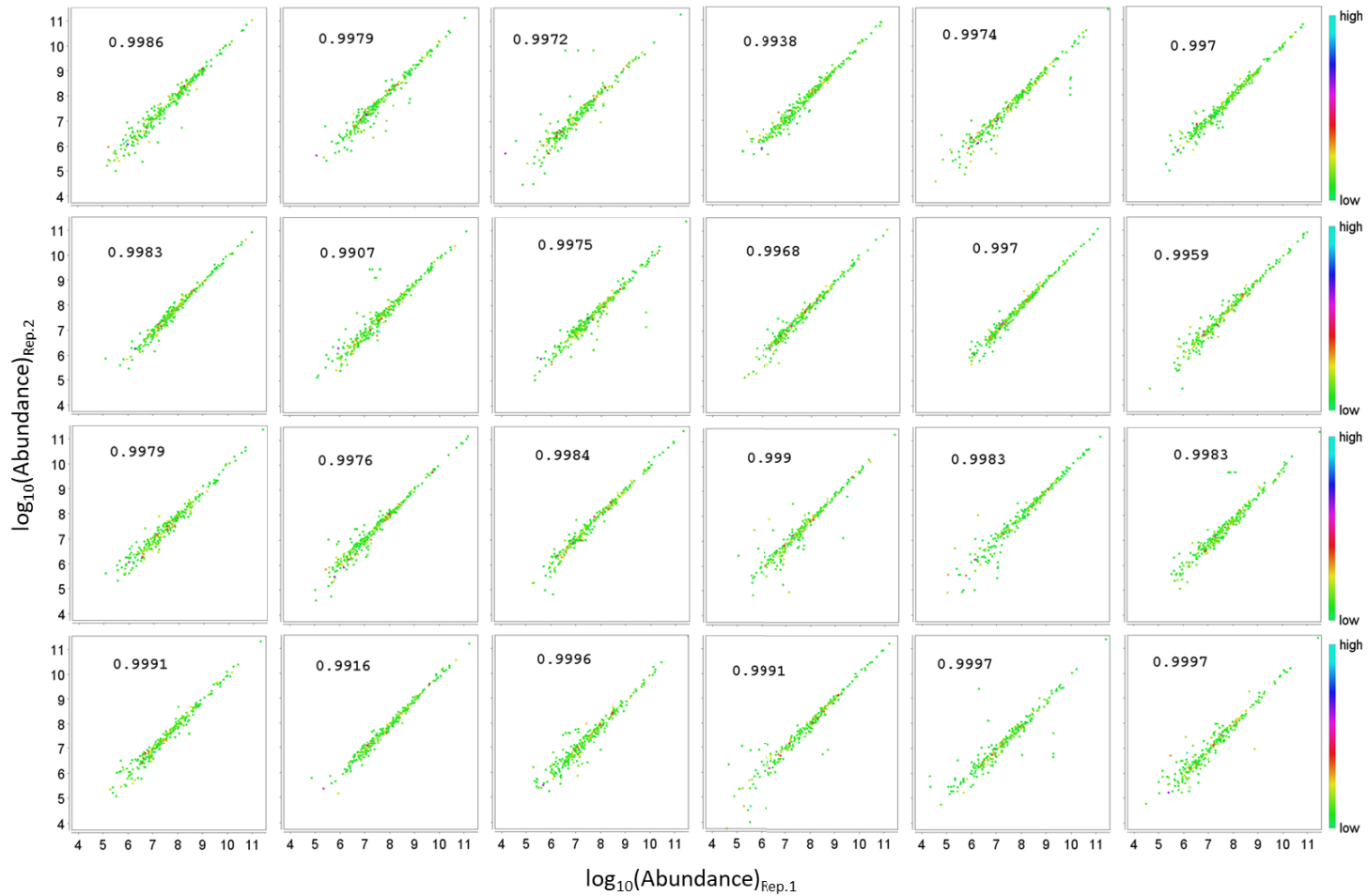
49. Mantel, P.-Y. & Marti, M. The role of extracellular vesicles in Plasmodium and other protozoan parasites. *Cell. Microbiol.* **16**, 344–354 (2014).
50. Antwi-Baffour, S. *et al.* Plasma mEV levels in Ghanaian malaria patients with low parasitaemia are higher than those of healthy controls, raising the potential for parasite markers in mEVs as diagnostic targets. *J. Extracell. Vesicles* **9**, 1697124 (2020).
51. Jung, A. L. *et al.* Surface proteome of plasma extracellular vesicles as mechanistic and clinical biomarkers for malaria. *Infection* **51**, 1491–1501 (2023).
52. Shabani, E. *et al.* High plasma erythropoietin levels are associated with prolonged coma duration and increased mortality in children with cerebral malaria. *Clin. Infect. Dis.* **60**, 27–35 (2015).
53. Bangirana, P. *et al.* Malaria with neurological involvement in Ugandan children: effect on cognitive ability, academic achievement and behaviour. *Malar. J.* **10**, 334 (2011).
54. John, C. C. *et al.* Cerebral malaria in children is associated with long-term cognitive impairment. *Pediatrics* **122**, e92-9 (2008).
55. Idro, R., Marsh, K., John, C. C. & Newton, C. R. J. Cerebral malaria: mechanisms of brain injury and strategies for improved neurocognitive outcome. *Pediatr. Res.* **68**, 267–274 (2010).
56. Tiberti, N. *et al.* Exploring experimental cerebral malaria pathogenesis through the characterisation of host-derived plasma microparticle protein content. *Sci. Rep.* **6**, 37871 (2016).
57. Comelli, L. *et al.* Characterization of secreted vesicles from vascular smooth muscle cells. *Mol. Biosyst.* **10**, 1146–1152 (2014).
58. Heberle, H., Meirelles, G. V., da Silva, F. R., Telles, G. P. & Minghim, R. InteractiVenn: a web-based tool for the analysis of sets through Venn diagrams. *BMC Bioinformatics* **16**, 169 (2015).
59. Oliveros, J. C. Venny 2.1.0. An interactive tool for comparing lists with Venn's diagrams. *Venny 2007-2015* <https://bioinfo.gp.cnb.csic.es/tools/venny/index.html> (2015).
60. Fernandez, N. F. *et al.* Clustergrammer, a web-based heatmap visualization and analysis tool for high-dimensional biological data. *Sci. Data* **4**, 170151 (2017).

61. Krämer, A., Green, J., Pollard, J. & Tugendreich, S. Causal analysis approaches in Ingenuity Pathway Analysis. *Bioinformatics* **30**, 523–530 (2014).
62. Fernandez-Becerra, C. *et al.* Naturally-acquired humoral immune responses against the N- and C-termini of the Plasmodium vivax MSP1 protein in endemic regions of Brazil and Papua New Guinea using a multiplex assay. *Malar. J.* **9**, 29 (2010).
63. Borre, M. B. *et al.* Primary structure and localization of a conserved immunogenic Plasmodium falciparum glutamate rich protein (GLURP) expressed in both the preerythrocytic and erythrocytic stages of the vertebrate life cycle. *Mol. Biochem. Parasitol.* **49**, 119–131 (1991).
64. Buchheim, J.-I. *et al.* Exploratory RNA-seq analysis in healthy subjects reveals vulnerability to viral infections during a 12- month period of isolation and confinement. *Brain Behav. Immun. Health* **9**, 100145 (2020).
65. O’Sullivan, J. M., Preston, R. J. S., O’Regan, N. & O’Donnell, J. S. Emerging roles for hemostatic dysfunction in malaria pathogenesis. *Blood* **127**, 2281–2288 (2016).
66. Pain, A. *et al.* Platelet-mediated clumping of Plasmodium falciparum-infected erythrocytes is a common adhesive phenotype and is associated with severe malaria. *Proc Natl Acad Sci USA* **98**, 1805–1810 (2001).
67. Francischetti, I. M. B., Seydel, K. B. & Monteiro, R. Q. Blood coagulation, inflammation, and malaria. *Microcirculation* **15**, 81–107 (2008).
68. Faille, D. *et al.* Platelet-endothelial cell interactions in cerebral malaria: the end of a cordial understanding. *Thromb. Haemost.* **102**, 1093–1102 (2009).
69. Kho, S. *et al.* Platelets kill circulating parasites of all major Plasmodium species in human malaria. *Blood* **132**, 1332–1344 (2018).
70. Martínez-Salazar, E. L. & Tobón-Castaño, A. Platelet profile is associated with clinical complications in patients with vivax and falciparum malaria in Colombia. *Rev. Soc. Bras. Med. Trop.* **47**, 341–349 (2014).
71. Baranowski, M. Biological role of liver X receptors. *J. Physiol. Pharmacol.* **59 Suppl 7**, 31–55 (2008).

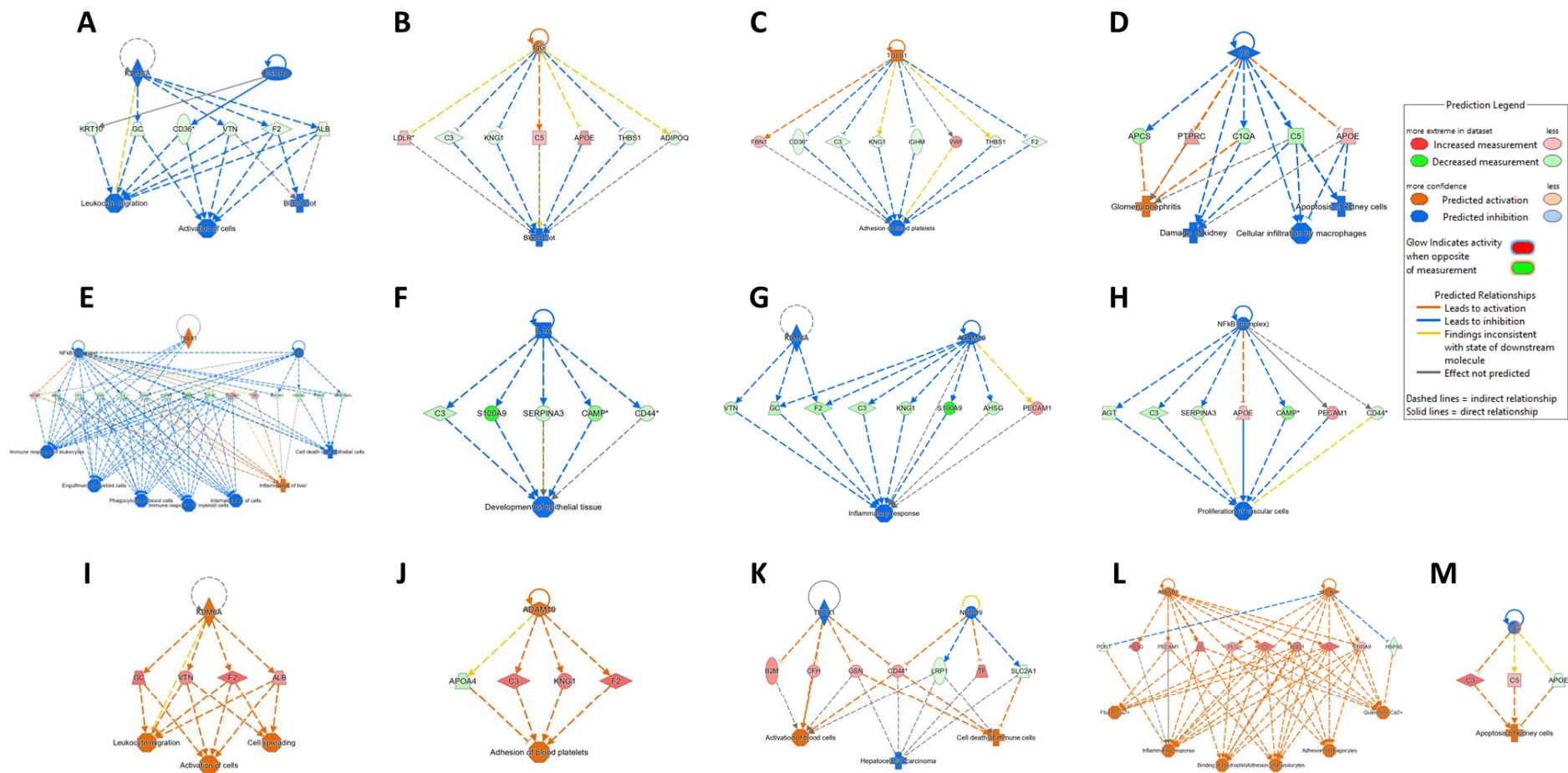
72. Laffitte, B. A. *et al.* Activation of liver X receptor improves glucose tolerance through coordinate regulation of glucose metabolism in liver and adipose tissue. *Proc Natl Acad Sci USA* **100**, 5419–5424 (2003).
73. Cermenati, G. *et al.* Diabetes-induced myelin abnormalities are associated with an altered lipid pattern: protective effects of LXR activation. *J. Lipid Res.* **53**, 300–310 (2012).
74. Ramírez, C. M. *et al.* Crosstalk Between LXR and Caveolin-1 Signaling Supports Cholesterol Efflux and Anti-Inflammatory Pathways in Macrophages. *Front Endocrinol (Lausanne)* **12**, 635923 (2021).
75. Wang, Z. *et al.* Nuclear receptor NR1H3 in familial multiple sclerosis. *Neuron* **90**, 948–954 (2016).
76. Shen, L. *et al.* Role of PRDM1 in Tumor Immunity and Drug Response: A Pan-Cancer Analysis. *Front. Pharmacol.* **11**, 593195 (2020).
77. Kiro Singh, A. S. *et al.* Malaria-specific Type 1 regulatory T cells are more abundant in first pregnancies and associated with placental malaria. *EBioMedicine* **95**, 104772 (2023).
78. Boyle, M. J. *et al.* The Development of Plasmodium falciparum-Specific IL10 CD4 T Cells and Protection from Malaria in Children in an Area of High Malaria Transmission. *Front. Immunol.* **8**, 1329 (2017).
79. Dooley, N. L. *et al.* Single cell transcriptomics shows that malaria promotes unique regulatory responses across multiple immune cell subsets. *Nat. Commun.* **14**, 7387 (2023).
80. Silva, G. B. da, Pinto, J. R., Barros, E. J. G., Farias, G. M. N. & Daher, E. D. F. Kidney involvement in malaria: an update. *Rev. Inst. Med. Trop. Sao Paulo* **59**, e53 (2017).
81. Kumar, R., Ng, S. & Engwerda, C. The Role of IL-10 in Malaria: A Double Edged Sword. *Front. Immunol.* **10**, 229 (2019).
82. Grand, M. *et al.* Hepatic inflammation confers protective immunity against liver stages of malaria parasite. *Front. Immunol.* **11**, 585502 (2020).
83. Jain, A., Kaushik, R. & Kaushik, R. M. Malarial hepatopathy: Clinical profile and association with other malarial complications. *Acta Trop.* **159**, 95–105 (2016).

84. Fazil, A. *et al.* Clinical profile and complication of malaria hepatopathy. *J. Infect. Public Health* **6**, 383–388 (2013).
85. de Oliveira, L. S. *et al.* Calcium in the backstage of malaria parasite biology. *Front. Cell. Infect. Microbiol.* **11**, 708834 (2021).
86. Wichapoon, B., Punsawad, C. & Viriyavejakul, P. Expression of cleaved caspase-3 in renal tubular cells in Plasmodium falciparum malaria patients. *Nephrology (Carlton)* **22**, 79–84 (2017).
87. Wu, Q. *et al.* Renal control of life-threatening malarial anemia. *Cell Rep.* **42**, 112057 (2023).
88. Wilairatana, P., Kwankaew, P., Kotepui, K. U. & Kotepui, M. Low Interleukin-12 Levels concerning Severe Malaria: A Systematic Review and Meta-Analysis. *Int. J. Environ. Res. Public Health* **19**, (2022).
89. Manganas, L. N. *et al.* BASP1 labels neural stem cells in the neurogenic niches of mammalian brain. *Sci. Rep.* **11**, 5546 (2021).
90. Sun, F. *et al.* BASP1 promotes high glucose-induced endothelial apoptosis in diabetes via activation of EGFR signaling. *J. Diabetes Investig.* **14**, 535–547 (2023).
91. Li, Y., Wu, T., Jiao, Z. & Yang, A. BASP1 is up-regulated in tongue squamous cell carcinoma and associated with a poor prognosis. *Asian J. Surg.* **45**, 1101–1106 (2022).
92. Song, F. *et al.* Plasma apolipoprotein levels are associated with cognitive status and decline in a community cohort of older individuals. *PLoS ONE* **7**, e34078 (2012).
93. Picard, C. *et al.* Apolipoprotein B is a novel marker for early tau pathology in Alzheimer's disease. *Alzheimers Dement* **18**, 875–887 (2022).
94. Liu, C.-C. *et al.* Tau and apolipoprotein E modulate cerebrovascular tight junction integrity independent of cerebral amyloid angiopathy in Alzheimer's disease. *Alzheimers Dement* **16**, 1372–1383 (2020).

## 5.6 Supplementary data



**Supplementary Figure 5.1** Pearson correlation plots depicting the relationship between technical replicates of patient sample. Numbers in the plots represent the r-value, all patient samples have an r-value greater than 0.99.

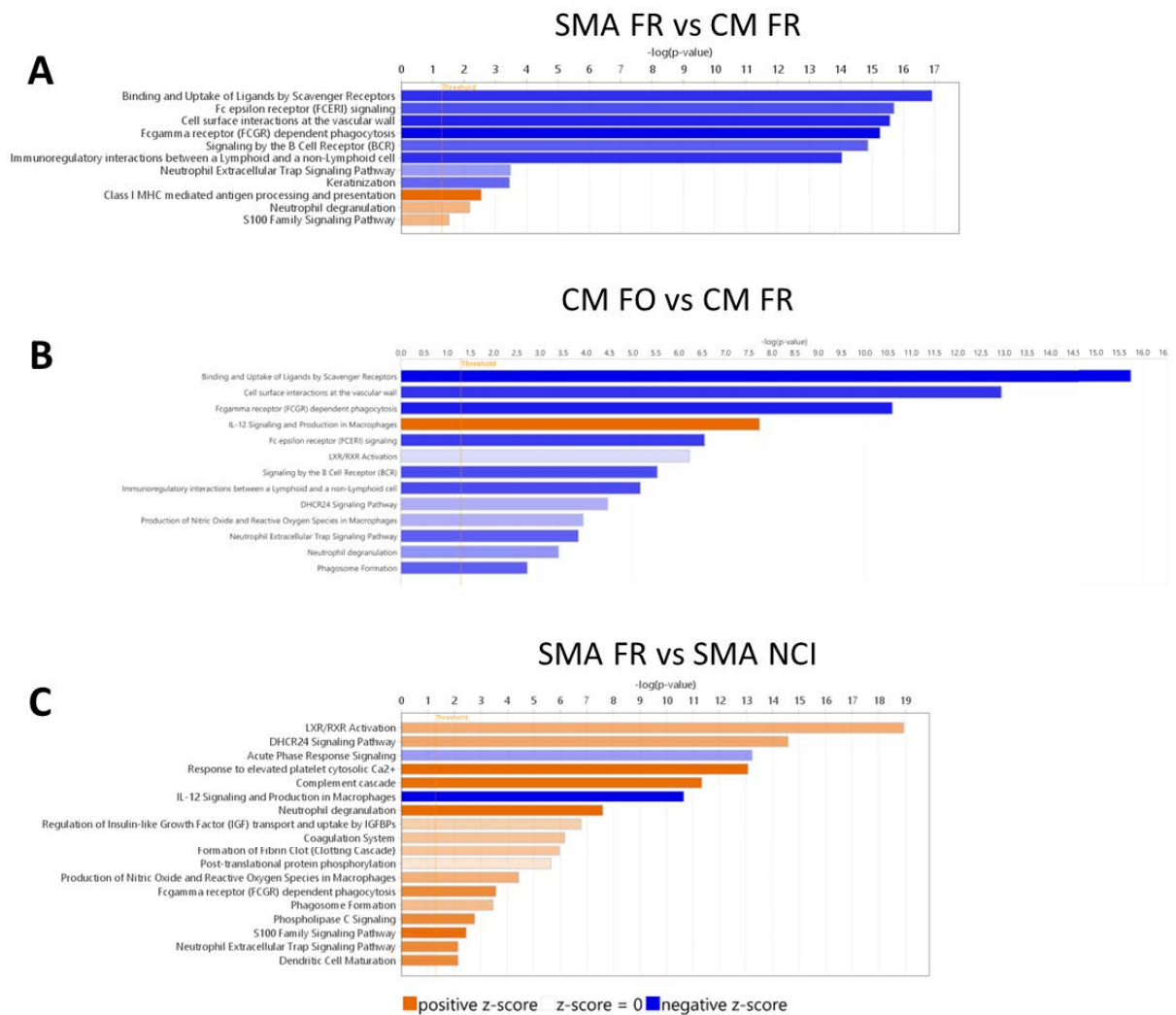


**Supplementary Figure 5.2** Predicted up- and downstream regulators using Ingenuity Pathway Analysis. Threshold cut-offs were set to FDR  $\leq$  1%, unique peptides  $\geq$  2, p-value  $<$  0.001. Depiction of inhibited networks and their regulators for (A-C) CM FR, (D) CM FO, and (E-H) SMA FR. (I-M) Portrayal of activated networks and their regulators for the SMA NCI sub-group.

## Supplementary Table 5.1 List of all differentially expressed proteins for the clinically relevant comparisons

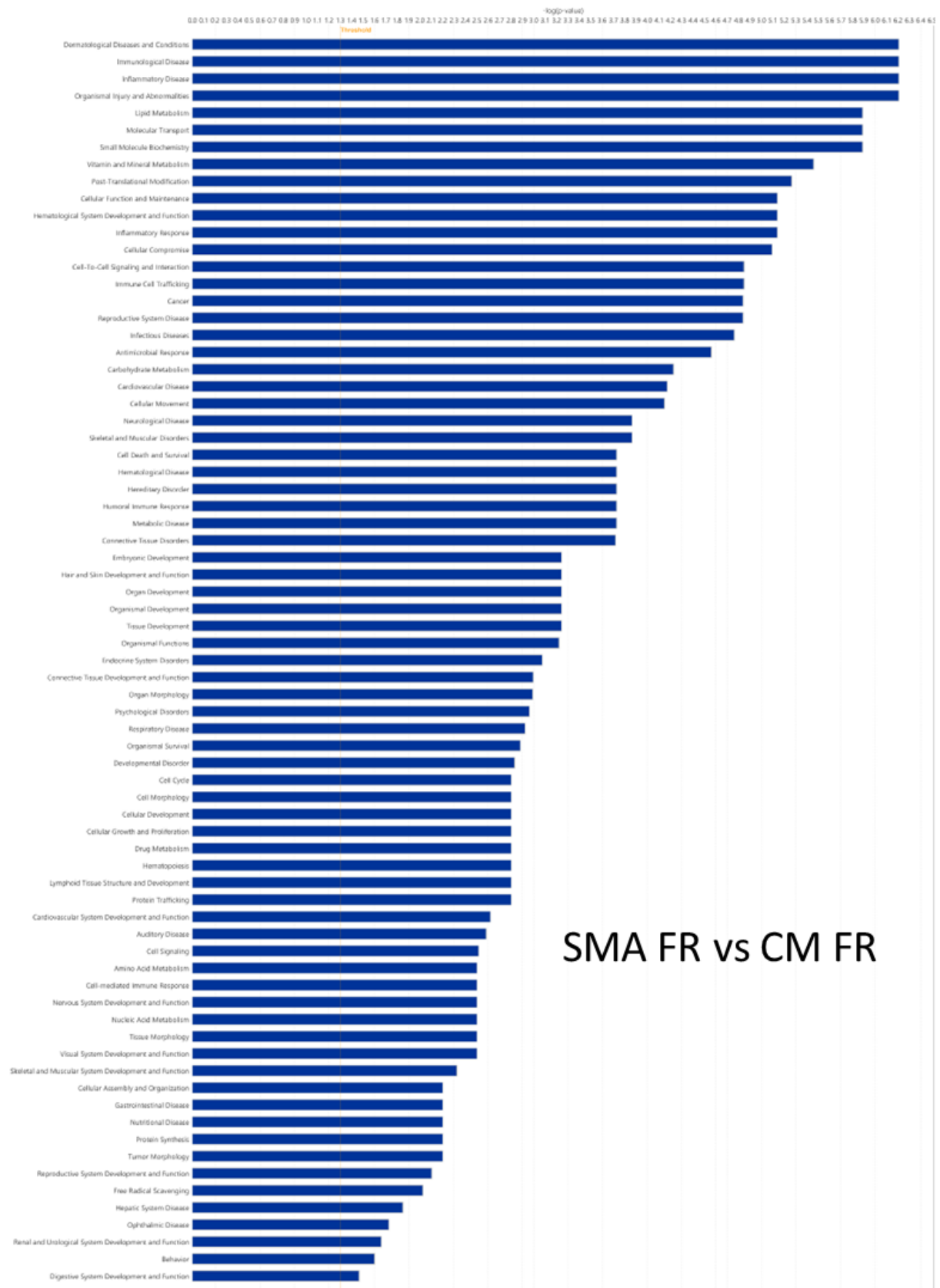
Supplementary Table 1. List of all differentially expressed proteins for the clinically relevant comparisons														
SMA FR vs CM FR					CM FO vs CM FR					SMA FR vs SMA NCI				
Entrez Gene Name	UniProtKB ID	Symbol	Log <sub>2</sub> FC	P value	Entrez Gene Name	UniProtKB ID	Symbol	Log <sub>2</sub> FC	P value	Entrez Gene Name	UniProtKB ID	Symbol	Log <sub>2</sub> FC	P value
Platelet factor 4	P02776	PF4	-6.67	1E-20	Immunoglobulin heavy constant gamma 2 (G2m marker)	P01859	IGHG2	-5.26	1E-20	Histone H4	P62805	H4C1	-11.11	1E-20
Immunoglobulin heavy variable 1-2	P23083	IGHV1-2	-5.26	1E-20	Immunoglobulin kappa variable 3D-20	AOA0C4DH25	IGKV3D-20	-5.26	1E-20	von Willebrand factor	P04275	VWF	-5.26	1E-20
Coagulation factor XIII A chain	P00488	F13A1	-5	0.0002	Haptoglobin	P00738	HP	-4.17	1E-20	Pentraxin 3	P26022	PTX3	-3.70	1E-20
Keratin 9	P35527	KRT9	-5	1E-20	Immunoglobulin heavy constant alpha 1	P01876	IGHA1	-3.85	1E-20	Serum amyloid A2	PODI9	SAA2	-3.45	1E-20
Lecithin-cholesterol acyltransferase	P04180	LCAT	-5	3.06E-06	Albumin	P02768	ALB	-3.70	1E-20	Cholesteryl ester transfer protein	P11597	CETP	-2.78	4.46E-05
Keratin 10	P13645	KRT10	-3.57	1E-20	Immunoglobulin heavy constant gamma 1 (G1m marker)	P01857	IGHG1	-3.33	1E-20	Keratin 2	P35908	KRT2	-2.70	1.19E-10
Immunoglobulin lambda variable 3-21	P80748	IGLV3-21	-3.33	1E-20	Immunoglobulin lambda variable 2-18	AOA075B69	IGLV2-18	-3.23	5.96E-10	Versican	P13611	VCAN	-2.44	0.0011
Solute carrier family 1 member 5	Q15758	SLC1A5	-3.23	1E-20	Merozoite surface protein 6	Q8IJ54	MSP6	-3.23	1E-20	Tenascin C	P24821	TNC	-2.38	0.0006
Immunoglobulin lambda variable 2-18	AOA075B69	IGLV2-18	-2.94	1E-20	Immunoglobulin heavy variable 3-49	AOA0A0MS15	IGHV3-49	-3.13	1E-20	Lipopolysaccharide binding protein	P18428	LBP	-2.17	3.66E-05
Immunoglobulin kappa variable 1-39	P01597	IGKV1-39	-2.86	1E-20	Immunoglobulin heavy constant gamma 3 (G3m marker)	P01860	IGHG3	-3.03	1E-20	Apolipoprotein D	P05090	APOD	-2.13	6.15E-13
Immunoglobulin kappa variable 1D-39	P04432	IGKV1D-39	-2.86	1E-20	Glutamate-rich protein	Q8IJ56	GLURP	-2.78	3.56E-07	Glutathione peroxidase 3	P22352	GPX3	1.5	7.18E-07
Immunoglobulin lambda variable 1-40	P01703	IGLV1-40	-2.78	9.18E-07	Hemopexin	P02790	HPX	-2.63	1E-20	Complement C3	P01024	C3	1.5	1.07E-14
Keratin 5	P13647	KRT5	-2.70	1E-20	Immunoglobulin heavy constant alpha 2 (A2m marker)	P01877	IGHA2	-2.56	1E-20	Coagulation factor X	P00742	F10	1.51	7.45E-09
Cholesteryl ester transfer protein	P11597	CETP	-2.63	1E-20	Proteasome 20S subunit alpha 4	P25789	PSMA4	-2.56	0.0011	Peptidylprolyl isomerase A	P62937	PP1A	1.51	1.66E-12
Immunoglobulin heavy variable 1-69	P01742	IGHV1-69	-2.63	1E-20	CEA cell adhesion molecule 8	P31997	CEACAM8	-2.5	1E-20	Cofilin 1	P23528	CF1	1.52	4.13E-12
Immunoglobulin heavy variable 1-69D	AOA084J2H0	IGHV1-69D	-2.63	1E-20	CD177 molecule	Q8N6Q3	CD177	-2.44	1E-20	Calmodulin 1-3	PODP25	CALM1 (includes others)	1.54	0.0003
Immunoglobulin heavy variable 2-5	P01817	IGHV2-5	-2.63	1E-20	Immunoglobulin lambda variable 1-40	P01703	IGLV1-40	-2.27	1E-20	Immunoglobulin heavy constant gamma 1 (G1m marker)	P01857	IGHG1	1.54	1E-20
Keratin 2	P35908	KRT2	-2.63	1E-20	Lysozyme	P61626	LYZ	-2.27	1E-20	S100 calcium binding protein A9	P06702	S100A9	1.55	2.13E-10
Complement factor properdin	P27918	CFP	-2.56	1E-20	Serpin family A member 7	P05543	SERPINA7	-2.27	1E-20	Orosomucoid 2	P19652	ORM2	1.55	1.47E-14
Transferrin receptor	P02786	TFRC	-2.56	1E-20	Immunoglobulin kappa variable 3-11	P04433	IGKV3-11	-2.22	1E-20	Orosomucoid 1	P02763	ORM1	1.55	2.44E-15
Dermcidin	P81605	DCD	-2.22	1E-20	Retinol binding protein 4	P02753	RBP4	-2.17	1E-20	Alpha-2-glycoprotein 1, zinc-binding	P25311	AZGP1	1.56	3.24E-14
Immunoglobulin lambda variable 6-57	P01721	IGLV6-57	-2.13	1E-20	Brain abundant membrane attached signal protein 1	P80723	BASP1	-2.13	1E-20	Beta-2-macroglobulin	P61769	B2M	1.57	1.87E-09
Immunoglobulin heavy constant gamma 3 (G3m marker)	P01860	IGHG3	-2.04	1E-20	Carbonic anhydrase 1	P00915	CA1	-2.04	8.38E-05	Serpin family A member 7	P05543	SERPINA7	1.57	4E-15
Immunoglobulin kappa variable 3-11	P04433	IGKV3-11	-2.04	1E-20	Immunoglobulin kappa variable 1-5	P01602	IGKV1-5	-2.04	4.44E-16	Alpha 2-HS glycoprotein	P02765	AHSG	1.57	2.22E-16
Low density lipoprotein receptor	P01130	LDLR	1.51	1E-20	Immunoglobulin heavy variable 1-69D	AOA084J2H0	IGHV1-69D	-2	1E-20	Kinogen 1	P01042	KNG1	1.58	2.71E-14
Proteasome 20S subunit alpha 1	P25786	PSMA1	1.52	6.68E-10	Protein 5	P07225	PROS1	1.5	1.78E-15	Complement factor B	B4E1Z4	CFB	1.59	1E-20
Proteasome 20S subunit alpha 4	P25789	PSMA4	1.52	3.87E-12	Apolipoprotein A4	P06727	APOA4	1.59	1E-20	Immunoglobulin kappa variable 1-13	PODP09	IGKV1-13	1.6	1.17E-10
Serum amyloid A2	PODI9	SAA2	1.56	1E-20	Inter-alpha-trypsin inhibitor heavy chain 2	P19823	ITH2	1.62	1E-20	Immunoglobulin kappa variable 1D-13	AOA084J2D9	IGKV1D-13	1.6	1.17E-10
Defensin alpha 1	P59666	DEFA1 (includes others)	1.64	1E-20	Complement factor H related 5	Q9BXR6	CFHR5	1.64	1E-20	Immunoglobulin heavy constant alpha 1	P01876	IGHA1	1.6	1E-20
S100 calcium binding protein A9	P06702	S100A9	1.67	1E-20	Aminolevulinatase	P13716	ALAD	1.65	0.0001	Coagulation factor II, thrombin	P00734	F2	1.62	1E-20
Apolipoprotein A4	P06727	APOA4	1.68	1E-20	Aggrecan	P16112	ACAN	1.86	1E-20	Lactate dehydrogenase A	P00338	LDHA	1.62	1E-20
S100 calcium binding protein A8	P05109	S100A8	1.69	1E-20					Complement C7	P10643	C7	1.63	3.08E-09	
Aggrecan	P16112	ACAN	1.77	1E-20					Brain abundant membrane attached signal protein 1	P80723	BASP1	1.63	1E-20	
Collagen type I alpha 1 chain	P02452	COL1A1	1.77	2.74E-08					Immunoglobulin heavy constant gamma 2 (G2m marker)	P01859	IGHG2	1.64	2.16E-10	
									Apolipoprotein H	P02749	APH	1.66	1E-20	
									Retinol binding protein 4	P02753	RBP4	1.66	1E-20	
									C-type lectin domain family 3 member B	P05452	CLEC3B	1.68	6.89E-15	
									Peptidoglycan recognition protein 2	Q96PD5	PGLYRP2	1.7	1E-20	
									Transthyretin	P02766	TTR	1.7	1E-20	
									Complement factor I	P05156	CFI	1.72	1.03E-08	
									S100 calcium binding prctein A8	P05109	S100A8	1.73	2.25E-09	
									Complement C8 beta chain	P07358	C8B	1.73	1E-20	
									Serpin family A member 6	P08185	SERPINA6	1.73	1E-20	
									Immunoglobulin heavy constant gamma 4 (G4m marker)	P01861	IGHG4	1.74	3.94E-11	
									Keratin 16	P08779	KRT16	1.8	1E-20	
									Complement factor H related 2	P36980	CFHR2	1.82	1.69E-14	

Abbreviations: CM, cerebral malaria; FO, fatal outcome; FR, full recovery; NCI, neurocognitive impairment; SMA, severe malarial anaemia



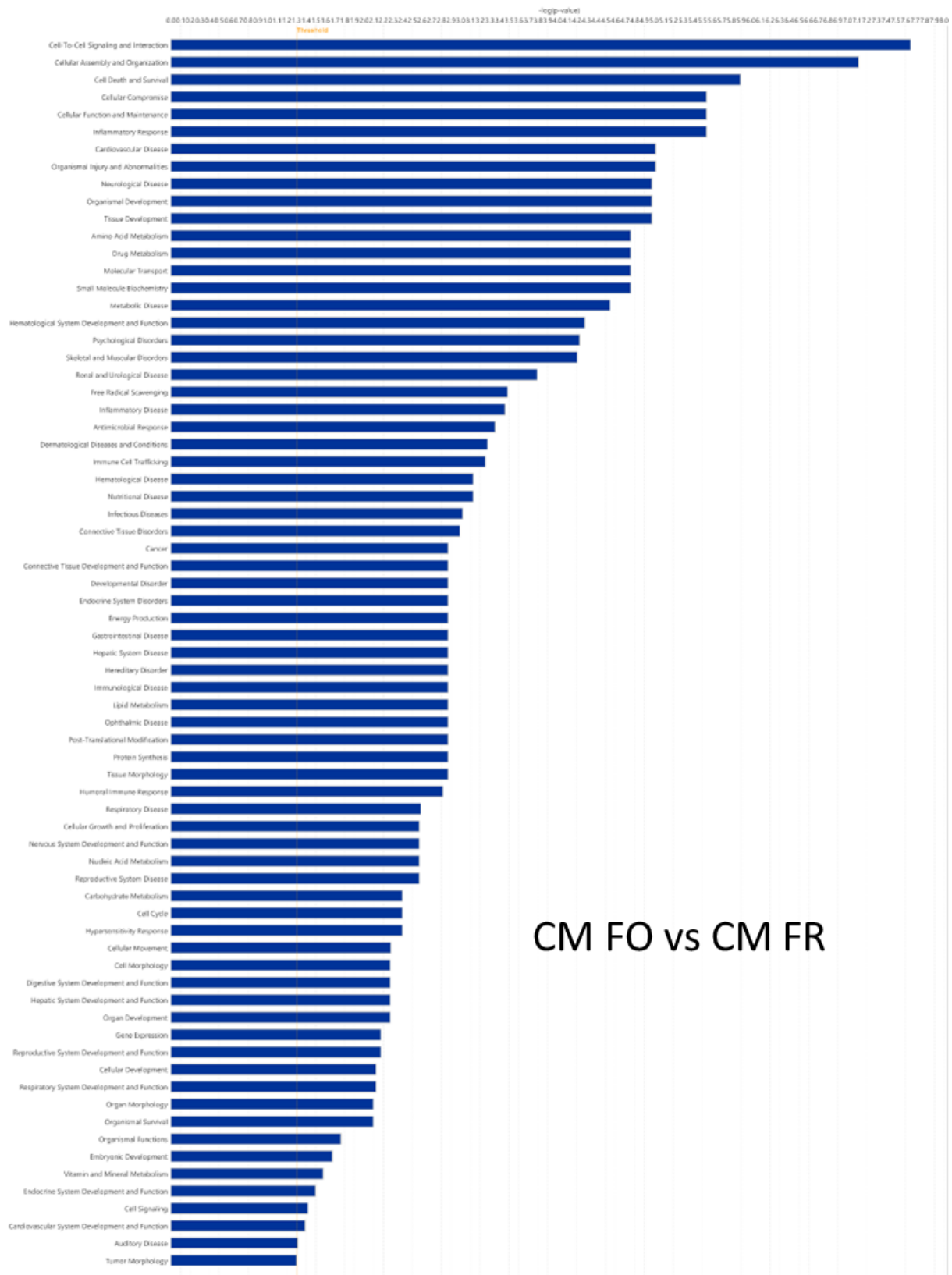
**Supplementary Figure 5.3** Canonical pathways for clinically relevant severe malaria comparisons. (A and B) Most of the canonical pathways were inhibited by the differentially expressed proteins in SMA FR vs CM FR and CM FR vs CM FR. (C) Most of the canonical pathways were activated by the differentially expressed protein in SMA FR vs SMA NCI. The z-score cut-off was at 2 for all. Abbreviations: CM, cerebral malaria; FO, fatal outcome; FR, full recovery; NCI, neurocognitive impairment; SMA, severe malarial anaemia.





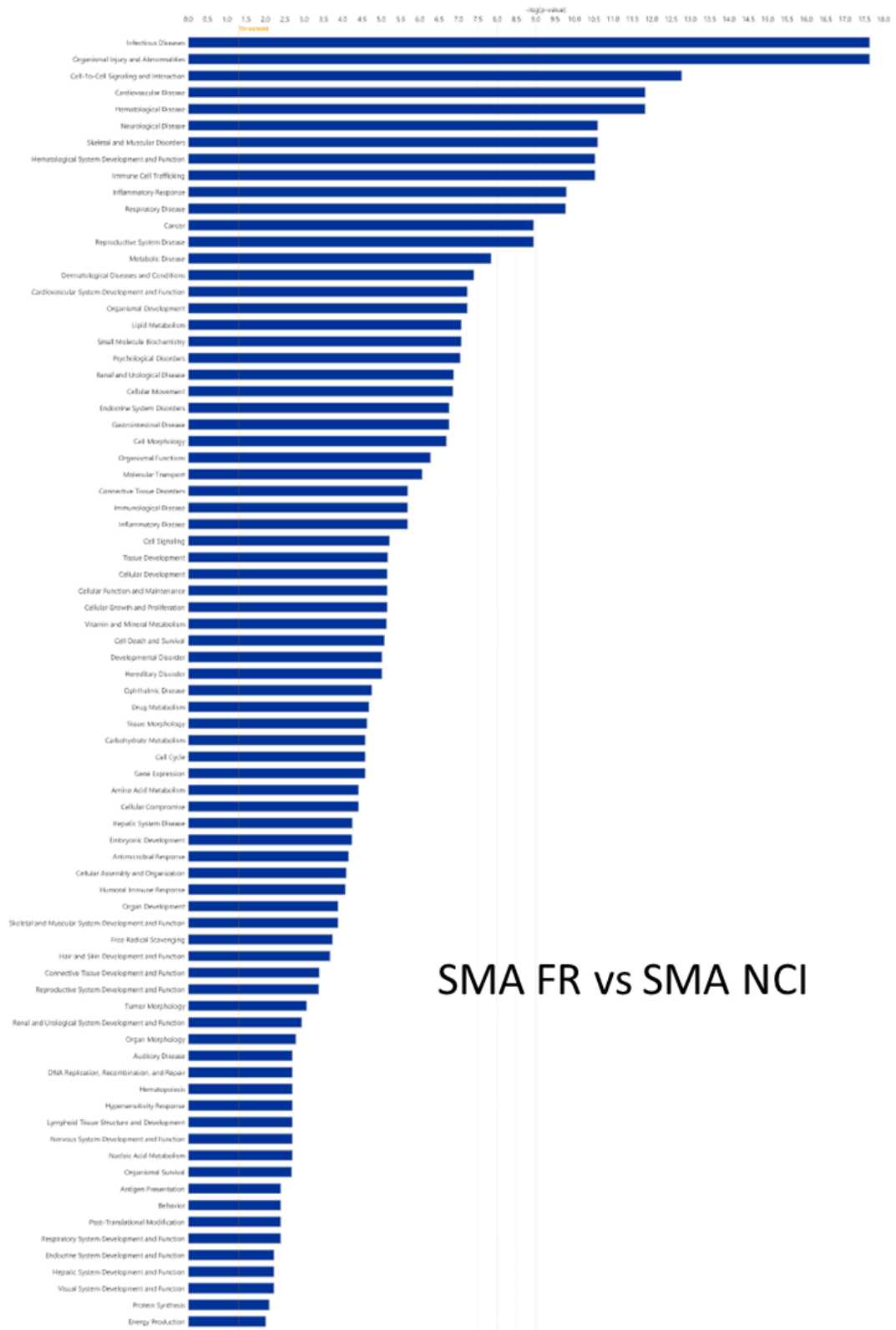
SMA FR vs CM FR

**Supplementary Figure 5.4** All diseases and biological functions significantly altered by the differentially expressed proteins between children with severe malarial anaemia (SMA) and cerebral malaria (CM) who fully recovered without complications.



CM FO vs CM FR

**Supplementary Figure 5.5** All diseases and biological functions significantly altered by the differentially expressed proteins between children with cerebral malaria who died (CM FO) and children with cerebral malaria who fully recovered without complications (CM FR).



## SMA FR vs SMA NCI

**Supplementary Figure 5.6** All diseases and biological functions significantly altered by the differentially expressed proteins between children with severe malarial anaemia who fully recovered without complications (SMA FR) and children with severe malarial anaemia who survived but developed neurocognitive impairment (SMA NCI).

**Chapter Six:**

**Characterisation of CSF and  
plasma extracellular vesicle  
from children with severe  
malaria**

## Chapter 6: Comparative phenotype and numbers of extracellular vesicles in the plasma and the cerebrospinal fluid of children with severe malaria

### Chapter overview

Cerebrospinal fluid and plasma EVs were phenotypically compared in this chapter to gain an understanding of the EV population during different severe malaria outcomes. The cerebrospinal fluid and plasma EVs were also compared to see if they reflect similar activity. This allowed us to study the cellular origins of the EV populations in further detail. Analysis showed strong negative correlation between the two sample types when comparing between samples from children with cerebral malaria who developed neurocognitive impairment.

### Authors' contributions

Author	Concept	Investigation	Methodology	Data curation	Formal Analysis	Writing-original draft	Writing-review & editing	Signature
Iris S. Cheng	X	X	X	X	X	X	X	Production Note: Signature removed prior to publication.
Natalie Sanders							X	Production Note: Signature removed prior to publication.
Robert O. Opoka							X	Production Note: Signature removed prior to publication.
Paul Bangirana							X	Production Note: Signature removed prior to publication.
Chandy C. John							X	Production Note: Signature removed prior to publication.
Valery Combes	X						X	Production Note: Signature removed prior to publication.

**Publication status:** In submission process

## **Comparative phenotype and numbers of extracellular vesicles in the plasma and the cerebrospinal fluid of children with severe malaria**

[Iris S. Cheng](#)<sup>1</sup>, [Natalie Sanders](#)<sup>2</sup>, [Robert O. Opoka](#)<sup>3</sup>, [Paul Bangirana](#)<sup>3,4</sup>, [Chandy C. John](#)<sup>5</sup>, [Valery Combes](#)<sup>1</sup>

<sup>1</sup>Malaria and Microvesicles Research Group, School of Life Sciences, Faculty of Sciences, University of Technology Sydney, Ultimo, Sydney, New South Wales, 2007, Australia

<sup>2</sup>Beckman Coulter Life Sciences, Mount Waterley, Victoria, 3149, Australia

<sup>3</sup>Global Health Uganda, Kampala, Uganda

<sup>4</sup>Department of Psychiatry, Makerere University College of Health Sciences, Kampala, Uganda

<sup>5</sup>Ryan White Center for Infectious Diseases and Global Health, Department of Pediatrics, Indiana University, Indianapolis, USA

Corresponding authors

Valery Combes, Email: [valery.combes@uts.edu.au](mailto:valery.combes@uts.edu.au)

Word Count: 6573

## **Abstract**

There is increased interest in methods for assessing extracellular vesicles (EVs) surface cargo in various diseases, as it can help discover clinically relevant information. Cerebral malaria (CM) and severe malarial anaemia (SMA) are two of the most severe complications of malaria infection, which can lead to neurocognitive impairments that can last for many years after the initial infection. The cellular origins of EVs have been previously compared between healthy controls and severe malaria patients; however, the different outcomes of severe malaria have never been assessed. In this study, for the first time, cerebrospinal fluid- (CSF) and platelet-free plasma- (PFP) derived EVs from Ugandan children were measured by flow cytometry and their cellular origin and numbers were compared in different groups of patients. Only patients who had received a lumbar puncture were selected for this study. Patients who were suffering from either CM or a combination of CM and SMA were classified according to their clinical outcome, i.e., full recovery, fatal outcome, and neurocognitive impairment (NCI). Pan-cellular EVs were identified using annexin V to label phosphatidylserine (PS) at their surface, and EVs from lymphocytic, monocytic/macrophage, platelet, endothelial, and erythrocytic origins were identified using antibodies against CD3, CD11b, CD41, CD105 and CD235a, respectively. The CSF from children with CM who had fatal outcomes had significantly more PS-positive (+) EVs than those who developed NCI and succumbed. The opposite was observed in the PFP, where the children who recovered without complications had more PS+ EVs than those with NCI and fatal outcomes. The T cell+/PS-negative (-) EV counts in the CSF of children with CM were significantly higher in those who had fatal outcomes than those who fully recovered without NCI. In the children with both CM and SMA, the number of T cell+/PS- EVs in the CSF was higher in those with fatal outcomes than those who developed NCI. The amount of monocyte+ or red blood cell+/PS- EVs in the CSF of children with both CM and SMA was significantly lower in those who recovered but developed NCI than in children who fully recovered. Children with CM who recovered but developed NCI had strong negative correlations between CSF and PFP EV levels. These findings highlight the role of EVs in CSF as potential prognostic biomarkers for children with CM who recovered but developed NCI and the pathophysiological differences between CSF and PFP.

**Keywords:** Extracellular vesicles (EVs), flow cytometry, plasma, cerebrospinal fluid, malaria, paediatric, cerebral malaria, severe malarial anaemia

## **6.1 Introduction**

Extracellular vesicles (EVs) are produced by most eukaryotic cells and include three main groups: exosomes, microvesicles, and apoptotic bodies. Each group of EVs is made via a different pathway: exosomes are produced when multivesicular bodies bind to the cell membrane and release its contents of vesicles 50-100 nm in diameter; microvesicles are produced through plasma membrane remodelling by outward budding, creating vesicles 100-1000 nm, and apoptotic bodies are produced during apoptosis and have a diameter of 1000-5000 nm<sup>1</sup>. Therefore, EVs are complex submicron particles that contain cytosolic proteins, lipids and nucleic acids, which contribute to intercellular communication and disease pathogenesis; they are also well-known sources of biomarkers for disease<sup>2-4</sup>. Since microvesicles have similar surface proteins as their parent cell, flow cytometry has been commonly used to determine their cell origin for many complex diseases, including malaria<sup>5-10</sup>.

An overarching issue is that the instrument's detection threshold limits the characterisation of exosomes by flow cytometry; therefore, other methods have been used, such as multiplex proximity extension assay for proteomic profiling of exosomes, allowing the identification of their cellular origin<sup>11,12</sup>. Due to the small size of extracellular vesicles, many studies have chosen to attach the EVs onto larger latex beads for detection via conventional flow cytometry. However, this method highly depends on the surface markers present on the EVs and requires large amounts of EVs. Recent advancements in flow cytometry technology and techniques have allowed the detection of exosomes within a sample. The BD FACSymphony™ A1 Cell Analyzer with the BD® Small Particle Detector can resolve polystyrene beads down to 90 nm, Nano-Flow Cytometry (NanoFCM) can analyse EVs as small as 40 nm, and the Beckman Coulter CytoFLEX™ can detect EVs at least as small as 65 nm<sup>13-16</sup>. It is essential to include exosomes during analysis as they carry important signalling molecules from parent cells and intercellular vesicles and organelle information<sup>17,18</sup>. Therefore, this study chose to use the CytoFLEX™ system for EV detection and numeration, as it can detect small EVs with a 4-laser configuration.

Malaria has been affecting human lives for thousands of years, yet its resilience allows it to remain a significant global health problem, infecting 249 million people and killing 608,000 in 2022<sup>19,20</sup>. This complex disease mainly affects people living in sub-Saharan Africa, where 95%



of the cases occur, affecting primarily children under the age of 5<sup>21</sup>. Uncomplicated malaria infections can progress to severe or complicated malaria in ~4.5% of patients, and the causes are still not fully understood<sup>21–25</sup>.

The primary complications of severe malaria include severe malaria anaemia (SMA) and cerebral malaria (CM), which can occur independently or in combination and can rapidly become fatal. CM is the most fatal syndrome associated with an uncontrolled systemic immune response and a mechanical obstruction of cerebral venules and capillaries by infected red blood cells (iRBCs) and other vascular cells<sup>26–28</sup>. SMA, on the other hand, is a more common complication with lower hospital mortality but increased risk of mortality after discharge or readmission<sup>29–31</sup>. SMA is characterised by the destruction of infected or non-infected red blood cells, sequestration of red blood cells in the spleen, dyserythropoiesis, and bone marrow suppression<sup>22,31,32</sup>. Despite effective treatment, up to 25% of the survivors can develop neurocognitive impairment (NCI), causing deficits in attention, cognitive ability, fine motor skills, memory, behaviour, and language comprehension<sup>33–35</sup>. These deficits may last for many years post-treatment, affecting education and livelihood<sup>36,37</sup>.

Malaria infections have been associated with EV production, and these EVs are thought to be involved in the modulation of host cell response and pathogenesis of the disease<sup>38,39</sup>. Uncovering that *P. falciparum* uses EVs to exchange genetic information and intra-parasite communication revealed new areas of malaria pathophysiology and possible interactions with the host immune system<sup>3,40</sup>. The past two decades of EV research in malaria have primarily been *in vitro*, *in vivo* and *in silico*, with few clinical studies<sup>38</sup>. *In vitro* and *in vivo* studies illustrate that EVs (specifically microvesicles, previously called microparticles) such as iRBC, endothelial, and platelet EVs, increase in amounts during malaria and severe malaria and that the EVs are markers of cellular activation, inflammation, and pathogenesis<sup>5,39,41–44</sup>. A study of Malawian children was the first to investigate and compare EV populations for different complications of malaria and linked higher levels of endothelial 'microparticles' in plasma with cerebral dysfunction<sup>10</sup>. Later, a study in Cameroon on children with severe malaria found significantly higher levels of plasma platelet, red blood cell, endothelial, monocyte and leukocyte 'microparticles' in children who developed CM<sup>6</sup>. Plasma levels of platelet, endothelial and red blood cell 'microparticles' were also elevated in patients with severe malaria from Thailand and India<sup>5,7,8</sup>.

Comparatively, many studies have investigated plasma EVs in the context of severe malaria, but none have assessed cerebrospinal fluid (CSF) EVs and their profiles. To our knowledge, only two studies have covered CSF EVs for protozoan parasites. One showed elevated levels of serum EVs, but not CSF EVs, in patients infected with *Toxoplasmosis* and the other described elevated levels of leukocyte 'microparticles' in the CSF of late-stage *Trypanosoma* infected patients<sup>45,46</sup>. EVs in CSF have been studied in neurological diseases such as Alzheimer's and dementia (higher concentrations of small EVs) and schizophrenia (elevated number of 'microparticles'), reflecting higher levels of EVs in the disease state<sup>47,48</sup>.

In malaria, investigations on the protein content of CSF in Ugandan children with CM showed elevated levels of Tau protein in the CSF at hospitalisation and was associated with long-term NCI and mortality<sup>49</sup> and elevated markers for neuronal injury (Tau) and impaired blood-brain-barrier were also detected in the CSF and were associated with kidney-brain injury<sup>50</sup>. There are precise pathophysiological mechanisms of disease severity occurring in the CSF of children with severe malaria, compelling the necessity to investigate these changes as cerebral dysfunction and neurological deficits are common complications. Another study of Ugandan children showed that acutely elevated plasma Tau levels were associated with long-term NCI and mortality in survivors of severe malaria (CM or SMA)<sup>51</sup>. This raises the question of whether CSF and plasma have similar, distinct or mixed profiles associated with neurological or deadly outcomes and whether the plasma profile can be used as a surrogate marker of what is happening in the CSF.

The characterisation of EV cellular origins in tissue and vasculature can help break down the complex heterogeneity of the EV populations. This could provide biological information on the functional status of parent cells to aid in understanding mechanisms behind disease pathogenesis and intercellular communication<sup>52-56</sup>. The EV profiles from body fluids such as plasma, CSF and urine can be used as non-invasive prognostic biomarkers for disease and diagnostic markers for neurological diseases<sup>52,57</sup>. By understanding their cellular origins, EVs can also become targets for pharmaceutical treatment to lessen disease severity and become tools for monitoring disease progression or treatment<sup>58-60</sup>.

This study compares the paired profiles of EVs (cellular origin and numbers) from CSF and platelet-free plasma (PFP) collected from children who developed severe malaria using antibody panels without the need for washing before detection via flow cytometry (Figure 6.1). The aim is to determine if the EV surface cargo and origin depend on disease outcome

and if the same patient's changes are reflected in the CSF and PFP. This could help further develop the understanding and role of EVs in malaria pathogenesis and the differences or similarities reflected in the CSF and PFP.

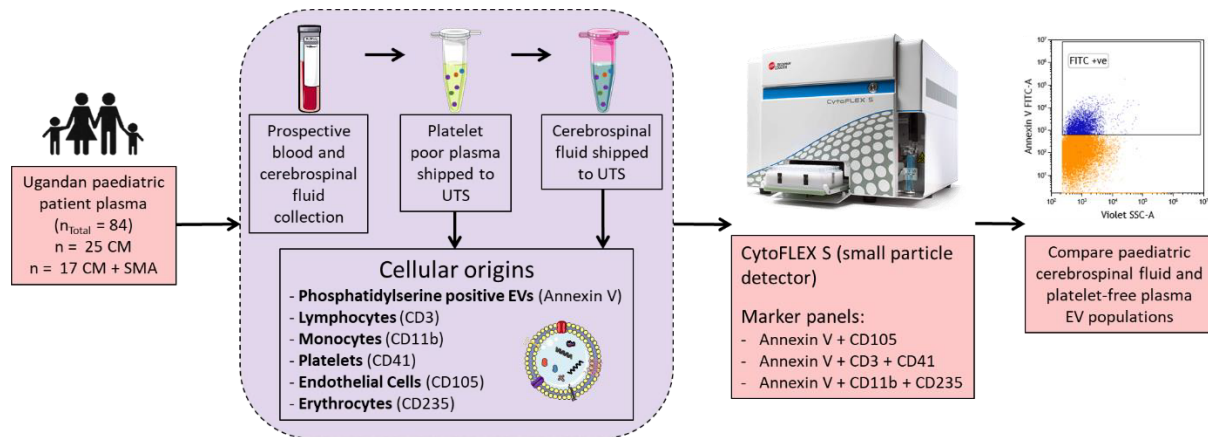


**Figure 6.1** Study pipeline, explaining the collection of paediatric samples and characterisation using flow cytometry. Abbreviations: CM, cerebral malaria; EV, extracellular vesicles; SMA, severe malarial anaemia; UTS, University of Technology Sydney.

## 6.2 Materials and methods

### 6.2.1 Participants

Ugandan children between 18 months and 10 years old were enrolled between 2008 and 2012 for long-term neurocognitive assessment by neurologists or paediatricians, as detailed in previous studies<sup>33,61–64</sup>. Samples from severe malaria patients were collected prospectively from children enrolled at Mulago National Referral and Teaching Hospital, Kampala, Uganda. Children were diagnosed with CM if they had blood smears positive for malaria parasites, coma, and a negative lumbar puncture to eliminate other causes of cerebral dysfunction. Children diagnosed with combined CM and SMA were defined as CM above in addition to haemoglobin < 5 g/dL. Clinical, biological, and neurological data, including clinical outcomes (i.e., survival, death, and NCI at baseline, 6, and 12 months), were recorded for all children involved in this project. The patient inclusion and exclusion criteria have been previously reported<sup>33,62</sup>. Community controls were not available as CSF is not collected during standard clinical assessment in hospitals unless the child presents with coma or cerebral meningitis-like symptoms to eliminate other causes of febrile encephalopathy<sup>65</sup>.

### 6.2.2 Informed consent and ethical approval

Please refer to section 4.2.2 for details regarding guardian consent and ethical approvals.

### 6.2.3 Study Design

A total of 42 children were selected for this project and distributed into six groups of patients following the demographic criteria illustrated in (Table 6.1): children fully recovered from CM (CM FR, n=16) or combined CM and SMA (CM + SMA FR, n=11), without complications; children who fully recovered from CM (CM NCI, n=5) or combined CM and SMA (CM + SMA NCI, n=4) but presented with NCI; children who succumbed from CM (CM FO, n=4) or combined CM and SMA (CM + SMA FO, n=2). The CSF and corresponding PFP were analysed by flow cytometry for each paediatric patient.

### 6.2.4 Cerebrospinal fluid and platelet-free plasma collection, preparation, and storage

Upon admission,  $\leq 5.5$  mL of whole blood was collected from each child via sodium citrate venipuncture. The whole blood was centrifuged at 1,500 g for 15 min at room temperature to remove cells and platelets<sup>6</sup>. The platelet-poor plasma was centrifuged at 13,000 g for 3 min at room temperature to remove cellular debris and any remaining platelets. The PFP containing the EVs was collected, stored at -80 °C and shipped to the University of Technology Sydney, where all the experiments were performed. CSF was collected through a lumbar puncture from the children and processed, stored, and shipped similarly to whole blood.

**Table 6.1** Characteristics of paediatric patient group baseline demographics and clinical findings

Demographic and clinical findings							
Paediatric patient group	CM FR (n = 16)	CM NCI (n = 5)	CM FO (n = 4)	CM SMA FR (n = 11)	CM SMA NCI (n = 4)	CM SMA FO (n=2)	P Value <sup>a</sup>
Age, y, mean (SD)	3.1 (0.50)	2.50 (0.54)	2.91 (0.27)	3.61 (0.47)	3.17 (0.36)	3.25 (0.41)	.02
Sex, male:female, No.	10:6	1:4	4:0	5:6	4:0	2:0	
Plasma volume, $\mu$ L, mean (SD)	165 (6.5)	169 (4.9)	179 (5.5)	178 (6.3)	172 (8.2)	167 (5.2)	.04
Blantyre coma scale <sup>§</sup> , mean	2	1	1	2	1	1	
Coma duration, hours, median (IQR)	80.20 (52.51-98)	75.00 (25-102.5)	0	72.3 (36.3-95)	85.6 (22-120.4)	0	
Haemoglobin, g/dL, mean (SD)	7.25 (1.24)	5.98 (1.56)	8.80 (2.01)	3.55 (0.42)	3.68 (0.26)	3.57 (0.23)	.001
Platelet count, $\times 10^9/L$ , median (IQR)	110 (40-153)	109 (35-213)	42 (21-62)	88 (36-103)	105 (55-168)	58 (18-72)	.04
Hypoxia Y:N/# (O <sub>2</sub> saturation <95%)	1:15	1:4	1:3	2:9	0:4	0:2	
Lactic acidosis Y:N/# (lactate >5 mmol/L)	1:15	1:4	2:2	3:8	1:3	0:2	
Plasmodium falciparum peripheral blood density, parasites/ $\mu$ L, median (IQR)	250 408 (95 025-260 975)*	26 690 (13 255-130 250)	390 240 (163 002-403 600)*	39 840 (6552-155 000)	209 100 (53 000 375-240 110)	70 700 (4002-90 044)	.008
PfHRP-2 level, ng/mL, median (IQR)	5214 (1084-6582)	5548 (2565- 9652)	2504 (865-5824)	695 (536-1666)	2269 (1445-3125)	1002 (695-1633)	.05

Abbreviations: CC, community children; CM, cerebral malaria; FO, fatal outcome; FR, full recovery; IQR, Interquartile Range; NCI, neurocognitive impairment; SD, standard deviation; SMA, severe malarial anaemia

<sup>a</sup> P Value based on one-way ANOVA Kruskal-Wallis

<sup>§</sup> Blantyre coma scale for preverbal children <5 years of age; minimum score: 0 (poor), maximum score: 5 (good), abnormal score  $\leq$  4

\* Two patients with hyperparasitaemia

### 6.2.5 Extracellular vesicle and cellular origin markers

FITC-Annexin V (phosphatidylserine, pan-cellular EVs) and corresponding 10X calcium binding buffer (10XBB), mouse anti-human krome orange-conjugated CD3 (lymphocytes, KrO-CD3, clone UCHT1), mouse anti-human allophycocyanin-conjugated CD11b (monocytes/macrophages, APC-CD11b, clone Bear1), mouse anti-human phycoerythrin-cyanine 7-conjugated CD41 (platelets, PC7-CD41, clone P2), mouse anti-human R-phycoerythrin-conjugated CD105 (endothelium, PE-CD105, clone TEA3/17.1.1) and mouse anti-human R-phycoerythrin-conjugated CD235 (erythrocytes, PE-CD235, clone 11E4B-7-6 (KC16)) monoclonal antibodies were sourced from Beckman Coulter. The annexin V and five monoclonal antibodies were centrifuged at 21,000 g for 1 hour at 15 °C to remove aggregates formed during storage that could interfere with the specificity of flow cytometry readings and increase the background noise.

### 6.2.6 Pre-analytical flow cytometer preparations

A nonionic, non-fluorescent, sterile and azide-free CytoFLEX™ sheath fluid from Beckman Coulter was used for all acquisitions. UltraPure™ DNase/RNase-free distilled molecular biology grade water from Invitrogen™ was used to dilute the 10XBB. Tissue culture grade, sterile phosphate-buffered saline (PBS) was purchased from Gibco. Sterile Contrad 70 and FlowClean from Beckman Coulter were used to clean the flow cytometer. All buffers and cleaning solutions were freshly made or newly opened on the day of acquisition, the solutions were kept sterile, and aliquots stored in 50 mL plastic falcon tubes were not reused in future runs to avoid microplastic noise.

It was essential that the Beckman Coulter CytoFLEX™ S flow cytometer, used for all measurements in this study, was exceptionally clean before running any precious paediatric samples, as the background could mask the presence of EVs, especially the smallest ones. After quality control, the 'system start-up program' followed by 'daily clean' were run using the acquisition software CytExpert™ version 2.4, the 'deep clean' was performed, and the diluted Contrad 70 (1:1 with UltraPure™ distilled water) was allowed to sit in the Flow Cell for 45 mins to 1 hour. The cytometer was primed at least three times, followed by running FlowClean and then PBS each for 10 mins on the fast setting. On the slow flow rate setting, a fresh aliquot of PBS was acquired twice for 5 minutes. The deep clean and subsequent washes

were repeated until debris build-up was removed. The cleaning was complete once there were consistently < 1,500 events per second while running PBS, on at least ten lots of 2-minute runs on a slow flow rate. Before any staining, all solutions were run three times for 2 minutes at a slow flow rate to ensure the solutions were not contaminated and that the monoclonal antibody centrifugation was successful. If the monoclonal antibodies still had aggregates, they were centrifuged again at 21,000 g for 1 hour at 15 °C.

#### 6.2.7 Staining and incubation

The CSF and PFP were thawed on ice and centrifuged at 13,000 g for 2 min to remove aggregates formed during cryostorage. Three staining panels were chosen: 1) FITC- annexin V + PE-CD105; 2) FITC- annexin V + KO-CD3 + PC7-CD41; and 3) FITC- annexin V + APC-CD11b + PE-CD235. Once the CytoFLEX™ was clean and ready, 5 µL of the sample (neat CSF or 1:100 PFP, diluted with PBS) was mixed with 0.5 µL of annexin V and 0.5 µL of 10XBB and incubated on ice in the dark for precisely 15 mins. Then, to the same tube/well, 1.5 µL of antibody was added for each monoclonal antibody and incubated on ice for 15 mins, protected from light. This staining procedure was done sequentially for each panel of annexin V plus monoclonal antibody. After incubation, the stained mixture was immediately topped up to 200 µL with 1X binding buffer (10XBB diluted with PBS) and run on the cytometer.

#### 6.2.8 Sizing beads used for extracellular vesicle gating strategy

Sizing beads from three manufacturers were analysed to determine the EV gate when analysing on a forward (FSC-A) versus violet side scattergram (VSSC-A) (Figure 6.2A-E). SPHERO™ nano fluorescent size standard kit consisting of 220 nm, 450 nm, 880 nm, and 1340 nm and 8 peak rainbow calibration particles 3.0-3.4 µm from Spherotech were acquired for acquisition settings, i.e. gain, threshold and width, 8 peak calibration plots not shown) (Figure 6.2A and B). Polystyrene latex bead mix (80 nm, 100 nm, 152 nm, and 296 nm) and photon correlation spectroscopy (PCS) control polystyrene latex beads 100 nm, 200 nm, 300 nm, and 500 nm from Beckman Coulter were acquired individually and as a pool to gauge the smallest detectable size (Figure 6.2C and D). NanoStandard™, consisting of highly uniform monodisperse polymer microspheres with a nominal diameter of 220 nm and mean diameter of 215 nm, were sourced from Applied Microspheres to further optimise the gating strategy

(Figure 6.2E). After acquiring the sizing beads, gates to encompass particles between 70-900 nm were established, which would include both exosomes and microparticles.

#### 6.2.9 Acquisition strategy and gating protocol

The samples were analysed using a Beckman Coulter CytoFLEX™ S instrument equipped with violet (405 nm), blue (488 nm), yellow-green (561 nm) and red (638 nm) laser excitation sources. This allowed the side scatter to be detected using the blue laser (SSC) and the violet laser (VSSC), with the VSSC configuration allowing for better nanoparticle resolution. The gain and threshold settings were optimised using the sizing beads and spare CSF EVs. Once the best gain was determined for each channel, a threshold trigger level on height was selected on the VSSC channel, and the same gain and threshold were used throughout all experiments. Based on the manufacturer's recommendation, the 'Event Rate (additional time added to the pulse/detection window) Setting' feature was set to 'high' for nanoparticle acquisition, narrowing the pulse window to reduce optical noise and background, improving event processing.

The acquisition gates were adjusted using spare patient CSF and PFP to ensure the EVs were not cut out, as latex beads do not precisely replicate the light scattering of biological membranes (Figure 6.3). Annexin V staining with and without calcium binding buffer was compared to confirm that positive events were not background noise or artefacts (Figure 6.3A). All samples (CSF and PFP) were acquired twice, each time 4 minutes on the lowest speed 'slow' (10 µL/min), a total of 8 minutes per sample, 80 µL of stained mixture, equating to 2 µL of CSF or 0.02 µL of PFP. In between acquisitions, a 15-second backflush was performed, and in between patient samples, after all the panels were acquired, a 3 min wash with FlowClean and 1 min with PBS on a fast flow rate (60 µL/min) was done to avoid cross-contamination between patient samples.

#### 6.2.10 Phenotype and statistical analysis

The flow cytometry standard (FCS) files were exported from the acquisition software CytExpert™ and imported into Kaluza™ version 2.2.1 for post-acquisition analysis. Post-acquisition compensation was performed for each staining condition and panel of annexin V plus monoclonal antibody. After confirming the fluorescent channels' thresholds, the



established gating strategy and compensation protocol were used for all CSF and PFP samples. EV phenotypes between patient outcomes and sample type (CSF and PFP) were compared by performing a Kruskal-Wallis test using GraphPad Prism version 10.0 for Windows. Using GraphPad Prism, the Spearman rank-order correlation coefficient ( $r$ ) between CSF and PFP was compared by evaluating the monotonic relationship. Comparison data were shown as correlation matrices, and  $r$ -values closer to  $|1|$  were considered to have a stronger association.

## 6.3 Results

### 6.3.1 Gating Strategy for EVs

Beads from different companies, fluorescent and non-fluorescents were compared and located on the forward and violet side scatter plots to optimise the EV gate definition (Figure 6.2B-E). The beads were used to identify where the EVs would approximately be on the graph located on the forward and violet side scatter plots. A gate was then drawn to encompass EVs ~60-480nm in size (Figure 6.2A).

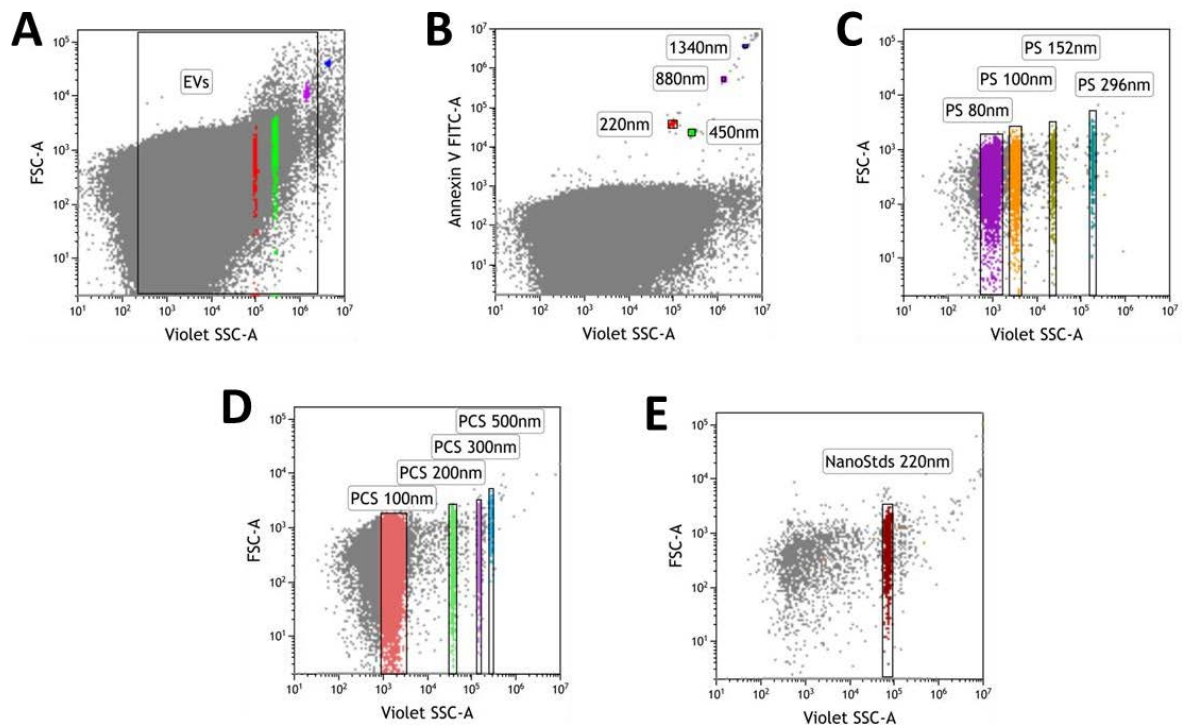


**Figure 6.2** Gating Strategy for particles between approximately 70-900 nm, acquisition on the CytoFLEX S flow cytometer. All plots are ungated, A) extracellular vesicles (EVs) gate created based on the comparison of all beads, colours correspond with SpheroTech sizing beads. B) SPHERO™ nano fluorescent size standard kit from SpheroTech, consisting of 220, 450, 880, and 1340 nm fluorescent sizing beads. C) and D) scatter plots show the position of polystyrene latex beads from Beckman Coulter (80, 100, 152, 200, 296, 300, and 500nm). E) Applied Microspheres Nanostandards™ with a nominal diameter of 220 nm and mean diameter of 215 nm.

### 6.3.2 Confirming events were extracellular vesicles

Fluorescent labelling of EVs improved resolution during flow cytometry by allowing the differentiation of particles from background noise. EVs were thus fluorescently labelled with various markers and fluorochromes, including annexin V-FITC, to label the population of EVs carrying phosphatidylserine (PS) on their surface. CSF and PFP samples were stained with and without binding buffer containing calcium. The absence of calcium in the staining mixture significantly decreased the number of PS-positive (+) events, with counts similar to unstained samples (Figure 6.3A). The decreased events confirmed the specificity of annexin V labelling and allowed for accurate discrimination of annexin V labelled EVs from background noise. Quadrant gates enabled the identification of double-positive EV populations for each panel of markers assessed on CSF and PFP, respectively (Figures 6.3B and C).

### 6.3.3 Phosphatidylserine profiles for CSF and PFP extracellular vesicles

The CSF and PFP EVs from two main groups of children, those with CM or combined CM and SMA, were characterised. Each group of children was subdivided into three sub-groups: children who fully recovered without complications (FR), children who recovered but developed neurocognitive impairment (NCI), and CM children with fatal outcomes (FO). We analysed the population of PS+ EVs in all sub-groups of children.

The PS+ events from the marker panels were used to compare EV counts between the patient sub-groups and the two types of samples (CSF and PFP). Within the CM patient group, significantly more PS EVs were identified in the CSF of children with CM FO than those with CM FR or CM NCI (Figure 6.4A). However, the opposite was seen in children with both CM and SMA, where more PS EVs were detected in the CSF of children with FR than in children with NCI or FO (Figure 6.4B).

When the PFP from the same patients was analysed, a profile opposite to that of the CSF was observed. There were more PS+ PFP EVs in patients with CM FR compared to CM NCI or CM FO (Figure 6.4C) and more PS EVs in children with fatal outcomes compared to those with complete recovery when analysing combined CM + SMA samples (Figure 6.4D). Overall, significantly more PS+ EVs were detected in the children's PFP than in the CSF for all patient groups and sub-groups, with more than a 100-fold difference (Figure 6.5). The significantly greater number of PFP EVs could reflect vascular cell activation during severe malaria.

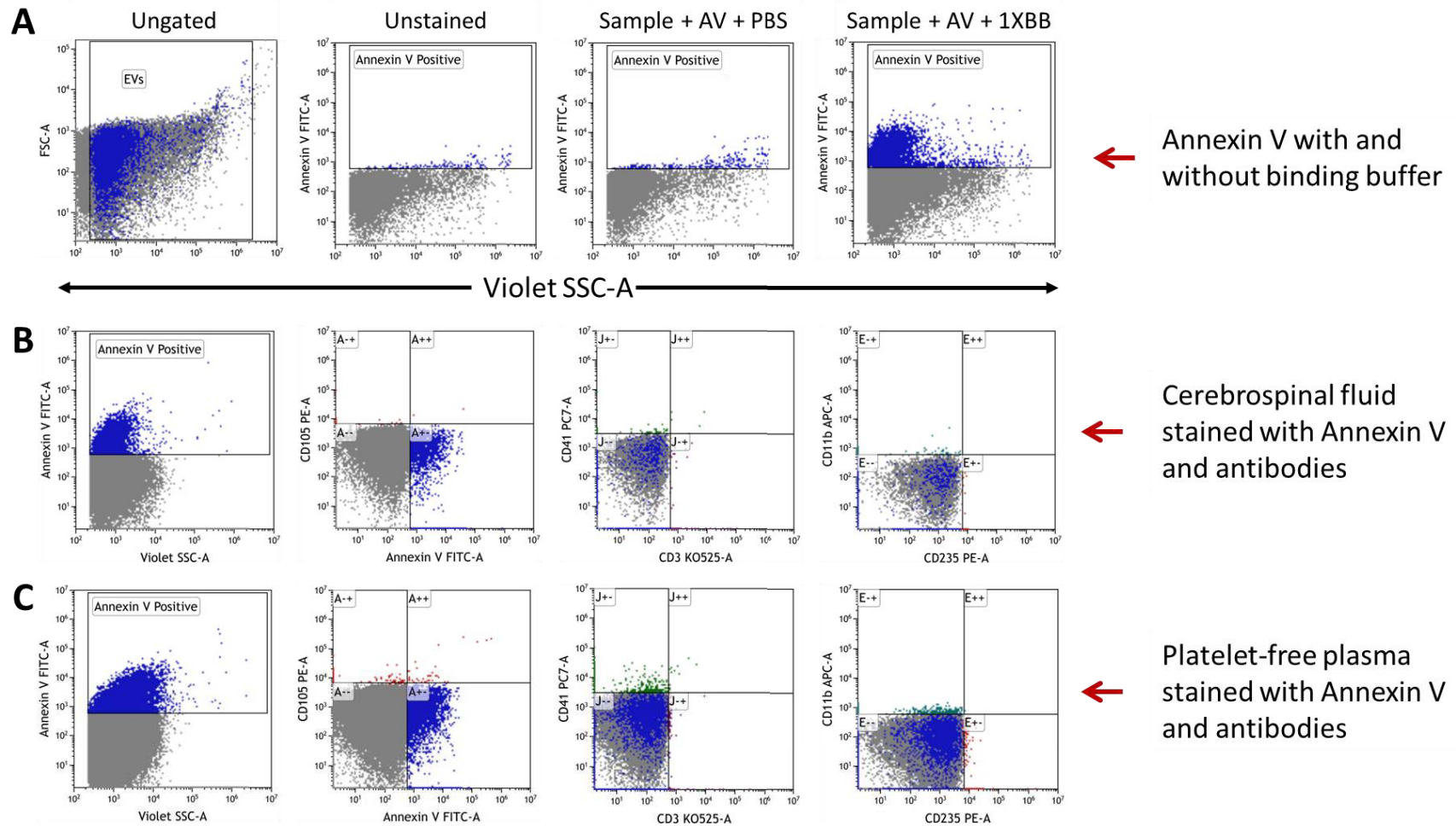


**Figure 6.3** Gating strategy for Annexin V and antibody labelled extracellular vesicles (EVs). A) A staining mixture with and without calcium binding buffer was used to see if EVs were being stained and the signal was not background noise. B) and C) Gates for the corresponding antibodies, CD3 (T cells), CD11b (monocytes), CD41 (platelets), CD105 (endothelial cells), and CD235 (red blood cells) were created and used for both cerebrospinal fluid and platelet-free plasma, respectively.

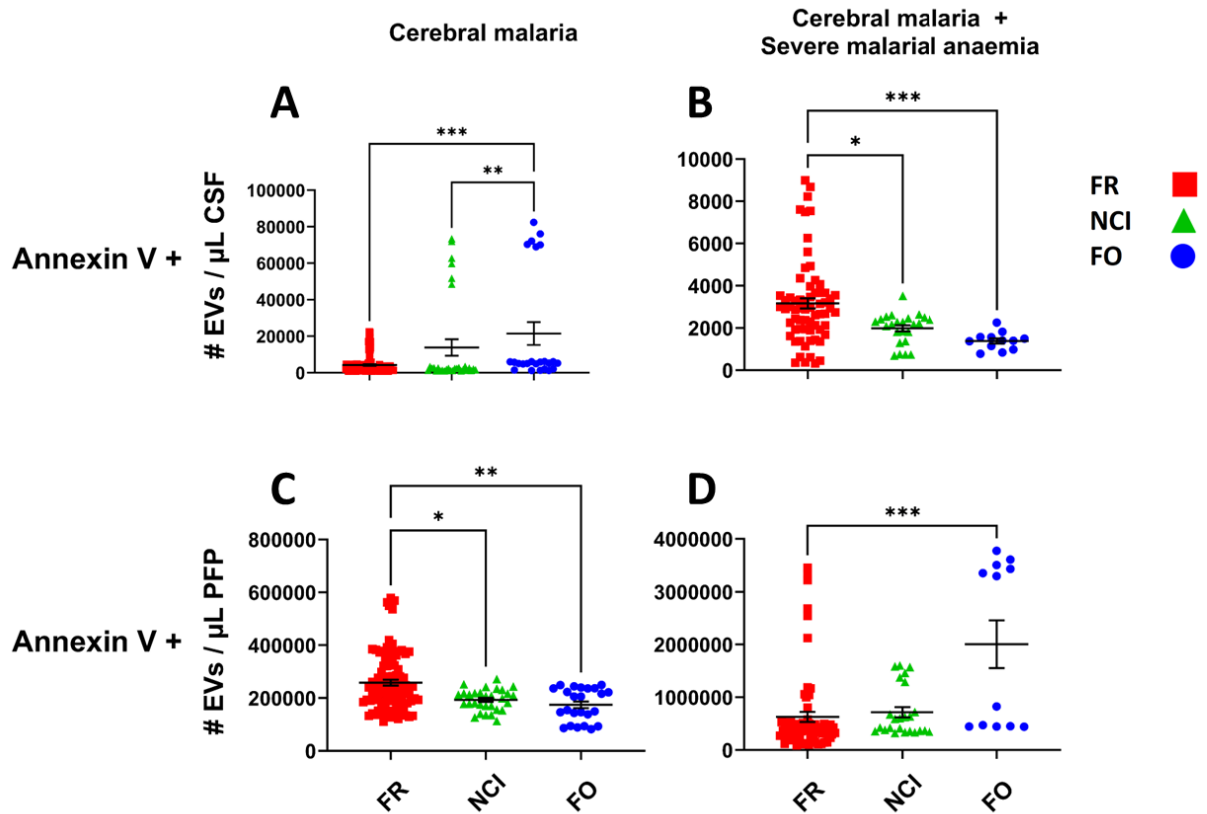


**Figure 6.4** Annexin V profiles for cerebrospinal fluid (CSF) and matching platelet-free plasma (PFP) extracellular vesicles (EVs). The annexin V-positive events from the three panels of markers were used to compare the three severe malaria outcomes for children with cerebral malaria (CM) and those with also severe malarial anaemia (SMA). (A and B) Children with CM who succumbed (FO) had more CSF EVs than those who fully recovered (FR) or developed neurocognitive impairment (NCI). The opposite was observed for children with both CM and SMA. (C and D) Children with CM FR had more PFP EVs than NCI and FO, as for children with CM and SMA, those with FO had more EVs than FR.



#### 6.3.4 Antibody+/PS-negative profiles of EVs in CSF and PFP during severe malaria

Five monoclonal antibodies were used for phenotyping the CSF and PFP EVs originating from T cells (CD3), monocytes (CD11b), platelets (CD41), endothelial cells (CD105), and red blood cells (CD235a). The antibody+ only (PS-negative) events were compared for each marker between the severe malaria patient subgroups.

##### *6.3.4.1 Cerebrospinal fluid*

Of all the cells of origin, only CD3 T cells displayed significant differences between the groups, with more CD3+ and PS-negative (-) events in the CSF from children with CM FO than children with CM FR. Although T cells were the only marker with significant differences, the other antibodies had similar trends (Figure 6.6, left column). The average number of antibody+ and PS- EVs in CSF from children with CM was similar for T cell, monocyte, platelet, and red blood cell origins, with only EVs from endothelial origin showing a slightly lower average (Figure 6.6, left column). In the CSF samples from children with combined CM and SMA, significantly more T cell-derived and PS- EVs were detected in patients with CM FO than in those with CM NCI (Figure 6.6, right column). There were also significantly more monocyte-derived and red blood cell-derived/PS- EVs in patients with CM FR than those with CM NCI (Figure 6.6, right column). The average number of EVs detected for each marker was approximately the same for all antibodies across all CSF samples from patients with CM and SMA (Figure 6.6, right column). Overall, children with CM had 2-3 times more PS- and antibody+ CSF EVs than children with both CM and SMA (Figure 6.6).

##### *6.3.4.2 Platelet-free plasma*

The antibody+/PS- PFP EVs showed no significant differences between the severe malaria outcomes for both main groups of patients, children with CM and children with both CM and SMA (Figure 6.7). However, the average trend showed that children with combined CM + SMA NCI had fewer antibody+/PS- PFP EVs for T cell, platelet, endothelial cell, and red blood cells of origin than the other two severe malaria outcomes (Figure 6.7, right column).

Similar to the levels of PS+ EVs described above, PS- and antibody+ EV levels were significantly higher in most PFP samples compared to the matching CSF (Figure 6.8). The significantly

elevated amounts of PFP EVs could once again indicate the activation of vascular cells during severe malaria.

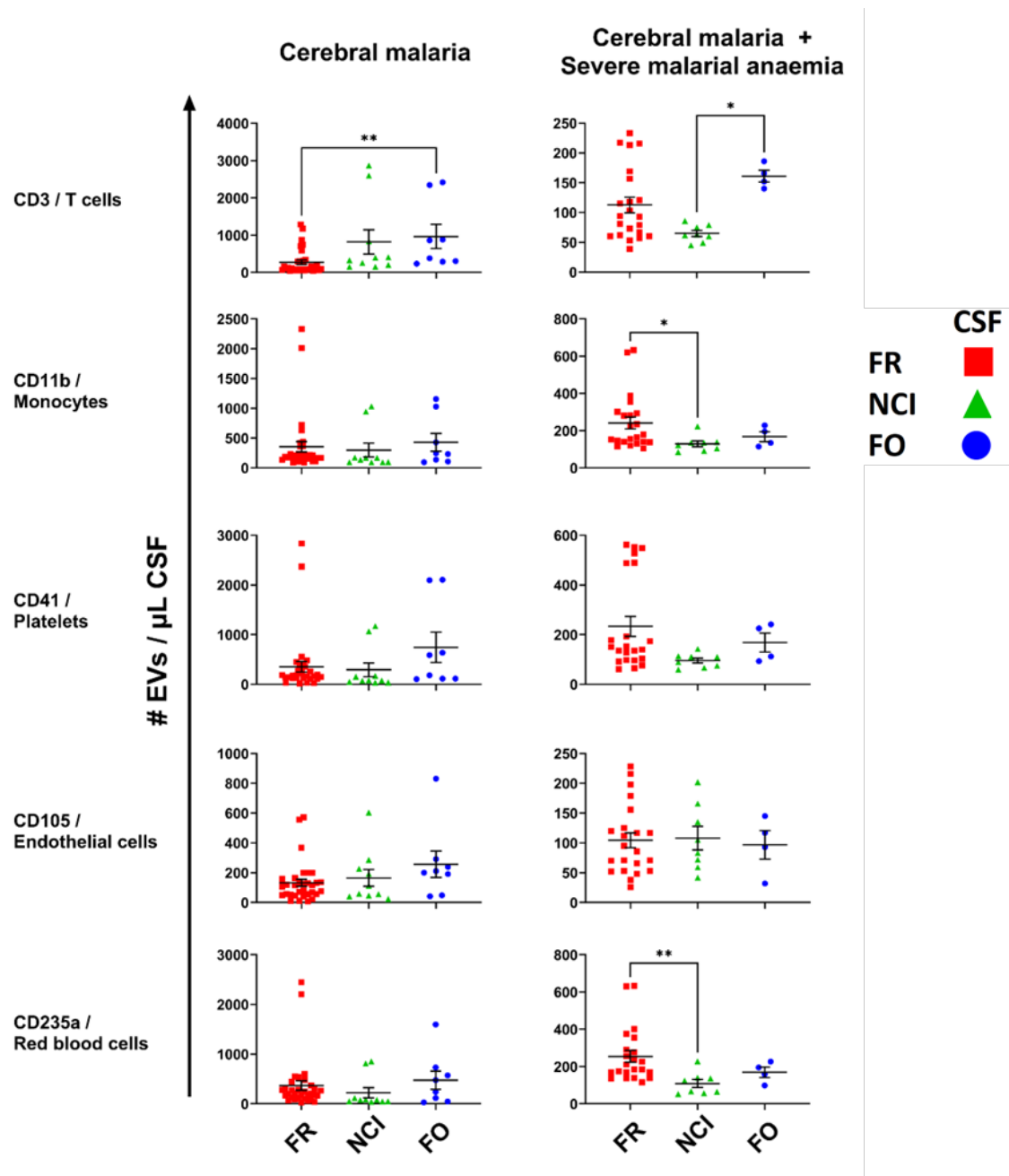


**Figure 6.6** Comparison of antibody-positive/annexin V-negative EVs in cerebrospinal fluid (CSF) between the different severe malaria outcomes. (Left column) Children with cerebral malaria (CM) FO had more T cell positive CSF EVs than FR, the other cellular markers were also higher in children with FO though not significantly. (Right column) Children with CM and severe malarial anaemia (SMA) FO had significantly more T cell EV in their CSF than those who developed NCI. Children with CM and SMA who developed NCI had significantly less monocyte and red blood cell positive CSF EV than those who fully recovered. Abbreviations: FO, fatal outcome; FR, full recovery; NCI, neurocognitive impairment.



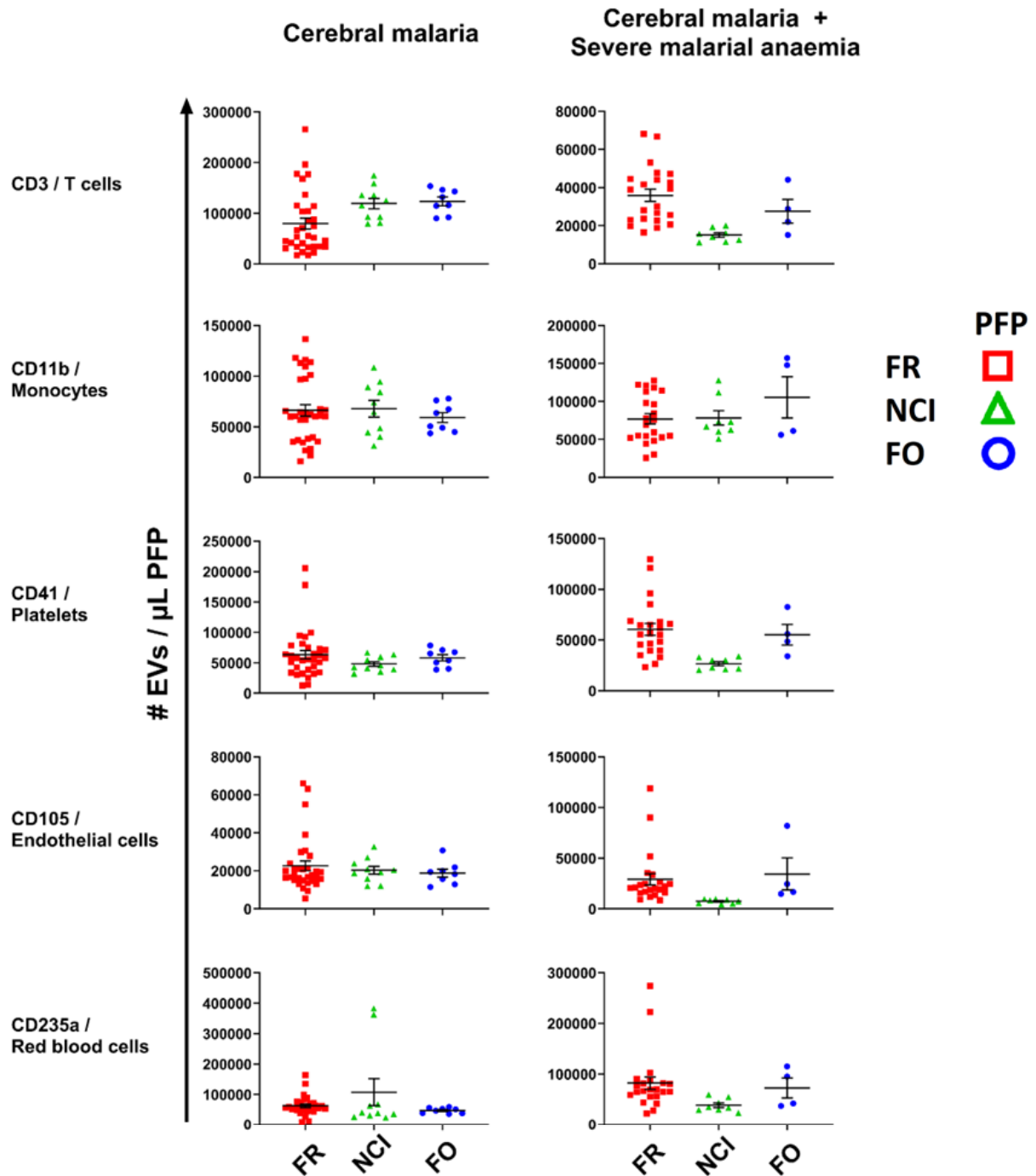


**Figure 6.7** Comparison of antibody-positive/annexin V-negative EVs in platelet-free plasma (PFP) between the different severe malaria outcomes. (Left and right columns) There were no significant differences in PFP EV populations for children with cerebral malaria (CM) and severe malarial anaemia (SMA). However, there was a slight trend showing children with CM and SMA who developed NCI had less antibody positive PFP EVs compared to the other patient groups. Abbreviations: FO, fatal outcome; FR, full recovery; NCI, neurocognitive impairment.

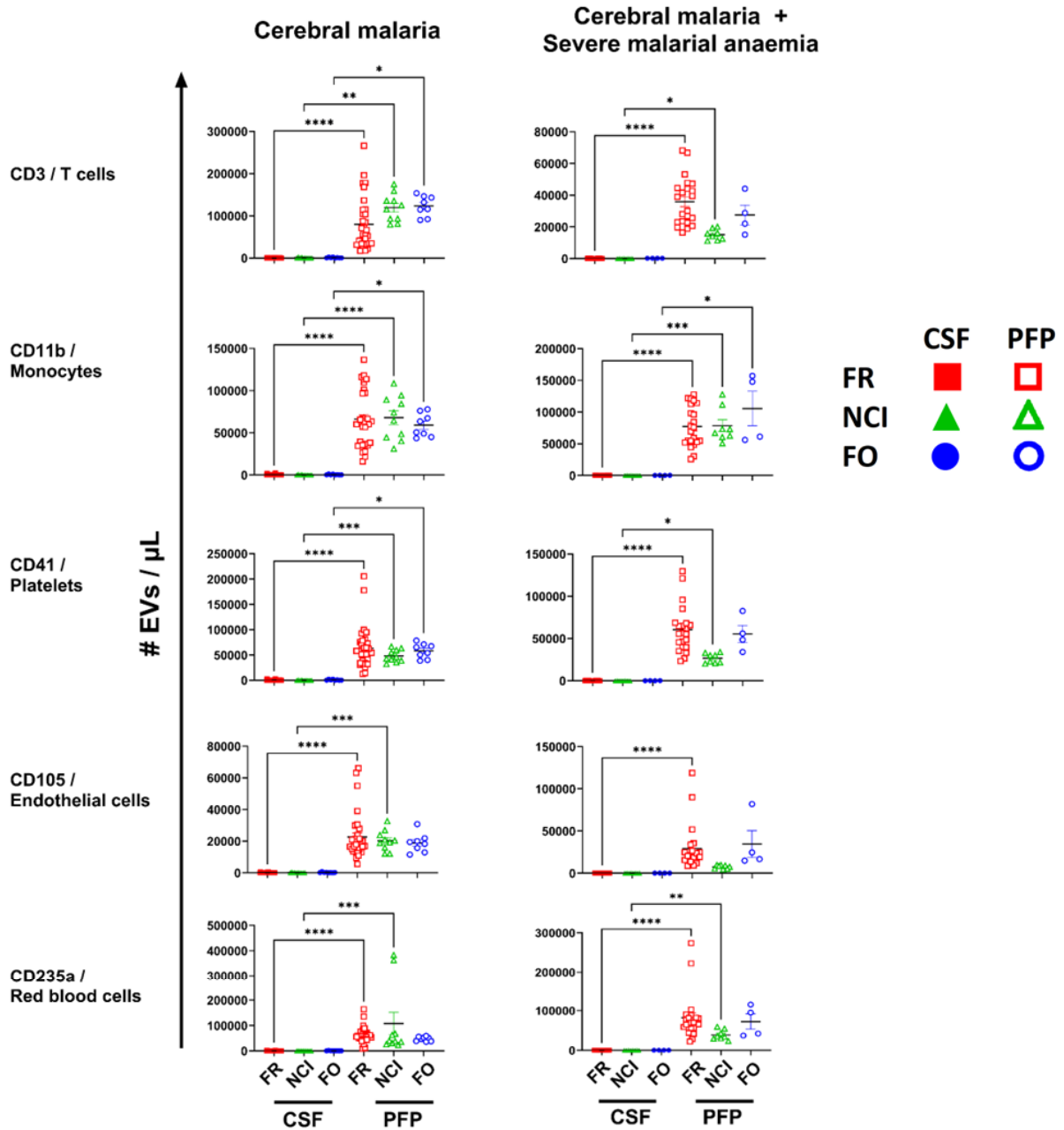


**Figure 6.8** Comparison of antibody-positive/annexin V-negative EVs between the cerebrospinal fluid (CSF) and platelet-free plasma (PFP) of children with severe malaria. (Left and right columns) There were significantly more EV in the PFP than CSF of children with cerebral malaria and those with also severe malarial anaemia. Abbreviations: FO, fatal outcome; FR, full recovery; NCI, neurocognitive impairment.

### 6.3.5 Antibody/PS double-positive profiles of EVs in CSF and PFP during severe malaria

#### 6.3.5.1 Cerebrospinal fluid

There were no significant differences in the number of CSF EVs positive for both PS and any vascular cell markers between the sub-groups of CM; however, the average trend showed lower numbers in the FR group compared to NCI and FO (Figure 6.9, left column). The average trend for double-positive CSF EVs in combined CM + SMA patients was higher in the children who fully recovered compared to those who developed NCI or had FO, with double-positive PS/CD41 EV counts being significantly higher in FR compared to NCI (Figure 6.9, right column). The number of PS+ CSF EVs detected for each vascular cell type was approximately the same among the CM CSF samples, likewise for the combined CM + SMA CSF samples (Figure 6.9). Overall, the average number of double-positive CSF EVs was 10-20 times higher in children with CM only than in those with both combined CM + SMA, especially for those with NCI and fatal outcomes (Figure 6.9).

#### 6.3.5.2 Platelet-free plasma

When comparing the PFP EVs in CM children, although not statistically significant, there was an observable trend for double-positive monocyte-, endothelial- and red blood cell-derived EVs where the average was higher in NCI compared to FR and FO (Figure 6.10, left column). In children with CM + SMA, the average number of double-positive monocytic PFP EVs was significantly higher in patients with fatal outcomes compared to the other two sub-groups (Figure 6.10, right column). Overall, the number of vascular cell-originating PFP EVs was approximately the same between the CM and CM + SMA patients (Figure 6.10).

The CM FR and CM NCI PFP detected significantly more PS+/antibody+ EVs than the matching CSF (Figure 6.11, left column). The EVs positive for PS and vascular cell markers appeared higher in the CM FO PFP than the matching CSF; however, only the T cell+ EVs were significantly higher (Figure 6.11, left column). For the sub-groups in children with both CM and SMA, the number of double-positive monocyte-, platelet- and red blood cell-derived PFP EVs was significantly higher than the matching CSF (Figure 6.11, right column). In addition, double-positive T cell EVs were more abundant in CM + SMA FR and NCI PFP than CSF; the FO sub-group had higher counts but not significantly (Figure 6.11, right column). The number of

endothelial/annexin double-positive CM + SMA EVs was also higher in PFP than in CSF, but only significantly for the FR sub-group (Figure 6.11, right column).

Similar to the above findings, PFP had more double-positive EVs than the matching CSF samples, possibly indicating more activation of vascular cell release of EVs (Figure 6.11). The differing amounts of EVs in CSF compared to PFP for the same phenotype may indicate different pathological processes in the brain vasculature compared to the blood vasculature.

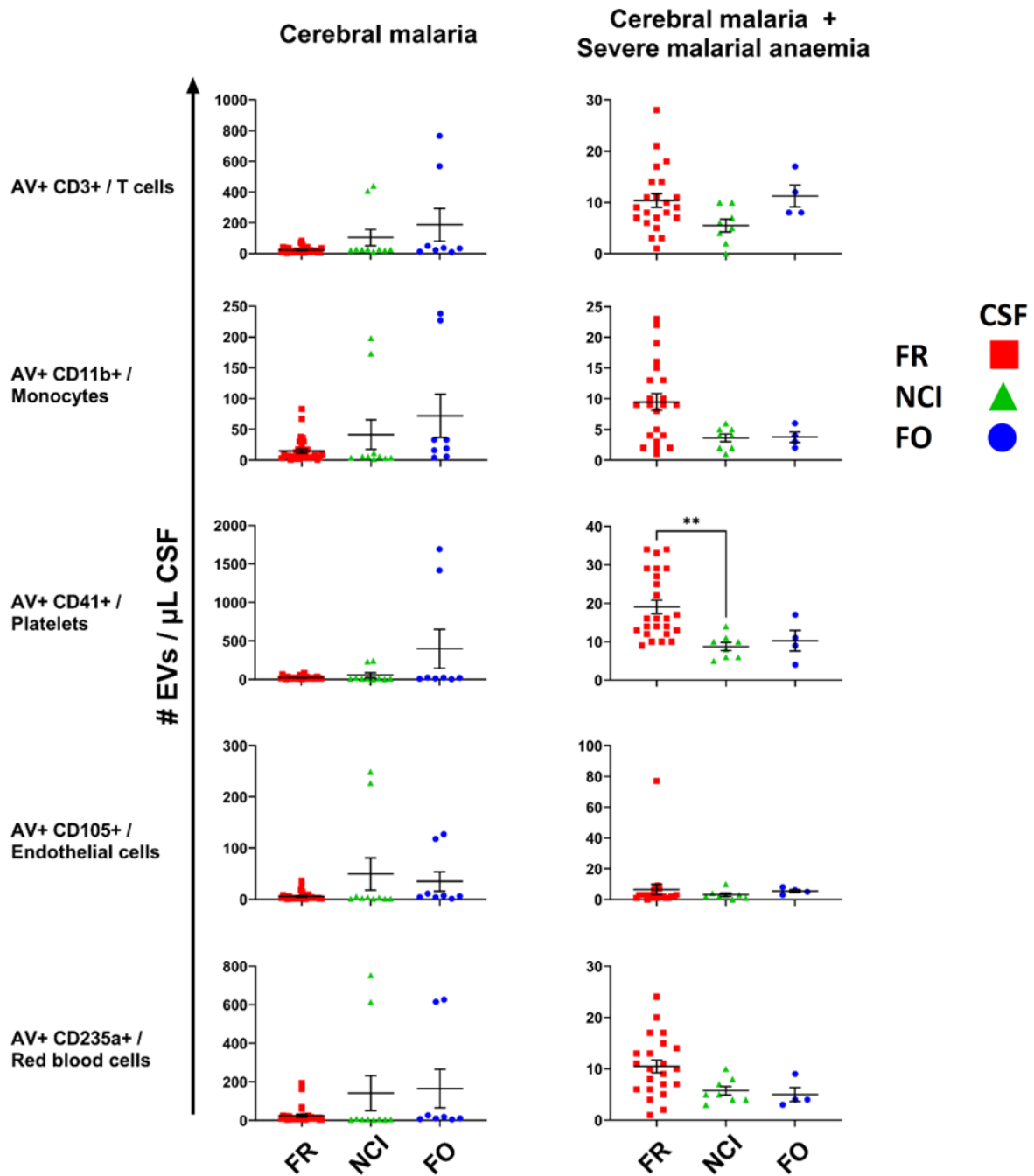


**Figure 6.9** Comparison of antibody-positive/annexin V-positive EVs in the cerebrospinal fluid (CSF) across the different severe malaria outcomes. (Left column) There were no significant differences between the outcomes of cerebral malaria (CM). However, the NCI and FO patients did show trend of more CSF EVs across all antibodies. (Right column) Children with CM and severe malarial anaemia who developed NCI had significantly less annexin V positive platelet CSF EVs than those who fully recovered, similar trends were seen in the other antibodies. Abbreviations: FO, fatal outcome; FR, full recovery; NCI, neurocognitive impairment.

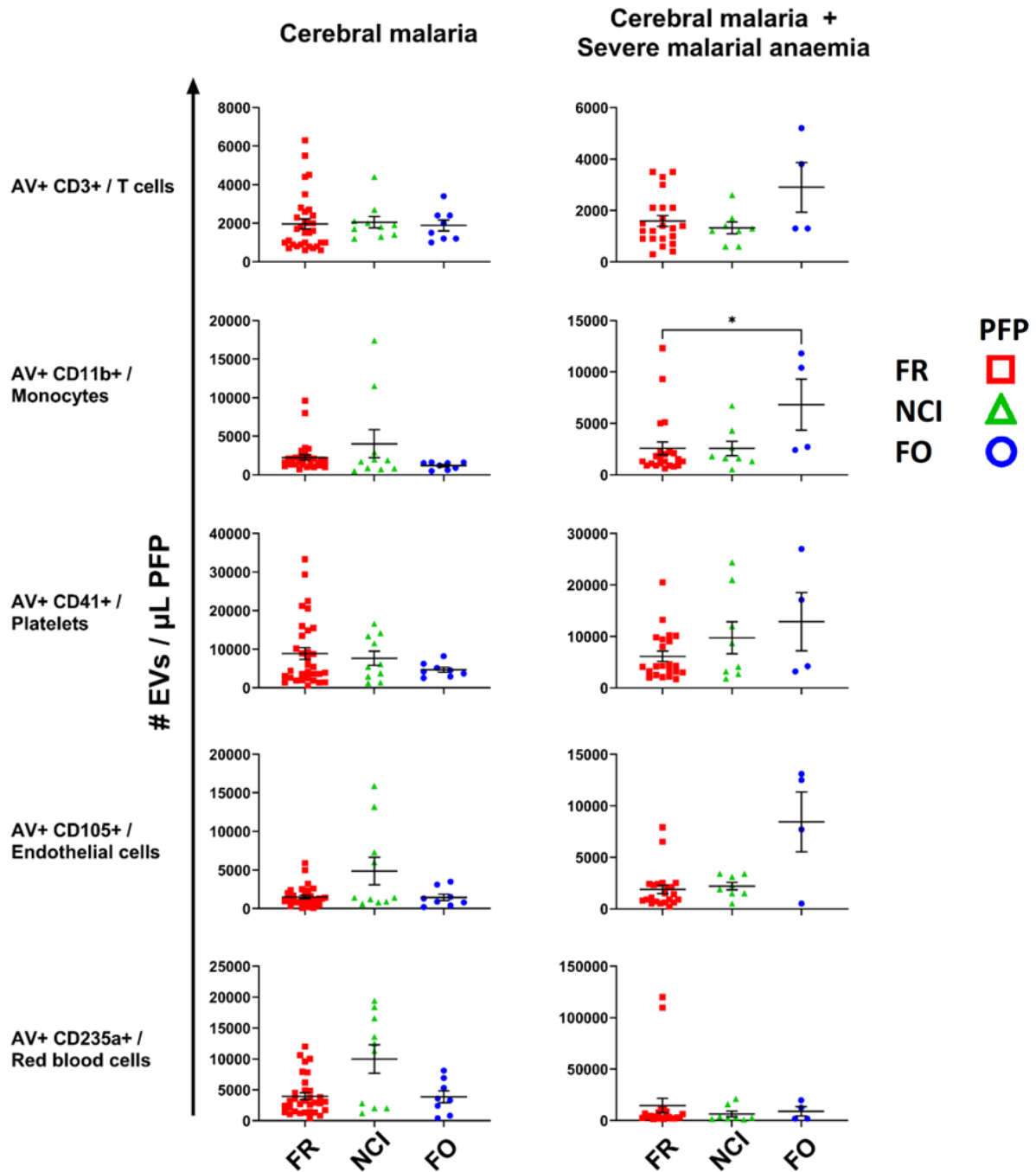


**Figure 6.10** Comparison of antibody-positive/annexin V-positive EVs in the platelet free plasma (PFP) across the different severe malaria outcomes. (Left column) There were no significant differences between the outcomes of cerebral malaria (CM). However, in the monocyte, endothelial, and red blood cell EVs NCI visually had more PFP EV than the other groups. (Right column) Children with CM and severe malarial anaemia FO had significantly more annexin V positive monocyte CSF EVs than those who fully recovered, similar trends were seen in the other antibodies. Abbreviations: FO, fatal outcome; FR, full recovery; NCI, neurocognitive impairment.

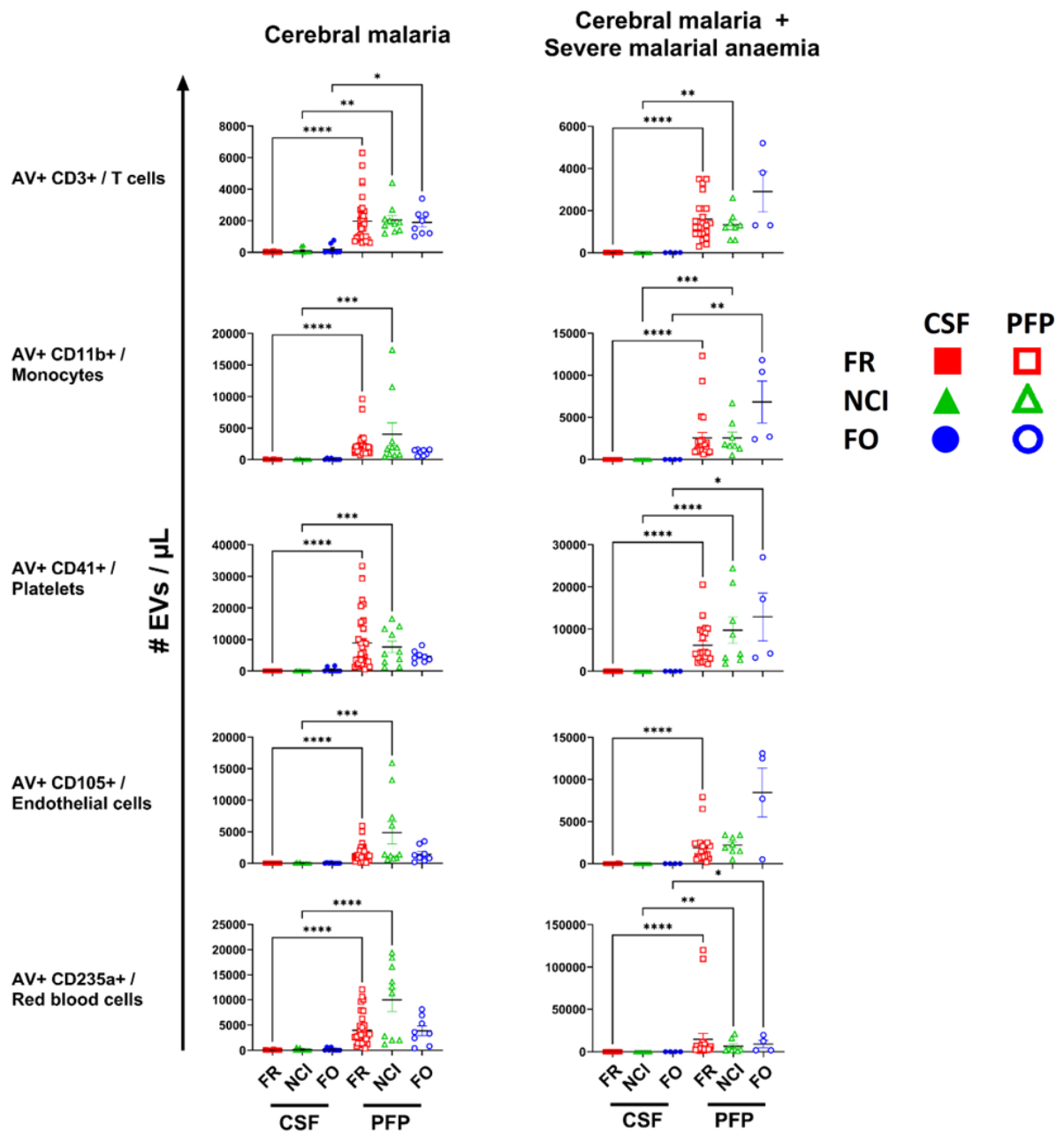


**Figure 6.11.** Comparison of antibody-positive/annexin V-positive EVs between the cerebrospinal fluid (CSF) and platelet-free plasma (PFP) across the different severe malaria outcomes. (Left and right columns) There were significantly more EV in the PFP than CSF of children with cerebral malaria and those with also severe malarial anaemia. Abbreviations: FO, fatal outcome; FR, full recovery; NCI, neurocognitive impairment.

### 6.3.6 Correlation between CSF and PFP EV profiles of severe malaria

Vascular phenotypes of EVs in CSF and PFP were compared to assess any potential association between the two sites (Figure 6.12). The closer the rank was to +1 or -1, the stronger the association; r-values between 0-0.30, 0.40-0.69, 0.70-0.89, and 0.90-1.00 have, respectively, weak (light blue/red), moderate, strong, and very strong (dark blue/red) correlations<sup>66</sup>. Correlations were performed for PS+ only, antibody+ only and double-positive PS/antibody analyses.

The Spearman's correlation matrices highlighted nine significant correlations (highlighted by yellow squares) among the patient sub-groups when comparing matching CSF and PFP samples (Figure 6.12). Seven of the nine significant correlations were for the EV profiles of children who developed NCI, specifically, six for CM and one for CM + SMA. The other two significant correlations were for children with CM FR and CM + SMA FR; however, both had much lower r-values. There was a moderate negative correlation for PS+ EVs from children with CM NCI ( $r = -0.62$ ,  $p\text{-value} = 0.0003$ ); this was the only significant correlation for PS+ EVs (Figure 6.12A). The antibody+ CM NCI EVs all had moderate to strong correlations, T cell only ( $r = -0.78$ ,  $p\text{-value} = 0.010$ , Figure 6.12B), platelet only ( $r = -0.77$ ,  $p\text{-value} = 0.013$ , Figure 6.12D), and endothelial cell only ( $r = -0.66$ ,  $p\text{-value} = 0.044$ , Figure 6.12E). Children with CM + SMA FR platelet+ EVs had significantly moderate correlations, although on the weaker end ( $r = -0.48$ ,  $p\text{-value} = 0.024$ , Figure 6.12D). As for the double-positive profiles, T cell+ EVs had weak correlations in CM FR children ( $r = -0.36$ ,  $p\text{-value} = 0.041$ ) but strong correlations in those with CM + SMA NCI ( $r = -0.88$ ,  $p\text{-value} = 0.007$ ) (Figure 6.12G). Lastly, double-positive EVs from children with CM NCI had strong correlations for endothelial+ EVs ( $r = -0.75$ ,  $p\text{-value} = 0.017$ , Figure 6.12J) and moderate correlation for red blood cell+ EVs ( $r = -0.69$ ,  $p\text{-value} = 0.030$ , Figure 6.12K). Overall, results indicated a moderate to strong negative correlation in the number of EVs in children with CM NCI (Figure 6.12).



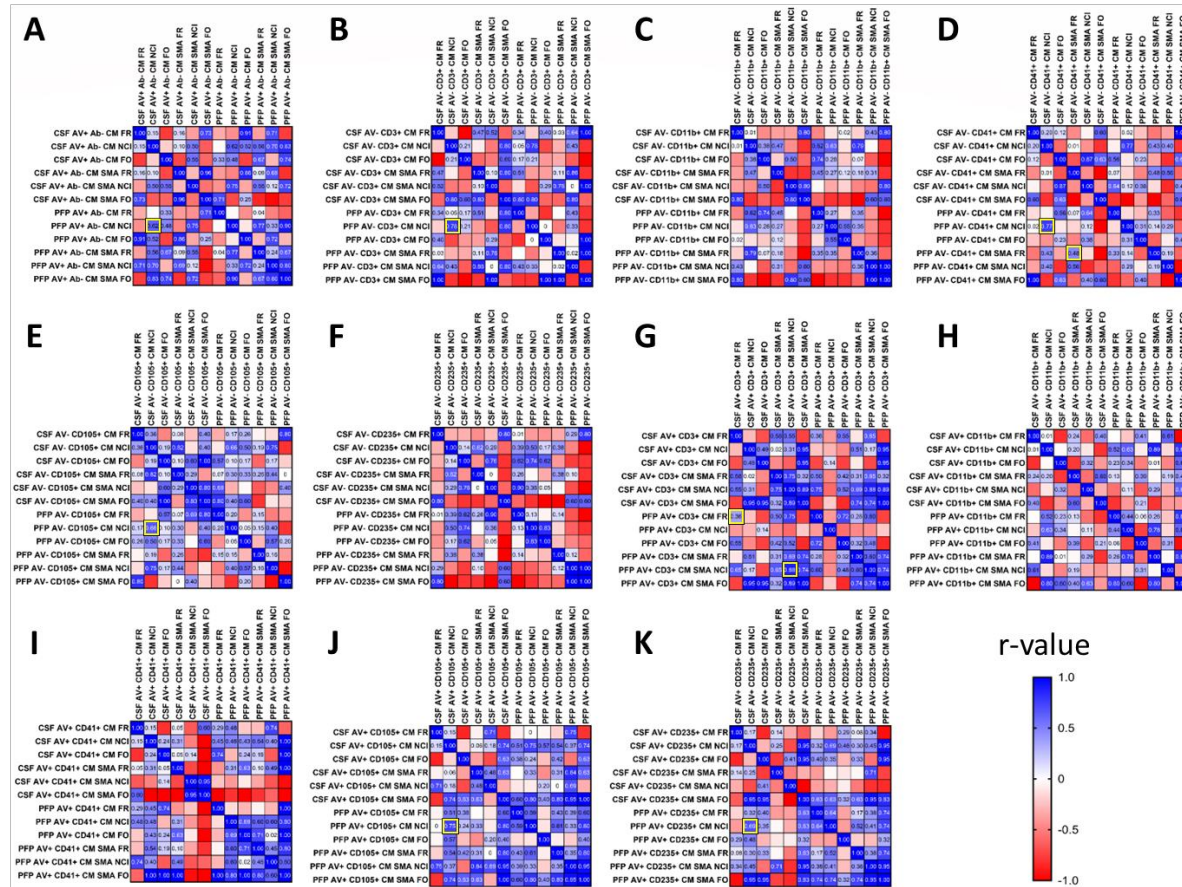


**Figure 6.12** Spearman's correlation matrix comparing the phenotypic profile of cerebrospinal fluid and platelet-free plasma extracellular vesicles from children with severe malaria. (A-K) The association between CSF and PFP is stronger the closer the rank is to +1 or -1, values between 0-0.30, 0.40-0.69, 0.70-0.89, and 0.90-1.00 have weak (light blue/red), moderate, strong, and very strong (dark blue/red) correlations, respectively. Significant correlations are highlighted with a yellow square. Overall, 9 comparisons were significantly correlated, six of them (CD3+, CD41+, CD105+, AV+CD105+ and AV+CD235+) had moderate to strong correlations and were in CM NCI patients, one (AV+CD3+) had strong correlations in CM SMA NCI patients, one (CD41+) had moderate correlations in CM SMA FR, and one (AV+CD3+) had weak correlations in CM FR. Abbreviations: AV, annexin V, CM, cerebral malaria; CSF, cerebrospinal fluid; FO, fatal outcome; FR, full recovery; NCI, neurocognitive impairment; PFP, platelet-free plasma; SMA, severe malarial anaemia. T cells (CD3), monocytes/macrophages (CD11b), platelets (CD41), endothelial cells (CD105), red blood cells (CD235a), positive (+), and negative (-).

## **6.4 Discussion**

EVs' essential roles in cell-to-cell communication during disease pathogenesis are increasingly recognised<sup>4,67,68</sup>. Flow cytometry remains a technique of choice to characterise EVs quantitatively and phenotypically in patients to study clinically relevant subpopulations. The presence of EVs in various accessible biofluids makes cytometric EV characterisation appealing for disease monitoring and longitudinal studies<sup>69</sup>. Studies have consistently shown for the past 20 years that elevated numbers of EVs in PFP are triggered by infections such as malaria<sup>38,67,70</sup>. This study, for the first time, has characterised EVs in the CSF and PFP of children with severe malaria and assessed the differences in EV numbers and cellular origin profiles depending on disease severity.

Previous studies on PFP EVs during malaria infection mainly investigated differences between clinical syndromes CM and SMA against healthy patients. In contrast, our study compared the EV populations and levels within a clinical presentation for different disease outcomes, i.e., full recovery, neurological impairment and fatal outcome in patients with either CM or combined CM and SMA. Only two studies have analysed CSF EVs in protozoan infections, but none during malaria. In Brazil, patients infected with *Toxoplasmosis gondii* had increased circulating serum EVs but not CSF EVs<sup>45</sup>. In the other study, patients from the Democratic Republic of the Congo infected with *Trypanosoma brucei gambiense* (Human African trypanosomiasis) had increased numbers of 'microvesicles' and specifically leukocyte 'microvesicles' were elevated in late-stage patient CSF compared to earlier stages<sup>46</sup>.

Using flow cytometry, the profiles of CSF and PFP EVs were analysed and compared after creating custom gates for the EV population using fluorescent beads for size estimation. The presence of PS was studied to investigate the total population of EVs. Although not consistently detectable in all subpopulations of EVs due to their low or absence of expression, PS allows the identification of EVs regardless of their cellular origin, providing a good approximation of the overall circulating EV population. Comparing paediatric patients with severe malaria showed that children with CM who died because of complications had more PS+ CSF EVs than those who survived, with or without future neurological deficits (Figure 6.4A). The trend identified aligns with the study on *Trypanosoma* in the Democratic Republic of the Congo, where the later, more severe stage of protozoan infection leads to increased EVs in CSF compared to the earlier stage<sup>46</sup>. However, the opposite was seen in the outcome

comparisons of patients with combined CM and SMA, and the overall number of PS+ CSF EVs in children with CM was higher than those with CM + SMA (Figure 6.4). This difference could hint at a possible change in pathogenesis within the ventricular system when the patient develops both CM and SMA.

Infections with protozoan parasites have been associated with EV production, and these EVs are thought to be involved in modulating the response of host cells and the pathogenesis of the disease<sup>71-74</sup>.

When the PFP of the same patients were analysed, our results exhibited the opposite to those in CSF, where children who fully recovered without complications had more PFP PS EVs than children with NCI or children who died (Figure 6.4C). The balance of anti- and pro-inflammatory responses is associated with the outcome of an individual's infection, where either side of the spectrum can lead to malaria complications<sup>75</sup>. The number of PS+ EVs in children with both CM and SMA was significantly higher than in children with only CM, and in the CM + SMA outcome comparisons, there were significantly more EVs in the children who died (Figure 6.4D). The involvement of severe anaemia might have contributed to the increase in EVs when the children died.

The different phenotypic profiles seen in children with combined symptoms of CM and SMA, where more PS+ CSF EVs were in the FR sub-group than NCI and FO, and more PS+ PFP EVs were in FO than FR, which could indicate syndrome-specific and non-specific changes due to varying degrees of inflammation (Figure 6.4B and D). Also, overall, children with CM had more PS+ EVs in their CSF and children with both CM and SMA had more PS+ EVs in their PFP. These differences between the CM and CM + SMA patients may reflect less cerebral activity and more vascular activity when the child also has SMA (Figure 6.4). The increase of PS+ PFP EVs in children with CM and SMA could also be attributed to extended hospital stays for SMA patients. Overall, PFP had higher numbers of PS+ EVs than CSF regardless of outcome or complication; this is similar to other neurological diseases such as Alzheimer's and dementia<sup>47</sup>.

The cellular origins of the PS- EVs were also compared, and once again, there were more EVs in the children with CM than both CM and SMA and more EVs in the PFP than CSF (Figure 6.6-8). The CSF from children with CM had an EV profile of T cells (leukocytes), platelets, monocytes, red blood cells, and endothelial cells, listed from most to least represented (Figure 6.6, left column). The CSF CM + SMA EV profile comprised monocytes, red blood cells,

platelets, T cells, and endothelial cells, listed from most to least represented (Figure 6.6, right column). Apart from endothelial EVs, the rest of the profile was reversed, which could indicate similar endothelial activation for both patient groups. For the PFP EVs, children with CM once again displayed higher numbers than those with CM + SMA (Figure 6.7). The CM PFP EV profile was T cells, monocytes, platelets, red blood cells, and endothelial cells, listed as most to least; the order was similar to the matching CSF EV profile (Figure 6.7, left column). As for children with both CM and SMA, the profile was monocytes, red blood cells, platelets, T cells, and endothelial cells, identical to the matching CSF (Figure 6.7, right column). Interestingly, the relative ratio of EVs per cellular marker was the same between PS- CSF and PFP EVs, with the number of endothelial cells EVs being the lowest.

Through the comparison of double-positive EVs, patients with CM once again had more EVs than those with CM + SMA, and PFP displayed more EVs than the corresponding CSF (Figure 6.9-11). The CM CSF EV profile was T cells, red blood cells, platelets, monocytes, and endothelial cells, listed most to least, and the CM + SMA CSF EV profiles was platelets, T cells, red blood cells, monocytes, and endothelial cells, listed most to least. The profiles were similar to the PS- comparisons except for the relatively lower monocytes EVs. The CM PFP EV profile included platelets, red blood cells, monocytes, endothelial cells, and T cells, which were listed as the most to least. Lastly, the CM + SMA PFP EV profile was red blood cells, platelets, monocytes, endothelial cells, and T cells. The double-positive PFP EVs seem to have shifted T cells to the least EVs, which could indicate a smaller population of large EVs, whereas the single-stained EVs had a relatively larger population of small EVs<sup>76</sup>. The comparisons suggest that many PS- EVs are most likely smaller EVs that need to be investigated further, as the 'microparticles' (larger EVs) have in the past 20 years.

Notably, when comparing the EV cellular origins of the different severe malaria outcomes, there were many differences; however, due to the limited number of patients in the more complex outcomes, NCI and FO, few were significant. However, when testing for CSF and PFP correlation, patients with CM NCI had the strongest negative correlation between CSF and PFP EV numbers, most likely due to syndrome-specific inflammatory responses. This indicates the need for studies to assess the pathogenic processes that occur within the CSF of patients with severe malaria, as it may provide insights into why these children develop impairments. Many variables seem to affect EV levels and phenotypical profiles of patients with malaria, such as age, endemic region, clinical history, and strength of immunity. Thus, matching these

details when analysing and comparing data is essential, as malaria pathogenesis is sufficiently complex. However, enforcing these differences excluded many patients from this study, decreasing the statistical strength of some cohorts, such as CM + SMA FO. Another limitation in this study is the duration of sample storage; some of the cohort was stored up to 13 years before analysis. Although past EV phenotyping studies have used plasma after long-term storage, CSF has not been in the field of malaria. Studies have shown that long-term storage of CSF does not affect specific biomarkers such as A $\beta$ <sub>1-42</sub>, T-tau, and P-tau<sup>77</sup>; however, not enough studies have shown the effect on surface markers, which could affect the antigenicity. New methods of staining to capture the entire population of EVs are still being developed. However, limitations still need to be overcome, such as unbound antibodies used during the staining process that should be removed by washing steps requiring long centrifuge times, leading to loss of EVs and low purification yield. A recent study has developed an antibody-free labelling method where only dyes are used during the staining process<sup>78</sup>. This method would be helpful in the detection of EVs that contain parasite DNA and allow for analysis without having to worry about unbound antibodies.

In combination with previous pathogenic results of EVs, this study highlights the potential for EVs to be used as biomarkers during severe malaria infection to distinguish the disease outcomes earlier and the potential to be pharmacological targets to decrease their production to protect from complications. Future studies are also needed to investigate the PS- portion of EVs to determine their subpopulations and the use of cohorts with a larger number of patients in the disease outcome groups.

## **Acknowledgements**

We are grateful to the children and their parents or guardians who participated in this study. We thank the study teams at Mulago Hospital, Makerere University, and the University of Minnesota for their commitment to treating the children and collecting the data. We also thank Beckman Coulter for assisting with the flow cytometry analysis with the CytoFLEX S.

## **Authors' contributions**

**Iris S. Cheng:** conceptualisation; investigation; methodology; data curation; formal analysis; validation; software; writing-original draft; writing-review & editing. **Natalie Sanders:** flow cytometry analysis; writing-review & editing. **Robert O. Opoka:** writing-review & editing. **Paul Bangirana:** writing-review & editing. **Chandy C. John:** writing-review & editing. **Valery Combes:** conceptualisation; funding acquisition; project administration; supervision; visualisation; formal analysis; writing-review & editing.

## **Competing interests**

The authors declare no competing interests.

## **Availability of data and material**

The data supporting this study's findings are available from the corresponding author upon reasonable request.

## **6.5 References**

1. György, B. *et al.* Detection and isolation of cell-derived microparticles are compromised by protein complexes resulting from shared biophysical parameters. *Blood* **117**, e39-48 (2011).
2. Palviainen, M. *et al.* Extracellular vesicles from human plasma and serum are carriers of extravesicular cargo-Implications for biomarker discovery. *PLoS ONE* **15**, e0236439 (2020).
3. Regev-Rudzki, N. *et al.* Cell-cell communication between malaria-infected red blood cells via exosome-like vesicles. *Cell* **153**, 1120–1133 (2013).
4. Sampaio, N. G., Cheng, L. & Eriksson, E. M. The role of extracellular vesicles in malaria biology and pathogenesis. *Malar. J.* **16**, 245 (2017).
5. Nantakomol, D. *et al.* Circulating red cell-derived microparticles in human malaria. *J. Infect. Dis.* **203**, 700–706 (2011).
6. Pankoui Mfonkeu, J. B. *et al.* Elevated cell-specific microparticles are a biological marker for cerebral dysfunctions in human severe malaria. *PLoS ONE* **5**, e13415 (2010).
7. Sahu, U., Mohapatra, B. N., Kar, S. K. & Ranjit, M. Promoter polymorphisms in the ATP binding cassette transporter gene influence production of cell-derived microparticles and are highly associated with susceptibility to severe malaria in humans. *Infect. Immun.* **81**, 1287–1294 (2013).
8. Sahu, U., Sahoo, P. K., Kar, S. K., Mohapatra, B. N. & Ranjit, M. Association of TNF level with production of circulating cellular microparticles during clinical manifestation of human cerebral malaria. *Hum. Immunol.* **74**, 713–721 (2013).
9. Nantakomol, D. *et al.* Quantitation of cell-derived microparticles in plasma using flow rate based calibration. *Southeast Asian J. Trop. Med. Public Health* **39**, 146–153 (2008).
10. Combes, V. *et al.* Circulating endothelial microparticles in malawian children with severe falciparum malaria complicated with coma. *JAMA* **291**, 2542–2544 (2004).

11. Larssen, P. *et al.* Tracing cellular origin of human exosomes using multiplex proximity extension assays. *Mol. Cell. Proteomics* **16**, 502–511 (2017).
12. Antwi-Baffour, S. S. Molecular characterisation of plasma membrane-derived vesicles. *J. Biomed. Sci.* **22**, 68 (2015).
13. McVey, M. J., Spring, C. M. & Kuebler, W. M. Improved resolution in extracellular vesicle populations using 405 instead of 488 nm side scatter. *J. Extracell. Vesicles* **7**, 1454776 (2018).
14. Brittain, G. C. *et al.* A Novel Semiconductor-Based Flow Cytometer with Enhanced Light-Scatter Sensitivity for the Analysis of Biological Nanoparticles. *Sci. Rep.* **9**, 16039 (2019).
15. Tian, Y. *et al.* Quality and efficiency assessment of six extracellular vesicle isolation methods by nano-flow cytometry. *J. Extracell. Vesicles* **9**, 1697028 (2020).
16. FACSymphony™ A1 | Laser Cell Analyzer. *BD FACSymphony™ A1 Cell Analyzer* <https://www.bdbiosciences.com/en-us/products/instruments/flow-cytometers/research-cell-analyzers/bd-facsymphony-a1> (2023).
17. Chen, H. *et al.* Exosomes, a new star for targeted delivery. *Front. Cell Dev. Biol.* **9**, 751079 (2021).
18. Kalluri, R. & LeBleu, V. S. The biology, function, and biomedical applications of exosomes. *Science* **367**, eaau6977 (2020).
19. Cox, F. E. History of the discovery of the malaria parasites and their vectors. *Parasit. Vectors* **3**, 5 (2010).
20. World Health Organization. *World malaria report 2023*. Geneva: World Health Organization; Licence:CC BY-NC-SA 3.0 IGO. <https://www.who.int/publications/i/item/9789240086173> (2023).
21. World Health Organization. *World malaria report 2022*. Geneva: World Health Organization; Licence:CC BY-NC-SA 3.0 IGO. <https://www.who.int/publications/i/item/9789240064898> (2022).
22. Winskill, P. *et al.* Estimating the burden of severe malarial anaemia and access to hospital care in East Africa. *Nat. Commun.* **14**, 5691 (2023).



23. Taylor, C., Namaste, S. M. L., Lowell, J., Useem, J. & Yé, Y. Estimating the Fraction of Severe Malaria among Malaria-Positive Children: Analysis of Household Surveys in 19 Malaria-Endemic Countries in Africa. *Am. J. Trop. Med. Hyg.* **104**, 1375–1382 (2021).
24. World Health Organization. *World malaria report 2019*. Geneva: World Health Organization; Licence:CC BY-NC-SA 3.0 IGO. <https://www.who.int/publications/i/item/9789241565721> (2019).
25. Cowman, A. F., Healer, J., Marapana, D. & Marsh, K. Malaria: biology and disease. *Cell* **167**, 610–624 (2016).
26. Combes, V. *et al.* Microvesiculation and cell interactions at the brain-endothelial interface in cerebral malaria pathogenesis. *Prog. Neurobiol.* **91**, 140–151 (2010).
27. Langfitt, J. T. *et al.* Neurodevelopmental impairments 1 year after cerebral malaria. *Pediatrics* **143**, (2019).
28. Cheng, I. S., Sealy, B. C., Tiberti, N. & Combes, V. Extracellular vesicles, from pathogenesis to biomarkers: the case for cerebral malaria. *VP* **2020**, (2020).
29. Perkins, D. J. *et al.* Severe malarial anemia: innate immunity and pathogenesis. *Int. J. Biol. Sci.* **7**, 1427–1442 (2011).
30. Phiri, K. *et al.* Intermittent preventive therapy for malaria with monthly artemether-lumefantrine for the post-discharge management of severe anaemia in children aged 4-59 months in southern Malawi: a multicentre, randomised, placebo-controlled trial. *Lancet Infect. Dis.* **12**, 191–200 (2012).
31. Severe malaria. *Trop. Med. Int. Health* **19 Suppl 1**, 7–131 (2014).
32. Bassat, Q. *et al.* Severe malaria and concomitant bacteraemia in children admitted to a rural Mozambican hospital. *Trop. Med. Int. Health* **14**, 1011–1019 (2009).
33. Bangirana, P. *et al.* Severe malarial anemia is associated with long-term neurocognitive impairment. *Clin. Infect. Dis.* **59**, 336–344 (2014).
34. Bangirana, P. *et al.* Neurocognitive domains affected by cerebral malaria and severe malarial anemia in children. *Learn. Individ. Differ.* **46**, 38–44 (2016).

35. Bruneel, F. Human cerebral malaria: 2019 mini review. *Rev Neurol (Paris)* **175**, 445–450 (2019).
36. Nakitende, A. J. *et al.* Severe malaria and academic achievement. *Pediatrics* **151**, (2023).
37. Rosa-Gonçalves, P., Ribeiro-Gomes, F. L. & Daniel-Ribeiro, C. T. Malaria related neurocognitive deficits and behavioral alterations. *Front. Cell. Infect. Microbiol.* **12**, 829413 (2022).
38. Opadokun, T. & Rohrbach, P. Extracellular vesicles in malaria: an agglomeration of two decades of research. *Malar. J.* **20**, 442 (2021).
39. Babatunde, K. A. *et al.* Role of extracellular vesicles in cellular cross talk in malaria. *Front. Immunol.* **11**, 22 (2020).
40. Mantel, P.-Y. *et al.* Malaria-infected erythrocyte-derived microvesicles mediate cellular communication within the parasite population and with the host immune system. *Cell Host Microbe* **13**, 521–534 (2013).
41. Freyssinet, J. M. Cellular microparticles: what are they bad or good for? *J. Thromb. Haemost.* **1**, 1655–1662 (2003).
42. Combes, V., Coltel, N., Faille, D., Wassmer, S. C. & Grau, G. E. Cerebral malaria: role of microparticles and platelets in alterations of the blood-brain barrier. *Int. J. Parasitol.* **36**, 541–546 (2006).
43. El-Assaad, F., Wheway, J., Hunt, N. H., Grau, G. E. R. & Combes, V. Production, fate and pathogenicity of plasma microparticles in murine cerebral malaria. *PLoS Pathog.* **10**, e1003839 (2014).
44. Faille, D. *et al.* Platelet microparticles: a new player in malaria parasite cytoadherence to human brain endothelium. *FASEB J.* **23**, 3449–3458 (2009).
45. da Cruz, A. B. *et al.* Human extracellular vesicles and correlation with two clinical forms of toxoplasmosis. *PLoS ONE* **15**, e0229602 (2020).
46. Dozio, V. *et al.* Cerebrospinal Fluid-Derived Microvesicles From Sleeping Sickness Patients Alter Protein Expression in Human Astrocytes. *Front. Cell. Infect. Microbiol.* **9**, 391 (2019).

47. Longobardi, A. *et al.* Cerebrospinal Fluid EV Concentration and Size Are Altered in Alzheimer's Disease and Dementia with Lewy Bodies. *Cells* **11**, (2022).
48. Mobarrez, F. *et al.* Microparticles and microscopic structures in three fractions of fresh cerebrospinal fluid in schizophrenia: case report of twins. *Schizophr. Res.* **143**, 192–197 (2013).
49. Datta, D. *et al.* Elevated Cerebrospinal Fluid Tau Protein Concentrations on Admission Are Associated With Long-term Neurologic and Cognitive Impairment in Ugandan Children With Cerebral Malaria. *Clin. Infect. Dis.* **70**, 1161–1168 (2020).
50. Conroy, A. L. *et al.* Cerebrospinal fluid biomarkers provide evidence for kidney-brain axis involvement in cerebral malaria pathogenesis. *Front. Hum. Neurosci.* **17**, 1177242 (2023).
51. Datta, D. *et al.* Association of Plasma Tau With Mortality and Long-term Neurocognitive Impairment in Survivors of Pediatric Cerebral Malaria and Severe Malarial Anemia. *JAMA Netw. Open* **4**, e2138515 (2021).
52. Li, Y. *et al.* EV-origin: Enumerating the tissue-cellular origin of circulating extracellular vesicles using exLR profile. *Comput. Struct. Biotechnol. J.* **18**, 2851–2859 (2020).
53. Doyle, L. M. & Wang, M. Z. Overview of extracellular vesicles, their origin, composition, purpose, and methods for exosome isolation and analysis. *Cells* **8**, (2019).
54. Brenner, A. W., Su, G. H. & Momen-Heravi, F. Isolation of extracellular vesicles for cancer diagnosis and functional studies. *Methods Mol. Biol.* **1882**, 229–237 (2019).
55. Hallal, S., Túzesi, Á., Grau, G. E., Buckland, M. E. & Alexander, K. L. Understanding the extracellular vesicle surface for clinical molecular biology. *J. Extracell. Vesicles* **11**, e12260 (2022).
56. Mathews, P. M. & Levy, E. Exosome production is key to neuronal endosomal pathway integrity in neurodegenerative diseases. *Front. Neurosci.* **13**, 1347 (2019).
57. Sanz-Ros, J. *et al.* Extracellular vesicles as therapeutic resources in the clinical environment. *Int. J. Mol. Sci.* **24**, (2023).
58. Buzas, E. I. The roles of extracellular vesicles in the immune system. *Nat. Rev. Immunol.* **23**, 236–250 (2023).

59. Wang, K. & Zeng, C. Extracellular vesicles and obesity. *Adv. Exp. Med. Biol.* **1418**, 143–153 (2023).
60. Zeng, Y. *et al.* Biological features of extracellular vesicles and challenges. *Front. Cell Dev. Biol.* **10**, 816698 (2022).
61. Bangirana, P. *et al.* Malaria with neurological involvement in Ugandan children: effect on cognitive ability, academic achievement and behaviour. *Malar. J.* **10**, 334 (2011).
62. Shabani, E. *et al.* High plasma erythropoietin levels are associated with prolonged coma duration and increased mortality in children with cerebral malaria. *Clin. Infect. Dis.* **60**, 27–35 (2015).
63. John, C. C. *et al.* Cerebral malaria in children is associated with long-term cognitive impairment. *Pediatrics* **122**, e92-9 (2008).
64. Idro, R., Marsh, K., John, C. C. & Newton, C. R. J. Cerebral malaria: mechanisms of brain injury and strategies for improved neurocognitive outcome. *Pediatr. Res.* **68**, 267–274 (2010).
65. Misra, U. K. *et al.* Cerebral malaria and bacterial meningitis. *Ann. Indian Acad. Neurol.* **14**, S35-9 (2011).
66. Akoglu, H. User's guide to correlation coefficients. *Turk. J. Emerg. Med.* **18**, 91–93 (2018).
67. Mantel, P.-Y. & Marti, M. The role of extracellular vesicles in Plasmodium and other protozoan parasites. *Cell. Microbiol.* **16**, 344–354 (2014).
68. Liu, Y.-J. & Wang, C. A review of the regulatory mechanisms of extracellular vesicles-mediated intercellular communication. *Cell Commun. Signal.* **21**, 77 (2023).
69. Lucchetti, D. *et al.* Measuring extracellular vesicles by conventional flow cytometry: dream or reality? *Int. J. Mol. Sci.* **21**, (2020).
70. Coltel, N., Combes, V., Wassmer, S. C., Chimini, G. & Grau, G. E. Cell vesiculation and immunopathology: implications in cerebral malaria. *Microbes Infect.* **8**, 2305–2316 (2006).

71. Szempruch, A. J., Dennison, L., Kieft, R., Harrington, J. M. & Hajduk, S. L. Sending a message: extracellular vesicles of pathogenic protozoan parasites. *Nat. Rev. Microbiol.* **14**, 669–675 (2016).
72. Twu, O. *et al.* Trichomonas vaginalis exosomes deliver cargo to host cells and mediate host:parasite interactions. *PLoS Pathog.* **9**, e1003482 (2013).
73. Buck, A. H. *et al.* Exosomes secreted by nematode parasites transfer small RNAs to mammalian cells and modulate innate immunity. *Nat. Commun.* **5**, 5488 (2014).
74. Silverman, J. M. *et al.* Leishmania exosomes modulate innate and adaptive immune responses through effects on monocytes and dendritic cells. *J. Immunol.* **185**, 5011–5022 (2010).
75. Kumar, R., Ng, S. & Engwerda, C. The Role of IL-10 in Malaria: A Double Edged Sword. *Front. Immunol.* **10**, 229 (2019).
76. Jeppesen, D. K. *et al.* Reassessment of exosome composition. *Cell* **177**, 428–445.e18 (2019).
77. Willemse, E. A. J., van Uffelen, K. W. J., van der Flier, W. M. & Teunissen, C. E. Effect of long-term storage in biobanks on cerebrospinal fluid biomarker A $\beta$ 1-42, T-tau, and P-tau values. *Alzheimers Dement (Amst)* **8**, 45–50 (2017).
78. Dekel, E. *et al.* Antibody-Free Labeling of Malaria-Derived Extracellular Vesicles Using Flow Cytometry. *Biomedicines* **8**, (2020).

**Chapter Seven:**  
**Concluding remarks and future  
directions**

## Chapter 7: Concluding remarks and future directions

Research and knowledge on the *Plasmodium* parasite's complex biology and pathophysiology has exponentially grown. Novel findings have allowed the development of malaria prevention strategies, antimalarial treatment, and vaccinations, significantly decreasing malaria's incidence and death rates<sup>111</sup>. An estimated 2.1 billion cases of malaria and 11.7 million deaths were avoided globally between the years 2000 and 2022<sup>5</sup>.

Even with so much success, malaria still poses significant global health issues; where in 2022, 249 million cases and 608,000 deaths occurred, as morbidity and mortality rates have stalled since 2015, the COVID-19 pandemic further impacted this<sup>5</sup>. Not all *P. falciparum* infections lead to severe malaria, i.e., ~4.5% of symptomatic patients. However, because the patients at highest risk are usually young children, early detection, diagnosis and treatment are crucial to saving lives<sup>1,50,51</sup>.

Currently, malaria is a treatable and curable disease if treatment is provided without delay; however, this can be difficult in countries where hospital care and access are poor. Therefore, with delayed intervention, notably for children under five years old, malaria infection can quickly evolve into severe and lethal complications with a mortality rate of up to 30% and neurocognitive impairment in 25-50% of survivors<sup>53,65-67,73,74,112,113</sup>. Many adjunctive therapies to prevent complications have been investigated, but success has been minimal with contrasting results; this could be due to late administration<sup>114</sup>. Hence, the need for markers that can predict children who will develop severe complications is essential, as physicians can then provide prompt and effective treatment using antimalarial agents and combination therapy to minimise harm and neurocognitive impairment<sup>114</sup>.

This PhD aimed to investigate extracellular vesicles in the plasma and cerebrospinal fluid of patients with severe or uncomplicated malaria from Uganda and Thailand. Sensitive and accurate high-throughput techniques such as next-generation sequencing, mass spectroscopy and flow cytometry were used to discover biomarkers of disease severity that allow for the early identification of children at risk of developing lethal complications. These techniques also allowed for a better understanding of the composition and cellular origin of the circulating EVs and their potential role in disease pathogenesis.

Most biomarkers studied for severe malaria distinguish uncomplicated malaria from CM and SMA, with only a few studies focusing on biomarkers to determine disease severity and

outcomes and even fewer investigating prognostic biomarkers of severe disease outcome. A common source of biomarkers for disease is blood, as it is commonly collected during routine clinical assessments. In the past, most of the potential plasma biomarkers investigated were proteins, and only until advancements in transcriptomics did studies shift to investigate miRNAs as plasma biomarkers. CSF is also an essential source of biomarkers in severe malaria, as cerebral dysfunction is a large part of CM pathogenesis. CSF protein profiles in children with CM have been reported to differ from those of other encephalopathies, and these CM unique proteins suggest distinct pathophysiological mechanisms that occur in the CSF<sup>115</sup>. Thus, it would be beneficial to investigate CSF content in severe malaria cases for biomarkers linked to severity, as most are investigating diagnostic markers, and only a handful are studying markers to predict disease outcomes.

In this thesis, we explored EVs in the context of different clinical presentations of malaria infection: uncomplicated malaria in Thai adult patients infected with *P. falciparum* or *P. vivax* (Chapter 3), cerebral malaria and severe malarial anaemia in children from Uganda with a further dichotomy into children who survived without complication and those who either developed neurological impairment or succumbed to the disease (Chapters 4 and 5). We further compared EVs from plasma to those present in the cerebrospinal fluid in the children from the Ugandan cohort who developed cerebral malaria or a combination of cerebral malaria and severe malarial anaemia (Chapter 6). This unique combination of patient profiles allowed us to better understand the EV profile and cargo during different disease outcomes. The detection of miRNAs in EVs isolated from healthy Thai adult patients and those with uncomplicated malaria showed that miRNA expressions differed depending on the species of *Plasmodium* the person is infected with (Chapter 3). The differences between *P. falciparum* and *P. vivax* indicated possible differences in pathogenesis, even in uncomplicated malaria. They supported the notion that EVs in malaria carry potential markers of disease severity. Differentially expressed miRNAs and proteins were then identified in plasma-EVs from children with *P. falciparum* severe malaria, distinguishing the disease outcomes within a syndrome (CM or SMA) (Chapters 4 and 5). We observed differences in the miRNA and proteins packaged in EVs before the children fully recovered or developed NCI or succumbed, and these differences appeared to be related to the patient's age, suggesting a relationship with the maturity of the immune system. The EV proteome results also identified proteins strongly associated with inflammation, immune activation, liver damage, cellular signalling



and communication, and developmental pathways within plasma-EVs of children with CM who later succumbed to infection and SMA children who, after treatment, developed NCI. The EV profiles for severe malaria disease outcomes were then phenotypically characterised to show where the EVs are coming from in circulation and the ventricular system (Chapter 6). Interestingly, children with CM NCI had negatively correlated CSF and plasma EV profiles, indicating distinct pathways of pathogenesis occurring in the CSF, which can be inversely reflected in the plasma.

This thesis reports minimally invasive prognostic biomarkers of severe malaria, which have the potential to be used in regions such as Sub-Saharan Africa to identify children at risk of persistent NCI. These markers require additional validation in children from various malaria-endemic countries, and if validated as prognostic biomarkers, an EV point-of-care test for children at risk of mortality and NCI can be identified and subsequently provided cognitive rehabilitation and relevant combination therapy and antimalarials. Researchers must also ensure that new techniques are cost-effective, minimally invasive, easy to use, and provide rapid, highly accurate results. One of the main concerns for EV biomarkers is how to implement their use in resource-limited countries, as consistent EV isolation can be challenging<sup>110</sup>. Last year, a team in Switzerland compared polyethylene glycol and sodium acetate precipitation methods of EV isolation and found both to be efficient purification methods<sup>116</sup>. This would eliminate the need for ultracentrifugation or expensive isolation columns, with the addition of easily scalable procedures<sup>116</sup>. Biomarker point-of-care tests are also advancing, protein rapid tests have been clinically used for many years now; however, miRNA tests are still being developed. Currently, various promising miRNA detection techniques such as chemiluminescence, bioluminescence, fluorescent, and colourimetric are being researched<sup>117</sup>. The detection limit is also promising, with some enzymatic chromogenic-based colourimetric detection methods measuring 0.15aM ( $10^{-18}$ ) of serum miRNA in 5 minutes<sup>118</sup>. These pocket-sized devices with visual readout methods would greatly improve diagnostic and prognostic test availability in the field and in resource-limited countries such as Uganda, as expensive machinery is not required<sup>117</sup>. Even though these point-of-care devices are promising, research is still required for multiplex miRNA and protein detection, as it is difficult to make the device accurate, small and affordable. Extensive clinical testing will also be necessary prior to deployment for clinician use.

The findings need further validation before moving on to prognostic devices, as this is the first time plasma-EVs from severe malaria paediatric patients have been investigated via high-throughput -omic techniques. Although the number of samples can be lower when performing -omics studies, the validation should be performed with greater patient numbers to increase the study's power, which was not possible for this thesis, as there were not enough qualifying patients to meet the strict criteria. Future studies with at least 50 patients per group would be the next step to validate these findings, followed by comparing other endemic countries. In addition, we were also restricted with the number of CSF samples, as they can only be collected from patients with cerebral malaria or other encephalopathies. Thus, we could not compare CSF-EV profiles to healthy children or children with only severe malarial anaemia. Using the EV phenotype profiles highlighted in this thesis as a starting point, future studies can build upon the marker panels to include additional circulatory and ventricular system markers to elucidate the different cellular activity further. In this thesis, healthy individuals were analysed alongside malaria patients to confirm the presence or quantity of markers and EVs. During validation studies, additional patient groups, such as asymptomatic and uncomplicated malaria, could strengthen the sensitivity and specificity of these prognostic markers, allowing treatment as early as feasible. There were also limitations in the transcriptomics analysis; an exogenous control, cel-miR-39-3p, was added during RNA isolation for both NGS and RT-qPCR samples; however, due to time constraints, the exogenous control was not run via RT-qPCR. Instead, an endogenous control, hsa-miR-16-5p was selected for RT-qPCR normalisation. Although hsa-miR-16-5p has previously been used in malaria RT-qPCR studies for normalisation, if time had permitted, exogenous control cel-miR-39-3p would have been a better choice.

The EVs' transcriptomic, proteomic, and phenotypic profiles from children with severe malaria have all shown potential as prognostic biomarkers for disease outcome/severity. To further increase sensitivity and specificity, these biomarkers can be combined into a panel to differentiate severe malaria outcomes accurately. However, when doing so, it is essential to match clinical data, age and region, as done in this thesis, as these factors may affect the results. This thesis further highlights the importance of future studies investigating the pathophysiology of severe malaria to develop a more efficient and effective treatment that can work hand in hand with biomarkers by treating patients earlier, minimising complications, and bettering the well-being of patients.

## Chapter 8: References (Chapter 1 and 7)

1. World Health Organization. *World malaria report 2019*. Geneva: World Health Organization; Licence:CC BY-NC-SA 3.0 IGO. <https://www.who.int/publications/i/item/9789241565721> (2019).
2. World Health Organization. *World malaria report 2022*. Geneva: World Health Organization; Licence:CC BY-NC-SA 3.0 IGO. <https://www.who.int/publications/i/item/9789240064898> (2022).
3. Kochar, D. K. *et al.* Plasmodium vivax malaria. *Emerging Infect. Dis.* **11**, 132–134 (2005).
4. González-Sanz, M., Berzosa, P. & Norman, F. F. Updates on malaria epidemiology and prevention strategies. *Curr. Infect. Dis. Rep.* 1–9 (2023) doi:10.1007/s11908-023-00805-9.
5. World Health Organization. *World malaria report 2023*. Geneva: World Health Organization; Licence:CC BY-NC-SA 3.0 IGO. <https://www.who.int/publications/i/item/9789240086173> (2023).
6. Imboumy-Limoukou, R. K. *et al.* Malaria in children and women of childbearing age: infection prevalence, knowledge and use of malaria prevention tools in the province of Nyanga, Gabon. *Malar. J.* **19**, 387 (2020).
7. Chilot, D. *et al.* Pooled prevalence and risk factors of malaria among children aged 6-59 months in 13 sub-Saharan African countries: A multilevel analysis using recent malaria indicator surveys. *PLoS ONE* **18**, e0285265 (2023).
8. Calle, C. L., Mordmüller, B. & Singh, A. Immunosuppression in Malaria: Do Plasmodium falciparum Parasites Hijack the Host? *Pathogens* **10**, (2021).
9. Chua, C. L. L. *et al.* Malaria in pregnancy: from placental infection to its abnormal development and damage. *Front. Microbiol.* **12**, 777343 (2021).
10. Cirera, L., Castelló, J. V., Brew, J., Saúte, F. & Sicuri, E. The impact of a malaria elimination initiative on school outcomes: Evidence from Southern Mozambique. *Econ. Hum. Biol.* **44**, 101100 (2022).

11. Lukwa, A. T., Mawoyo, R., Zablou, K. N., Siya, A. & Alaba, O. Effect of malaria on productivity in a workplace: the case of a banana plantation in Zimbabwe. *Malar. J.* **18**, 390 (2019).
12. Birbeck, G. L. *et al.* Blantyre Malaria Project Epilepsy Study (BMPES) of neurological outcomes in retinopathy-positive paediatric cerebral malaria survivors: a prospective cohort study. *Lancet Neurol.* **9**, 1173–1181 (2010).
13. Bangirana, P. *et al.* Malaria with neurological involvement in Ugandan children: effect on cognitive ability, academic achievement and behaviour. *Malar. J.* **10**, 334 (2011).
14. Sachs, J. & Malaney, P. The economic and social burden of malaria. *Nature* **415**, 680–685 (2002).
15. Degarege, A., Fennie, K., Degarege, D., Chennupati, S. & Madhivanan, P. Improving socioeconomic status may reduce the burden of malaria in sub Saharan Africa: A systematic review and meta-analysis. *PLoS ONE* **14**, e0211205 (2019).
16. Kooko, R., Wafula, S. & Orishaba, P. Socio-economic determinants of malaria prevalence among under five children in Uganda: Evidence from 2018-19 Uganda malaria indicator survey. *J. Vector Borne Dis.* **0**, 0 (2022).
17. Gonçalves, N. V. *et al.* Malaria and environmental, socioeconomics and public health conditions in the municipality of São Félix do Xingu, Pará, Eastern Amazon, Brazil: An ecological and cross-sectional study. *Rev. Soc. Bras. Med. Trop.* **56**, e0502 (2023).
18. Patrick, S. M. *et al.* Household living conditions and individual behaviours associated with malaria risk: a community-based survey in the Limpopo River Valley, 2020, South Africa. *Malar. J.* **22**, 156 (2023).
19. Daca, C. S. L., Sebastian, M. S., Arnaldo, C., Schumann, B. & Namatovu, F. Socioeconomic and geographical inequalities in health care coverage in Mozambique: a repeated cross-sectional study of the 2015 and 2018 national surveys. *BMC Public Health* **23**, 1007 (2023).
20. Guin, P., Kumar, E. L. & Mukhopadhyay, I. Do climatic and socioeconomic factors explain population vulnerability to malaria? Evidence from a national survey, India. *Indian J. Public Health* **67**, 226–234 (2023).

21. Ingstad, B., Munthali, A. C., Braathen, S. H. & Grut, L. The evil circle of poverty: a qualitative study of malaria and disability. *Malar. J.* **11**, 15 (2012).
22. Ge, Y. *et al.* How socioeconomic status affected the access to health facilities and malaria diagnosis in children under five years: findings from 19 sub-Saharan African countries. *Infect. Dis. Poverty* **12**, 29 (2023).
23. Chahine, Z. & Le Roch, K. G. Decrypting the complexity of the human malaria parasite biology through systems biology approaches. *Front. Syst. Biol.* **2**, (2022).
24. Josling, G. A. & Llinás, M. Sexual development in Plasmodium parasites: knowing when it's time to commit. *Nat. Rev. Microbiol.* **13**, 573–587 (2015).
25. Phillips, M. A. *et al.* Malaria. *Nat. Rev. Dis. Primers* **3**, 17050 (2017).
26. Vaughan, A. M. *et al.* Complete Plasmodium falciparum liver-stage development in liver-chimeric mice. *J. Clin. Invest.* **122**, 3618–3628 (2012).
27. Vaughan, A. M. & Kappe, S. H. I. Malaria parasite liver infection and exoerythrocytic biology. *Cold Spring Harb. Perspect. Med.* **7**, (2017).
28. White, N. J. Malaria. in *Manson's tropical infectious diseases* 532-600.e1 (Elsevier, 2014). doi:10.1016/B978-0-7020-5101-2.00044-3.
29. Coatney, G. R., Collins, W. E., Warren, M. & Contacos, P. G. *The primate malarias [original book published 1971]*. vol. 1 (Atlanta: Centers for Disease Control and Prevention, 2003).
30. Yang, A. S. P. *et al.* Development of Plasmodium falciparum liver-stages in hepatocytes derived from human fetal liver organoid cultures. *Nat. Commun.* **14**, 4631 (2023).
31. Breman, J. G. Eradicating malaria. *Sci. Prog.* **92**, 1–38 (2009).
32. Mehra, S., Stadler, E., Houry, D., McCaw, J. M. & Flegg, J. A. Hypnozoite dynamics for Plasmodium vivax malaria: The epidemiological effects of radical cure. *J. Theor. Biol.* **537**, 111014 (2022).
33. White, N. J. Determinants of relapse periodicity in Plasmodium vivax malaria. *Malar. J.* **10**, 297 (2011).

34. Meibalan, E. & Marti, M. Biology of malaria transmission. *Cold Spring Harb. Perspect. Med.* **7**, (2017).
35. Bannister, L. & Mitchell, G. The ins, outs and roundabouts of malaria. *Trends Parasitol.* **19**, 209–213 (2003).
36. White, N. J. Malaria parasite clearance. *Malar. J.* **16**, 88 (2017).
37. Taylor, L. H. & Read, A. F. Why so few transmission stages? Reproductive restraint by malaria parasites. *Parasitol Today (Regul Ed)* **13**, 135–140 (1997).
38. Amoah, L. E. *et al.* Comparative analysis of asexual and sexual stage Plasmodium falciparum development in different red blood cell types. *Malar. J.* **19**, 200 (2020).
39. Chawla, J., Oberstaller, J. & Adams, J. H. Targeting Gametocytes of the Malaria Parasite Plasmodium falciparum in a Functional Genomics Era: Next Steps. *Pathogens* **10**, (2021).
40. Schofield, L. & Grau, G. E. Immunological processes in malaria pathogenesis. *Nat. Rev. Immunol.* **5**, 722–735 (2005).
41. Miller, L. H., Ackerman, H. C., Su, X. & Wellems, T. E. Malaria biology and disease pathogenesis: insights for new treatments. *Nat. Med.* **19**, 156–167 (2013).
42. Korzeniewski, K., Bylicka-Szczepanowska, E. & Lass, A. Prevalence of asymptomatic malaria infections in seemingly healthy children, the rural dzanga sangha region, central african republic. *Int. J. Environ. Res. Public Health* **18**, (2021).
43. Agaba, B. B. *et al.* Asymptomatic malaria infection, associated factors and accuracy of diagnostic tests in a historically high transmission setting in Northern Uganda. *Malar. J.* **21**, 392 (2022).
44. Kotepui, M., Kotepui, K. U., Masangkay, F. R., Mahittikorn, A. & Wilairatana, P. Prevalence and proportion estimate of asymptomatic Plasmodium infection in Asia: a systematic review and meta-analysis. *Sci. Rep.* **13**, 10379 (2023).
45. Prusty, D. *et al.* Asymptomatic malaria infection prevailing risks for human health and malaria elimination. *Infect. Genet. Evol.* **93**, 104987 (2021).

46. Ashley, E. A., Pyae Phyo, A. & Woodrow, C. J. Malaria. *Lancet* **391**, 1608–1621 (2018).
47. Oakley, M. S., Gerald, N., McCutchan, T. F., Aravind, L. & Kumar, S. Clinical and molecular aspects of malaria fever. *Trends Parasitol.* **27**, 442–449 (2011).
48. Trampuz, A., Jereb, M., Muzlovic, I. & Prabhu, R. M. Clinical review: Severe malaria. *Crit. Care* **7**, 315–323 (2003).
49. White, N. J. Severe malaria. *Malar. J.* **21**, 284 (2022).
50. Winskill, P. *et al.* Estimating the burden of severe malarial anaemia and access to hospital care in East Africa. *Nat. Commun.* **14**, 5691 (2023).
51. Taylor, C., Namaste, S. M. L., Lowell, J., Useem, J. & Yé, Y. Estimating the Fraction of Severe Malaria among Malaria-Positive Children: Analysis of Household Surveys in 19 Malaria-Endemic Countries in Africa. *Am. J. Trop. Med. Hyg.* **104**, 1375–1382 (2021).
52. Murray, C. J. L. *et al.* Global malaria mortality between 1980 and 2010: a systematic analysis. *Lancet* **379**, 413–431 (2012).
53. Severe malaria. *Trop. Med. Int. Health* **19 Suppl 1**, 7–131 (2014).
54. Teuscher, F. *et al.* Artemisinin-induced dormancy in plasmodium falciparum: duration, recovery rates, and implications in treatment failure. *J. Infect. Dis.* **202**, 1362–1368 (2010).
55. Peatey, C. *et al.* Dormant Plasmodium falciparum Parasites in Human Infections Following Artesunate Therapy. *J. Infect. Dis.* **223**, 1631–1638 (2021).
56. Venugopal, K., Hentzschel, F., Valkiūnas, G. & Marti, M. Plasmodium asexual growth and sexual development in the haematopoietic niche of the host. *Nat. Rev. Microbiol.* **18**, 177–189 (2020).
57. Joice, R. *et al.* Plasmodium falciparum transmission stages accumulate in the human bone marrow. *Sci. Transl. Med.* **6**, 244re5 (2014).
58. Obaldia, N. *et al.* Bone Marrow Is a Major Parasite Reservoir in Plasmodium vivax Infection. *MBio* **9**, (2018).

59. Wassmer, S. C. *et al.* Investigating the Pathogenesis of Severe Malaria: A Multidisciplinary and Cross-Geographical Approach. *Am. J. Trop. Med. Hyg.* **93**, 42–56 (2015).
60. Miller, L. H., Good, M. F. & Milon, G. Malaria pathogenesis. *Science* **264**, 1878–1883 (1994).
61. Chua, C. L. L., Ng, I. M. J., Yap, B. J. M. & Teo, A. Factors influencing phagocytosis of malaria parasites: the story so far. *Malar. J.* **20**, 319 (2021).
62. Cowman, A. F., Healer, J., Marapana, D. & Marsh, K. Malaria: biology and disease. *Cell* **167**, 610–624 (2016).
63. Wassmer, S. C. & Grau, G. E. R. Severe malaria: What's new on the pathogenesis front? *International journal for parasitology* **47**, 145–152 (2017).
64. White, N. J. *et al.* Malaria. *Lancet* **383**, 723–735 (2014).
65. Bruneel, F. Human cerebral malaria: 2019 mini review. *Rev Neurol (Paris)* **175**, 445–450 (2019).
66. Bangirana, P. *et al.* Severe malarial anemia is associated with long-term neurocognitive impairment. *Clin. Infect. Dis.* **59**, 336–344 (2014).
67. Bangirana, P. *et al.* Neurocognitive domains affected by cerebral malaria and severe malarial anemia in children. *Learn. Individ. Differ.* **46**, 38–44 (2016).
68. Song, X. *et al.* Cerebral malaria induced by plasmodium falciparum: clinical features, pathogenesis, diagnosis, and treatment. *Front. Cell. Infect. Microbiol.* **12**, 939532 (2022).
69. Lozoff, B. & Georgieff, M. K. Iron deficiency and brain development. *Semin. Pediatr. Neurol.* **13**, 158–165 (2006).
70. John, C. C. *et al.* Cerebral malaria in children is associated with long-term cognitive impairment. *Pediatrics* **122**, e92-9 (2008).
71. Idro, R. *et al.* Severe neurological sequelae and behaviour problems after cerebral malaria in Ugandan children. *BMC Res. Notes* **3**, 104 (2010).
72. Carter, J. A. *et al.* Persistent neurocognitive impairments associated with severe falciparum malaria in Kenyan children. *J. Neurol. Neurosurg. Psychiatr.* **76**, 476–481 (2005).



73. Idro, R. *et al.* Cerebral malaria is associated with long-term mental health disorders: a cross sectional survey of a long-term cohort. *Malar. J.* **15**, 184 (2016).
74. Ssenkusu, J. M. *et al.* Long-term Behavioral Problems in Children With Severe Malaria. *Pediatrics* **138**, (2016).
75. Fernando, S. D. *et al.* The impact of repeated malaria attacks on the school performance of children. *Am. J. Trop. Med. Hyg.* **69**, 582–588 (2003).
76. Fernando, D., Wickremasinghe, R., Mendis, K. N. & Wickremasinghe, A. R. Cognitive performance at school entry of children living in malaria-endemic areas of Sri Lanka. *Trans. R. Soc. Trop. Med. Hyg.* **97**, 161–165 (2003).
77. Fernando, D., de Silva, D. & Wickremasinghe, R. Short-term impact of an acute attack of malaria on the cognitive performance of schoolchildren living in a malaria-endemic area of Sri Lanka. *Trans. R. Soc. Trop. Med. Hyg.* **97**, 633–639 (2003).
78. World Health Organization. *World malaria report 2016*. Geneva: World Health Organization; Licence:CC BY-NC-SA 3.0 IGO. <https://www.who.int/publications/i/item/9789241511711> (2016).
79. Enayati, A. & Hemingway, J. Malaria management: past, present, and future. *Annu. Rev. Entomol.* **55**, 569–591 (2010).
80. RTS,S Clinical Trials Partnership. Efficacy and safety of RTS,S/AS01 malaria vaccine with or without a booster dose in infants and children in Africa: final results of a phase 3, individually randomised, controlled trial. *Lancet* **386**, 31–45 (2015).
81. Datto, M. S. *et al.* Efficacy and immunogenicity of R21/Matrix-M vaccine against clinical malaria after 2 years' follow-up in children in Burkina Faso: a phase 1/2b randomised controlled trial. *Lancet Infect. Dis.* **22**, 1728–1736 (2022).
82. Dalko, E. *et al.* Erythropoietin Levels Increase during Cerebral Malaria and Correlate with Heme, Interleukin-10 and Tumor Necrosis Factor-Alpha in India. *PLoS ONE* **11**, e0158420 (2016).
83. Casals-Pascual, C. *et al.* High levels of erythropoietin are associated with protection against neurological sequelae in African children with cerebral malaria. *Proc Natl Acad Sci USA* **105**, 2634–2639 (2008).

84. Phiri, H. T. *et al.* Elevated plasma von Willebrand factor and propeptide levels in Malawian children with malaria. *PLoS ONE* **6**, e25626 (2011).
85. Hollestelle, M. J. *et al.* von Willebrand factor propeptide in malaria: evidence of acute endothelial cell activation. *Br. J. Haematol.* **133**, 562–569 (2006).
86. Bridges, D. J. *et al.* Rapid activation of endothelial cells enables Plasmodium falciparum adhesion to platelet-decorated von Willebrand factor strings. *Blood* **115**, 1472–1474 (2010).
87. Oluboyo, A. O., Chukwu, S. I., Oluboyo, B. O. & Odewusi, O. O. Evaluation of Angiopoietins 1 and 2 in Malaria-Infested Children. *J. Environ. Public Health* **2020**, 2169763 (2020).
88. Conroy, A. L. *et al.* Whole blood angiopoietin-1 and -2 levels discriminate cerebral and severe (non-cerebral) malaria from uncomplicated malaria. *Malar. J.* **8**, 295 (2009).
89. Thakur, K., Vareta, J., Carson, K., Taylor, T. & Sullivan, D. Performance of Cerebrospinal Fluid (CSF) Plasmodium Falciparum Histidine-Rich Protein-2 (pfHRP-2) in Prediction of Death in Cerebral Malaria (I10-2.005). (2014).
90. Adukpo, S. *et al.* High plasma levels of soluble intercellular adhesion molecule (ICAM)-1 are associated with cerebral malaria. *PLoS ONE* **8**, e84181 (2013).
91. Gupta, H. *et al.* Plasma levels of hsa-miR-3158-3p microRNA on admission correlate with MRI findings and predict outcome in cerebral malaria. *Clin. Transl. Med.* **11**, e396 (2021).
92. Zeng, Y. *et al.* Biological features of extracellular vesicles and challenges. *Front. Cell Dev. Biol.* **10**, 816698 (2022).
93. Sanz-Ros, J. *et al.* Extracellular vesicles as therapeutic resources in the clinical environment. *Int. J. Mol. Sci.* **24**, (2023).
94. Buzas, E. I. The roles of extracellular vesicles in the immune system. *Nat. Rev. Immunol.* **23**, 236–250 (2023).
95. Hallal, S., Túzesi, Á., Grau, G. E., Buckland, M. E. & Alexander, K. L. Understanding the extracellular vesicle surface for clinical molecular biology. *J. Extracell. Vesicles* **11**, e12260 (2022).

96. Lu, S. *et al.* Challenges and opportunities for extracellular vesicles in clinical oncology therapy. *Bioengineering (Basel)* **10**, (2023).
97. Zhang, X. *et al.* Engineered extracellular vesicles for cancer therapy. *Adv. Mater.* **33**, e2005709 (2021).
98. Sheta, M., Taha, E. A., Lu, Y. & Eguchi, T. Extracellular vesicles: new classification and tumor immunosuppression. *Biology (Basel)* **12**, (2023).
99. Yokoi, A. & Ochiya, T. Exosomes and extracellular vesicles: Rethinking the essential values in cancer biology. *Semin. Cancer Biol.* **74**, 79–91 (2021).
100. Ciferri, M. C., Quarto, R. & Tasso, R. Extracellular Vesicles as Biomarkers and Therapeutic Tools: From Pre-Clinical to Clinical Applications. *Biology (Basel)* **10**, (2021).
101. Huda, M. N. *et al.* Potential use of exosomes as diagnostic biomarkers and in targeted drug delivery: progress in clinical and preclinical applications. *ACS Biomater. Sci. Eng.* **7**, 2106–2149 (2021).
102. Zhou, X. *et al.* Emerging technologies for engineering of extracellular vesicles. *Front. Bioeng. Biotechnol.* **11**, 1298746 (2023).
103. György, B. *et al.* Membrane vesicles, current state-of-the-art: emerging role of extracellular vesicles. *Cell. Mol. Life Sci.* **68**, 2667–2688 (2011).
104. Théry, C. *et al.* Minimal information for studies of extracellular vesicles 2018 (MISEV2018): a position statement of the International Society for Extracellular Vesicles and update of the MISEV2014 guidelines. *J. Extracell. Vesicles* **7**, 1535750 (2018).
105. Valadi, H. *et al.* Exosome-mediated transfer of mRNAs and microRNAs is a novel mechanism of genetic exchange between cells. *Nat. Cell Biol.* **9**, 654–659 (2007).
106. Colombo, M., Raposo, G. & Théry, C. Biogenesis, secretion, and intercellular interactions of exosomes and other extracellular vesicles. *Annu. Rev. Cell Dev. Biol.* **30**, 255–289 (2014).
107. Mathews, P. M. & Levy, E. Exosome production is key to neuronal endosomal pathway integrity in neurodegenerative diseases. *Front. Neurosci.* **13**, 1347 (2019).

108. Zhu, J., Wang, S., Yang, D., Xu, W. & Qian, H. Extracellular vesicles: emerging roles, biomarkers and therapeutic strategies in fibrotic diseases. *J. Nanobiotechnology* **21**, 164 (2023).
109. Opadokun, T. & Rohrbach, P. Extracellular vesicles in malaria: an agglomeration of two decades of research. *Malar. J.* **20**, 442 (2021).
110. Couch, Y. Challenges associated with using extracellular vesicles as biomarkers in neurodegenerative disease. *Expert Rev. Mol. Diagn.* **23**, 1091–1105 (2023).
111. Sankineni, S., Chauhan, S., Shegokar, R. & Pathak, Y. Global health and malaria: past and present. in *Malarial drug delivery systems: advances in treatment of infectious diseases* (eds. Shegokar, R. & Pathak, Y.) 1–16 (Springer International Publishing, 2023). doi:10.1007/978-3-031-15848-3\_1.
112. Langfitt, J. T. *et al.* Neurodevelopmental impairments 1 year after cerebral malaria. *Pediatrics* **143**, (2019).
113. John, C. C. *et al.* Cerebral malaria in children is associated with long-term cognitive impairment. *Pediatrics* **122**, e92-9 (2008).
114. Akide Ndunge, O. B., Kilian, N. & Salman, M. M. Cerebral malaria and neuronal implications of plasmodium falciparum infection: from mechanisms to advanced models. *Adv Sci (Weinh)* **9**, e2202944 (2022).
115. Gitau, E. N., Kokwaro, G. O., Karanja, H., Newton, C. R. J. C. & Ward, S. A. Plasma and cerebrospinal proteomes from children with cerebral malaria differ from those of children with other encephalopathies. *J. Infect. Dis.* **208**, 1494–1503 (2013).
116. Zoia, M. *et al.* Validation of effective extracellular vesicles isolation methods adapted to field studies in malaria endemic regions. *Front. Cell Dev. Biol.* **10**, 812244 (2022).
117. Wang, Z.-Y. *et al.* Advances in Point-of-Care Testing of microRNAs Based on Portable Instruments and Visual Detection. *Biosensors (Basel)* **13**, (2023).
118. Tang, S. *et al.* Magnetic three-phase single-drop microextraction for rapid amplification of the signals of DNA and microRNA analysis. *Anal. Chem.* (2020) doi:10.1021/acs.analchem.0c01936.